SOME STUDIES ON AUTOMATIC GENERATION CONTROL OF MULTI-AREA INTERCONNECTED RESTRUCTURED POWER SYSTEMS

A Thesis Submitted in Partial Fulfillment of the Requirements for the Award of the Degree of

DOCTOR OF PHILOSOPHY

Submitted by

YOGENDRA ARYA

(Enrollment No. 2K11/PhD/EE/11)

Under the Supervision of

Prof. NARENDRA KUMAR

Department of Electrical Engineering
Delhi Technological University
Bawana Road, Delhi-110042
DECEMBER, 2017

SOME STUDIES ON AUTOMATIC GENERATION CONTROL OF MULTI-AREA INTERCONNECTED RESTRUCTURED POWER SYSTEMS

A Thesis Submitted in Partial Fulfillment of the Requirements for the Award of the Degree of

DOCTOR OF PHILOSOPHY

Submitted by

YOGENDRA ARYA

(Enrollment No. 2K11/PhD/EE/11)

Under the Supervision of

Prof. NARENDRA KUMAR

Department of Electrical Engineering
Delhi Technological University
Bawana Road, Delhi-110042
DECEMBER, 2017

CANDIDATE'S DECLARATION

I hereby certify that the work which is being presented in this thesis entitled **"Some Studies on Automatic Generation Control of Multi-Area Interconnected Restructured Power Systems"** submitted in partial fulfillment of the requirements for the award of the degree of Doctor of Philosophy in the Department of Electrical Engineering, Delhi Technological University, Delhi is an authentic record of my own work carried out under the supervision of Dr. Narendra Kumar, Professor and Director, Internal Quality Assurance Cell (IQAC). The matter presented in this thesis has not been submitted elsewhere for the award of a degree.

Place: Delhi   **(Yogendra Arya)**
Date:

CERTIFICATE

On the basis of candidate's declaration, I hereby certify that the thesis entitled **"Some Studies on Automatic Generation Control of Multi-Area Interconnected Restructured Power Systems"** submitted to the Department of Electrical Engineering, Delhi Technological University, Delhi in partial fulfillment of the requirements for the award of degree of Doctor of Philosophy, is an original contribution with the existing knowledge and faithful record of the research work carried out by him under my guidance and supervision.

To the best of my knowledge, this work has not been submitted in part or full for the award of any degree elsewhere.

Dr. Narendra Kumar

Former Head & Professor
Department of Electrical Engineering
Director IQAC
Delhi Technological University
Bawana road, Delhi-110042, India

The Ph.D. viva-voce of Mr. Yogendra Arya, research scholar has been held on ……………

Signature of   Signature of   Signature of
Supervisor   **External Examiner**   **Head, Dept. of Electrical Engg.**

ACKNOWLEDGEMENTS

I thank the college management, Director and HOD of Electrical & Electronics Engineering Department, Dr. Meena Tushir of my institute for deputing me to pursue Ph.D. degree.

The completion of this work came at the expense of my long hours of absence from home. No words are adequate to express my indebtedness to my family for all the pains and suffering they have undergone to bring me up to this stage. I am extremely thankful to all my relatives too for their sincere good wishes.

(Yogendra Arya)

ABSTRACT

The prime objective of automatic generation control (AGC) is to adjust the active power generation in response to variable power demands and hence to maintain scheduled system frequency and scheduled tie-line power flows with neighboring control areas at desired tolerance values. A sizeable fall in frequency might badly affect the timing of electric clocks, magnetizing currents in transformers/induction motors, constant speed of AC motors, continuous operation of processes and synchronous operation of various units in power system. Additionally, power system may face a serious instability problem at substantial drop in the frequency. In steady state, automatically these variations must be zero. Enhanced power system stability is achieved with the proper design of supplementary controller adopted in an AGC system. However, continuous growth in size and complexity, stochastically changing power demands, system modeling errors, alterations in electric power system structures and variations in the system parameters over the time has turned AGC task into a challenging one. Consequently, conventional control strategies may be incompetent to handle such unpredictable variations in an AGC system. Hence, the researchers over the world are trying to propose several novel control strategies that fuse knowledge, techniques and methodologies from varied sources to tackle AGC problem of power system effectively. The literature survey indicates that several researchers, to tackle AGC issue in restructured system, have presented various types of controllers optimized using various conventional and intelligent soft computing techniques. The literature survey also unveils that the performance of AGC system depends chiefly on the sort of intelligent technique exploited and structure of the controller. Hence, the goal of the present study is to propose different types of new

supplementary controller structures for various types of restructured as well as traditional power systems.

The presented work is divided into ten chapters. Chapter 1 deals with the introduction of AGC topic in deregulated environment. Chapter 2 presents a critical review of AGC schemes in restructured power system. Chapter 3 stresses on the modeling of traditional and restructured power systems under the study. The main simulation work starts from Chapter 4.

In Chapter 4, the study is firstly conducted on a proposed restructured two-area multi-source hydrothermal and hydrothermal gas power systems interconnected via AC and AC/DC parallel tie-lines. Modern optimal control theory based optimal PI structured controllers are designed with full state vector feedback control strategy employing performance index minimization criterion. From the results obtained in the study, it is substantiated that the use of AC/DC parallel links as an area interconnection shows enrichment in the dynamic performance of the system in terms of less oscillations, settling time and peak overshoots/undershoots in the deviation in frequency and tie-line power responses. Eigenvalue study confirmed the positive effect of AC/DC parallel links on the system dynamic performance and stability. It is also observed that the multi-source hydrothermal system shows inferior performance in comparison to the single-source thermal system due the presence of hydro source in each area of the multi-source hydrothermal system due to the non-minimum phase characteristics of hydro turbines.

The full state feedback optimal PI controllers work well and are very much robust but in realistic environments, the measurement of all states is not feasible all the time. Hence, next, in Chapter 5, some modern methods are adopted to conduct the study. In first attempt, a modified fuzzy PI (FPI) controller optimized using genetic algorithm

(GA) is proposed for different electric power system models such as traditional two-area non-reheat thermal, reheat thermal, multi-source hydrothermal and restructured two-area reheat thermal systems. In traditional two-area multi-source hydrothermal system, each control area owns two generating units, one non-reheat thermal and one mechanical governor based hydro power plant. However, in restructured two-area single-source system, each control area owns two single reheat thermal generating units. Firstly, a FPI-1 controller is designed with nominal range of membership functions (mfs) and GA tuned output scaling factors. Secondly, to test the impact of alteration in horizontal range of mfs of FPI-1, it is further optimized to get FPI-2 controller. The results of FPI-1 and 2 controllers are compared and the results due to later controller are found to be superior. Yet, FPI controllers are designed only for a traditional two-area non-reheat thermal system; they are successfully applied on other system under studies. The performance of FPI controllers is found significantly superior in terms of lesser numerical values of settling times (STs), peak undershoots (PUs) and various performance indices (PIs) compared to conventional controllers based on optimal, GA, gravitational search algorithm (GSA), bacterial foraging optimization algorithm (BFOA), hybrid BFOA-particle swarm optimization (hBFOA-PSO) and hybrid firefly algorithm-pattern search (hFA-PS) techniques.

Next, in Chapter 6, BFOA optimized fuzzy PI (FPI) and fuzzy PID (FPID) controllers are proposed for traditional two-area non-reheat thermal, reheat thermal, multi-source hydrothermal and restructured multi-source hydrothermal power systems. BFOA is used to simultaneously tune the input and output scaling factors of FPI/FPID controller keeping mfs and fuzzy rules invariant. It is observed that FPI controller shows superior results in terms of lesser values of STs/PUs/PIs compared to PI controller based on recently reported techniques like GA/PSO/BFOA/hBFOA-

PSO/hFA-PS/FA/artificial bee colony (ABC) and FPI controller tuned using PS/PSO algorithms for the same system design.

Further, a fractional order PID (FOPID) structured controller is suggested for AGC problem solution of power systems in Chapter 7. The parameters of FOPID controller are optimized exploiting BFOA. At first, a traditional two-area multi-source hydrothermal system is considered and the advantage of FOPID is established over PI/PID controller optimized using hFA-PS and PID controller optimized using grey wolf optimization (GWO) techniques. To show the effectiveness of the method, the approach is further extended to restructured two-area multi-source hydrothermal and thermal gas systems. The analysis of the simulation results discloses the efficacy of FOPID controller over BFOA/differential evolution (DE)/GA optimized PID controller. Then, the study is extended to a restructured three-area multi-source hydrothermal power system.

In the next step of the study, a maiden attempt is made to propose a fractional order fuzzy PID (FOFPID) controller for traditional two-area multi-source hydrothermal, restructured two-area multi-source hydrothermal, restructured two-area multi-source thermal gas and restructured three-area multi-source hydrothermal AGC systems in Chapter 8. The parameters of FOFPID controller are also tuned utilizing BFOA. The critical analysis of the obtained results revealed the worth of FOFPID controller over FOPID controller in terms of less numerical value of STs, PUs and PIs. It is also experienced that FOFPID controller satisfies the AGC requirements in different power transactions taking place under deregulated environment more fruitfully than FOPID controller.

In Chapter 9, FOFPID controller is implemented in AGC of restructured three-area multi-source hydrothermal system considering appropriate generation rate

constraint (GRC), deadzone (DZ), boiler dynamics (BD) and time delay (TD). However, controller is optimized for linear system it works robustly in the presence of GRC/DZ/BD/TD physical constraints; though in the presence of GRC/DZ/BD/TD the system performance degraded drastically in comparison to the linear or the system with GRC only. Further, investigations clearly reveal that the controller is found to perform well when the system is subjected to higher degree of uncontracted load demands and simultaneous occurrence of uncontracted load demands. Thus, controller parameters obtained for the linear system are robust enough and need not be retuned for the system having appropriate GRC or GRC/DZ/BD/TD or wide changes in the size and location of contract violations. Thus, BFOA tuned FOFPID controller and other controllers proposed in the previous chapters may be options to supply reliable power with quality to the consumers.

Finally, Chapter 10 presents an overview of the contributions made in the current thesis. Few suggestions are also given to extend the research in the future.

CONTENTS

LIST OF FIGURES

xvii

time t = 0 s

LIST OF TABLES

NOMENCLATURE

Symbols	Name of the parameter/constant
F	Frequency
U_{PS}	Incremental change in power generation function
U_P	Input signal to primary control loop
U_S	Input signal to secondary control loop
U_{LS}	Incremental change in load shading function
U_{TU}	Incremental change in tripping unit function
β_i	Bias constant in i^{th} area
R_{ti}	Thermal power generation regulation constant in i^{th} area
R_{hi}	Hydro power generation regulation constant in i^{th} area
R_{gi}	Gas power generation regulation constant in i^{th} area
T_{Gi}	Steam turbine governor time constant in i^{th} area
T_{Ti}	Steam turbine time constant in i^{th} area
K_{ri}	Coefficient of reheater steam turbine in i^{th} area
T_{ri}	Steam turbine reheater time constant in i^{th} area
T_{RHi}	Hydro turbine speed governor transient droop time constant in i^{th} area
T_{GHi}	Hydro turbine speed governor main servo time constant in i^{th} area
T_{Ri}	Hydro turbine speed governor reset time in i^{th} area
T_{Wi}	Nominal starting time of water in penstock in i^{th} area
X_i	Gas turbine speed governor lead time constant in i^{th} area
Y_i	Gas turbine speed governor lag time constant in i^{th} area
a_i, b_i & c_i	Gas turbine constant of valve positioner in i^{th} area

T_{CRi}	Gas turbine combustion reaction time delay in i^{th} area
T_{Fi}	Gas turbine fuel time constant in i^{th} area
T_{CDi}	Gas turbine compressor discharge volume time constant in i^{th} area
P_{Ghi}	Output power of hydro turbine in i^{th} area
P_{Gti}	Output power of thermal turbine in i^{th} area
P_{Ggi}	Output power of gas turbine in i^{th} area
P_{Gi}	Power output in i^{th} GENCO
P_{gi}	Total power output in i^{th} area
$P_{ij\,max}$	Maximum power flow from i^{th} area to j^{th} area
P_{Ci}	Control signal in i^{th} area or speed changer setting in i^{th} area
α_{ij}	Area size ratio
ACE_i	Area control error in i^{th} area
K_{PSi}	Gain constant of power system in i^{th} area
T_{PSi}	Time constant of power system in i^{th} area
D_i	Load frequency characteristics in i^{th} area
T_{ij}	Tie-line synchronization power coefficient
H_i	Inertia constant in i^{th} area
F_r	Rated frequency
P_{ri}	Power rating of each control area in i^{th} area
ΔF_i	Frequency deviation in i^{th} area
$\Delta Ptie_{ij}$	Tie-line deviation between i^{th} and j^{th} area
ΔP_{Gti}	Deviation in thermal turbine output in i^{th} area
ΔP_{Rti}	Deviation in intermediate state of reheat turbine in i^{th} area
ΔX_{Ei}	Deviation in steam turbine governor output in i^{th} area
ΔP_{Ghi}	Deviation in hydro turbine output in i^{th} area

ΔX_{hi}	Deviation in output of mechanical hydraulic governor of hydro turbine in i^{th} area
ΔP_{RHi}	Deviation in intermediate state of hydro turbine governor in i^{th} area
ΔP_{Ggi}	Deviation in gas turbine output in i^{th} area
ΔP_{FCi}	Deviation in intermediate state of fuel sytsem and combustor of gas turbine in i^{th} area
ΔP_{VPi}	Deviation in valve positioner of gas turbine in i^{th} area
ΔX_{gi}	Deviation in intermediate state of speed governor of gas turbine in i^{th} area
ΔP_{Gi}	Deviation in total power output in i^{th} area
ΔP_{Di}	Deviation in load disturbance in i^{th} area
ΔP_{Li}	Deviation in power demand of DISCO-i
$\Delta P_{Li,LOC}$	Deviation in contracted local load demandin i^{th} area
ΔP_{UCi}	Deviation in uncontracted load demandin i^{th} area
$\underline{X}$	State vector
$\underline{U}$	Control vector
$\underline{P_d}$	Disturbance vector
$\underline{Y}$	Output vector
A	System matrix
B, Γ and C	Control, disturbance and output matrices
Q	Positive semi-definite symmetric state cost weighting matrix
R	Positive definite symmetric control cost weighting matrix
K	Optimal feedback gain matrix
J	Performance Index
$*$	Optimal value
K_1 - K_3	Boiler gains boiler dynamics (BD)
T_D	fuel firing system delay time in BD

T_f	fuel system time constant in BD
C_B	boiler storage time constant in BD
T_{RB}	lead-lag compensator time in BD
K_{IB}	boiler integrator gain IN BD
T_{IB}	proportional-integral ratio of gains in BD
N_C	Number of iterations of chemotaxis loops
N_{re}	Number of iterations of reproduction loops
N_{ed}	Number of iterations of elimination-dispersal loops
P_{ed}	Probability value for elimination dispersal process of BFOA
$\omega_{attract}$, $d_{attract}$, $h_{repellent}$ & $\omega_{repellent}$	Parameters of BFOA for computing cost function

CHAPTER 1

INTRODUCTION

1.1   General

Large-scale power systems are normally represented by control areas or regions representing coherent groups of generators. The various areas are interwoven through tie-lines [1]. The tie-lines are utilized for contractual energy exchange between different areas and provide inter-area support in case of abnormal conditions. The real and reactive power demands on the power system are never steady but continuously vary with the rising or falling trend. The real and reactive power generations must therefore vary continuously to match the load perturbations. The unbalancing between generated power and load demand causes the system frequency to deviate from its nominal value and creates inadvertent power exchanges between control areas. As load demand changes during different hours of a day, the use of manual control to maintain precise balance would be ineffective. To accomplish this, it becomes necessary to automatically regulate the operation of the main steam valves or hydro gates as per a suitable control strategy, which, in turn, controls the real power output of the alternators. The problem of controlling the output of electric generators in this way is termed as automatic generation control (AGC) which is detailed in the subsequent section.

The world's power demand is spiraling day by day, so to enhance competition and to supply reliable, economic and quality electric power, modern power systems are now transforming from traditional regulated environment to complex deregulated environment. In these modern restructured power systems, without changing the basic ideas, the engineering aspects of the planning and operation have to be reformulated.

In a deregulated electric power market, the vertically integrated utility does not exist, but various players like distribution companies (DISCOs), generation companies (GENCOs), transmission companies and independent system operator (ISO) have emerged. Among various ancillary services performed by ISO is the AGC. In the open market scenario, under the supervision of ISO, a DISCO (or buyer) of an area is free to choose from GENCOs (or seller) operating in the same or other control areas for power contracts. All power transactions are to be cleared mandatorily from ISO, which aims to assist system security and stability. At the time of execution of these power contracts, the system frequency profile deviates from nominal values. Hence, a sophisticated AGC controller is required to control the deviations in frequency, tie-line power flows and GENCOs outputs. In this work, starting from a conventional optimal controller, some new controller structures optimized using genetic algorithm and bacterial foraging optimization techniques have been proposed for AGC of restructured as well as traditionally interconnected electric power systems.

1.2 Automatic generation control (AGC)

The maintenance of nominal voltage and frequency is necessary to achieve high efficiency, minimum wear and tear of the consumer equipment and to enhance the stability and quality of the electric power supply. The frequency variations are mainly due to active power mismatch between generations and load, whereas voltage deviations are mainly due to reactive power imbalance in the system. The reactive power is produced close to the requirements as it engages only capital cost but no fuel cost and it is not exported on the lines to avoid large transmission losses. In a power system, active power balance can be achieved by controlling the generation.

For small load perturbations, a mismatch in real power balance influences mainly the system frequency but leaves the bus voltage levels unaltered and similarly a

mismatch in reactive power balance affects mainly the bus voltage levels but leaves the system frequency unaffected. In view of this, the real power-frequency (p-f) and reactive power-voltage (q-v) control problems are treated as two independent or decoupled control problems for all practical studies/purposes [1–6]. The main requirement of AGC is to ensure that the operating frequency of various bus voltages and currents are maintained at or very near to the specified nominal values. The tie-line power flows among the interconnected areas are maintained at specified nominal levels. The total power obligation on the system as a whole is shared optimally by the individual generators. The first two functions are ensured by designing an effective AGC controller. The third function engrosses another set of control termed as active power dispatch.

1.3   Control loops in AGC system

The execution of AGC schemes involves a number of control functions. These control functions are implemented by the primary and supplementary AGC loops as shown in Fig. 1.1. The responsibility of primary AGC loop is to regulate the real power output and the speed of the generator. It comprises of the speed governor mounted on the prime mover. It uses feedback of the generator speed or frequency and the real power output of the generator. The supplementary AGC loop regulates the net interchange, real power output of units and frequency. It consists of a feedback system which injects a signal into the speed governor. This signal is termed as the area control error (ACE) which is the combination of frequency deviation (ΔF) and tie-line power deviation ($\Delta Ptie$). The supplementary loop gives feedback via ACE and incremental change (U_S) adds it to the primary control loop through a suitable controller. The incremental change in the power generation (ΔP_{GS}) is obtained from the generator

3

Generation Side Control

Demand Side Control

Natural regulation

Primary control

ΔF

Governor & turbine

U_P
U_S

ΔP_{GS}

Power System

AGC

Supplementary Control

ACE

$\frac{dF}{dt}$

F

U_{LS}

Under frequency load shedding (UFLS)

ΔF

U_{TU}

Connection and tripping of the power system

Operator

Emergency control
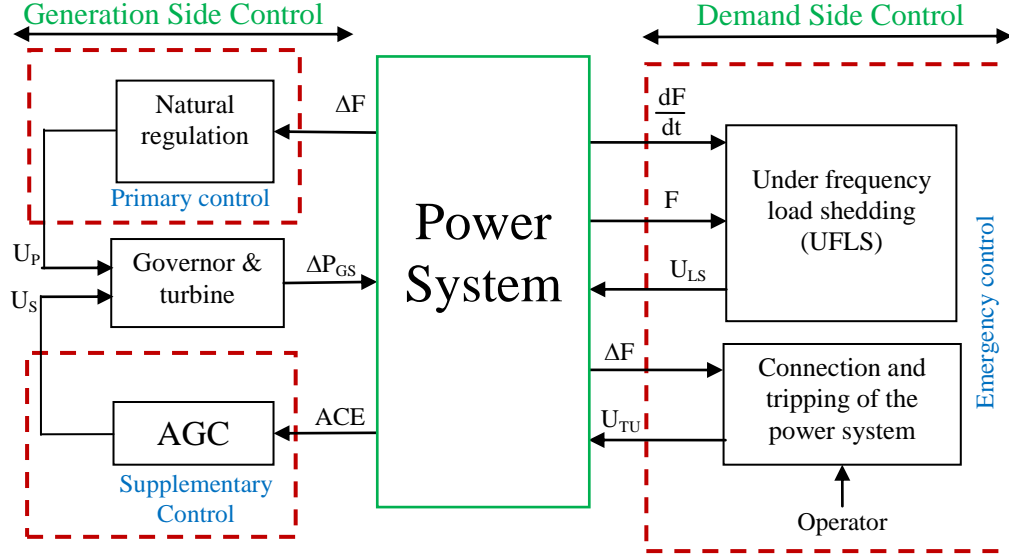
Fig. 1.1 Control loops in AGC system.

by using its input signals from primary (U_P) and supplementary (U_S) control loops.

Following a significant fault, there is a serious demand-generation imbalance associated with rapid frequency changes. The AGC controller might not be able to repair frequency change via the supplementary control loop. In this circumstance, the emergency control and protection schemes like under frequency load shedding (UFLS) are to be initiated to eliminate the risk of cascaded contingencies, which may lead to interruption of power supply. In case of emergency control, UFLS and protection system act as a tertiary control. Whenever, supplementary controller fails to regulate unwanted change in operating condition, the UFLS control system senses the signals (frequency and its derivative) and produces an appropriate increment function (U_{LS}) for load shedding while protection unit produces an increment change (U_{TU}) for tripping of the power system network to get the power system in nominal state.

The time hierarchy of execution of control functions in power system arises because of the extremely wide range of response time intrinsic in power system operation and control. Time decomposition is always carried out to subdivide a difficult problem into smaller sub-problems [7]. The overall operation and control of a

power system on time scale may be clubbed in four major groups as: governor actions (few seconds), AGC (many second), economic dispatching (minutes) and unit commitment (hours). However, there are still some slower and faster functions than the time decomposition which are not mentioned here. For example, maintenance scheduling has a time scale of days while relay action is faster than governor action.

It often happens that control function at higher-level take place with a slower time scale than control function at a lower level. An example of this is that UC control action take place at interconnected power system levels while economic dispatch control (EDC), AGC and governor action take place at individual plants level. However, this is not a general rule. For example, boiler control action done at the power plant level can be slower than AGC done at system level [7]. Apart from that, control functions for governor action and AGC are executed as on-line functions while UC and other slower functions (i.e., maintenance, planning etc.) are considered to be executed as off-line functions. The economic dispatch is carried out as on-line and off-line function depending upon the situation.

1.4 Power system restructuring and deregulation

Electricity is a concurrent subject in the Indian constitution, where decision-making and implementation involve both the state and central governments. Power development in India has been carried out predominantly by the state owned electricity boards. Until 1990, the power industry was solely governed by the government through various provisions envisaged in various Electricity Acts [i.e., Indian Electricity Act 1910 and Electricity Supply Act 1948] by the government agencies/authorities. However, all the government agencies and authorities were supposed to work under the central government through Ministry of Power (MOP).

The duties of MOP include the formulation of policies and plans, processing power projects for investment decisions, research and development, formulation of legislation pertaining to power generation and providing the required linkages between other ministries and departments dealing various aspects like, finance, environmental issues, land use, natural resources etc., at state and central levels.

The electric power industry has functioned with the vertically integrated utility (VIU) structure till late eighties where most of the operations like; generation, transmission and distribution are regulated by a single utility. Due to the VIU structure of the electricity industry, it was not possible to split the costs incurred in generation, transmission and distribution. Consequently, the utilities charge their customers an average tariff rate based on the aggregated cost during a period which sometimes causes an over pricing of electricity. The other restrictions associated with VIU structure are incompetence in generation and use of power, elevated losses, infrastructure deterioration and poor management. Therefore, it became essential to introduce deregulation in the electric power industry. Fig. 1.2 presents unbundling of one power system entity into three power entities. The last two decades have witnessed a transition of electric power industries throughout the world from regulated i.e., VIU structure to deregulated structure adding a market based competition in the supply system of electricity. The objectives of this reform are the creation of retail wheeling and the partition between production and other services. The main advantages expected from the market-based system are reduction in electricity charges, long-term gains in efficiency and the influx of private capital. The structure of this new electric power supply industry is normally based on either pool
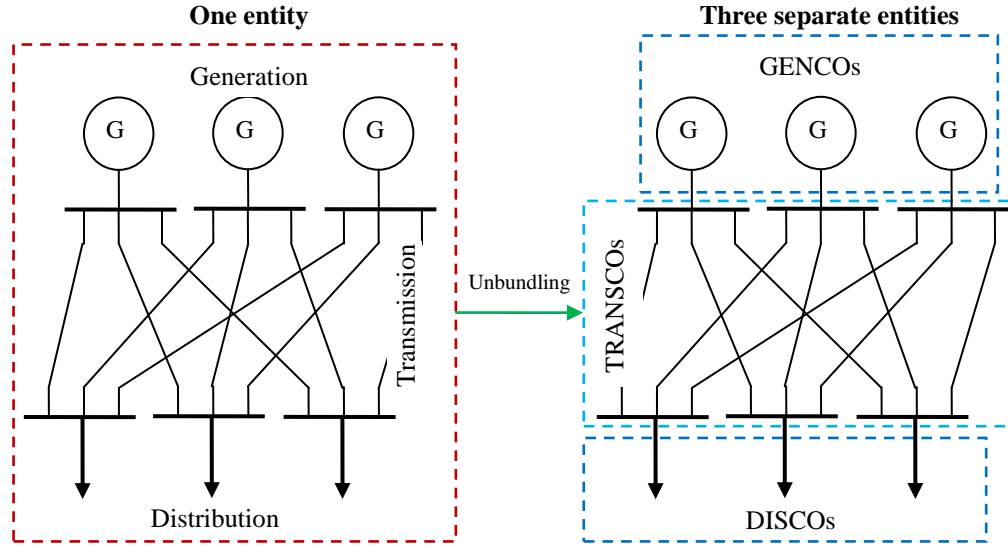
Fig. 1.2   Unbundling of power system utilities.

or markets for primary energy transaction. The competition in the wholesale generation market and the retail market together with the open access to the transmission network may bring many benefits to the end consumers. However, this transition has posed many new technical issues and challenges to the operation of power system under deregulated scenario. Therefore, there is an urgent need to modify the existing fundamental principles of operational and control philosophies to handle power supply system operating in deregulated environment [8–11].

1.5   AGC in deregulated environment

As there are many generation companies (GENCOs), distribution companies (DISCOs) and transmission companies (TRANSCOs) participating in deregulated environment, a DISCO has the freedom to select any GENCO to have a contract for receiving power. All possible market transactions have to be cleared through an impartial entity called an independent system operator (ISO). The duty of ISO is to control a number of ancillary services assigned to it and AGC is one of these ancillary services. AGC operation is accountable to load following contracts described in inter-
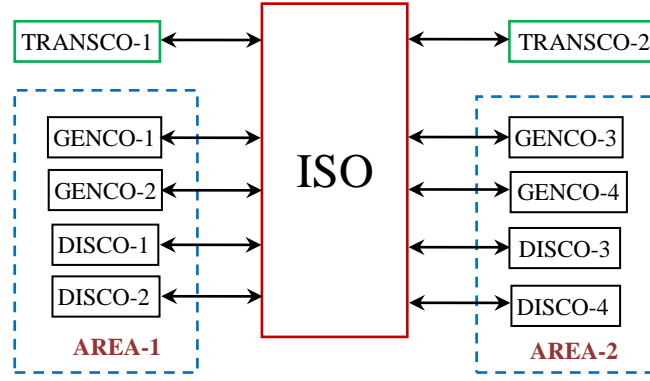
Fig. 1.3 Interconnection of GENCOs/DISCOs/TRANSCOs.
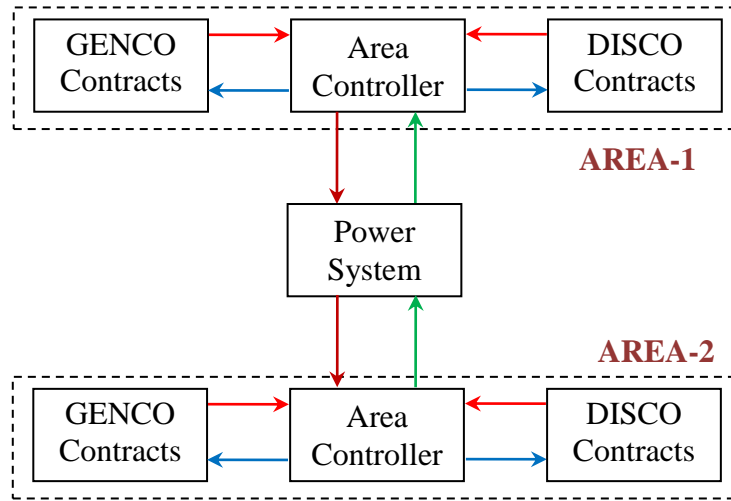
Fig. 1.4 Schematic diagram of an interconnected restructured power system model.

connected power system under deregulated environment. Fig. 1.3 presents transactions in deregulated market between GENCOs, DISCOs and TRANSCOs through the ISO. This deregulated power system has two DISCOs and two GENCOs in each control area. However, interconnection between power system control areas is via two TRANSCOs. The schematic representation of an interconnected power system for AGC in deregulated environment is shown in Fig. 1.4. However, implementation of these contracts will also meet the North American Electric Reliability Council (NERC) criteria of control performance as long as ACE is a part of the control objectives [12–14]. In such a market place, the AGC systems will need

all the information required in a vertically operated utility industry plus the contract data and measurements.

Players violating the contractual agreements are subjected to high penalty. In real time operation, the contract violation is reflected in higher cost of area regulation requirement. DISCOs may also participate in area regulation by using demand side management techniques. The deregulated power market framework requires establishment of standards for the electronic communication of contract data, as well as, measurements among the ISO and the market players. However, a variety of technical regulations will be needed to ensure secure power system operation and a fair marketplace. Moreover, all the transactions are coordinated and implemented by the ISO.

1.5.1 DISCO participation matrix

In restructured or deregulated power system, GENCOs sell power to various DISCOs at competitive prices. Thus, DISCOs have the liberty to choose the GENCOs for power contracts. They may or may not have power contracts with the GENCOs in their own area. This makes various combinations of GENCO-DISCO contracts possible in practice. This can be introduced by a concept of DISCO participation matrix (DPM). DPM is a matrix with number of rows equal to number of GENCOs and number of columns equal to number of DISCOs. Each entry in this matrix is a fraction of total load contracted by n^{th} DISCO towards the mth GENCO, so entry is named as contract participation factor cpf_{mn} [12]. For a power system operating in deregulated environment, if m-number of GENCOs and n-number of DISCOs are participating to honor a contract, the generalized structure of DPM may have the following representation:

$$
\text{DPM} =
\begin{bmatrix}
\text{cpf}_{11} & \text{cpf}_{12} & . & . & . & \text{cpf}_{1n} \\
\text{cpf}_{21} & \text{cpf}_{22} & . & . & . & \text{cpf}_{2n} \\
. & . & . & . & . & . \\
. & . & . & . & . & . \\
. & . & . & . & . & . \\
\text{cpf}_{m1} & \text{cpf}_{m2} & . & . & . & \text{cpf}_{mn}
\end{bmatrix}
$$

(Columns indicated by downward arrows: DISCO-1, DISCO-2, . . ., DISCO-n. Rows indicated by arrows on the right: GENCO-1, GENCO-2, . . ., GENCO-m)

1.5.2 Transactions in deregulated environment

Poolco based transactions

In this type of transaction, GENCOs and DISCOs negotiate inner contracts among each other in their own area only and submit their contractual agreements to ISO to get the clearance [12]. Therefore, there is no transaction of power from one control area to other control areas in case of implementation of AGC schemes when load disturbance occurs in any of the control areas. For example, in a two-area system, there will be no contracts between DISCOs of area-1 and GENCOs of area-2 or vice versa. The parameter cpf_{mn} is set to zero for DISCOs and GENCOs for different control areas. In such an arrangement, a GENCO sends a pulse to a governor to follow the predicted load as long as it does not exceed the contracted value. For these types of transactions, the structure of DPM may be given as shown on next page.

Poolco plus bilateral based transactions

Here, DISCOs are free to have a contract with any GENCO in their own control area or another control area. In poolco plus bilateral contract based transactions, all the

$$
\text{DPM} = \begin{bmatrix} \text{cpf}_{11} & \text{cpf}_{12} & 0 & 0 \\ \text{cpf}_{21} & \text{cpf}_{22} & 0 & 0 \\ 0 & 0 & \text{cpf}_{33} & \text{cpf}_{34} \\ 0 & 0 & \text{cpf}_{43} & \text{cpf}_{44} \end{bmatrix}
$$

Columns: DISCO-1, DISCO-2, DISCO-3, DISCO-4 (top). Rows: GENCO-1, GENCO-2, GENCO-3, GENCO-4 (right).

DISCOs can contract with all available GENCOs to fulfill the requirements of AGC scheme of a power system. The participation of GENCOs to meet the demand of DISCOs is characterized by the structure of corresponding DPM. Each load-matching contract requires a separate control process. These control process must cooperatively interact to maintain system frequency and minimize deviation in tie-line scheduled exchanges. A DISCO can control its load by using demand side management (DSM) techniques also [13]. The example of such type of DPM can be given as follows:

$$
\text{DPM} = \begin{bmatrix} \text{cpf}_{11} & \text{cpf}_{12} & \text{cpf}_{13} & \text{cpf}_{14} \\ \text{cpf}_{21} & \text{cpf}_{22} & \text{cpf}_{23} & \text{cpf}_{24} \\ \text{cpf}_{31} & \text{cpf}_{32} & \text{cpf}_{33} & \text{cpf}_{34} \\ \text{cpf}_{41} & \text{cpf}_{42} & \text{cpf}_{43} & \text{cpf}_{44} \end{bmatrix}
$$

Columns: DISCO-1, DISCO-2, DISCO-3, DISCO-4 (top). Rows: GENCO-1, GENCO-2, GENCO-3, GENCO-4 (right).

Contract violation based transactions

There may be circumstances where any of the DISCOs draws power more than that specified in the contract agreement and cleared by ISO [12]. This uncontracted power must be supplied by GENCOs in the same area as DISCOs and it is considered as a local load of the area and not as contract demand. For poolco and poolco plus bilateral

contract based transactions, DPM remains unchanged in the event of contract violations. This uncontracted power is supplied by the area GENCOs on the basis of concerned ACE participation factors (apfs). DISCOs are being penalized by ISO for such contracts violations as per the provisions laid down in the mutual transaction agreements and cleared by ISO.

1.6 Objectives of the thesis

In the literature a heap of articles have been appeared regarding the investigation of AGC in vertically integrated and deregulated power systems. Various control strategies have also been proposed to achieve better system dynamic performance. In the design of AGC regulators, classical, modern control and intelligent techniques have been incorporated from time to time. Still, there is a scope to carry out the investigations in deregulated power systems to deal certain important issues comprehensively.

There are many types of market transactions in practice for which a widely accepted control strategy has to be evolved. The investigations are required to be carried out considering all types of power transactions possible in a deregulated power environment. The various aspects of power system models and AGC strategies which have been dealt in regulated power system environment still have not found a considerable attention of researchers in deregulated power system environment. Therefore, efficacy of control strategies working well in traditional systems should also be checked in deregulated power systems. Most of the studies relating to optimal AGC of interconnected power systems in deregulated environment are based on single-source models. The effectiveness of optimal control strategy should be judged in multi-source restructured systems. Further, the studies relating to restructured power system are largely based on single-source models with conventional PI/PID

AGC controller. Therefore, new controllers in conjunction with appropriate optimization algorithms are to be implemented on single-source and multi-source restructured as well as traditional power systems.

Keeping in view the foregoing discussion, the motivation and main objectives of the thesis are stated as follows:

1. To develop dynamic model of two-area interconnected power system in deregulated environment considering two multi-source GENCOs and two DISCOs in each control area. The two control areas are interconnected via AC and AC/DC parallel links.

2. To propose optimal AGC controller design based on PI control strategy for multi-source power systems operating in deregulated environment considering (i) poolco based transaction, (ii) poolco plus bilateral based transactions and (iii) contract violations based transactions. The effect of incorporating the dynamics of DC link in parallel with AC link in system dynamic model on system dynamic performance has to be investigated under various market transactions.

3. To suggest genetic algorithm (GA) tuned fuzzy PI (FPI) controller for different power systems interconnected in regulated as well as deregulated environments. The effect of optimizing the horizontal range of membership functions (mfs) on system dynamic performance is to be investigated.

4. To design bacterial foraging optimization algorithm (BFOA) tuned fuzzy PI (FPI) and fuzzy PID (FPID) controllers for various traditional and restructured power system models. The effectiveness of FPID controller is to be compared with FPI designed in the current study and other PI and FPI controllers prevalent in the literature.

5. To present BFOA based fractional order PID (FOPID) controller for two and three-area multi-source power systems interconnected in regulated and deregulated scenarios.

6. To propose BFOA based fractional order fuzzy PID (FOFPID) controller for two and three-area multi-source power systems interconnected in regulated and deregulated fashion and to compare the performance of FOFPID and FOPID controllers.

7. To study the effect of system nonlinearities like generation rate constraint (GRC), governor deadzone (DZ), boiler dynamics (BD) and time delay (TD) on the performance of three-area multi-source restructured power system with FOFPID controller and hence, to check the robustness of the proposed BFOA tuned FOFPID controller.

1.7 Outline of the thesis

The thesis is organized into ten chapters. The chapter wise summary of the thesis is presented in the subsequent paragraphs:

Chapter 1: It presents a brief operational and control aspects and the identification of primary, secondary and emergency controls in overall control of power systems operating in interconnected craze. The AGC problem under vertically integrated and deregulated environment is conversed. The importance is conferred upon typical AGC systems, AGC in deregulated environment, DPM, various types of market transactions like poolco contract based transactions, poolco plus bilateral contract based transactions and transactions with contract violation.

Chapter 2: Following a brief description of AGC scheme in regulated environment, a widespread review of the literature on AGC of interconnected power system in

deregulated environment is presented in Chapter-2. Besides citing the most recent research works in the area of AGC in deregulated environment, the advanced control concepts like fuzzy, neural, neuro-fuzzy and intelligent optimization algorithms based AGC methods are reviewed comprehensively.

Chapter 3: It deals with the development of transfer function models of speed governor systems, turbines and associated components of thermal, hydro and gas power plants. Using the same, the dynamic models of two-area interconnected power systems having single and multi-sources in each area in regulated and deregulated environment are developed. The modification in ACE, tie-line power and generation formula of GENCOs in deregulated environment is also discussed.

Chapter 4: It is concerned with the study of optimal PI controllers for AGC study of two-area multi-source interconnected power systems in deregulated environment incorporating AC/DC parallel links as an interconnection between control areas with various market transactions. The differential equations of two-area interconnected power systems are developed considering deregulated environment with AC/DC parallel links. The state space design matrices are developed to design optimal gain of optimal AGC controllers. The dynamic plots, performance index value and patterns of open loop and close loop eigenvalues are discussed in AC and AC/DC parallel tie-line scenarios. The simulation results are obtained using MATLAB/SIMULINK software version 7.5.0 (R2007b).

Chapter 5: It deals with the application of genetic algorithm (GA) tuned fuzzy PI (FPI) controllers for AGC study of two-area interconnected traditional and restructured power systems. The superiority of GA tuned FPI approach is established over various lately published controllers.

Chapter 6: Here bacterial foraging optimization algorithm (BFOA) technique is used to design fuzzy PI (FPI) and fuzzy PID (FPID) controllers for two-area single/multi-source interconnected traditional/restructured power system. The simulation results obtained are compared with each other and with recent controllers available in the literature.

Chapter 7: It presents AGC study of traditional two-area multi-source hydrothermal, restructured two-area multi-source hydrothermal, restructured two-area multi-source thermal gas and restructured three-area multi-source hydrothermal power systems employing BFOA tuned fractional order PID (FOPID) supplementary controller. The dominance of FOPID controller is demonstrated over optimized PI/PID structured controller.

Chapter 8: A BFOA tuned fractional order fuzzy PID (FOFPID) supplementary controller is proposed for AGC study of various power system models studied in the previous chapter. It is observed that for different traditional/restructured two-area and restructured three-area power systems, the proposed FOFPID controller outperforms FOPID controller.

Chapter 9: The proposed FOFPID controller optimized for restructured linear three-area system is implemented on restructured three-area system incorporating nonlinearities like governor deadzone (DZ), generation rate constraint (GRC), boiler dynamics (BD) and time delays (TD). A desirable performance is achieved using FOFPID controller in the presence of system nonlinearities, however the system performance degrades drastically. The controller is also tested against different amounts and positions of uncontracted power demands to check the robustness. Investigations clearly reveal that the controller is found to perform well when the

system is subjected to higher degree of uncontracted demands and simultaneous occurrence of different uncontracted demands.

Chapter 10: It provides a review of the major contributions made out of the research work presented in the thesis. The scope for further work in the area of AGC of multi-area interconnected restructured power systems is also presented.

CHAPTER 2

LITERATURE SURVEY

2.1 Introduction

The literature review shows an incessant progress in the design and implementation of AGC strategies over a period of more than six decades. Apart from conventional methods, recently, new intelligent methods are gaining the potential implementation in the design and analysis of AGC schemes. These concepts are helping the power engineers to handle the power system becoming more complex, nonlinear and uncertain year by year. Despite advances in control concepts, many operating structural changes have taken place during last three decades. Deregulation of power industry is one of the most imperative changes witnessed by the power industry worldwide. In the following sections, these schemes are reviewed expansively.

2.2 Brief review of traditional AGC schemes

The very early effort in AGC has been to control the frequency of power system via the flywheel governor of the synchronous machine. Later on, a supplementary control was incorporated with the governor with the help of a signal directly proportional to the frequency deviation plus its integral or integral of summation of deviation in frequency plus tie-line power i.e., area control area (ACE). This scheme is the classical approach for AGC of electrical power system.

Very early works in classical AGC were based on tie-line bias control approach [15–18]. The examinations with large signal dynamics of AGC systems by using an optimization technique based on nonlinear programming might be a maiden attempt [19]. With the advent of modern control theory and its revolutionary applications by

Fosha and Elgerd [20] in power system control, there has been an incessant effort to suggest optimal AGC schemes to circumvent many limitations of classical methods during 1970. The design of linear optimal PI regulator for a two and three-area power systems was presented by Calovic [21–22]. An enhanced optimal control scheme for a two-area hydrothermal system was proposed by Kothari at al., [23]. Further, modified optimal AGC regulators were proposed in [24–26]. Some recent applications of optimal AGC regulators are available in the literature [27–32]. Although optimal AGC schemes offered deliberately improved system dynamic performance, they are associated with the measurement of all the system states, which is not practically possible sometimes. To circumvent these inadequacies, suboptimal AGC schemes are proposed in the literature [33–40]. To improve the dynamic performance of AGC system under changeable system parameters and operating conditions, variable structure controller has offered healthier potential [41–51]. Since digital control is more flexible, reliable, accurate, compact and fewer vulnerable to noise and drift, different researchers have suggested digital or discrete or sampled data AGC control schemes in AGC of power system [52–70].

Over the last decades, intelligent techniques have emerged in a big way to deal with the problems associated with successful design and implementation of control methods for large and complex electrical power system. Their potential applications in the area of AGC of power system have continuously been witnessed in the literature for more than last two decades [71–75]. Various intelligent techniques like artificial neural networks [76–86], fuzzy logic [87–111], neural fuzzy [112–121], big bang-big crunch optimization (BB-BCO) [101], hybrid differential evolution-pattern search (DEPS) [104], genetic algorithm (GA) [100,103,106,122–125], simulated annealing (SA) [126], particle swarm optimization (PSO) algorithm [110,121,127–

19

132], artificial bee colony (ABC) algorithm [133–135], gravitational search algorithm (GSA) [136–141], bacterial foraging optimization algorithm (BFOA) [99,142–146], pattern search (PS) [147], firefly algorithm (FA) [148–150], hybrid FA-PS (hFA-PS) [107,150], hybrid PSO-PS [151], grey wolf optimization (GWO) [152], bat algorithm (BA) [109,153–154], teaching-learning based optimization (TLBO) algorithm [105,155–156], differential evolution (DE) algorithm [157], cat swarm optimization (CSO) algorithm [158], cuckoo search (CS) algorithm [159–160], flower pollination algorithm (FPA) [161–162], imperialist competitive algorithm (ICA) [163], gases Brownian motion optimization (GBMO) [164], kriging based surrogate modeling technique [165], robust optimization [166], chaotic multi-objective optimization [167], chaotic PSO [168], ITAE optimization [169] etc. The capacious literature that has been published in national/international journals, conferences, seminars, books, magazines etc., is critically reviewed in [71–75].

2.3 AGC schemes in restructured power systems

The power system industries have witnessed numerous structural and operational changes besides the control and other facets since its inception. One of the key changes in power system operation and control is its changeover from regulated to deregulated environment. Accordingly, the control methodologies have been modified to deal with the changed power environment. Over, more than two decades, AGC strategies, which have been identified efficient to control large and complex restructured power system, have found an amicable space in the literature. The following aspects of restructured power system have been covered to review the literature in this field:

2.3.1 Restructuring and deregulation

The process of deregulation in California began in 1992, but it became more overt in 1996, after when The Federal Energy Regulatory Commission (FERC) issued an order to permit the free access of transmission grids. In deregulated environment, the traditional vertically monopolistic structure which performed all the functions involved in power generation, transmission and distribution, is disaggregated into separate companies termed as GENCOs, TRANSCOs and DISCOs each dedicated to function individually. A fair contest is introduced to GENCOs and DISCOs in order to reach higher efficiency in electricity production and utilization. Sood et al., reviewed the research articles on restructuring power industry in general [170] and wheeling of power under deregulated environment in particular [171]. In traditional unit commitment (UC), the objective is to produce power to satisfy the consumers with minimum production cost to meet the demand, whereas in the deregulated power market the GENCOs schedule their generators with a very different objective of maximizing their profit with an inequality demand constraint. Considering this aspect, various market models in practice in the area of UC under deregulated environment are presented in [172]. The issues in energy segment [173], evaluation techniques of electricity price forecasting [174] and survey of critical research areas in power generation planning [175] in deregulated markets have appeared in the literature. The emerging issues associated with restructuring the electric power industry, their solution methods and tools are addressed in [176]. In [177], the basis for a new strategy for solving the problem of inter-utility power transactions in deregulated electricity markets is discussed. The problem is formulated as an optimization problem with a nonlinear objective function and linear constraints.

The role of flexible alternating current transmission system (FACTS) technology to complement the conventional choices to provide a reliable and adequate transmission system in new scenario is discussed [178–179]. However, advanced power technology development for potential application in bidding system, demand side technology, smart power system such as gas-insulated substations, HVDC, EMS/SCADA and static VAR compensators and energy saving technologies are advised in [180].

The primary step in the restructuring process of the power industry has been separation of the transmission and distribution activities from the generation activity. The next step is to place electricity generation sector in open market via creation of power pools, provision for direct bilateral transactions or bidding in the spot markets. It will be followed by offering competition in distribution and transmission activities. The transition from VIU structure to deregulated one is constantly in progress worldwide. The research articles telling the state-of-the-art of deregulation process of electric industry in Russia [181], Japan [182], China [183–184], USA [184], Iran [185], Italy [186–187], Britain [188], Asia [189], India [190–194], Bolivia, Chile, Peru [195] etc., have appeared over the time in the literature to benefit the power engineers and planners working in power restructuring area.

The main causes behind the power sector reforms in India were accumulation of commercial losses due to poor fiscal health of state utilities, endemic capacity and energy shortages and increasing subsidy burden on the states utilities. Investment in the sector was falling far short of demand in power supply. In 1991, Government of India initiated the process for reforming the power sector with the major purpose of transforming the electricity sector into a proficient enterprise. As a primary step, 'Electricity Act-2003' came into force on June 10, 2003. Some of the key issues

addressed by this Act and their impact on power system restructuring are discussed in [190–194].

2.3.2   Ancillary services under open market

Ancillary services are those services performed by generators, transmission and control equipment, which are necessary to support fundamental services and to preserve trustworthy operations and system security. These services are essential to ensure reliable operation of an electric power system. The various aspects of ancillary services are addressed in [196–209]. A summary of practical experiences concerning performance of ancillary services in several competitive markets in Europe, Australia and New Zealand are talked about in [196]. The design aspects of ancillary service markets and their procurement are explored in [196–198]. The design, implementation and experience with ancillary service market procurement in different countries are provided in [199–205]. Cheung [199–200] talks about the design and implementation of ancillary service markets in North America. A unified framework for competitive electricity market and grid reliability based on the duality theory is described. The design and implementation experiences of ancillary services auction markets in the regional electricity markets of China [201], Nordiac [202], California [203], RTO market [204] and in ERCOT [205] are available in the literature. Hemandez et al., [206] proposed a methodology for ancillary reactive power service allocation cost in deregulated markets. The suggested method is based on sensitivities and the postage-stamp method in order to allocate the total costs service amongst all participants. With the purpose of achieving this goal, the system operator identifies voltage support and/or reactive power necessities, and looks out for appropriate providers. In [207], essential technical/economical features of management of frequency and voltage control ancillary services across a variety of jurisdictions are described and the

technical requirements adopted in North America, Europe, Germany, France, Spain, Netherlands, Belgium and Great Britain are contrasted. A new market based method for acquiring VAR ancillary service in the electricity market is developed in [208]. A hybrid PSO technique for procuring VAR ancillary service in the deregulated electricity markets is proposed in [209].

2.3.3   AGC in restructured power system

With the transition of power industry from regulated to deregulated one, there is a need to modify the traditional operating practices of AGC so that they may be capable to fulfill the AGC necessities in new operating environment. In a deregulated environment, the AGC turns into a commodity, which can be traded. GENCOs participating in the AGC provide a service for which they must be compensated. In competitive market scenario, AGC is essential for maintaining the system reliability. It facilitates power exchanges and provides better conditions for power trading. In the open electricity market, AGC system is faced by new uncertainties, therefore, a reevaluation in traditional modeling and control structures is fundamentally desirable. Large numbers of research papers in the field of AGC/LFC in restructured power systems have appeared in the literature [12–14,210–399].

The majority of the studies in the area of AGC for restructured power system were based on the identification of important technical, operational and control issues arising due to the changed operating environment. Major space of the articles has been dedicated to converse the issues, modifications in the presented control philosophies to meet out the requirements of effective control and the proposals to improve the control efforts. Christie et al., [210] try to identify likely deregulation scenarios, technical issues associated with LFC and technical solutions like standards and algorithms needed for the operation of this key component of national

infrastructure in the face of profound structural changes. Bevrani et al., [211] have compared various types of prevalent LFC approaches. The approaches were categorized broadly in three categories namely classical, robust/adaptive and intelligent approaches. A formulation of AGC in deregulated environment is presented in [212–214]. The objective to attain a degree of social welfare using LFC methods in power systems operating in deregulated environment is envisaged by Genki and Masakazu [215]. Authors explained the LFC methods in order to maximize the social welfare, assuming the ancillary service market like in PJM interconnection in America. Some control aspects to improve reliability in a deregulated environment are outlined in [216]. The frequency linked pricing is identified as an alternative to frequency regulation in deregulated electricity markets [217–218]. Wang et al., [219] have formulated a new approach of AGC cost allocation on the customer side. The load curves of a single load and a control area are investigated and decomposed, then an AGC demand curve is got, which can reflect AGC costs. Chanana and Kumar present a price based AGC employing unscheduled interchange price signals in Indian electric power scenario [220]. Unlike developed nations, AGC has not been implemented in India to provide supplementary control to preserve the frequency. In India, as per the Central Electricity Regulatory Commission (CERC) guidelines, 2005 all the dedicated generators are complied to function under free governor mode of action at all the time, which offers primary frequency control. The divergences from scheduled generation and scheduled demand are balanced by both generators and beneficiaries, which are being reimbursed via frequency dependent unscheduled interchange (UI) rates, set by CERC. The UI mechanism operates as the supplementary control for keeping the frequency within normal operating band [221]. Katende and Okafore investigated some of the technical problems associated with

AGC in Nigerian power system after deregulation [222]. Baken and Uhlen [223] tried to include marked bidding procedures in a closed loop AGC application taken from the Norwegian Regulating Power Market. Egido et al., reviewed the structure of Spanish AGC under new competitive environment [224].

Load following, an ancillary service with frequency control comes broadly under AGC in deregulated regime and is discussed broadly in [225–230]. Authors in [231] proposed a model for evaluating the performance of the LFC problem in deregulated environment where units may elect to offer or receive the service.

Wang et al., [232] proposed a new framework for forecasting and procuring AGC capacity so as to well balance the economic efficiency and system security in the competitive electricity market using the historical data of Zhejiang provincial electricity market. Delfino et al., [233] evaluated AGC and inadvertent interchange evaluation in an IEEE reliability test system arranged in a three-area configured restructured power system. Fathima and Abdullah [234] performed analysis on frequency related market structure in restructured system. In AGC, the penalty factor is important for optimal generation allocation. Under deregulation the transmission loss assessment for the individual plant becomes more important than that for the entire system. This needs the introduction of slack-bus independent penalty factors [235]. Various fundamental and control concepts of LFC in the new context of open access for electrical energy market implementation are critically reviewed in [236].

2.3.4 AGC control strategies in restructured power system

Numerous control schemes have been suggested for AGC/LFC in various types of interconnected restructured power systems [236]. In Europe, three types of control schemes are defined by the union for the coordination of transmission of electricity (UCTE): centralized network control, decentralized pluralistic network control and

decentralized hierarchical network control [212]. The nations with a central electricity supply system use AGC schemes based on centralized control strategy. In this scheme, a single secondary controller is used. The other two decentralized methods believe some separate control areas and each control area owns separate controller. The concepts of centralized [244] and decentralized [12,14,213–220,225,228–231,233–234,237–399] controls under competitive environments have surfaced in the literature.

2.3.5 *Optimal AGC schemes in restructured power system*

The studies done using classical control approaches, result in relatively large overshoots and transient frequency deviations [71–75]. Moreover, the settling time of the system frequency deviation is comparatively long and is of the order of 10–20 seconds. The optimal AGC regulator design techniques enable the power engineers to design an optimal controller via minimization a given performance criterion. Fosha and Elgerd [20] were the first to propose their pioneering work on optimal AGC regulator design via this concept. In restructured power system, the concept of optimal control theory using full state vector feedback is visible in [237–244]. In practical situations, access to all of the state variables is not possible in various power systems. This inadequacy of optimal AGC regulators is eradicated by proposing sub-optimal controller designs via output feedback control methods [243–251]. In output feedback technique, only the measurable states within each control area are necessary to employ for feedback. The investigations carried out reveal that the performance of optimal control strategy is superior but the output vector feed control approach also provides a desired solution. However, the un-measurable states can be reconstructed via Kalman filter or an observer in optimal control method [243–244,246–251]. The structure-preserving model of power system in order to consider the characteristics of

loads, the optimization problem is constrained by differential equations as well as algebraic equations. A quasi-Newton algorithm is used to solve the formulated optimal DAE-constrained optimization problem for developing optimal LFC scheme in deregulated power system [252].

2.3.6 Robust AGC techniques in restructured power system

Robust linear control theory has provided powerful tools such as µ synthesis/analysis, quantitative feedback theory (QFT), linear matrix inequality (LMI), optimal H_2, H_∞ and mixed H_2/H_∞ techniques for AGC regulator design. The concept of robust control strategy is utilized in AGC regulator design for deregulated market [253–268].

2.3.7 AGC in restructured power system with AC/DC tie-lines

Major part of the works reported by the researchers regarding AGC of restructured power systems is limited to multi-area power systems interconnected via AC tie-lines. As the load demands are raising day by day, the power engineers in the current scenario are motivated to pay their attention to transmit large chunks of electric power via HVDC system. Besides other applications, commissioning of an HVDC link in parallel with an existing AC link has shown beneficial impacts from the point of view of stabilization of the system [28–32,36–37,40].

Increased operational complexities due to the introduction of HVDC links between operating areas will put extra burden on system operators to maintain the current manual control system. A model of the interconnected power systems of Norway and Sweden is used to show how introduction of AGC might aid the system operator in handling the increased complexity. A flexible approach is devised where selected units are automatically following load changes on the HVDC links. It is proposed by Baken et al., that ramp following controller (RFC) supported by

manual control may be a promising option to deal with such systems [225]. AGC schemes of power systems interconnected via AC/DC tie-lines under deregulated power environment are reported in [237,239,241,257,269–272]. AGC study with AC/DC tie-lines is performed in two-area non-reheat thermal system using optimal and PSO tuned fuzzy controllers by Sinha et al., in [237], optimal controller by Hasan et al., in [239], optimal controller in two-area reheat thermal system by Ibraheem et al., in [241], optimal sliding mode/H_∞ controller in two-area non-reheat thermal system by Kumar et al., in [257], conventional controller in two-area non/reheat thermal-mechanical governor based hydro system by Rao et al., [269–270] and artificial cooperative search algorithm (ACSA) tuned PI controller in two-area non/reheat thermal system by Selvaraju and Somaskandan in [271–272].

2.3.8 *Intelligent techniques in restructured power system*

In the recent years, intelligent methods, such as artificial neural networks (ANNs), fuzzy logic, various optimization algorithms and hybrid intelligent techniques have been applied to evade the problems, which were not solved, via conventional techniques. These methods are found very capable and reliable in synthesis and analysis of AGC schemes in power system. The intelligent techniques due to their inherent salient features have been gained a revered space for AGC schemes in restructured power systems since more than last two decades. Some of the important intelligent methods for AGC of restructured power systems are reviewed in the following subsections.

2.3.8.1 *Fuzzy logic based AGC schemes*

Due to simplicity, robustness and reliability, fuzzy logic control (FLC) is used in almost all fields of science and technology, including solving AGC problems in

restructured power systems. Contrasting the traditional control approaches, which are essentially based on the linearized mathematical models of the systems, the FLC technique tries to establish the controller directly based on the measurements, long-term knowledge and experiences of domain experts. Various types of possible FLC structures are available in the literature. These structures are derived by considering various numbers and types of inputs and outputs, fuzzy sets, membership functions (mfs), control rules, inference engine (fis) and defuzzification methods. Several studies exploiting polar/multi-stage/PI/PID/PIDF/type-2 structured un-optimized FLCs and FLCs with mfs and/or input/output scaling factors optimized via suitable optimization techniques in AGC regulator design under open market scenario are reported in the literature [273–296].

2.3.8.2 ANN based AGC schemes

Artificial neural networks (ANNs) promote great interest due to their potential to learn better approximation of any arbitrary nonlinear function and their aptitude for use in parallel processing and multivariable systems. Power systems are imagined to be highly nonlinear as a whole and it is very difficult to model them mathematically for the analysis purpose. The ANNs have solved this problem to a great extent. The neural technology offers many more benefits in the area of nonlinear control problems, particularly when the system is operating over the nonlinear operating range. The applications of neural networks in restructured power system for solving AGC problem are witnessed in [297–304].

A new approach based on artificial flexible neural networks (FNNs) is proposed to design controller for a large-scale three-area power system in a deregulated environment in [297]. The designed controllers have shown their capability to minimize the effect of disturbances and achieve acceptable frequency regulation in

the presence of load variations and tie-line disturbances. In [298], a decentralized radial basis function neural network (RBFNN) based controller for LFC in a three-area deregulated power system is presented. The design of ANN controller is based on the mixed H_2/H_∞ control techniques. The effectiveness of the designed scheme is tested favorably in minimizing the effects of area load disturbances and maintaining robust performance in the presence of plant parameter changes and system nonlinearities like generation rate constraint (GRC). An ANN based controller for multi-area AGC scheme in a restructured system is presented in [299]. A three layer feed forward neural network is suggested for controller design and trained with back propagation algorithm (BPA). The ACE signal and load variation in the system have been used as input to the ANN controller. The ANN controller has been developed for multi-area system having poolco, bilateral and mixed transactions. The functioning of the proposed controller has been demonstrated on a 75-bus Indian power system network and the result of the ANN controller is compared with GA tuned PID controller. A new adaptive controller based on unsupervised learning approach, named feedback error learning, is suggested for AGC of two-area power system in deregulated environment by Sabahi et al., [300]. The dynamic neural network is used for feed forward controller to get an improvement in overall system dynamic performance. In [301], an ANN controller is proposed for a 75-bus Indian power system consisting of 95-lines and 15 generators interconnected in four-areas with superconducting magnetic energy storage (SMES) units included in area-1 and area-3. A hybrid genetic-neural network approach is proposed in [302]. In [303], back propagation-through-time algorithm tuned ANN controller is presented for two-area thermal system. A mixed H_2/H_∞ control technique trained ANN controller is proposed

in [304] for two-area restructured power system having two DISCOs and two GENCOs in each area.

2.3.8.3 *ANFIS based AGC schemes*

The adaptive neuro-fuzzy inference system (ANFIS) is used as a supplementary controller which perform better compared to fuzzy and ANN controllers [113,305–310]. In [113], an ANFIS controller is designed for a two-area non-reheat thermal restructured power system that outperforms the controller designed in [12]. In [305–306], an ANFIS controller is implemented on a two-area hydrothermal restructured power system, which outperforms dual mode controller. In [307–309], an ANFIS controller is designed for a three-area hydrothermal gas multi-source restructured power system that outperforms various intelligent controllers. In [310], an ANFIS controller designed for a two-area hydrothermal restructured power system with SMES-thyristor controlled phase shifter (TCPS) combination outperforms conventional PI and FLC controllers.

2.3.8.4 *GA based AGC schemes*

The genetic algorithm (GA) is a searching algorithm that uses the mechanism of natural selection and natural genetics. GA operates without the knowledge of the task domain and utilizes only the fitness of evaluated individuals. From the random initial population, GA starts a loop of evolution processes consisting of selection, crossover and mutation in order to improve the average fitness function of the whole population.

The GA has been used to adjust parameters for different AGC controllers like I, PI, PID, sliding mode or variable structure controller etc. In the recent past, many studies exploiting GA dealing with different restructured power systems have appeared in the literature [266,274,284–287,289,294,302,311–324]. A GA tuned PI

controller shows improved results compared to a H_∞ controller in traditional and restructured power systems [266]. A GA based multi-stage fuzzy controller is implemented successfully in three-area restructured system [274]. GA based PI controller is presented in [284] for an interconnected two-area power system under deregulated environment and a GA based PID controller is presented in [285] for an interconnected three-area power system under deregulated environment. Bhateshvar et al., presents GA based I/PID and fuzzy controllers in [286–287,294]. Chathoth et al., presents GA based non-integer controller in a two-area restructured non-reheat thermal power system [289]. Some other controller like hybrid genetic-neural [302], GA based I/PI/PID [311–315,317–324] and GA based PSS [316] are also prevalent.

2.3.8.5   PSO based AGC schemes

Particle swarm optimization (PSO) technique is based on a model of social interaction between independent agents and uses social knowledge or swarm intelligence to get global maximum/minimum of a cost function. PSO uses social rules to search in the parameter space by controlling the trajectories of a set of autonomous particles. The position of each particle representing a particular solution of the problem is used to compute the value of the fitness function to be optimized. Each particle may change its position and consequently may explore the solution space simply varying its coupled velocity. The main PSO operator is the velocity update that takes the best position in terms of fitness value, reached by all the particles during their paths, and the best position that the agent itself has reached during its search resulting in a migration of the entire swarm towards the global optimum. At every iteration, the particle moves around according to its velocity and position. In restructured

environment, PSO has been applied for tuning AGC controllers as stated in [237,249–250,276,285,294–295,325–333].

Sinha et al., optimized fuzzy controller via PSO in two-area non-reheat thermal system [237]. Rakhshani and Sadeh proposed a PSO and adaptive weighted PSO (AWPSO) assisted intelligent output feedback controller obtained via optimization of the feedback gains of measurable system states in a two-area restructured non-reheat thermal power system [249–250]. The AWPSO output feedback controller outperforms conventional, PSO and ICA based linear quadratic regulators (LQRs). A PSO tuned multi-stage FLC work superiorly in comparison to GA tuned multi-stage FLC for a two-area restructured non-reheat thermal power system [276]. A PSO tuned PID controller work satisfactorily in a three-area restructured multi-source power system [285]. A PSO tuned two-stage FLC show enhanced results compared to PSO/GA tuned PID controller in a two-area restructured non-reheat thermal power system [294]. A PSO tuned FLC show better results compared to unturned FLC designed for a two-area restructured non-reheat thermal power system [295]. Taher et al., [325] applied hybrid PSO to optimize the gains of I/PI controllers for LFC in two-area power system. Rao et al., [326] addressed I controller tuning of TCPS based hydrothermal AGC system under open market scenario using PSO technique. Further, hybrid PSO tuned PID controllers work superbly over real/binary coded GA based PID for AGC of a four-area restructured reheat thermal power system as proposed by Bhatt et al. [327]. AGC I controller is tuned via craziness-based PSO (CPSO) in two-area hydrothermal system under open market scenario considering the impacts of static synchronous series compensator (SSSC) in series with tie-line and SMES at the terminal of area [328]. Further, CPSO based I controller is implemented in restructured two-area hydro system with SMES and TCPS located in series with tie-

line [329]. PSO based dual mode controller is proposed for two-area hydrothermal restructured power system with SSSC and TCPS [330]. In [331], hybrid chaotic PSO based I controller is proposed for AGC of two-area non-reheat thermal restructured power system. Further, a statistically tracked PSO is proposed for AGC of four-area reheat thermal restructured power system in [332]. Lakshmi et al., in [333] proposed a PSO tuned PI controller for restructured two-area non-reheat thermal power system. The responses of the PSO PI are compared with the responses of the conventional PI controller for poolco, bilateral and contract violation based transactions.

2.3.8.6 ACO based AGC schemes

The ant colony optimization (ACO) algorithm is a probabilistic technique for solving the problems, which may reduce the path length through graphs. Although real ants are blind, they are capable of finding the shortest path from food source to their nest by exploiting a liquid substance called pheromone, which they release on the transit route. ACO is a population-based general search method for the solution of complex continuous problems, which is inspired by the pheromone track laying behavior of real ant colonies. Rao et al., [334] demonstrated ant colony system algorithm for AGC of hydrothermal system under open market scenario. Gain setting of I controller is optimized via ACO technique following a step load power demand in either areas. The performance of the approach outperforms GA technique.

2.3.8.7 ABC based AGC schemes

The artificial bee colony (ABC) algorithm, one of the most recently introduced optimization algorithm, simulates the intelligent foraging behavior of a honey bee swarm. It incorporates a flexible and well-balanced mechanism to adapt the global and local exploration and exploitation abilities within a short computation time.

Hence, this method is efficient in handling large and complex search spaces. Due to its simplicity and simple implementation, ABC algorithm has captured much attention and has been applied to solve many practical optimization problems. Javidan and Ghasemi in [281] proposed an interactive ABC (IABC) optimization based fuzzy (IABCF) to tune optimal gains of a robust PID (RPID) controller for the solution of restructured two/four-area thermal power system. The method outperforms GA/PSO technique. Shayeghi et al., in [335] addressed market based LFC design using ABC tuned PID controller for solution of LFC problem in the restructured two-area non-reheat thermal power system. The simulation results obtained show enhanced performance of ABC tuned PID controller over GA/PSO tuned PID controller. An ABC tuned controller is proposed for AGC of a four-area power system incorporating SMES with possible contracted scenarios under large load power demand in comparison with conventional tuning of control parameters through ITAE performance indices by Taher et al., in [336]. The robust design of a power system stabilizer (PSS) to improve the stability of a restructured two-area non-reheat thermal system with automatic voltage regulator (AVR) using ABC tuned PID controller is proposed by Abedinia et al., in [337]. Moreover, the proposed control strategy has simple structure, easy to implement and tune, which can be useful for the real world restructured power system.

2.3.8.8 DE based AGC schemes

Differential evolution (DE) algorithm, a search heuristic algorithm, is a simple, efficient, reliable algorithm with simple coding. The major advantage of DE over GA is that GA uses crossover operator for evolution while DE relies on mutation act. Different types of controllers optimized via DE are available in the literature for restructured power systems [288,290–291,323,338–339]. DE algorithm based

structure preserving controller in three-area power system with boiler dynamics (BD), governor deadband (GDB), GRC and parametric uncertainties under deregulated environment is presented in [288]. A DE optimized fuzzy PID controller with derivative filter for LFC of two-area restructured multi-source hydrothermal gas power system is proposed by Sahu et al., in [290]. PID with filter (PIDF) controller is optimized via DE algorithm using ITAE criterion for restructured two-area four units thermal system without any physical constraints and restructured two-area six units hydrothermal system with physical constraints under the presence of redox flow batteries (RFB) and interline power flow controller (IPFC) by Gorripotu et al., in [291]. A DE optimized PID controller show better dynamic performance in a restructured two-area thermal gas multi-source system over GA tuned PID controller [323]. DE algorithm is utilized to tuned fractional order PID controller for AGC of restructured three-area hydrothermal gas power system with thyristor controlled phase angle regulator (TCPAR) in tie-lines [338]. Shaik et al., in [339] presents a DE based PID controller to solve AGC problem in nonlinear restructured two-area hydrothermal power system with doubly fed induction generator (DFIG) based wind turbine. DE based PID outperforms PSO based PID controller.

2.3.8.9 *BFOA based AGC schemes*

The bacterial foraging optimization algorithm (BFOA) is a fresh evolutionary technique in which the number of parameters used for searching the total solution space is much higher as compared to GA. The BFOA is inspired by the natural selection, which tends to get rid of the animals with poor foraging strategies and favor those having triumphant foraging strategies. This optimization technique has been successfully implemented to solve AGC problems under deregulated environment [340–344]. Saikia et al., designed and implemented a BFOA tuned FOPID controller

for nonlinear restructured two-area non-reheat thermal [340] and nonlinear restructured three-area reheat thermal [341] power system models successfully. Further, Thirunavukarasu et al., suggested BFOA tuned PI controller for restructured two-area reheat thermal-mechanical/electrical governor based hydro power system [342]. Chidambaram and Paramasivam proposed a BFOA tuned I controller for restructured two-area reheat thermal power system with RFB and IPFC [343]. Further, Thirunavukarasu et al., proposed a PI^2 controller tuned using BFOA for restructured two-area reheat thermal power system with RFB and unified power flow controller (UPFC) [344].

2.3.8.10 ICA based AGC schemes

The concept of imperialistic competitive algorithm (ICA) is derived from the notion of imperialistic competitions. The ICA is similar to other evolutionary algorithms in such a manner that it starts with an initial population denoted as countries. The ICA is applied to various multi-area restructured power systems as denoted in the literature [249,283,285,324,345]. An ICA optimized intelligent linear-quadratic optimal output feedback controller is proposed for restructured two-area non-reheat thermal power system [249]. Here, ICA method outperforms conventional method. Hosseini et al., in [283] proposed an ICA optimized PID controller for a new three-area steam hydro diesel restructured power system. Rouhani et al., in [285] proposed an ICA optimized fuzzy controller for a new three-area wind-steam, hydro-steam, and hydro-diesel restructured power system with PSS-AVR-TCPS. Here, ICA tuned fuzzy method outperforms GA/PSO/ICA tuned conventional PID method. Kumar et al., in [324] proposed an ICA optimized PID for restructured two-area system with non-reheat turbine and three-area system with reheat turbine and GRC. Here, ICA tuned PID controller show better results in comparison to the results offered by GA tuned PID

controller. An I controller is designed for LFC of SSSC and capacitive energy source (CES) incorporated two-area single-source hydrothermal system employing ICA [345].

2.3.8.11 HBMO based AGC schemes

Honey bee mating optimization (HBMO) algorithm is a recently developed nature inspired intelligence technique that has shown great potential for the solution of highly nonlinear tuning problems. It may be considered as a typical swarm based approach for optimization where the search algorithm is inspired by the process of real honey bees mating. In the current years, HBMO has been extensively used as specific research and optimization tools in numerous domains that has critical issues related to commerce, engineering, science and technology. Due to the simple and flexible nature of the HBMO, it has been used in restructured power system in order to solve AGC problem effectively [346–349]. A HBMO based fuzzy controller is proposed for solution of AGC problem in a restructured two-area non-reheat thermal power system with GRC [346–347]. The effectiveness of the proposed method is demonstrated over PSO/GA tuned fuzzy controller. A strength pareto HBMO (SPHBMO) based multi-stage fuzzy (MSF) PID controller is proposed for AGC of a restructured three-area non-reheat thermal power system with GRC [348]. The superiority of proposed SPHBMO based MSF PID controller is demonstrated over PSOMSF PID and conventional fuzzy PID controllers. In [349], a HBMO based fuzzy controller is proposed for AGC of restructured two-area non-reheat thermal power system with PSS and AVR. The advantage of method is demonstrated over PSO/GA fuzzy controller.

2.3.8.12 FA based AGC schemes

The firefly algorithm (FA) is a nature-inspired metaheuristic optimization technique, which is based on the flashing activities of fireflies in the summer sky in the tropical temperature regions. Its major benefit is the fact that it employs mainly real random numbers and is based on the global communication among the swarming particles i.e., fireflies and consequently, it appears further effective in multi objective optimization. The use of FA in AGC under deregulated environment is available in the literature [293,350–351]. Gorripotu et al., in reference [293] proposed a FA optimized fuzzy PID controller with derivative filter for AGC of restructured four-area reheat thermal power system with GRC and GDB. The FA tuned I controller work effectively in comparison to GA tuned I controller. Also, FA tuned fuzzy PID controller with derivative filter and triangular mfs outperforms FA tuned fuzzy PID controller with derivative filter and trapezoidal mfs, FA tuned PID controller with derivative filter and FA tuned PI controller. Abedinia et al., in reference [350] proposed a FA optimized fuzzy PID controller for AGC of a restructured power system and it shows better results in comparison to classical fuzzy PID and PID controllers. Gorripotu et al., in reference [351] proposed a FA optimized PID controller with derivative filter for AGC of restructured four-area reheat thermal power system with GRC and GDB. The FA tuned PID controller with derivative filter outperforms FA tuned I/PI controller.

2.3.8.13 FPA based AGC schemes

Flower pollination algorithm (FPA) is one of the lately proposed nature inspired algorithm that replicates the behavior of flower pollination in the nature. Some papers on AGC of restructured power system with FPA based controllers have appeared in

the literature [352–353]. In reference [352] authors have proposed a FPA optimized PI controller for AGC of restructured two-area non-reheat thermal-hydro power system with RFB. The FPA tuned PI controller show enhanced performance compared to conventional PI controller. In [353], authors have proposed a FPA optimized fractional order integral-derivative with filter ($I^{\lambda}D^{\mu}F$) controller for AGC of restructured three-area reheat thermal-hydro-gas power system with electric vehicles and incorporating the effects of GRC/GDB/TD. The FPA tuned $I^{\lambda}D^{\mu}F$ controller show enhanced performance over PID with filter (PIDF) controller.

2.3.8.14 HSA based AGC schemes

Harmony search algorithm (HSA) is a new derivative free, real parameter, optimization algorithm inspired from the musical improvisation process of searching for a perfect state of harmony. In comparison to other meta-heuristic algorithms reported in the literature, HSA imposes a fewer mathematical calculations, identifies the high performance region of the solution space and may be implemented in many aspects of optimization problem. In AGC field, HSA and its improved forms are available [354–359]. In [354], authors have proposed a HSA optimized fuzzy PID controller for AGC of restructured two-area non-reheat thermal system. However, a multi-objective HAS (MOHSA) tuned multi-stage FLC is presented for AGC in a three-area non-reheat thermal system in [355]. Shankar et al., proposed an opposition based HS (OHS) algorithm to tune I controller in AGC of two-area hydrothermal gas multi-source system with RFB/GRC [356]. Shiva et al., proposed an improved version of HAS termed as quasi-oppositional HSA (QOHSA) [357–359]. QOHSA optimized Sugeno fuzzy-logic (QOHSA-SFL) controller is proposed in [357] for four-area reheat thermal restructured system. QOHSA-SFL controller shows superior performance in comparison to GA-SFL in a three-area reheat thermal-hydro

restructured system [358]. Further, a QOHSA tuned PID controller is suggested for a five-area reheat thermal-hydro-gas restructured system with GRC/GDB/TD [359].

2.3.8.15 *Some other techniques based AGC schemes*

Some other optimization algorithms are applied recently in AGC of restructured power systems; however, to tune various controllers, their presence in the literature is observed scanty [360–369]. In [360], authors have proposed a fruit fly optimization algorithm (FFOA) optimized I/PI/PID/IDD/PIDD controller for AGC of restructured two-area reheat thermal-hydro-nuclear power system. Rahman et al., proposed a biogeography-based optimization (BBO) technique tuned three-degree-of-freedom integral-derivative (3DOF-ID) controller for a restructured two-area reheat thermal-hydro power system [361]. Selvaraju et al., proposed an artificial cooperative search (ACS) technique in power system [271–272,362]. An ACS tuned PI controller for a restructured two-area non/reheat thermal power system with SMES/RFB is proposed in [362]. Kumar et al., proposed a big bang big crunch (BBBC) algorithm tuned PID (BBBC-PID) controller for a restructured two-area and four-area power systems [363]. The BBBC-PID outperforms HSA-PID and ICA-PID controllers. A new strength pareto gravitational search algorithm (SPGSA) based PID controller is suggested for a restructured three-area restructured power system with GRC [364]. A disrupted oppositional-based gravitational search algorithm (DOGSA) tuned sliding mode controller (SMC) is proposed for the AGC problem solution of interconnected two-area thermal gas multi-source power system under deregulated environment [365]. The superior performance of DOGSA method is shown via comparison with basic GSA and GA/DE techniques detailed in the literature. Farook and Raju [366] proposed a hybrid GA-FA algorithm to optimize gains of a PID controller for AGC study of a multi-source two-area power system. A modified group search optimization

(MGSO) algorithm is proposed in AGC of two-area hydrothermal gas multi-source restructured power system with GRC/GDB and gate controlled series capacitor (GCSC) to tune tilt integral-derivative (TID)-based damping controller [367]. A hybrid DE-PS (hDE-PS) algorithm is proposed to tune a modified integral derivative (MID) controller for AGC of a two-area multi-source restructured power system in [368]. A new minority charge carrier inspired algorithm is proposed for AGC of a two-area multi-source hydrothermal restructured power system in [369].

2.3.9 Multi-area restructured power system

The most of the studies under deregulated environment have been performed by the researchers on two-area power system. The literature survey indicates that some of the studies have also been conducted on three-area restructured power systems [273–274,283,285,288,307–309,313,338,348,353,355,358,364,370,374–375,388–389,391]. However, very little work has been reported so far for the interconnected four-area restructured power systems [281,293,324,351,357,363,370,383,387,396]. Only two research papers related to AGC study of five-area restructured power systems have been observed in the recent literature [321,359].

2.3.10 Multi-source restructured power system

The most of the studies specifically in restructured power systems have been performed by the researchers so far only on single-source thermal or hydro power systems. Each area of single-source system incorporates only thermal or hydro generating units. But in practical power generation environment, each control area of multi-area interconnected power system owns thermal, hydro, gas, nuclear, diesel, wind etc. sources for power generation. The AGC study of traditionally interconnected multi-source power systems is available in the literature [30–31,38,

100,103–104,126,132,143,150–152,155–157]. However, in this section, a collection of papers only on restructured multi-area multi-source AGC systems has been discussed [245,290–291,323,356,360,365–369,371]. A two-area system with hydro-thermal-gas diverse sources in each area is simulated in [245]. The same system with TD and GRC is simulated in [290]. A two-area system with two thermal power generating units and one hydro power generating unit in each area of the system is studied in [291]. A two-area system with one thermal unit with GRC and one gas unit in each area of the system is studied in [323,365]. A two-area system with hydro-thermal-gas diverse sources is again examined considering GRC only in thermal units in [356]. In [360] authors have proposed a restructured two-area reheat thermal-hydro-nuclear multi-source power system. A two-area system with hydrothermal power generating units in area first and thermal gas power generating units in second area of the system is studied in [366]. A two-area system having hydro with GRC, thermal with GRC-GDB and gas power generating units in each area of the system is investigated in [367,371]. A two-area multi-source restructured power system having thermal plant with GRC/BD/GDB, hydro plant with GRC and wind plant in area-1 and thermal plant with GRC/BD/GDB, hydro plant with GRC and diesel incorporating RFB and UPFC is studied in [368]. A two-area system with electrical/mechanical governor based hydro with GRC and reheat thermal with GRC multi-source generations in each area is simulated in [369].

2.3.11 AGC with energy storage and FACTS devices

The researchers over the worldwide have proposed various control strategies, as discussed in the previous sections, for various types of restructured power system to control the governor action so that the system frequency and tie-lie power deviations are kept minimal and GENCOs may generate the required electrical power in the most

effective manner. The effectiveness of these novel control strategies can further be enhanced in the presence of energy storage and flexible AC transmission systems (FACTS) devices.

Energy storage units such as battery energy storage (BES), CES, RFB and SMES can successfully damp oscillations in a power system because they offer storage capacity in addition to the kinetic energy of the generator rotor, which can share the sudden alterations in the power requirement. An attempt to use BES to improve the AGC dynamics under deregulated power system has appeared in the literature [372]. The incorporation of CES [345,370,374], RFB [272,291,343–344,352,356, 362,368] and SMES [265,310,328–329,336,362,374] in AGC of restructured system is available in the literature.

FACTS devices also play a crucial role to controlling the power flow in an interconnected restructured power system [178–179]. Different FACTS devices are TCPS, SSSC, IPFC, thyristor controlled series compensator (TCSC), UPFC, GCSC etc. Numerous studies have explored the prospective of FACTS devices for enhanced power system control since they provide more flexibility. The concepts of TCPS [269,272,278–279,310,314,326,329–330,367], SSSC [328,330,345, 367,373], IPFC [291,343], TCSC [322,367], UPFC [344,368] and GCSC [367] are augmented with AGC under deregulated environment to get improved system dynamic performance.

2.3.12 Some other AGC schemes

Some other useful contributions in restructured power systems are also available in the literature [375–399].

2.4 Conclusion

A comprehensive and critical review of the published literature in the area of AGC of traditional and restructured power systems has been presented in this chapter. Though, the chief thrust is laid on the review of the literature on AGC schemes in restructured power systems. The literature on recent developments like AGC schemes based on the concepts of intelligent strategies including fuzzy logic, neural networks, mixed fuzzy-neural and various soft computing techniques like GA, PSO, BFOA, ABC, FA, DE etc., have been reviewed significantly. Various AGC strategies, types of multi-area single/multi-source systems with and without energy storage units, FACTS devices and AC/DC tie-lines have also been reviewed and discussed efficiently.

CHAPTER 3

DEVELOPMENT OF MATHEMATICAL MODELS FOR AGC OF POWER SYSTEMS

3.1 Introduction

The fossil fuels such as coal, oil, natural gas and nuclear energy and water are commonly utilized energy sources in the power generating plants. As a consequence, in the current scenario, the control areas are supposed to have various types of generating sources. In this chapter, mathematical models of two-area interconnected power systems are developed consisting of power plants having single-source thermal, multi-source hydrothermal and thermal gas sources in a control area. The two-areas are interconnected in traditional as well as restructured configurations. The dynamic models of the systems in state variable form are developed for each component of the system.

3.2 Mathematical modeling of power system

In a power system, the synchronous generators are normally driven by prime mover getting energy from sources like hydro, thermal, gas etc. Each turbine is equipped with a speed governing system to provide a means by which the turbine can be started, run up to the operating speed and operate on load with the required power output. The load damping constant (D_i), power system gain constant (K_{PSi}), power system time constant (T_{PSi}) and area frequency response characteristic (β_i) are defined in Eqns. (3.1-3.8) [2]:

$$D_i = \frac{\partial P_{Li}}{\partial F_i} \frac{1}{P_{ri}} \ \text{puMW/Hz} \tag{3.1}$$

$$K_{PSi} = \frac{1}{D_i} \quad \text{Hz/puMW} \tag{3.2}$$

$$T_{PSi} = \frac{2H_i}{F_i D_i} \quad s \tag{3.3}$$

$$\beta_i = D_i + \frac{1}{R_i} \quad \text{puMW/Hz} \tag{3.4}$$

Similarly, these parameters for j^{th} area can be given as:

$$D_j = \frac{\partial P_{Lj}}{\partial F_j} \frac{1}{P_{rj}} \quad \text{puMW/Hz} \tag{3.5}$$

$$K_{Pj} = \frac{1}{D_j} \quad \text{Hz/puMW} \tag{3.6}$$

$$T_{Pj} = \frac{2H_j}{F_r D_j} \quad s \tag{3.7}$$

$$\beta_j = D_j + \frac{1}{R_j} \quad \text{puMW/Hz} \tag{3.8}$$

where, P_r is the total area capacity in MW, ∂P_L is the nominal operating load in MW, R is the speed regulation parameter in Hz/puMW and H is the inertia constant in second.

3.2.1 Modeling of thermal power plant

In coal-based plants, the energy contained in the fuel is used to generate high pressure and high temperature steam in the boiler. The steam energy is then transformed into mechanical energy in axial flow steam turbines. Each turbine consists of a number of stationary and rotating blades concentrated into groups or stages. As the high-pressure steam enters the fixed set of stationary blades, it is accelerated and acquires increased kinetic energy as it expands to a lower pressure. The stream is then guided onto the rotating blades where it experiences a change in momentum and direction, thereby exerting a tangential force on the turbine blade and output torque on the turbine shaft.

As the steam passes axially along the turbine shaft its pressure reduces, so its volume increases and the length of the blades must increase from the steam entrance to the exhaust to accommodate this change. Typically a complete steam turbine will be divided into three or more stages, with each turbine stage being connected in tandem on a common shaft. Dividing the turbine into stages so that the steam is to be reheated between stages to increase its enthalpy and consequently increase the overall efficiency of the steam cycle.

Steam turbines can be classified as non-reheat, single-reheat or double-reheat turbines. Non-reheat turbines have one turbine stage and are usually built for use in units below 100 MW. The most common configuration used for large steam turbines is the single tandem-reheat arrangement. The steam flow in the turbine is controlled by the governing system. The speed signal to the governor is provided by the speed measuring device. The main amplifier of the governing system and the valve mover is an oil servomotor controlled by the pilot valve. When the generator is synchronized, the emergency stop valves are only used to stop the generator under emergency conditions, although they are often used to control the initial start-up of the turbine.

Fig. 3.1 shows a schematic diagram of tandem-compound single reheat steam turbine system and Fig. 3.2 shows its approximate linear transfer function model (TFM) [49,55,70]. The time constants T_t, T_r and T_c are respectively the delays due to steam chest and inlet piping, reheaters and crossover piping. The fractions F_{HP}, F_{IP} and F_{LP} represent parts of the total turbine power of high, intermediate and low-pressure cylinders of the turbine. It should be noted that $F_{HP} + F_{IP} + F_{LP} = 1$. The T_c may be neglected due to its small value compared with other time constants. The reduced order transfer function is given in Fig. 3.3. The portion of total power generated in the intermediate and low-pressure cylinders $= F_{IP} + F_{LP} = 1 - F_{HP}$. From Fig. 3.3:
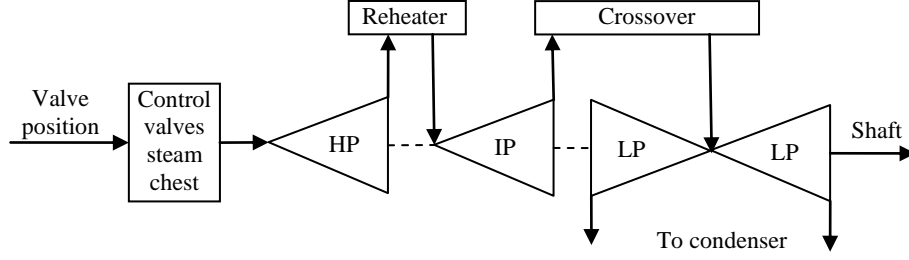
Fig. 3.1 Configuration diagram of single reheat tandem compound steam system.
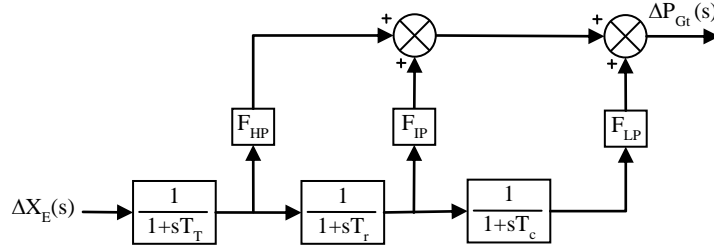
Fig. 3.2 Approximate linear TFM for reheat thermal turbine.
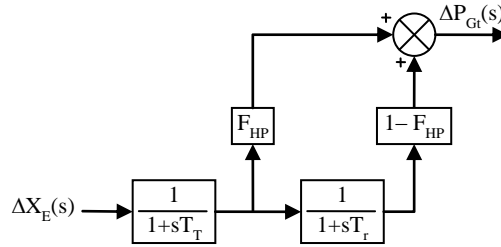
Fig. 3.3 Reduced order model of Fig. 3.2.

$$\Delta P_{Gt}(s) = \frac{1}{1+sT_T}\left[F_{HP} + \frac{1-F_{HP}}{1+sT_r}\right]\Delta X_E(s) \qquad (3.9)$$

or

$$\Delta P_{Gt}(s) = \frac{1+sK_rT_r}{(1+sT_T)(1+sT_r)}\Delta X_E(s). \qquad (3.10)$$

Where, K_r is the reheat coefficient which is the fraction of the power generated in the high-pressure cylinder (= F_{HP}). The deviation in output power of single reheat steam turbine in response of change in governor setting is represented Eqn. (3.10). The out
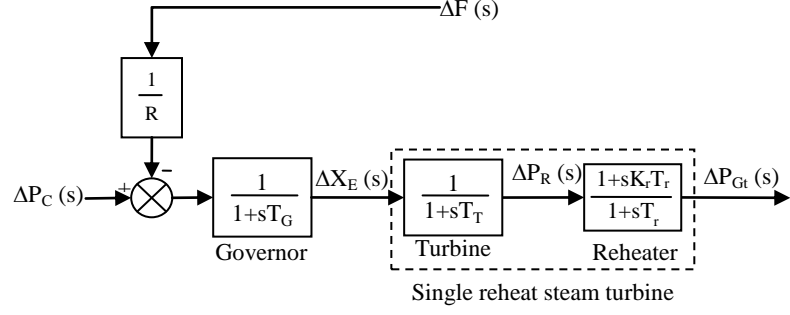
Fig. 3.4 TFM of reheated steam turbine with speed governing system.

put of speed governor will be given by Eqn. (3.11).

$$\Delta X_E (s) = \left(\frac{1}{1+sT_G} \right) \left(\Delta P_C(s) - \frac{\Delta F(s)}{R} \right) \tag{3.11}$$

The block diagram representation of reheated steam turbine with its speed governing system is shown in Fig. 3.4.

3.2.2 *Modeling of hydro power plant*

Hydraulic turbines use the force exerted by water as it falls from an upper reservoir to a lower reservoir. The vertical distance between the upper reservoir and the level of the turbine is called the head. The size of the head is used to categorize hydroelectric power plants like high head, medium head and low head (run-of-river) plants, though there is no harsh demarcation line. Low and medium head hydro plants are built employing reaction turbines such as a Francis turbine. Because of the relatively low-pressure head, reaction turbines normally use large volume of water, need large water passages and function at low speeds. Because of the low revolving speed, the generators have a large diameter.

Development of the transfer function models for hydro turbine penstock and hydro governors is detailed in [56]. The hydro turbine and penstock model is given by Eqn. (3.12):

51

$$\frac{\Delta P_{Gh}(s)}{\Delta X_E(s)} = \frac{a_{23}\left[1+\left(a_{11}-\dfrac{a_{13}a_{21}}{a_{23}}\right)\right]sT_W}{1+a_{11}sT_W} \tag{3.12}$$

where a_{11} and a_{13} are partial derivatives of flow regarding head and gate opening while a_{21} and a_{23} are partial derivatives of torque relating to head and gate opening. However, the impact of speed deviation on the torque is ignored as turbine speed changes are small, particularly when operating in conjunction with a system. T_W is water starting time in seconds. For an ideal lossless hydro turbine, $a_{11} = 0.5Z_o$, $a_{21} = 1.5Z_o$, $a_{13} = a_{23} = 1$ [56]. Z_o stand for the initial gate opening in pu. Hence, Eqn. (3.12) turns to Eqn. (3.13).

$$\frac{\Delta P_{Gh}(s)}{\Delta X_E(s)} = \frac{1 - sZ_0T_W}{1 + 0.5sZ_0T_W} \tag{3.13}$$
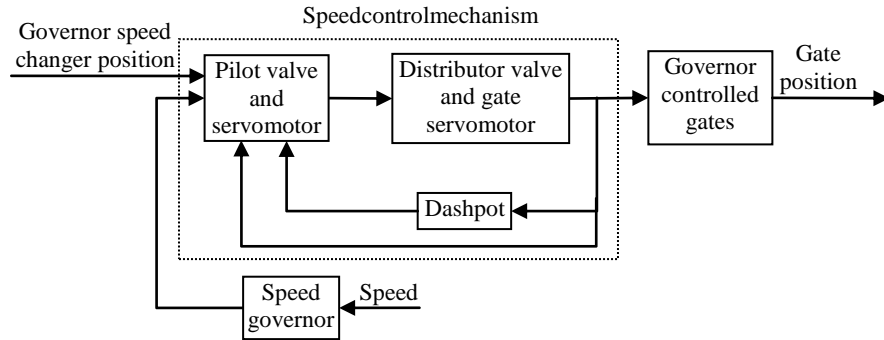
Fig. 3.5 Configuration diagram of mechanical hydraulic speed governing system.
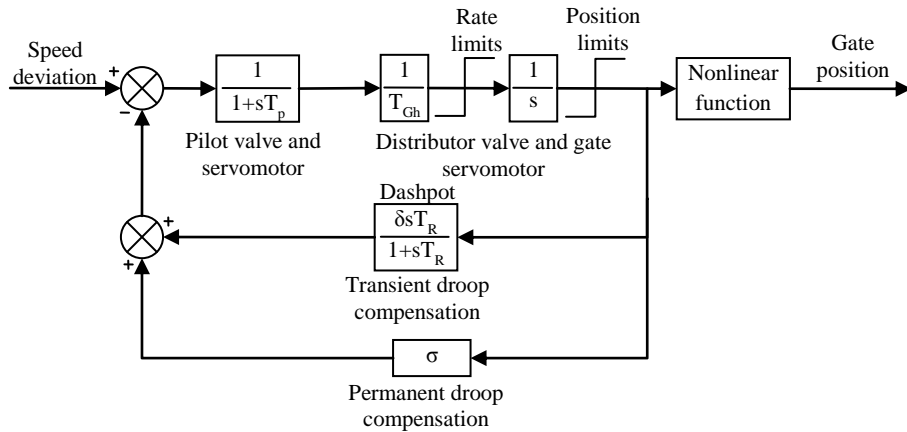
Fig. 3.6 Approximate nonlinear model of mechanical hydraulic governing system.

At full load, $Z_o = 1$. Hence, Eqn. (3.13) turns to Eqn. (3.14).

$$\frac{\Delta P_{Gh}(s)}{\Delta X_E(s)} = \frac{1 - sT_W}{1 + 0.5sT_W} \tag{3.14}$$

The configuration diagram for a mechanical hydraulic speed governing system for a hydro turbine is given in Fig. 3.5. The speed governing necessities for hydro turbines are sturdily influenced by the impacts of water inertia. The dashpot feedback in Fig. 3.5 is requisite to attain stable performance. The block diagram of Fig. 3.6 is an approximate nonlinear model for such a hydro speed governing scheme. The gate servomotor may be rate limited for large speedy speed departures [56], though, the transient droop feedback decreases the probability of rate limiting in AGC. The position limits exist matching to the boundaries of the gate opening. Ignoring nonlinearities like rate/position limits and the small time constant of the pilot valve, the transfer function of the hydrogovernor may be given by Eqn. (3.15):

$$\frac{\Delta X_E(s)}{\Delta F(s)} = \frac{\frac{1}{R}\left(1 + sT_R\right)}{\frac{T_R T_G}{\sigma}s^2 + \frac{T_G + T_R\left(\sigma + \delta\right)}{\sigma}s + 1} \tag{3.15}$$

where, ΔF is frequency deviation in Hz, σ is permanent droop in pu ($R = F\sigma$), δ is temporary droop in pu, T_R is dashpot time constant in seconds and T_{Gh} is governor response time in seconds. The hydro governor transfer function may be approximated by the easy transfer function as:

$$\frac{\Delta X_E(s)}{\Delta F(s)} = \frac{\frac{1}{R}\left(1 + sT_R\right)}{\left(1 + sT_{RH}\right)\left(1 + sT_{GH}\right)} \tag{3.16}$$

where, $T_{RH} = \dfrac{T_G + T_R\left(\sigma + \delta\right)}{\sigma}$ and $T_{GH} = \dfrac{T_R T_G\left(\sigma + \delta\right)}{T_G + T_R\left(\sigma + \delta\right)}$.
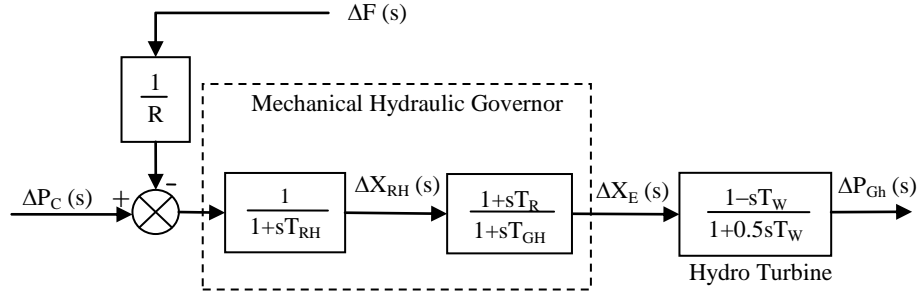
Fig. 3.7 Transfer function model of hydro turbine with speed governing system.

The Eqn. (3.16) is obtained by avoiding $T_R T_G \sigma$ with respect to $[T_G + T_R (\sigma + \delta)]^2$, as $T_R T_G \sigma \ll [T_G + T_R(\sigma + \delta)]^2$.

Considering the speed changer position (ΔP_C), Eqns. (3.14) and (3.16) can be written as Eqn. (3.17) and represented by Fig. 3.7.

$$\Delta X_{Eh} \ (s) = \left(\frac{1}{1+sT_{RH}}\right)\left(\frac{1+sT_R}{1+sT_{GH}}\right)\left(\frac{1-sT_W}{1+0.5sT_W}\right)\left(\Delta P_C \ (s) - \frac{\Delta F \ (s)}{R}\right). \tag{3.17}$$

3.2.3 Modeling of gas power plant

Disparate steam turbines, gas turbines do not need an intermediate working fluid and in its place the fuel thermal energy is converted into mechanical energy employing the hot turbine exhaust gases. Air is normally used as the working fluid with the fuel being natural gas or heavy/medium fuel oil. The most popular system for gas turbines is the open regenerative cycle and comprises of a compressor, combustion chamber and turbine. The fuel is supplied through the governor valve to the combustion chamber to be burnt in the presence of air supplied by the compressor. The hot, compressed air, mixed with the burning products, is then directed into the turbine where it expands and transfers its energy to the moving blades in much the same way as in the steam turbine. The exhaust gases are then used to heat the air delivered by the compressor. There are also other, more complicated cycles that use either
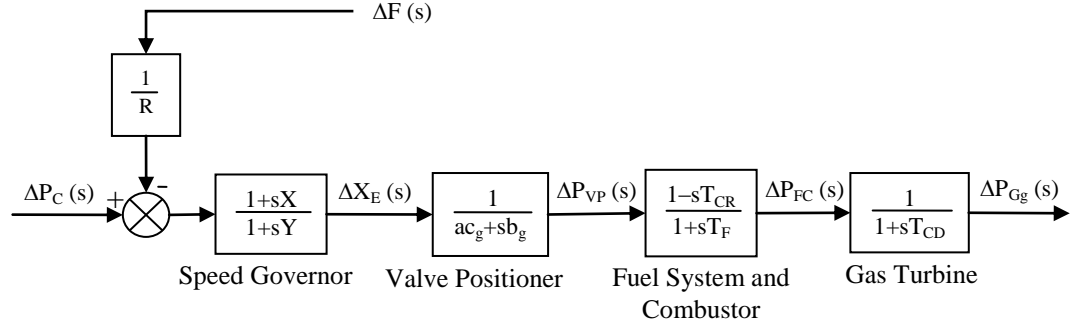
Fig. 3.8 Transfer function model of gas turbine with speed governing system.

compressor inter-cooling and reheating, or inter-cooling with regeneration and reheating. For small load perturbation, the change in setting of gas turbine governor (ΔX_g), valve positioner (ΔP_{VP}), fuel and combustor system (ΔP_{FC}) and gas turbine power output (ΔP_{Gg}) are given by subsequent mathematical relations [30].

$$\Delta X_E\ (s) = \left(\frac{1+sX}{1+sY}\right)\left(\Delta P_C\ (s) - \frac{\Delta F\ (s)}{R}\right)$$

(3.18)

$$\Delta P_{VP}\ (s) = \left(\frac{a}{c_g + sb_g}\right)\Delta X_E\ (s) \tag{3.19}$$

$$\Delta P_{FC}\ (s) = \left(\frac{1-sT_{CR}}{1+sT_F}\right)\Delta P_{VP}\ (s) \tag{3.20}$$

$$\Delta P_{Gg}\ (s) = \left(\frac{1}{1+sT_{CDi}}\right)\Delta P_{FC}\ (s) \tag{3.21}$$

The overall transfer function model for gas turbines can be given by uniting Eqns. (3.18-3.21). Fig. 3.8 shows block diagram of gas turbine with speed governing system.

3.2.4 Modeling of tie-line

When two control areas of a power system are interconnected via AC tie-line, the synchronizing coefficient (T_{12}) is given by [30].

55
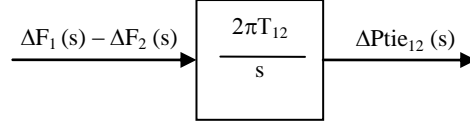
Fig. 3.9 Transfer function model of AC tie-line.
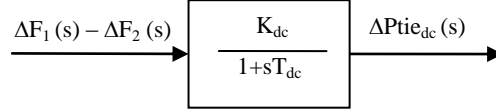
Fig. 3.10 Transfer function model of DC tie-line.

$$T_{12} = P_{12max} \cos(\delta_1 - \delta_2) \tag{3.22}$$

For small load perturbation, the deviation in tie-line power flow ($\Delta Ptie_{12}$) is given by Fig. 3.9.

$$\Delta Ptie_{12} \ (s) = \frac{2\pi T_{12}}{s} \left(\Delta F_1 \ (s) - \Delta F_2 \ (s) \right) \tag{3.23}$$

The above equation can be represented by the block diagram shown in Fig. 3.9. If two control areas of a power system are interconnected by a DC link, the transfer function model of incremental power flow on DC tie-line is given by (3.24) [27–31].

$$\Delta Ptie_{dc} \ (s) = \frac{K_{dc}}{1+sT_{dc}} \left(\Delta F_1 \ (s) - \Delta F_2 \ (s) \right) \tag{3.24}$$

The Eqn. (3.24) is subjected to the condition that the DC tie-line is operating in the constant current mode. The above equation can be represented by block diagram shown in Fig. 310.

The ratio of area power rating (α_{12}) can be defined as [32].

$$\alpha_{12} = -\frac{P_{r1}}{P_{r2}} \tag{3.25}$$

3.3 Power system models under investigation

The Eqns. (3.1-3.25) are used to develop generalized models of the power systems under study. Different traditional and restructured power system models are extensively studied in this study. A traditional, two-area power system having one non
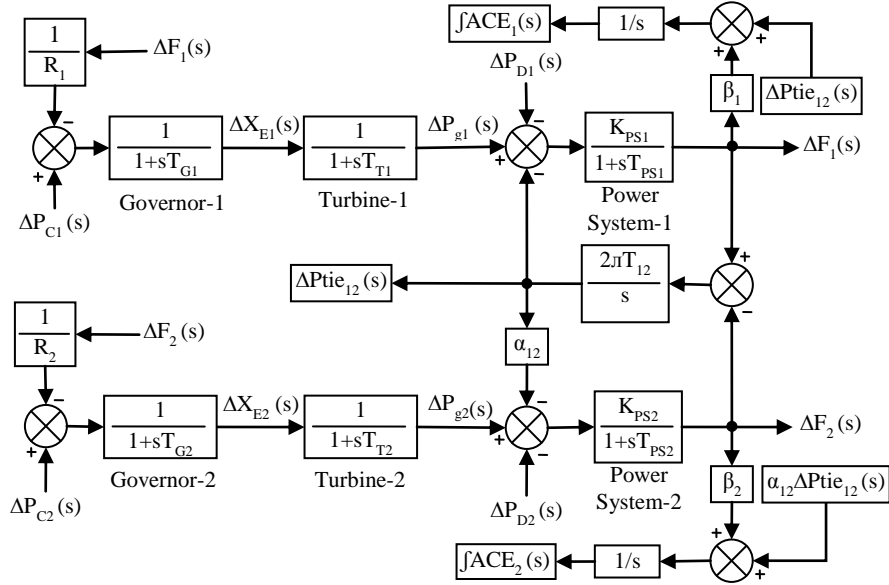
Fig. 3.11 Transfer function model of two-area non-reheat thermal power system.
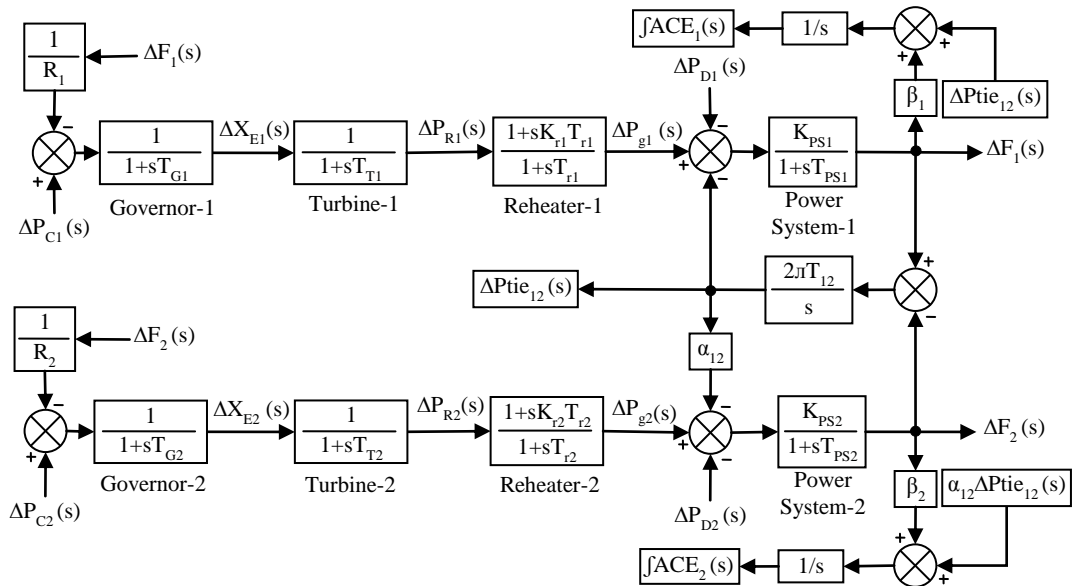
Fig. 3.12 Transfer function model of two-area reheat thermal power system.
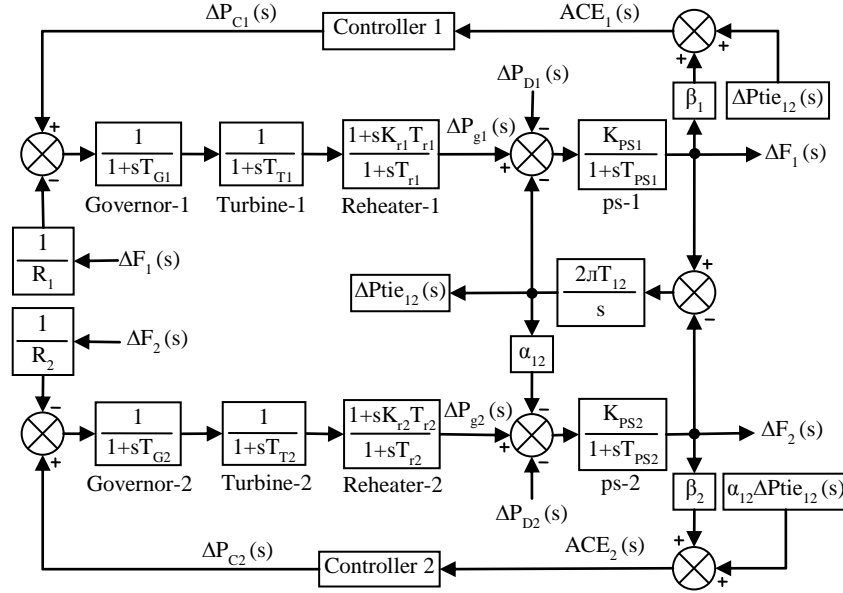
Fig. 3.13 Two-area reheat thermal power system model with a controller in each area.

-reheat thermal unit in each area is shown in Fig. 3.11. However, a traditional two-area power system with one single reheat thermal unit in each area is shown in Figs. 3.12 and 3.13. Figs. 3.11 and 3.12 do not show controllers while position of controllers is shown in Figs. 3.13. A traditional two-area multi-source hydrothermal power system is shown in Fig. 3.14. Each area of this system incorporates two sources first non-reheat thermal plant and second mechanical governor based hydro power plant. The area control error (ACE) is defined as:

$$ACE_1(s) = \beta_1 \Delta F_1(s) + \Delta Ptie_{12}(s), \tag{3.26}$$

$$ACE_2(s) = \beta_2 \Delta F_2(s) + \alpha_{12} \Delta Ptie_{12}(s). \tag{3.27}$$

The system shown in Fig. 3.14 is interconnected in restructured fashion under deregulated environment in Fig. 3.15. The formula for scheduled tie-line power i.e., $\Delta Ptie_{scheduled}$, GENCO power output i.e., ΔP_G and power demand in the area i.e., ΔP_D signals shown in Figs. 3.15 and 16 are stated as follows.

$$\Delta Ptie_{scheduled}(s) = (cpf_{13} + cpf_{23})\Delta P_{L3} + (cpf_{14} + cpf_{24})\Delta P_{L4}$$

$$- (cpf_{31} + cpf_{41})\Delta P_{L1} - (cpf_{32} + cpf_{42})\Delta P_{L2}, \tag{3.28}$$

$$\Delta P_{Gi}(s) = cpf_{i1}\,\Delta P_{L1} + cpf_{i2}\,\Delta P_{L2} + cpf_{i3}\,\Delta P_{L3} + cpf_{i4}\,\Delta P_{L4},\ i = 1,\ldots,4 \text{ and} \qquad (3.29)$$

$$\Delta P_{D1}(s) = \Delta P_{L1} + \Delta P_{L2} + P_{UC1} \text{ and } \Delta P_{D2} = \Delta P_{L3} + \Delta P_{L4} + P_{UC2}. \qquad (3.30)$$

Fig. 3.14 Transfer function model of traditional two-area multi-source hydrothermal power system.

Fig. 3.15 Model of restructured two-area multi-source hydrothermal power system.
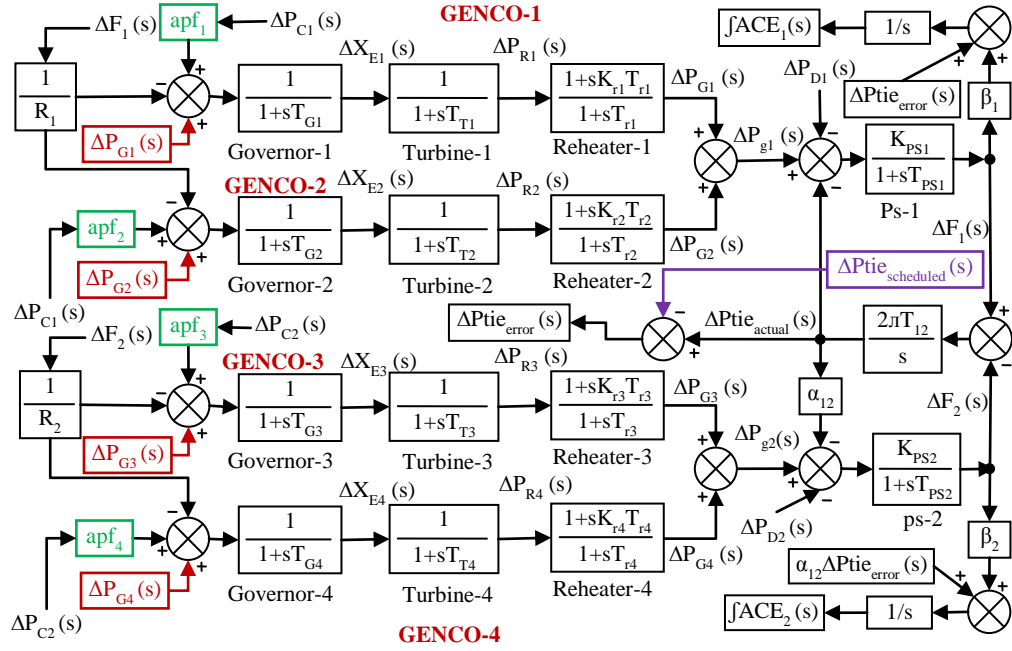
Fig. 3.16 Transfer function model of restructured thermal power system.

The ΔP_{Li} and P_{UCi} are demand of DISCO-i and uncontracted demand in area-i, respectively. In restructured power system, the tie-line power error is defined as:

$$\Delta Ptie_{error}(s) = \Delta Ptie_{actual}(s) - \Delta Ptie_{scheduled}(s). \tag{3.31}$$

$\Delta Ptie_{actual}$ in restructured power system is equivalent to $\Delta Ptie_{12}$ in traditional two-area power system. ACE stated in Eqns. (3.26-3.27) for traditional system will be modified in restructured power system as:

$$ACE_1(s) = \beta_1 \Delta F_1(s) + \Delta Ptie_{error}(s), \tag{3.32}$$

$$ACE_2(s) = \beta_2 \Delta F_2(s) + \alpha_{12} \Delta Ptie_{error}(s). \tag{3.33}$$

A restructured two-area single-source thermal power system shown in Fig. 3.16 is also examined in the current study. Each area of the system is equipped with two single reheat thermal units.

The transfer function models of reheater of thermal plant, hydraulic mechanical governor, hydro turbine, gas governor and fuel system and combustor of gas plant are modeled in the split form as shown in Fig. 3.17. The modeling of the components has
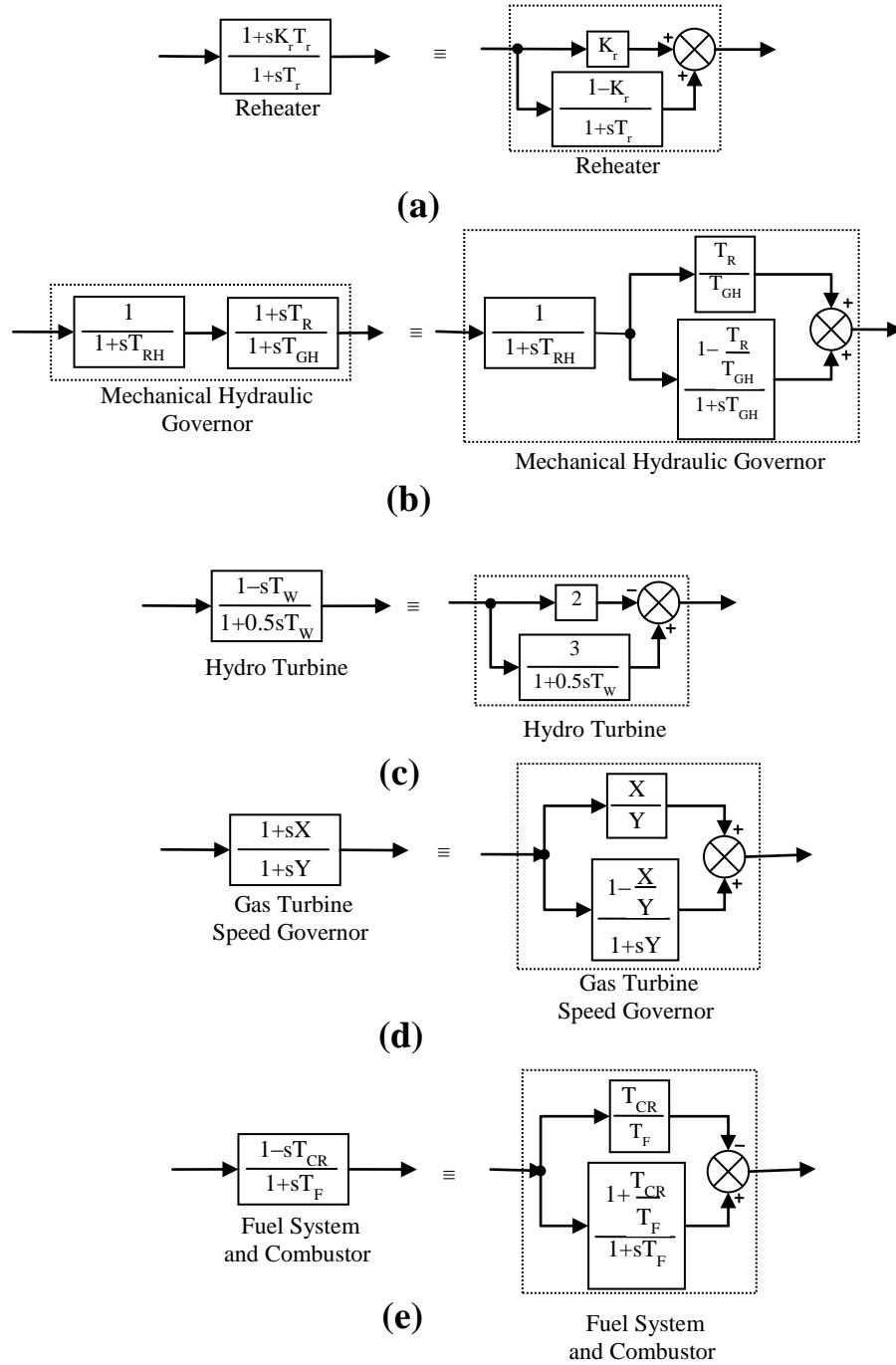
Fig. 3.17 Transfer function models in split form (a) reheater, (b) mechanical hydraulic governor, (c) hydro turbine, (d) gas turbine speed governor and (e) fuel system and combustor.
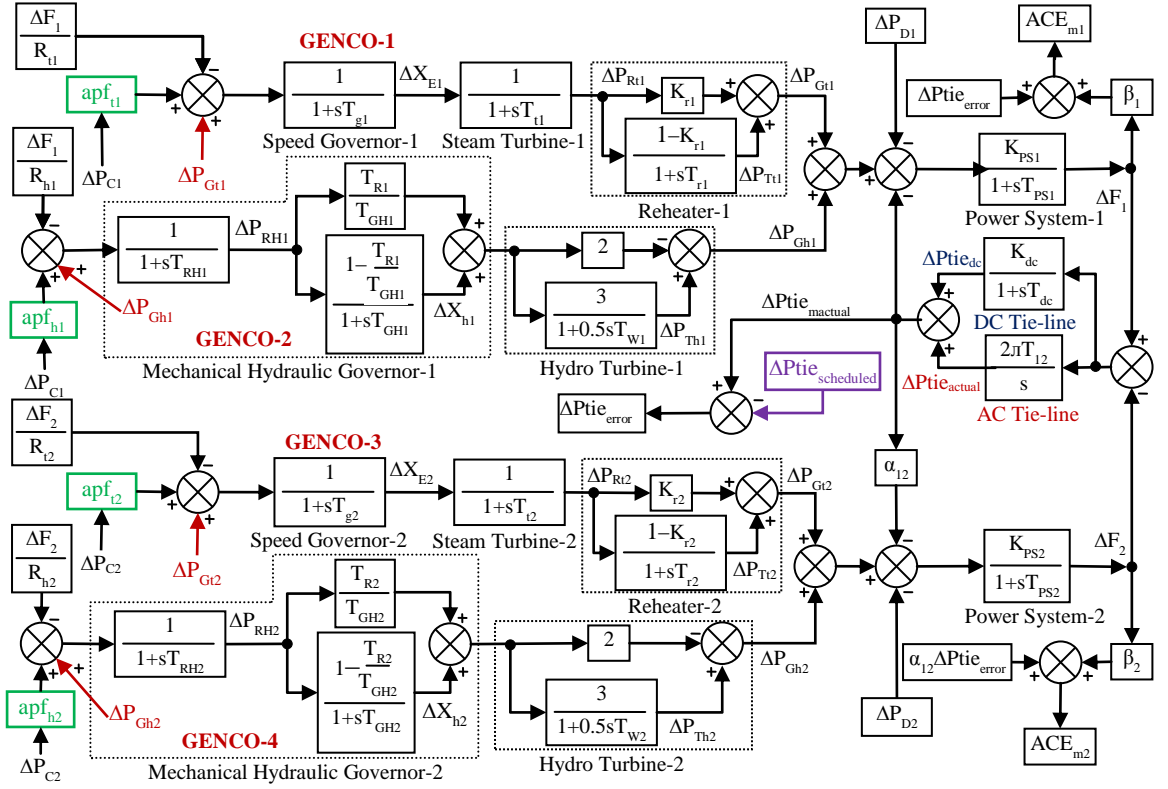
Fig. 3.18 Model of restructured two-area multi-source hydrothermal power system.
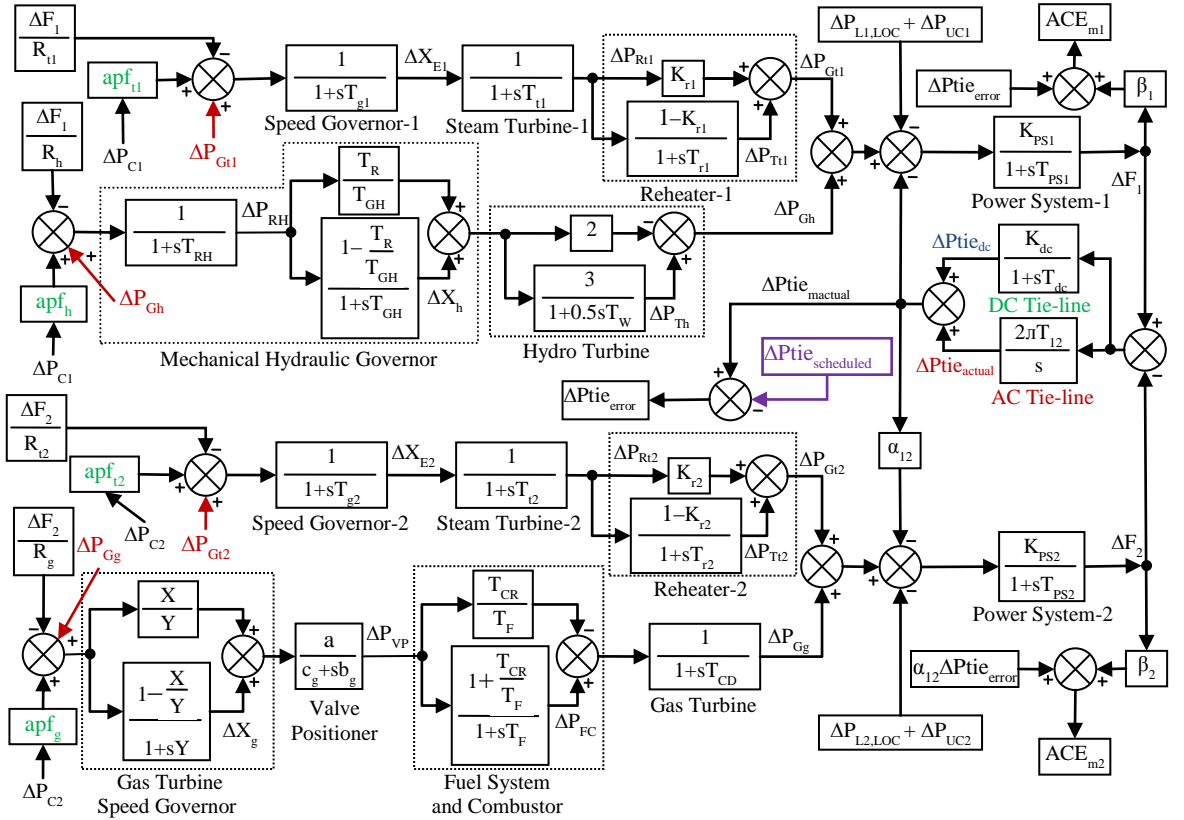
Fig. 3.19 Model of restructured two-area multi-source hydrothermal/gas power system.

been done to simplify the differential equations used to develop the state space model of the systems [30–31].

Further, restructured two-area two-source hydrothermal (Fig. 3.18) and hydrothermal gas (Fig. 3.19) systems are also modeled and studied. The system shown in Fig. 3.18 has thermal and hydro multi-sources in each area of the system. However, the system shown in Fig. 3.19 has thermal hydro multi-sources in area-1 and thermal gas multi-sources in area-2. The transfer function models of reheater of thermal plant, hydraulic mechanical governor and hydro turbine of hydro plant and gas turbine speed governor and fuel system and combustor of gas plant are considered in the split form. The system is interconnected via AC/DC parallel tie-lines. The ACE, which is defined by Eqns. (3.32-3.33) is modified (ACE_m) in the presence of AC/DC parallel tie-line as stated in Eqns. (3.34-3.35) and shown in Figs. 3.18-3.19.

$$ACE_{m1}(s) = \beta_1 \Delta F_1(s) + \Delta Ptie_{error}(s), \tag{3.34}$$

$$ACE_{m2}(s) = \beta_2 \Delta F_2(s) + \alpha_{12} \Delta Ptie_{error}(s). \tag{3.35}$$

A three-area multi-source hydrothermal power system under deregulated power environment can further be modeled accordingly.

3.4   Conclusion

The transfer function model of thermal, hydro and gas turbines and their governing systems, tie-lines and other components have been developed in this chapter. The transfer function models of various traditional two-area interconnected power systems such as non-reheat thermal power system, single reheat thermal power system, multi-source multi-unit hydrothermal power system are formulated. Various restructured single-source multi-unit single reheat thermal power system, multi-source multi-unit hydrothermal power system and multi-source multi-unit hydrothermal gas power

system models with and without considering AC and AC/DC parallel tie-lines are also designed in this chapter.

CHAPTER 4

OPTIMAL AGC OF RESTRUCTURED MULTI-SOURCE HYDROTHERMAL/GAS SYSTEM

4.1 Introduction

The early studies concerning the design of automatic generation control (AGC) controllers of power systems were based on conventional control methods. This method engages two variables namely, variation in frequency and tie-line power flows. Their deviations are weighted together by a linear combination to a single variable called ACE which is used as the input signal to a proportional integral (PI) controller. The PI gains are not based on any specific criterion, but are calculated on the basis of operator' experience. With the advent of modern optimal control theory, many concepts for AGC schemes have been presented which were having several virtues over conventional AGC designs. Based on this concept, following the pioneering work of Fosha and Elgerd [20] many optimal AGC schemes have appeared in the literature [21–32,237–244].

One of the chief developments which the electricity industry has gone through in recent decades is its shift from regulated to deregulated operating environment. It offers several advantages to the power producers, distributors and consumers as well. In deregulated environment, the vertically integrated utilities (VIUs) no longer evince interest on but various entities like distribution companies (DISCOs), generation companies (GENCOs), transmission companies (TRANSCOs) and independent system operator (ISO) have been introduced [12,14,213–220,225,228–231,233–234,237–398]. ISO is independent agent for market participants who perform various

ancillary services and among them is the AGC [12]. In the new environment, optimal AGC schemes have also been developed and modified according to the new market structure as reported in the literature [237–244].

Keeping the above discussion in view, this chapter presents a comprehensive investigation on AGC of restructured two-area multi-source power systems. Two areas are interconnected via AC and AC/DC parallel tie-lines under deregulated power environment.

The modern advances in the power electronic devices led to the development of fast acting flexible alternating current transmission system (FACTS) devices to enhance the stability of the interconnected modern power system. FACTS devices offer more flexibility in power system operation and control to continue an invariable system voltage and frequency profiles. Developments in power electronics industry further helped to produce high voltage direct current (HVDC) transmission to transmit bulk power over remote places with lesser capital outlays and power losses than high voltage alternating current (HVAC) transmission system [241]. Some significant benefits of HVDC transmission comprise controlled huge power transmission between unsynchronized AC distribution systems, no limitation of distance for transfer of power, need fewer number of conductors; hence it decreases the line expenditure and can transmit more power per conductor than HVAC system. On the other side, many problems exist in the power system interconnected via long AC tie-lines like frequent tripping due to power oscillations, huge fault current level and decline in system recital due to transmission of disturbances among systems [30]. Hence, in order to enhance controllability, one imperative application of HVDC transmission line is to operate in tandem with an existing AC transmission line acting as AC/DC parallel links interconnecting two-areas.

Recently some researchers have explored AGC in conventional [30–31,38, 100,103–104,126,132,143,150–152,155–157] and restructured [245,290–291,323,356, 360,365–367,369,371] power systems with multi-sources such as hydro, thermal, gas, nuclear etc., operating in each control area, as discussed in Chapter 2 in details. Optimal AGC controllers are implemented successfully on a two-area system with hydrothermal gas units in each area [30–31]. Optimal full state feedback and output feedback controllers are proposed for a realistic single-area multi-source system [38]. An optimal output feedback controller is proposed for two-area system with hydro thermal gas diverse sources in each area under deregulated environment [245]. To perform the present study, optimal PI AGC controllers are designed exploiting modern control theory. To the best of authors' knowledge, no attempt has been made so far to design optimal PI controllers for AGC of two-area multi-source hydrothermal power system under deregulated environment and interconnected via AC/DC parallel links. In order to assess the stability of the system, eigenvalue study is also carried out. The feasibility of designed optimal PI controllers is tested in the wake of step load perturbation (SLP) in anyone or both control areas depending on various power contracts among various GENCOs and DISCOs. The dynamic performance of multi-source system is also compared with single-source system. Finally, the study is extended to a restructured two-area multi-source hydrothermal-thermal gas system.

4.2 Power system models under study

A restructured two-area multi-source power system model is considered under the present study. Two-areas are interconnected via AC and AC/DC parallel links. The power system configuration is shown in Fig. 4.1. Each area of the system consists of hydro and thermal units for electrical power generation. Thermal system is single

reheat turbine type while hydro system is mechanical governor based plant. The model of the system is shown in Fig. 4.2. A two-area multi-source hydrothermal/gas system interconnected via AC and AC/DC parallel links shown in Fig. 4.5 is also explored at the last. Area-1 of hydrothermal/gas system owns hydrothermal units while area-2 is equipped with thermal and gas units.

4.3 AGC under deregulated environment

In deregulated environment, GENCOs sell electricity they generate to various DISCOs at competitive rates. The entity which wheels this power between DISCOs and GENCOs is termed as TRANSCO. In the open market, a DISCO can contract individually with GENCOs to purchase the power and these contracts must be approved from the ISO [12]. DISCOs have liberty to make contracts with the GENCOs of different areas called bilateral transactions [12,244]. While in poolco based transactions, GENCOs have contracts only with the DISCOs of the same control area [12,244]. An AGC study on restructured power systems should accommodate all power transactions possible like poolco, bilateral and an amalgamation of these two transactions.

   In the proposed model, each control area has two DISCOs and two GENCOs. Let GENCO-1, GENCO-2, DISCO-1, DISCO-2 be in area-1, while GENCO-3, GENCO-4, DISCO-3, DISCO-4 be in area-2. To make the realization of contracts simpler, a
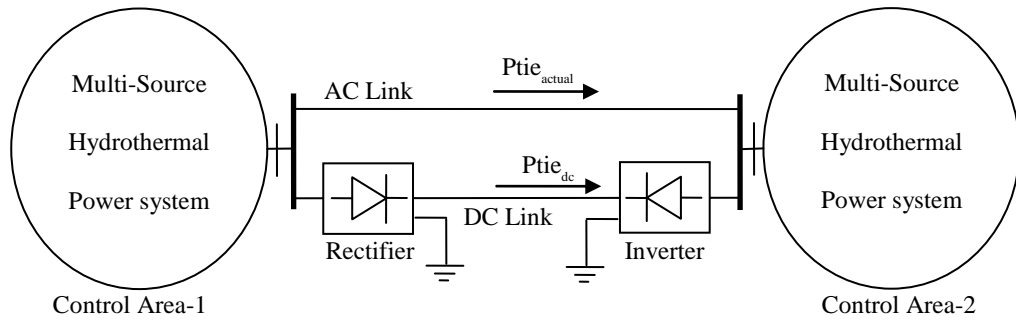
Fig. 4.1   Two-area multi-source power system interconnected via AC/DC parallel links [29–30,241].
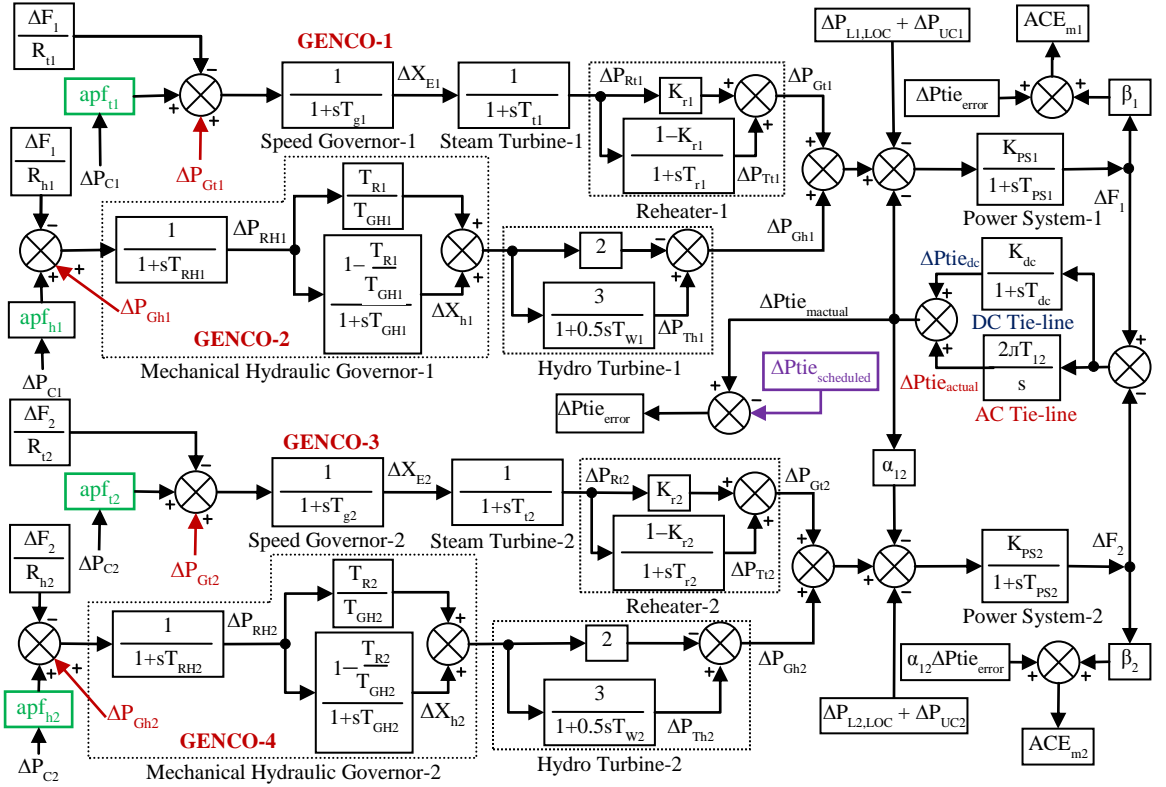
Fig. 4.2 Model of two-area multi-source hydrothermal system under deregulated environment.

DPM is usually employed [5,12,228,293,313,322,341,343] as given by Eqn. (4.1).

$$\text{DPM} = \begin{bmatrix} \text{cpf}_{11} & \text{cpf}_{12} & \text{cpf}_{13} & \text{cpf}_{14} \\ \text{cpf}_{21} & \text{cpf}_{22} & \text{cpf}_{23} & \text{cpf}_{24} \\ \text{cpf}_{31} & \text{cpf}_{32} & \text{cpf}_{33} & \text{cpf}_{34} \\ \text{cpf}_{41} & \text{cpf}_{42} & \text{cpf}_{43} & \text{cpf}_{44} \end{bmatrix}. \tag{4.1}$$

The number of rows and columns in a DPM corresponds to the number of GENCOs and DISCOs, respectively. An entry in DPM is termed as contract participation factor (cpf), which corresponds to contracted load of a DISCO from a corresponding GENCO. Sum of the entries of any column of DPM is $\sum_i^{\text{nGENCO}} \text{cpf}_{ij} = 1$, $j = 1,2,\ldots,\text{nDISCO}$, where nGENCO is number of GENCOs and nDISCO is number of DISCOs [228]. The actual steady state tie-line power flows in a two-area system interconnected via AC link is given as [12]:

69

$$\Delta Ptie_{actual} = \frac{2\pi T_{12}}{s} [\Delta F_1 - \Delta F_2]. \tag{4.2}$$

The DC link is supposed to work in constant current control mode [30]. The transfer function model of DC link is taken from [29–30,39,104,237,241] as shown in Fig. 4.2. For small perturbation, the DC tie-line power flow (Eqn. 3.24) is given as:

$$\Delta Ptie_{dc} = \frac{K_{dc}}{1 + sT_{dc}} [\Delta F_1 - \Delta F_2]. \tag{4.3}$$

For small step load perturbation (SLP), the actual tie-line power flow, as given by Eqn. (4.2) for the system interconnected via AC link is tailored in the presence of DC link in parallel with AC link as:

$$\Delta Ptie_{mactual} = \Delta Ptie_{actual} + \Delta Ptie_{dc}. \tag{4.4}$$

The scheduled steady state power flow on the tie-line is stated in Eqn. (3.28) as [5,12,228,241,245,313,341,343]:

$$\Delta Ptie_{scheduled} = \sum_{i=1}^{2} \sum_{j=3}^{4} cpf_{ij} \Delta P_{Lj} - \sum_{i=3}^{4} \sum_{j=1}^{2} cpf_{ij} \Delta P_{Lj}, \tag{4.5}$$

$$\Delta Ptie_{scheduled} = [P_{exp1}] - [P_{imp1}].$$

Where $[P_{exp1}]$ is the total power exported from area-1 and equal to the demand of DISCOs in area-2 from GENCOs in area-1, while $[P_{imp1}]$ is the total power imported in area-1 and equal to the demand of DISCOs in area-1 from the GENCOs in area-2 [245]. The tie-line power flow error is stated as:

$$\Delta Ptie_{error} = \Delta Ptie_{mactual} - \Delta Ptie_{scheduled}. \tag{4.6}$$

In the steady state, $\Delta Ptie_{error}$ vanishes as $\Delta Ptie_{mactual}$ attains $\Delta Ptie_{scheduled}$. The area control error (ACE) is also altered in the presence of AC/DC parallel links (Eqns. (3.34-3.35)) as:

$$ACE_{m1} = \beta_1 \Delta F_1 + \Delta Ptie_{error}, \tag{4.7}$$

$$ACE_{m2} = \beta_2 \Delta F_2 + \alpha_{12} \Delta Ptie_{error}. \tag{4.8}$$

where, α_{12} is area size ratio and β_1, β_2 are frequency bias constants of the respective control area. Since, more than one GENCO is available usually in each control area; the modified area control error (ACE$_m$) signal must be distributed between GENCOs in proportion to their involvement in AGC. The factor used to perform this sharing is termed as ACE participation factor (apf). It should be noted that in all the current simulations, apfs are kept at the same values of 0.5. The steady state generated powers of GENCOs in contract with DISCOs are stated in Eqn. (3.29) as:

$$\Delta P_{Gti} = cpf_{i1}\,\Delta P_{L1} + cpf_{i2}\,\Delta P_{L2} + cpf_{i3}\,\Delta P_{L3} + cpf_{i4}\,\Delta P_{L4}, \; i = 1,3, \tag{4.9}$$

$$\Delta P_{Ghi} = cpf_{i1}\,\Delta P_{L1} + cpf_{i2}\,\Delta P_{L2} + cpf_{i3}\,\Delta P_{L3} + cpf_{i4}\,\Delta P_{L4}, \; i = 2,4. \tag{4.10}$$

The ΔP_{Gti} and ΔP_{Ghi} are generations of thermal and hydro power plants, respectively. In Fig. 4.2, the market disturbance signal $\Delta P_{L1,LOC}$ ($= \Delta P_{L1} + \Delta P_{L2}$) can be defined as the total local demand in area-1 and $\Delta P_{L2,LOC}$ ($= \Delta P_{L3} + \Delta P_{L4}$) the total local load demand in area-2. ΔP_{Li} denotes the power demand made by DISCO-i. The disturbance signal ΔP_{UCi} is the uncontracted power demanded by any DISCO in area-i.

4.4 State space model of the system

The linear continuous-time power system model under examination shown in Fig. 4.2 can be represented by the following standard state space equations:

$$\frac{d}{dt}\underline{X} = A\underline{X} + B\underline{U} + \Gamma\underline{P}_d, \; \underline{X(0)} = 0 \tag{4.11}$$

$$\underline{Y} = C\underline{X} \tag{4.12}$$

where $\underline{X}$ is system state vector of the dimension n × 1, n is no. of states = 18, $\underline{U}$ is control input vector of the dimension m × 1, m is no. of control variables = 2, $\underline{P}_d$ is disturbance vector of the dimension p × 1, p is no. of disturbance variables = 6, $\underline{Y}$ is

output vector of the dimension q × 1, q is no. of output variables = 18. A, B, C, and Γ are system, control, output and disturbance matrices with dimensions of n × n, n × m, q × n and n × p, respectively, and are given in Appendix A. In the application of optimal control theory, the term $\underline{P}_d$ in Eqn. (4.11) is removed in steady state occurring after a SLP. So the Eqn. (4.11) can be rephrased as:

$$\frac{d}{dt}\underline{X} = A\underline{X} + B\underline{U}, \quad \underline{X}(0) = -X_{ss} \tag{4.13}$$

where new state vector is equal to the old state vector minus its steady state value X_{ss} [41,43]. The state, control and disturbance vectors selected for the power system under study are given as follows:

State vector [18×1]:

$$\underline{X} = [\Delta F_1 \ \Delta Ptie_{actual} \ \Delta F_2 \ \Delta P_{Tt1} \ \Delta P_{Th1} \ \Delta P_{Tt2} \ \Delta P_{Th2} \ \Delta P_{Rt1} \ \Delta X_{h1} \ \Delta P_{Rt2} \ \Delta X_{h2} \ \Delta X_{t1} \ \Delta P_{RH1}$$

$$\Delta X_{t2} \ \Delta P_{RH2} \ \smallint ACE_{m1}dt \ \smallint ACE_{m2}dt \ \Delta Ptie_{dc}]^T \tag{4.14}$$

Control vector [2×1]:

$$\underline{U} = [\Delta P_{C1} \ \Delta P_{C2}]^T \tag{4.15}$$

Disturbance vector [6×1]:

$$\underline{P}_d = [\Delta P_{L1} \ \Delta P_{L2} \ \Delta P_{L3} \ \Delta P_{L4} \ \Delta P_{UC1} \ \Delta P_{UC2}]^T \tag{4.16}$$

4.5 Design of optimal PI controllers

The design of optimal PI controllers is detailed in the literature [1,20,23–32, 39,41,43,237,241]. The power system model in the state variable form is given by Eqns. (4.11–4.12). The control vector $\underline{U}$ defines the performance criterion to minimize the performance index J given by Eqn. (4.17).

$$J = \smallint_0^\infty \frac{1}{2}[\underline{X}^T Q\underline{X} + \underline{U}^T R\underline{U}] \ dt. \tag{4.17}$$

where, Q is a positive semi-definite symmetric state cost weighting matrix and R is a positive definite symmetric control cost weighting matrix as given in Appendix A. The optimal control law is given [20,23] as:

$$\underline{U}^* = -K^*\underline{X} \qquad (4.18)$$

where,

$$K^* = R^{-1}B^T P \qquad (4.19)$$

and P is the solution of algebraic matrix Riccati equation

$$PA + A^T P - PBR^{-1}B^T P + Q = 0. \qquad (4.20)$$

Table 4.1

Optimal gain matrices for two-area multi-source restructured power system.

Optimal feedback gain matrices $[K^*]$

AC link only, $[2\times17]$, $J^* = 3.6800e^{+3}$

[0.6377	−1.5684	0.0974	5.1642	2.0584	0.4118	0.1356	0.8880	−0.2779
0.0196	0.5464	0.4448	−2.3890	0.0016	4.3984	1.0000	−0.0000;	
0.0974	1.5684	0.6377	0.4118	0.1356	5.1642	2.0584	0.0196	0.5464
0.8880	−0.2779	0.0016	4.3984	0.4448	−2.3890	0.0000	1.0000]	

AC/DC links, $[2\times18]$, $J^* = 2.9347e^{+3}$

[0.4060	−0.1332	0.3290	4.4167	1.3850	1.1592	0.8089	0.6380	0.3429
0.2696	−0.0744	0.3846	4.2529	0.0618	−2.2435	1.0000	0.0000	−0.0174;
0.3290	0.1332	0.4060	1.1592	0.8089	4.4167	1.3850	0.2696	−0.0744
0.6380	0.3429	0.0618	−2.2435	0.3846	4.2529	0.0000	1.0000	0.0174]

Table 4.2

Pattern of open/closed-loop eigenvalues for two-area multi-source restructured power system.

State variables	Eigenvalues with AC link		Eigenvalues with AC/DC links	
	Open-loop	Closed-loop	Open-loop	Closed-loop
ΔF_1	−0.0000	−14.2205	−0.0000	−14.2205
$\Delta Ptie_{actual}$	−0.0000	−14.2105	−0.0000	−14.1122
ΔF_2	−12.9224	−0.5128 + 2.8721i	−12.9224	−2.1258 + 7.8182i
ΔP_{Tt1}	−12.9074	−0.5128 − 2.8721i	−12.7630	−2.1258 − 7.8182i
ΔP_{Th1}	−0.1628 + 2.9641i	−2.8032 + 0.8295i	−2.0752 + 7.8229i	−3.7737
ΔP_{Tt2}	−0.1628 − 2.9641i	−2.8032 − 0.8295i	−2.0752 −7.8229i	− 2.8032 + 0.8295i
ΔP_{Th2}	−2.6410 + 0.8493i	−2.7959 + 0.4668i	−3.4881	−2.8032 − 0.8295i
ΔP_{Rt1}	−2.6410 − 0.8493i	−2.7959 − 0.4668i	−2.6410 + 0.8493i	−1.1848 + 1.2818i
ΔX_{h1}	−2.6553 + 0.6186i	−1.1848 + 1.2818i	−2.6410 −0.8493i	−1.1848 − 1.2818i
ΔP_{Rt2}	−2.6553 − 0.6186i	−1.1848 − 1.2818i	−0.7514 + 1.3220i	−1.9882 + 0.3470i
ΔX_{h2}	−0.7514 + 1.3220i	−1.3861	−0.7514 −1.3220i	−1.9882 − 0.3470i
ΔX_{t1}	−0.7514 − 1.3220i	−0.3352	−1.9876 + 0.3891i	−0.4896
ΔP_{RH1}	−1.2913	−0.2026 + 0.0778i	−1.9876 −0.3891i	−0.3352
ΔX_{t2}	−0.2113	−0.2026 − 0.0778i	−0.4585	−0.1996 + 0.0755i
ΔP_{RH2}	−0.0980	−0.1974	−0.2113	−0.1996 − 0.0755i
$\int ACE_{m1}dt$	−0.0347	−0.0347	−0.0976	−0.1974
$\int ACE_{m2}dt$	−0.0204	−0.0344	−0.0347	−0.0347
$\Delta Ptie_{dc}$			−0.0204	−0.0344

4.6 Simulation and discussion of results

The state space model of the restructured multi-area system shown in Fig. 4.2 is simulated using the optimum regulator gains obtained adopting workspace of MATLAB software version 7.5.0(R2007b) installed on an Intel Core2 Duo processor of 1.66 GHz and 2 GB of RAM computer. The system data are given in Appendix B. The following two case studies are investigated extensively:

4.6.1 Multi-source hydrothermal system with different transactions

The system model under study is simulated for all types of probable transaction like poolco, bilateral and a combination of these two transactions taking place in a deregulated environment. The optimal feedback gains of optimal PI controllers are obtained for power system considering (i) AC link and (ii) AC/DC parallel links in conjunction with the minimum performance index values J^* given in Table 4.1. The open-loop and closed-loop system eigenvalues for the system model with AC link and AC/DC parallel links are given in Table 4.2. The study of Table 4.1 reveals that system performance index J^* is reduced when AC/DC parallel links ($J^* = 2.9347e^{+3}$) are used as area interconnection than those obtained with AC link ($J^* = 3.6800e^{+3}$). Next, the analysis of Table 4.2 indicates that open-loop eigenvalues of both systems corresponding to first two states lie on the $j\omega$-axis in s-plane, while all other values lie in the left half of s-plane. Therefore, system is marginally stable in open-loop interconnected via AC or AC/DC parallel links. On the other hand, all close-loop eigenvalues have negative real parts, which ensure system stability with excellent stability margins for both cases. Moreover, the magnitudes of imaginary parts of closed-loop eigenvalues of some states are less compared to open-loop, which may improve the system dynamic results. Some eigenvalues show more negative real parts

74

in case of AC/DC links, which improve the stability margins of the system. The cases for different transactions are discussed as follows:

Case A: Poolco based transactions

In poolco based transactions GENCOs contribute in AGC of their own control area, here area-1 only i.e., power is demanded only by DISCO-1 and DISCO-2 [5,12,293,298,307,343]. Let, the power demand of each DISCO be 10%, i.e., $\Delta P_{L1,LOC}$ = 0.2 puMW and $\Delta P_{L2,LOC}$ = 0 puMW. Area control error (ACE) participation factor of thermal (apf_{t1} = apf_{t2}) and hydro (apf_{h1} = apf_{h2}) are kept equal to 0.5. The DPM for this case is given as:

$$DPM = \begin{bmatrix} 0.5 & 0.5 & 0 & 0 \\ 0.5 & 0.5 & 0 & 0 \\ 0 & 0 & 0 & 0 \\ 0 & 0 & 0 & 0 \end{bmatrix}. \tag{4.21}$$

Generations of GENCOs must match the demanded power of the DISCOs in contract with them in the steady state. From Eqns. (4.9–4.10), in steady state, the theoretical values of deviation in generations are ΔP_{Gt1} = 0.1 puMW, ΔP_{Gh1} = 0.1 puMW and ΔP_{Gt2} = ΔP_{Gh2} = 0 puMW. Also the scheduled power flow on the tie-line can be calculated by Eqn. (4.5), i.e., $\Delta Ptie_{scheduled}$ = 0 puMW. The simulation results for the power system interconnected via AC/DC parallel links are shown in Fig. 4.3. For Case-A, it is observed that in the steady state, the deviations in each area frequency, settle to zero under a step load power demand change of DISCO-1 and DISCO-2, hence AGC requirement is fulfilled. The $\Delta Ptie_{scheduled}$ = $\Delta Ptie_{actual}$ = $\Delta Ptie_{mactual}$ = 0 puMW. Therefore, $\Delta Ptie_{error}$ = 0 puMW. The actual generations of all GENCOs attain the desired values in the steady state as shown in Figs. 4.3(e–h). As GENCOs situated in area-2 do not have contracts with any GENCO, ΔP_{Gt2} = ΔP_{Gh2} = 0 puMW in steady state. It is also examined that the system results belonging to area

of power demand i.e., area-1, experience more peak undershoots compared to area-2 with zero power demand. Consequently, it is concluded that the outcome of disturbance show local dominance but it also influences the outcomes of other interconnected area due to the presence of weak tie-line.

Case B: Combination of poolco and bilateral transactions

In this case, DISCOs have the freedom to have contracts with the GENCOs available in its own or other control areas [6,12,245,293,298,307,343]. For this scenario, the DPM is given by Eqn. (4.22).

$$
DPM = \begin{bmatrix} 0.1 & 0.1 & 0.1 & 0.1 \\ 0.1 & 0.1 & 0.1 & 0.3 \\ 0.5 & 0.2 & 0.5 & 0.3 \\ 0.3 & 0.6 & 0.3 & 0.3 \end{bmatrix}.
\tag{4.22}
$$

Let each DISCO demands 6% power from GENCOs as per the pattern of cpfs shown in the DPM, i.e., $\Delta P_{L1,LOC} = \Delta P_{L2,LOC} = 0.12$ puMW. Using Eqn. (3.28 or 4.5), $\Delta Ptie_{scheduled} = \{(0.1 + 0.1 + 0.1 + 0.3) - (0.5 + 0.3 + 0.2 + 0.6)\}0.06 = -0.06$ puMW. For Case-B, the simulation results for the system with AC/DC parallel links are also shown in Fig. 4.3. In steady state the deviation in frequency settles to zero. The actual tie-line powers shown in Figs. 4.3(c–d) settle to the desired value of –0.06 puMW, which is $\Delta Ptie_{scheduled}$ in the steady state. The steady state desired values of power

(a)   (b)
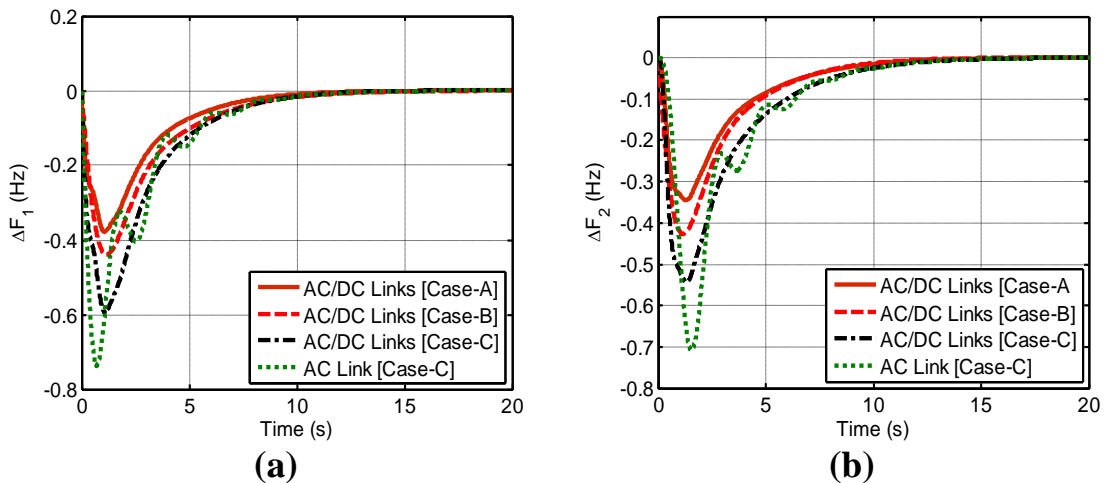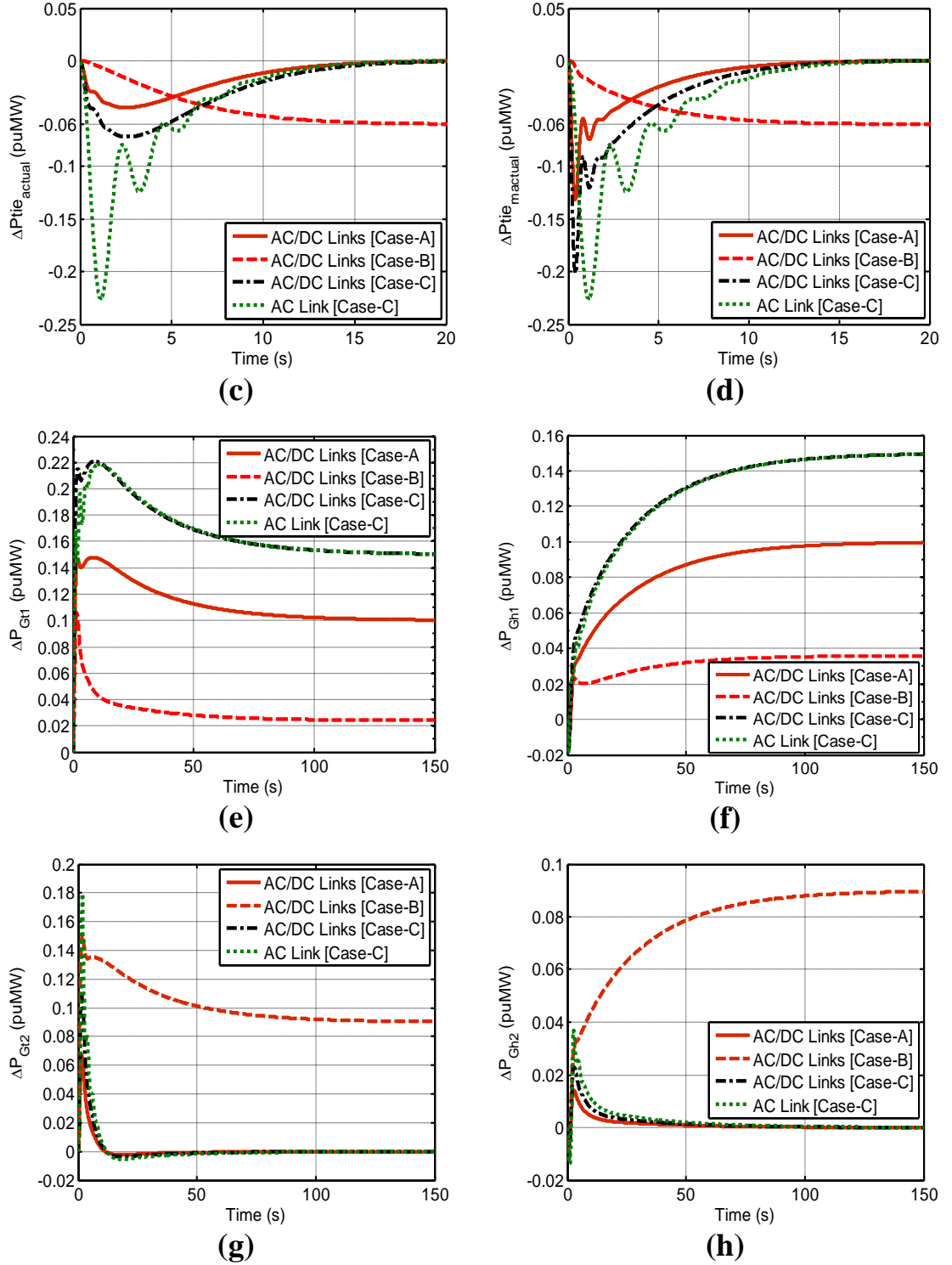
Fig. 4.3 Dynamic performance of two-area multi-source hydrothermal power system (a) ΔF_1, (b) ΔF_2, (c) $\Delta Ptie_{actual}$, (d) $\Delta Ptie_{mactual}$, (e) ΔP_{Gt1}, (f) ΔP_{Gh1}, (g) ΔP_{Gt2} and (h) ΔP_{Gh2}.

generations are $\Delta P_{Gt1} = 0.024$ puMW, $\Delta P_{Gh1} = 0.036$ puMW, $\Delta P_{Gt2} = 0.09$ puMW, and $\Delta P_{Gh2} = 0.09$ puMW. These are verified in Figs. 4.3(e–h).

Case C: Contract violation

It is possible that a DISCO might violate a contract by demanding extra power than that specified in the contract. This excess power must be supplied by the GENCOs situated in the same control area as the DISCO [6,12,228,237,241,278,293,298, 307,322,341,396]. Hence, it must be revealed as a local load of the control area but not as the contract demand. Consider Case-A once again with an amendment that DISCO-1 demands excess power of 0.1 puMW. Therefore, the total load demand in area-1 = $\Delta P_{L1,LOC} + \Delta P_{UC1} = 0.2 + 0.1 = 0.3$ puMW. However, load demand in area-2 will be same as was in Case-A, i.e., 0 puMW. In the steady state, apfs of area-1 will decide the distribution of this excess load power demand. Therefore, the steady state desired values of generations are $\Delta P_{Gt1} = \Delta P_{Gt1} + (apf_{t1} \times \Delta P_{UC1}) = 0.1 + (0.5 \times 0.1) = 0.15$ puMW, $\Delta P_{Gh1} = \Delta P_{Gh1} + (apf_{h1} \times \Delta P_{UC1}) = 0.1 + (0.5 \times 0.1) = 0.15$ puMW and verified in Figs. 4.3(e–h) for Case-C. Regarding the system with AC/DC links for Case-C from Fig. 4.3, it is observed that the system interconnected via AC/DC parallel links compared to the system interconnected via AC link only, successfully suppress the oscillations with reduced settling times and peak undershoots for the frequency, tie-line power and generation deviations. The frequency deviations evaporate in the steady state as shown in Figs. 4.3(a–b). The actual tie-line powers are same to Case-A as confirmed via Figs. 4.3(c–d). In the steady state, the outputs of GENCO-3 and GENCO-4 are not influenced by the excess power demand of DISCO-1, i.e., $\Delta P_{Gt2} = \Delta P_{Gh2} = 0$ puMW as shown in Figs. 4.3(g–h). Therefore, optimal PI controllers perform competently to accomplish AGC goals in restructured system.

4.6.2 Comparison with single-source system

In this section, a comparison is made between the two-area multi-source hydrothermal system and a two-area single-source thermal system with AC/DC parallel links under

deregulated environment [241]. The system data are given in Appendix B. The DPM is taken from [241] as:

$$\text{DPM}=\begin{bmatrix} 0.5 & 0.0 & 0.5 & 0.1 \\ 0.0 & 0.5 & 0.0 & 0.4 \\ 0.5 & 0.5 & 0.5 & 0.0 \\ 0.0 & 0.0 & 0.0 & 0.5 \end{bmatrix}. \tag{4.23}$$

Consider Case 4 of [241] where load demands of DISCO-1, 2, 3 and 4 is 0%, 0%, 1% and 1% puMW, respectively. In addition, DISCO-3 demands excess power of 1% puMW. Accordingly, the total load demand in area-2 = 0.03 puMW. Therefore, the steady state desired values of GENCOs outputs are $\Delta P_{Gt1} = 0.06$ puMW, $\Delta P_{Gh1} = 0.04$ puMW, $\Delta P_{Gt2} = 0.01$ puMW and $\Delta P_{Gh2} = 0.01$ puMW and $\Delta Ptie_{scheduled} = 0.01$ puMW. As per state vector given in Eqn. (4.14), the full state optimal feedback gains and optimal performance index values for hydrothermal system, are given in Table 4.3 and for the single-source system are given in Table 2 of [241]. Table 4.3 reveals that the optimal performance index condenses with AC/DC parallel links ($J^* = 3.0556e^{+3}$) compared to AC link ($J^* = 4.5654e^{+3}$). It can also be noted that these values are larger than the corresponding values i.e., 48.8422 and 42.3037, respectively (see Table 2 of [241]). The simulation results are shown in Fig. 4.4. Figs. 4.4(c,e–h) validate the desired values of tie-line power flows and different generations. It is noticed that ΔF_1

Table 4.3

Optimal gain matrices of optimal PI controllers for multi-source restructured power system while comparing with single-source restructured power system.

Optimal feedback gain matrices [K*]								
AC link only, [2×17], $J^* = 4.5654e^{+3}$								
[0.5732	–2.1986	0.2294	5.7910	2.3543	0.9526	0.2429	0.7772	0.4333
0.0671	0.5850	0.4199	4.3255	0.0109	4.9256	1.0000	–0.0000;	0.2294
2.1986	0.5732	0.9526	0.2429	5.7910	2.3543	0.0671	0.5850	0.7772
0.4333	0.0109	4.9256	0.4199	4.3255	–0.0000	1.0000]		
AC/DC links, [2×18], $3.0556e^{+3}$								
[0.4219	1.4145	0.3807	4.6428	1.5300	2.1008	1.0671	0.5892	0.7510
0.2551	0.2674	0.3725	8.3368	0.0582	0.9143	1.0000	–0.0000	–0.1575;
0.3807	–1.4145	0.4219	2.1008	1.0671	4.6428	1.5300	0.2551	0.2674
0.5892	0.7510	0.0582	0.9143	0.3725	8.3368	0.0000	1.0000	0.1575]

(a)   **(b)**

(c)   **(d)**

(e)   **(f)**
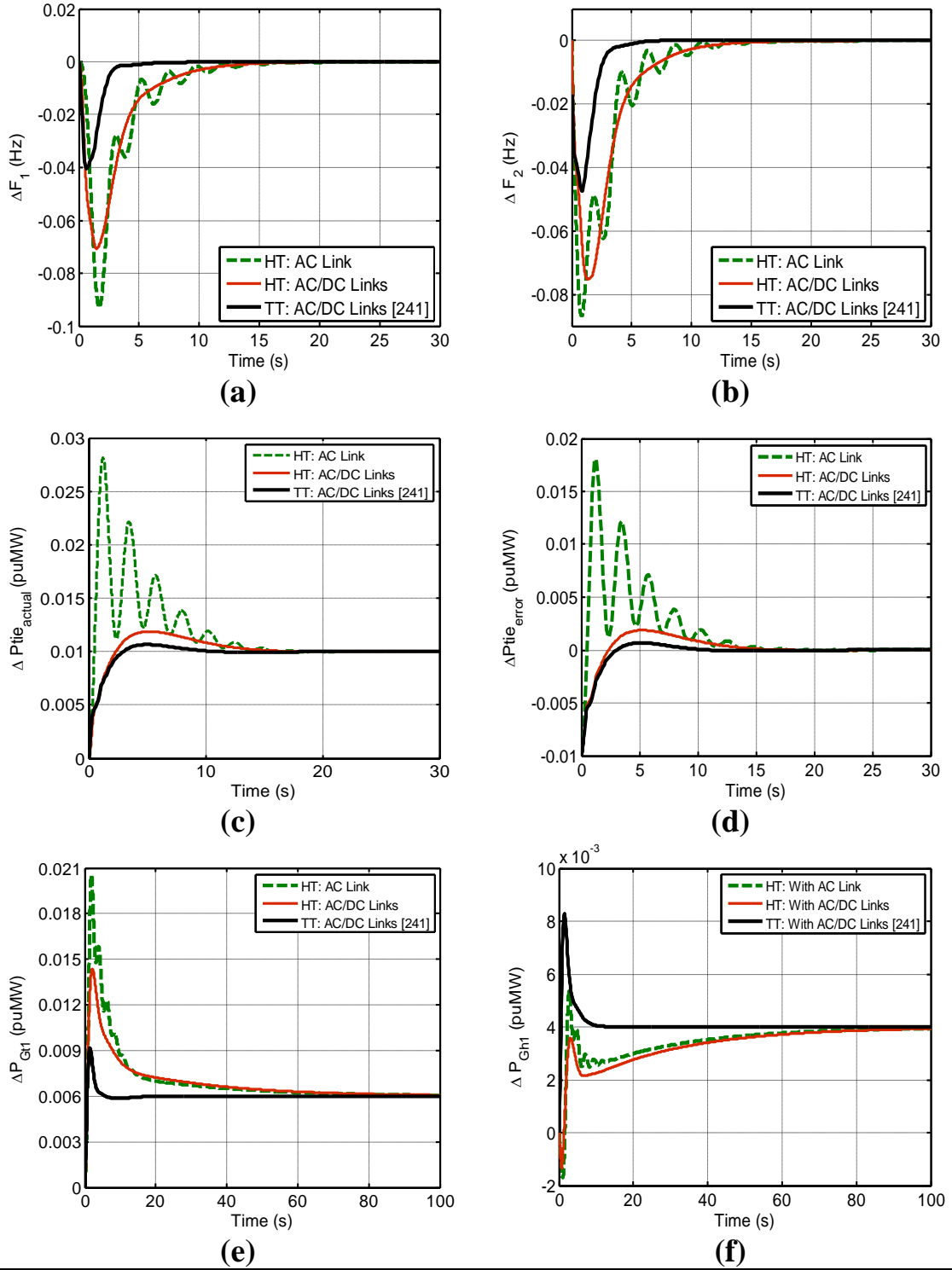
and ΔF_2 results in Figs. 4.4(a–b) and $\Delta Ptie_{error}$ in Fig. 4.4(d) settle to zero in steady

state. From Figs. 4.4(f,h), it is observed that the results of power generations due to

hydro units are characterized by an initial fast negative dip followed by slower

exponential increase in power generation. This is due to non-minimum phase charac-
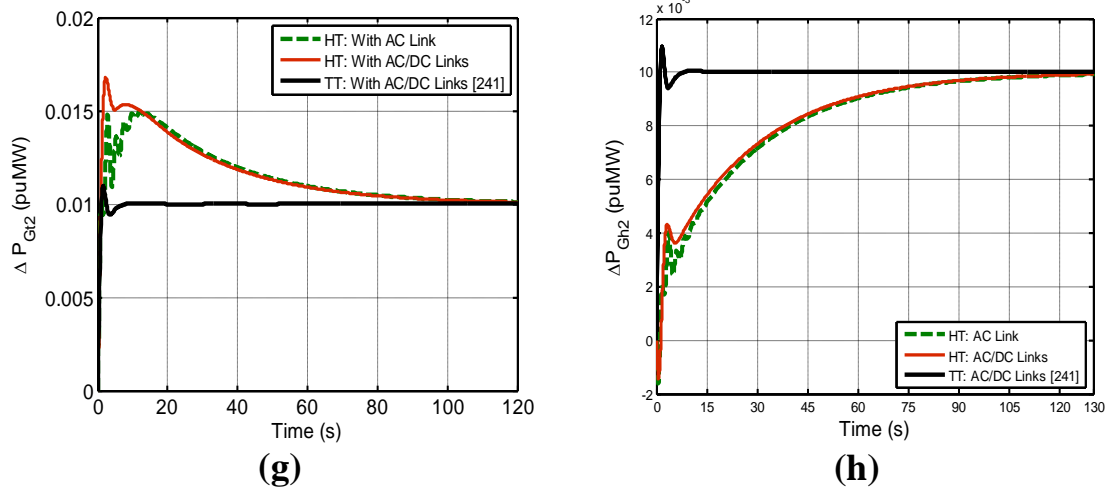
Fig. 4.4 Comparison of dynamic performance of multi-source and single-source systems (a) ΔF_1, (b) ΔF_2, (c) $\Delta Ptie_{actual}$, (d) $\Delta Ptie_{error}$, (e) ΔP_{Gt1}, (f) ΔP_{Gh1}, (g) ΔP_{Gt2} and (h) ΔP_{Gh2}.
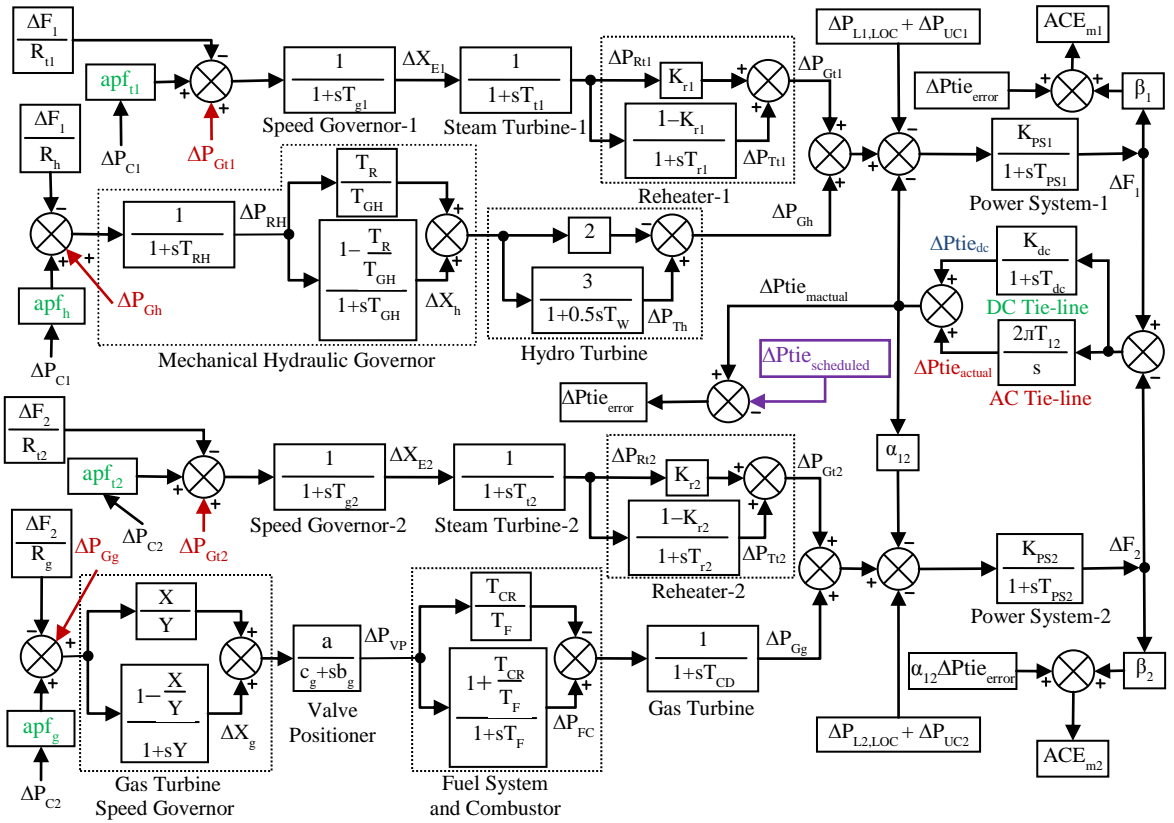
Fig. 4.5 Model of restructured two-area multi-source hydrothermal/gas system.

teristic of hydro turbines. Hence, hydro plants in comparison to thermal necessitate more time to meet desired power demand of DISCOs. Hence, it is observed and established that the hydrothermal system show deteriorated and sluggish results compared to those obtained with thermal system.

81

4.6.3 Multi-source hydrothermal/gas system

To show the scalability and effectiveness of the optimal PI controllers, the study is also extended to a two-area multi-source hydrothermal/gas system. Area-1 of the power system is outfitted with single reheat thermal and mechanical governor based hydro units while area-2 is equipped with single reheat thermal and gas units. The two-area system is interconnected via AC/DC parallel links. Model of the system is given in Fig. 4.5. The system state matrices are given in Appendix A and the parameters in Appendix B. Frequently used transactions type i.e., poolco plus bilateral transactions is simulated to conduct the study. The state vector selected is of the order of [19×1] for system with AC/DC links and is given by Eqn. (4.24).

$$X = [\Delta F_1 \ \Delta F_2 \ \Delta Ptie_{actual} \ \Delta P_{Tt1} \ \Delta P_{Th} \ \Delta P_{Tt2} \ \Delta P_{Gg} \ \Delta P_{Rt1} \ \Delta X_h \ \Delta P_{Rt2} \ \Delta P_{FC} \ \Delta P_{VP} \ \Delta X_{t1}$$

$$\Delta P_{RH} \ \Delta X_{t2} \ \Delta X_g \ \int ACE_{m1}dt \ \int ACE_{m2}dt \ \Delta Ptie_{dc}]^T \qquad (4.24)$$

For this scenario the DPM engaged is given as:

$$DPM = \begin{bmatrix} 0.6 & 0.0 & 0.4 & 0.1 \\ 0.1 & 0.1 & 0.1 & 0.2 \\ 0.1 & 0.1 & 0.3 & 0.3 \\ 0.2 & 0.8 & 0.2 & 0.4 \end{bmatrix} \qquad (4.25)$$

All apfs are kept at the same values i.e., $apf_{t1} = apf_h = apf_{t2} = apf_g = 0.5$. Let, $\Delta P_{L1} = \Delta P_{L2} = \Delta P_{L3} = \Delta P_{L4} = 0.01$ puMW. Hence, $\Delta P_{D1} = \Delta P_{D2} = 0.02$ puMW. The thermal generations are defined via Eqn. (4.9) while hydro and gas generations in steady state can be calculated using Eqns. (4.26-4.27).

$$\Delta P_{Gh} = cpf_{21} \ \Delta P_{L1} + cpf_{22} \ \Delta P_{L2} + cpf_{23} \ \Delta P_{L3} + cpf_{24} \ \Delta P_{L4}, \qquad (4.26)$$

$$\Delta P_{Gg} = cpf_{41} \ \Delta P_{L1} + cpf_{42} \ \Delta P_{L2} + cpf_{43} \ \Delta P_{L3} + cpf_{44} \ \Delta P_{L4}. \qquad (4.27)$$

Fig. 4.6 incorporates the MATLAB simulation results of the system interconnected via AC and AC/DC parallel links. In steady state the deviations in
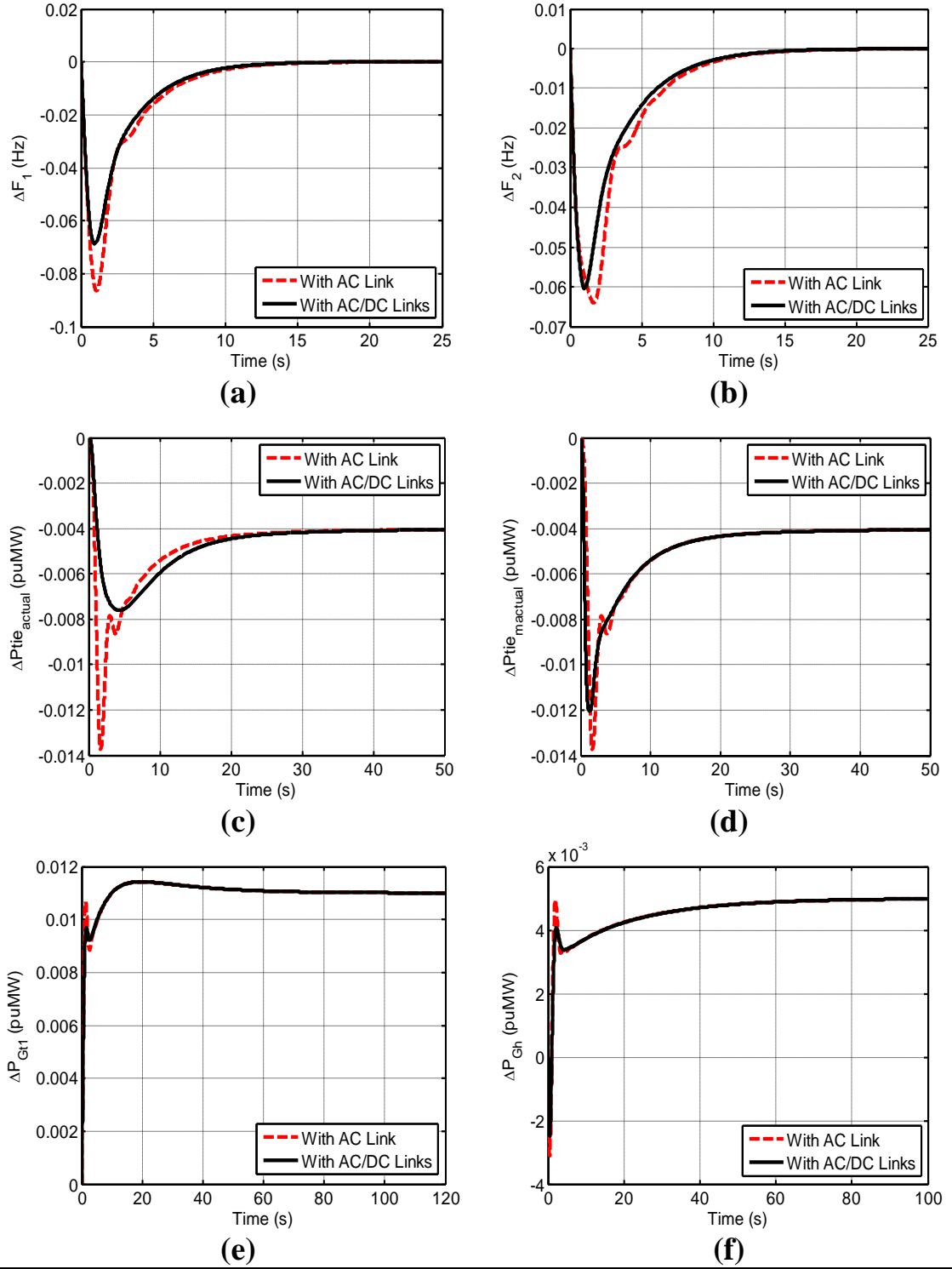
frequency of both areas settle to zero as shown Figs. 4.6(a-b). The scheduled tie-line power flows are calculated using Eqn. (4.5), and found out as: $\Delta Ptie_{scheduled} = -0.04$ puMW. The $\Delta Ptie_{actual}$ and $\Delta Ptie_{mactual}$ power flows shown in Figs. 4.6(c-d) settle to -0.04 puMW, which is equal to the $\Delta Ptie_{scheduled}$ in the steady state. Hence, in the steady
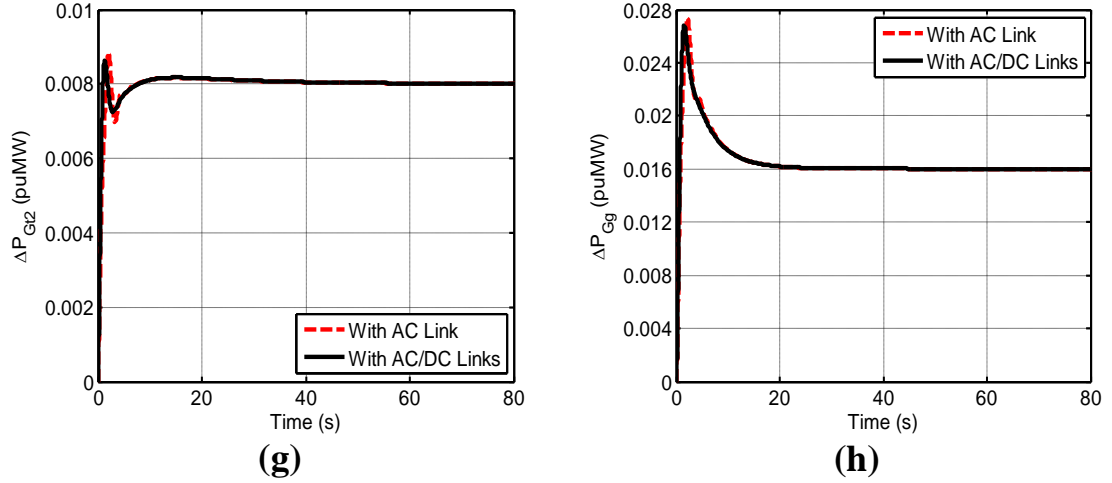
Fig. 4.6 Dynamic performance of two-area multi-source hydrothermal/gas system (a) ΔF_1, (b) ΔF_2, (c) $\Delta Ptie_{actual}$, (d) $\Delta Ptie_{mactual}$, (e) ΔP_{Gt1}, (f) ΔP_{Gh}, (g) ΔP_{Gt2} and (h) ΔP_{Gg}.

Table 4.4
Optimal feedback gain matrices of the AGC controllers.

Optimal feedback gain matrices [K^*]							
AC link only, [2×18], J* = 5.0442e^{+3}							
[0.2219	0.4306	−2.1118	6.7735	1.9337	0.5281	0.2963	0.5939
0.9873	0.1053	0.1364	0.0183	0.3782	29.6221	0.0170	0.0483
0.9915	−0.1304;	−0.0463	0.8791	1.1545	0.5253	0.2782	4.6015
1.3298	0.0082	0.6706	0.6895	1.3830	0.4082	0.0004	12.8169
0.3591	1.1792	0.1304	0.9915]				
AC/DC links, [2×19], J* = 4.2425e^{+3}							
[0.1550	0.1265	−0.2122	5.4207	1.1021	0.5763	0.1722	0.4337
0.5504	0.0719	0.1844	0.0368	0.3376	20.5249	0.0123	0.2276
0.9446	−0.3281	0.0393;	0.5677	0.4887	−0.0593	1.8205	1.3166
3.6493	0.8162	0.2832	0.0137	0.4913	0.9509	0.3298	0.0649
−3.5863	0.3216	1.1876	0.3281	0.9446	−0.0130]		

state, $\Delta Ptie_{error}$ = 0 puMW. The steady state desired generations of different four GENCOs are calculated using Eqns. (4.9 and 4.26-4.27) as: ΔP_{Gt1} = 0.011 puMW, ΔP_{Gh} = 0.005 puMW, ΔP_{Gt2} = 0.008 puMW and ΔP_{Gg} = 0.016 puMW. The optimal AGC controllers work adequately as these generations are attained by the simulated actual responses shown in Figs. 4.6(e–h). All figures in Fig. 4.6 show smooth and fast responses with no oscillations and lesser peak undershoots with AC/DC links compared to AC link. Hence, from Figs. 4.6(a–h), it is observed that the system offer superior performance when AC/DC parallel links are employed to connect the two areas compared to when only AC link is used as an area interconnection.

Table 4.5
Pattern of open-loop and closed-loop eigenvalues.

State variables	Eigenvalues with AC link		Eigenvalues with AC/DC links	
	Open-loop	Closed-loop	Open-loop	Closed-loop
Δf_1	-0.0000	-20.8143	-0.0000	-20.8260
Δf_2	-0.0000	-14.1532	-0.0000	-14.1259
$\Delta Ptie_{actual}$	-19.8333	-13.9922	-19.8476	-13.9340
ΔP_{Tt1}	-12.7836	-6.8092	$-1.9516 + 7.6572i$	$-2.0509 + 7.6934i$
ΔP_{Th}	-12.7636	-5.7927	$-1.9516 - 7.6572i$	$-2.0509 - 7.6934i$
ΔP_{Tt2}	-7.0161	$-0.8314 + 2.9896i$	-12.6654	-6.5139
ΔP_{Gg}	-5.9117	$-0.8314 - 2.9896i$	-12.7793	-4.6762
ΔP_{Rt1}	$-0.0610 + 3.1982i$	-3.4567	-6.7009	-4.4951
ΔX_h	$-0.0610 - 3.1982i$	-3.2426	$-0.5490 + 1.7991i$	$-1.5132 + 1.7134i$
ΔP_{Rt2}	$-0.4456 + 1.7976i$	$-1.3954 + 1.8435i$	$-0.5490 - 1.7991i$	$-1.5132 - 1.7134i$
ΔP_{FC}	$-0.4456 - 1.7976i$	$-1.3954 - 1.8435i$	-3.9438	-3.4888
ΔP_{VP}	-3.5010	-2.0747	-3.4077	-2.8494
ΔX_{t1}	-3.0832	-1.2680	-2.8225	-1.4294
ΔP_{RH}	-1.9812	-0.3964	-1.3972	-0.0474
ΔX_{t2}	-1.1382	-0.3012	-0.4613	-0.4834
ΔX_g	-0.1853	-0.0474	-0.1841	-0.1549
$\int ACE_{m1} dt$	-0.0972	-0.2010	-0.0416	-0.1963
$\int ACE_{m2} dt$	-0.0416	-0.1546	-0.0966	-0.2999
ΔP_{dc}	$-$	$-$	-5.0000	-0.3932

The optimal feedback gains along with performance index (J^*) values are shown in Table 4.4. The pattern of open-loop and closed-loop system eigenvalues of the system interconnected via AC link and AC/DC parallel links is given in Table 4.5. The analysis of Tables 4.4 and 4.5 provides the same outcomes as offered by Tables 4.1 and 4.2. Therefore, with the use of AC/DC parallel links, the oscillations in the frequency and tie-line power flow can be suppressed effectively under the presence of sudden step load demands and consumers and hence, can get a quality electrical power.

4.7 Conclusion

This chapter presents a comprehensive study on AGC of two area restructured power system interconnected via AC and AC/DC parallel tie-lines under deregulated environment. Each area consists of hydro and thermal power units. To carry out the

study, PI control strategy based AGC optimal controllers are designed employing modern optimal control theory. A decisive investigation is performed for the proposed AGC scheme under poolco, bilateral and a combination of these two transactions. The MATLAB simulation results with optimal PI controllers for various generations and tie-line power flows of GENCOs are authenticated with the theoretical values. It is observed that with both AC and AC/DC parallel links, the power system is marginally stable in open-loop and stable with fine stability margins in closed-loop mode. It is observed that the real part of the some closed-loop eigenvalues is more negative compared to the open-loop eigenvalues. Consequently, the closed-loop hydrothermal system exhibits greater stability margins and ensures fast exponential decay of system time responses. Furthermore, the imaginary part of the eigenvalues of some states gets diminished resulting in lesser oscillation along with fast exponential decay. It is also found that the system performance index is reduced with AC/DC parallel links compared to the system with AC link only. Next, published results of a single-source restructured thermal system with optimal PI controllers are compared with the results obtained with the restructured multi-source hydrothermal system and it is established that the results of the hydrothermal system are sluggish/inferior due to the presence of one hydro unit in each control area. Finally, to demonstrate the effectiveness of the optimal PI controllers in different restructured two-area multi-source systems, the study is also extended to a restructured two-area multi-source hydrothermal/gas system interconnected via AC and AC/DC parallel links.

CHAPTER 5

AGC OF POWER SYSTEMS USING GA BASED FUZZY LOGIC CONTROLLERS

5.1   Introduction

Recently, fuzzy logic control (FLC) strategies have gained large attention to solve AGC problem of interconnected traditional and restructured power systems as discussed in Chapter 2 [87–111,151,168,273–296]. FLC is very efficient, robust and an alternate option to the conventional control method, particularly when the processes are too multifaceted for investigation by conventional control practices [101]. Fuzzy logic applies human knowledge and preferences using membership functions (mfs) and fuzzy rules. The mfs are typically designed on the basis of the obligation and constraints of the system under deliberation. The FLC in AGC systems offers amazingly enhanced results. FLC for AGC problems is mostly based on fuzzy gain scheduling of integral (I) [88], proportional (P) [115], integral derivative (ID) [96], PI [92–95,100] and PID [101] controllers. These controllers exhibit healthier dynamic performances compared with conventional I, PI and PID structured controllers. An interval type-2 fuzzy PID controller proposed in [101] performs better than type-1 fuzzy PID controller and the conventional PID controller in AGC of four-area system. A proportional controller based on hybrid neuro fuzzy (HNF) strategy is successfully applied to tackle AGC problem in a two-area thermal system [115]. A remarkable FPI controller is presented for AGC of hydro and thermal systems in [92–93,95], where it shows improved performance compared to other fuzzy and conventional PI controllers. Recently, some researchers examined AGC of power

systems consisting of multi-sources in each area [100,103]. A FPI controller is implemented in AGC of a multi-source hydrothermal system [100,103]. However, the method adopted to select output scaling factors and horizontal range of mfs is not presented in [100,103]. Also, structure of the controller is complex.

In view of the above, a modified fuzzy PI (FPI) controller tuned via genetic algorithm (GA) is presented for AGC of interconnected two-area power systems. Firstly, a FPI-1 controller is designed with nominal horizontal range of mfs and GA tuned output scaling factors. Secondly, to test the impact of alteration in horizontal range of mfs of FPI-1, it is further optimized to get FPI-2 controller. The results of FPI-1 and 2 controllers are compared and the results due to the latter controller are found to be superior. Yet, FPI controllers are designed only for a traditional two-area non-reheat thermal system; they are successfully applied on traditional two-area reheat/multi-source hydrothermal and restructured reheat thermal systems. The recital of FPI controllers is found considerably improved compared to conventional controllers based on optimal, GA, gravitational search algorithm (GSA), bacterial foraging optimization algorithm, (BFOA), hybrid bacterial foraging optimization algorithm-particle swarm optimization (hBFOA-PSO) and hybrid firefly algorithm-pattern search (hFA-PS) techniques and fuzzy gain scheduling controller presented in [100,103].

5.2   Power system models investigated

Four different power systems examined in this chapter are traditional non-reheat, reheat, multi-source multi-area (MSMA) and restructured reheat thermal power systems. Fig. 5.1 shows transfer function model of traditional two-area reheat thermal system. The transfer function model of traditional two-area non-reheat thermal system will be without reheater transfer function blocks shown in Fig. 5.1. The transfer

function model of traditional two-area multi-source hydrothermal system is shown in Fig. 5.6. Each area of multi-source system consists of one non-reheat thermal and one mechanical governor based hydro units [100,103,150]. The restructured system is an interconnected two-area system with two reheat thermal units (GENCOs) and two distribution companies (DISCOs) in each area. The test system is taken from [343] as shown in Fig. 5.8. Area capacity of each system is 2000 MW operating at initial loading of 1000 MW at 60 Hz. The frequency bias setting B is selected equivalent to the area frequency response characteristic β.

5.3 GA based FPI controllers

Because of intrinsic characteristics of the varying loads and intricacy of the power system, conventional control schemes may not offer acceptable solutions for AGC problems. Fuzzy logic controllers (FLCs) can be successfully applied to AGC problem for superior outcomes. A FLC includes four main modules: the fuzzification, the rule base, the inference engine and the defuzzification [94]. The fuzzifier converts the crisp value into fuzzy sets, therefore, this operation is called fuzzification. The rule base consists of mfs and control rules. The main component of the FLC is the inference engine, which executes all logic manipulations in a FLC. Lastly, the outcome of the inference process is an output represented by a fuzzy set, though the output of the FLC must be a crisp value. Consequently, fuzzy set is changed into a numeric value by using the defuzzifier, hence, this process is termed as defuzzification. The FPI controller (Fig. 5.2), designed to solve the two-area AGC problem, uses two input signals, viz., area control error (ACE) and derivative of ACE (dACE/dt) and the output signal (y), which is scaled to acquire control signal (ΔP_C) of the FPI controller [94]:

$$\Delta P_C = K_p y + \int K_i y dt \qquad (5.1)$$

For designing the FPI controllers, the output scaling factors K_p/K_i, control rules and mfs are to be determined. In the present study, 7 triangular mfs are selected for each input and the FPI output. So, 49 control rules are framed so that they can schedule output scaling factors. Appropriate rule base used in the study is taken from [92–94] and are detailed in Table 5.1. For the FPI controller shown in Fig. 5.2, a Mamdani fuzzy inference system (fis) is selected and the centroid method is used in defuzzification process.

Genetic algorithm (GA) is an artificial intelligent tuning method based on Darwinian theory of natural selection and survival of the fittest. The technique is similar to biological genetics, in which chromosome or string is made up by genes termed as binary bits or alleles. The chromosome organization is related to the parameters of the system under investigation. Though, in GA, an optimal solution is obtained employing intelligent utilization of a random search [266]. GA starts finding the optimal solution by creating an initial random population of several chromosomes. At every step, it computes the fitness value of each chromosome of the current population to generate the next generation. The fitness relates to the decoded value of the solution of the objective function, which is to be optimized. The fittest chromosomes are selected stochastically as parents to produce offspring for the next generation; however, the less fit chromosomes will pass away. Furthermore, roulette

Table 5.1
Rules of FPI controllers [92–94].

		dACE/dt						
		LN	**MN**	**SN**	**Z**	**SP**	**MP**	**LP**
	LN	LP	LP	LP	MP	MP	SP	Z
	MN	LP	MP	MP	MP	SP	Z	SN
	SN	LP	MP	SP	SP	Z	SN	MN
ACE	**Z**	MP	MP	SP	Z	SN	MN	MN
	SP	MP	SP	Z	SN	SN	MN	LN
	MP	SP	Z	SN	MN	MN	MN	LN
	LP	Z	SN	MN	MN	LN	LN	LN

LN: Large Negative, MN: Medium Negative, SN: Small Negative, Z: Zero, SP: Small Positive, MP: Medium Positive, LP: Large Positive
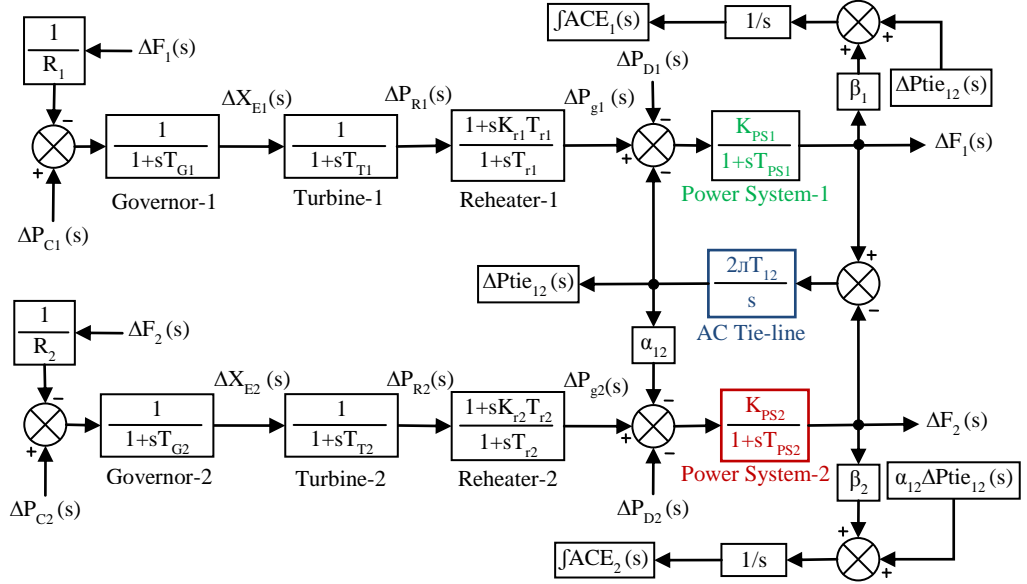
Fig. 5.1 Transfer function model of two-area reheat thermal power system.
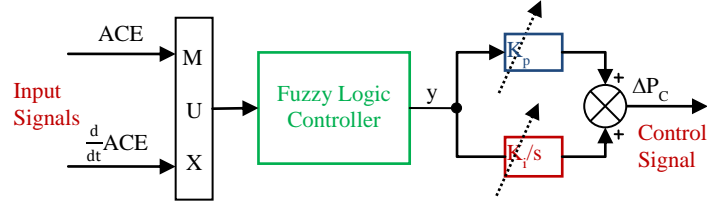
Fig. 5.2 Structure of FPI controller.
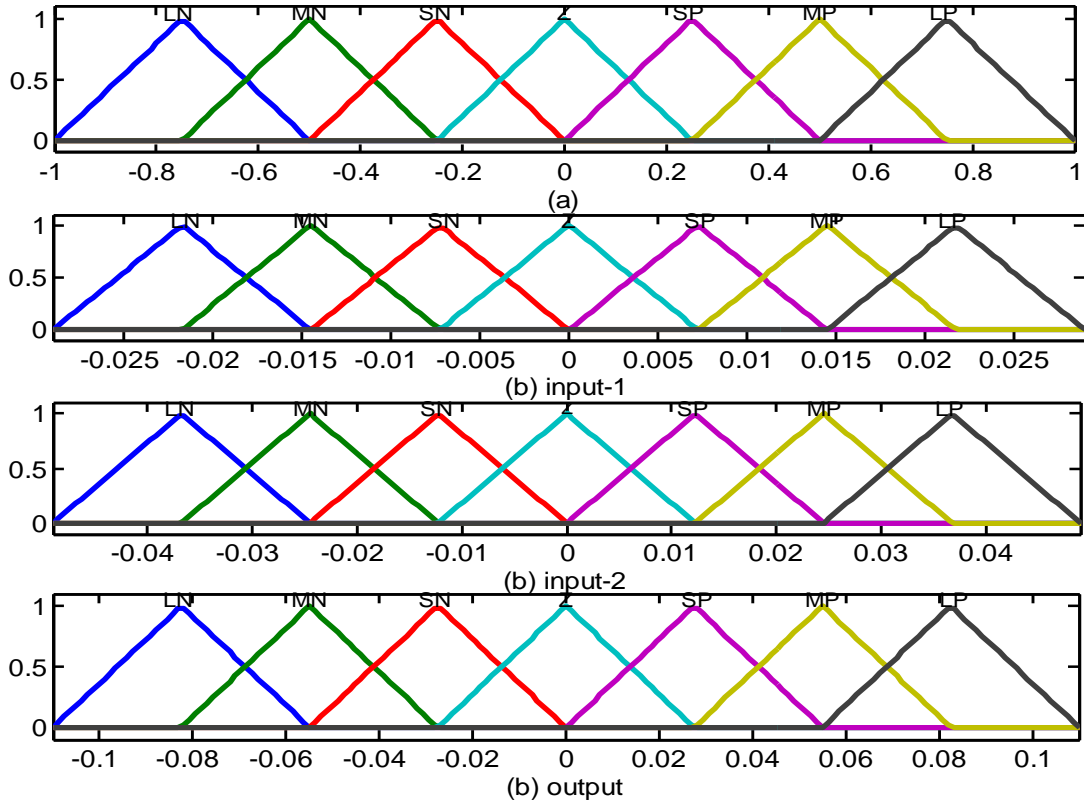
Fig. 5.3 Membership functions for FLC inputs and output (a) FPI-1 and (b) FPI-2.

wheel parent selection method is used here. An appropriate crossover probability should be selected to crossover a pair of chromosomes at a randomly chosen point to form two new offsprings. Based on some mutation probability, few offsprings undergo mutation operation to avoid suboptimal solution via premature convergence. Hence, a new population different from the old one is generated in every iteration. The total process is continued until optimal solution is attained.

In this study, the following objective function (J) is employed to get the optimal values of output scaling factors for area-1:

$$\text{Minimize J} = \int_0^T ACE_1^2 dt. \tag{5.2}$$

where, T is the time of simulation process. To optimize output scaling factors K_p/K_i of FPI-1; area-2 is kept uncontrolled and 2 variables with 10 bits for each are considered. Therefore, the chromosome length is 20 bits and the population size selected is 20. Crossover probability, mutation probability and number of generations are 0.8, 0.03 and 400, respectively. The optimal values of K_p and K_i are found to be 1.0110 and 2.891, respectively. The horizontal axis range of mfs for FPI-1 controller is taken as $[-1,1]$ for inputs and output mfs as shown in Fig. 5.3(a). The horizontal axis range of mfs for FPI-1 is optimized using GA to get FPI-2 controller. The universe of discourse (UOD), left base and right base of each triangular mfs of FPI-1 are selected as variables, hence, there are $16\{(2 \times 7) + 2\}$ variables. With 2 inputs and 1 output, FPI-1 has total $48(3 \times 16)$ parameters to be tuned. The UOD and left/right base are defined via upper and lower limit between which the optimum value is likely to exist to acquire minimum value of J stated in Eqn. (5.2). The mfs of FPI-2 controller are shown in Fig. 5.3(b). The similar methods are adopted and same tuned parameter values are obtained for area-2.

5.4 Simulation results and discussions

5.4.1 Two-area non-reheat thermal system

A two-area non-reheat thermal system is simulated considering 1% step load perturbation (SLP) at t = 0 s in area-1. To make comparison with the proposed FPI controllers, optimal PI controllers are also designed in the present study with the state vector of the order of [9×1] as given below:

State vector: $[X]^T = [X_1 X_2 \ X_3 \ X_4 X_5 \ X_6 X_7 \ X_8 \ X_9]$

$$= [\Delta F_1 \Delta P_{g1} \ \Delta X_{E1} \ \Delta F_2 \Delta P_{g2} \ \Delta X_{E2} \Delta P tie_{12} \int ACE_1 dt \int ACE_2 dt] \qquad (5.3)$$

Using the system data given in Appendix B, a MATLAB program written for optimal PI controllers is run to obtain optimal feedback gain matrix $[K^*]$ of [2×9] order given next, while the system results of ΔF_1, ΔF_2 and $\Delta P tie_{12}$ states are shown in Figs. 5.4(a-c).

$$K^* = \begin{bmatrix} 0.4246 & 0.6615 & 0.1628 & -0.0789 & -0.1148 & -0.0263 & -0.1773 & 1.0000 & 0.0000 \\ -0.0789 & -0.1148 & -0.0263 & 0.4246 & 0.6615 & 0.1628 & 0.1773 & -0.0000 & 1.0000 \end{bmatrix}$$

To show the superiority of the proposed FPI controllers, the results are compared with optimal PI controllers designed in the current study and several other controllers published recently and which are based on tuning methods like gravitational search algorithm (GSA) [136] and bacteria foraging optimization algorithm (BFOA) [144] based PID along with hybrid BFOA-particle swarm optimization (hBFOA-PSO) based PI controllers [146]. The enhancement in performance attained by the FPI controllers is apparent from the Figs. 5.4(a-c). It is concluded that the results due to FPI-1 controller are better than those offered by GSA: PID, BFOA: PID, optimal, hBFOA-J_1: PI and hBFOA-J_2: PI controllers. Analysis of the results plainly reveals that the performance of the system is notably enhanced further with FPI-2 compared to FPI-1. The numeric values of settling times (STs) and peak undershoots (PUs) for
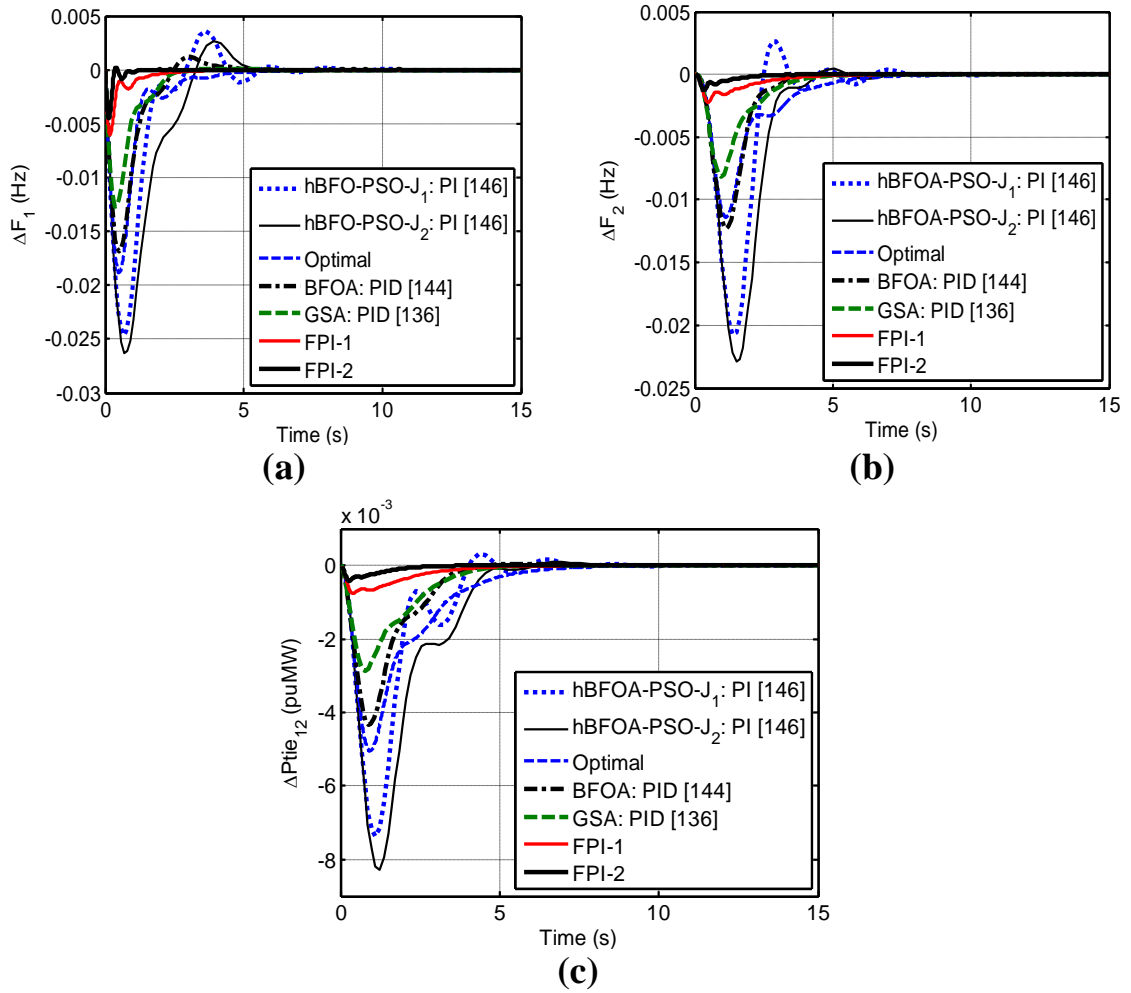
Fig. 5.4 System response with non-reheat turbine for SLP of 1% at t = 0 s in area-1 (a) ΔF_1, (b) ΔF_2 and (c) $\Delta Ptie_{12}$.

Table 5.2										
Numerical values of STs, PUs and PIs with non-reheat power system.										
Controller	STs (s)			PUs (–ve) (Hz or puMW)			PIs			
	ΔF_1	ΔF_2	$\Delta Ptie_{12}$	ΔF_1	ΔF_2	$\Delta Ptie_{12}$	ISE	ITSE	IAE	ITAE
hBFOA-PSO-J$_1$: PI [146]	5.36	6.15	3.814	0.0247	0.0204	0.00717	0.00094	0.00104	0.0729	0.1183
hBFOA-PSO-J$_2$: PI [146]	4.89	4.19	4.260	0.0262	0.0300	0.00825	0.00132	0.00165	0.0924	0.1492
Optimal	4.12	5.36	4.391	0.0188	0.0114	0.00503	0.00037	0.00035	0.0494	0.0817
BFOA: PID [144]	3.70	3.26	3.145	0.0168	0.0123	0.00433	0.00033	0.00029	0.0403	0.0493
GSA: PID [136]	2.32	3.68	3.097	0.0127	0.0081	0.00286	0.00016	0.00013	0.0289	0.0358
FPI-1	1.67	2.69	1.547	0.0060	0.0022	0.00075	1.49e^{-05}	9.07e^{-06}	0.0090	0.0134
FPI-2	**0.71**	**1.20**	**0.027**	**0.0045**	**0.0012**	**0.00041**	**4.15e^{-06}**	**1.15e^{-06}**	**0.0030**	**0.0038**

responses of change in frequency of area-1 (ΔF_1), area-2 (ΔF_2) and tie-line power

($\Delta Ptie_{12}$) states are shown in Table 5.2 for a tolerance band of ± 0.0005. Performance

of the controllers is also examined on the basis of different performance indices (PIs) such as integral of squared error (ISE), integral of time multiplied squared error (ITSE), integral of absolute error (IAE) and integral of time multiplied absolute error (ITAE) as stated follows:

$$\text{ISE} = \int (\Delta F_1^2 + \Delta F_2^2 + \Delta Ptie_{12}^2)dt \tag{5.4}$$

$$\text{ITSE} = \int (\Delta F_1^2 + \Delta F_2^2 + \Delta Ptie_{12}^2)t.\, dt \tag{5.5}$$

$$\text{IAE} = \int |\Delta F_1| + |\Delta F_2| + |\Delta Ptie_{12}|)dt \tag{5.6}$$

$$\text{ITAE} = \int |\Delta F_1| + |\Delta F_2| + |\Delta Ptie_{12}|)t.\, dt \tag{5.7}$$

The numerical values of STs, PUs and different PIs for various controllers under study are presented in Table 5.2. The simulation time of 15 s is considered for PIs of all controllers. After analysis, it is clearly evident that the values of STs/PUs and PIs such as ISE, ITSE, IAE and ITAE values are lowest with FPI-1 controller in comparison to others, except for the FPI-2 controller. Hence, it is concluded that FPI controllers are more capable of providing better performance with lesser values of STs/PUs/PIs compared to others.

5.4.2   *Two-area reheat thermal system*

The study is further extended by integrating the reheat effect in the non-reheat system model. Without varying the design, the FPI-1 and 2 controllers are implemented for AGC study of reheat thermal system shown in Fig. 5.1. The simulation results for ΔF_1, ΔF_2 and $\Delta Ptie_{12}$ under 1% SLP in area-1 at t = 0 s are shown in Figs. 5.5(a-c). The results of FPI controllers are compared with the literature containing three optimal PI [25], one PI [25] and one GA tuned I [124] controllers. The design details of optimal PI controllers used here is given in [25]. Critical scrutiny of the system

responses evidently indicate that the performance of the system is appreciably enhanced with the proposed FPI control approach in comparison to other methods.

The numerical values of STs, PUs and PIs are given in Table 5.3. The performance of GA tuned I controller [124] is better in comparison to conventional PI controller [25] in terms of same magnitude of PUs but less for STs and PIs of ΔF_1, ΔF_2 and $\Delta Ptie_{12}$ system results. The results of three optimal controllers [25] are far better than I controller while the performance of FPI-1 controller is better than that of optimal PI controllers. The numerical values of STs, PUs and PIs for all responses in case of FPI controllers are less than others and the least is with FPI-2. It is detected that for FPI-1/2 controller, due to the effect of reheater, all the numerical values of
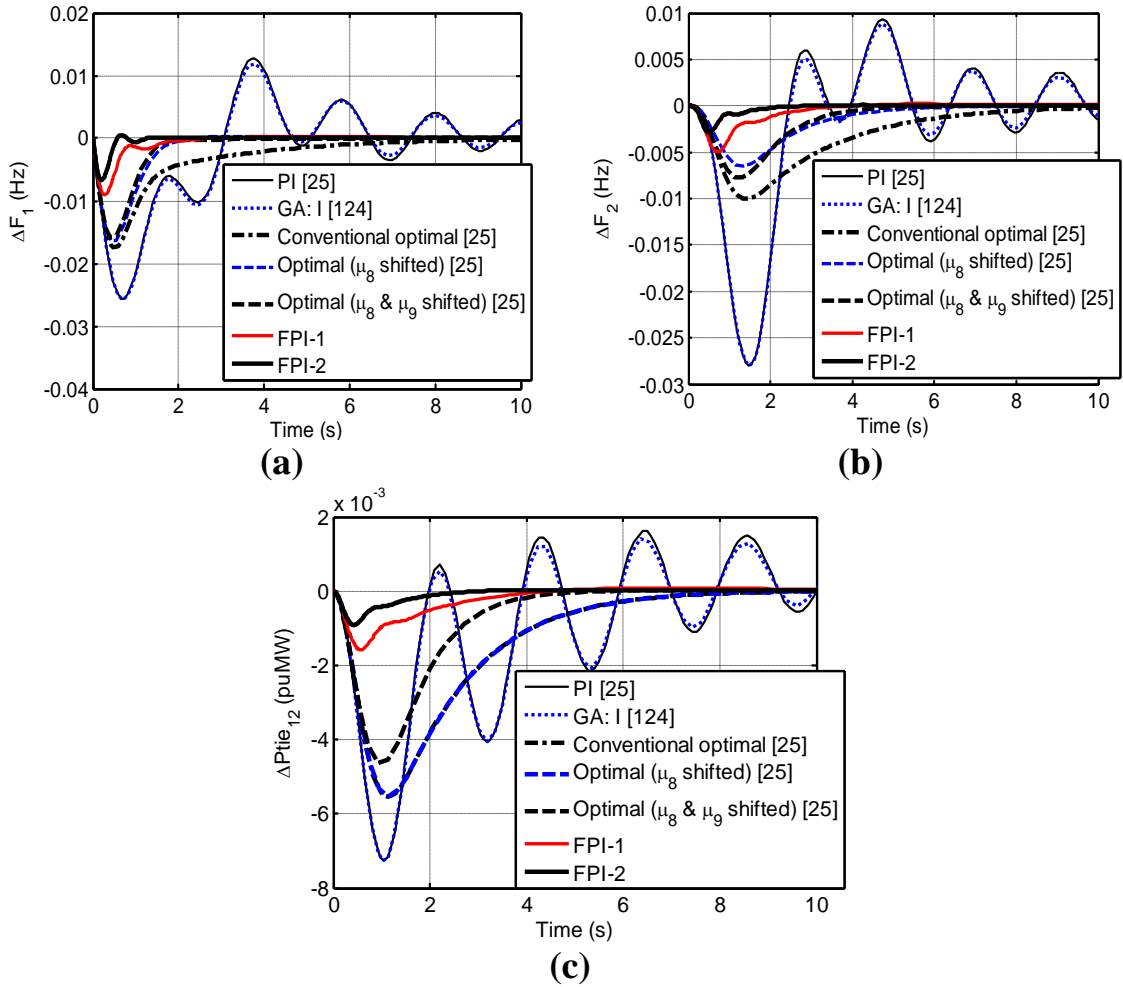
Fig. 5.5 System response with reheat turbine for SLP of 1% at t = 0 s in area-1 (a) ΔF_1, (b) ΔF_2 and (c) $\Delta Ptie_{12}$.

Table 5.3
Numerical values of STs, PUs and PIs with reheat power system.

Contr-oller	STs (s)			PUs (−ve) (Hz or puMW)			PIs			
	ΔF_1	ΔF_2	$\Delta Ptie_{12}$	ΔF_1	ΔF_2	$\Delta Ptie_{12}$	ISE	ITSE	IAE	ITAE
Conv. PI [25]	20.84	19.96	15.242	0.0257	0.0280	0.00724	0.00166	0.00327	0.1488	0.5798
GA: I [124]	16.64	17.62	14.938	0.0257	0.0280	0.00724	0.00164	0.00304	0.1424	0.5139
Conv. opt. [25]	7.73	8.18	5.147	0.0174	0.0100	0.00553	0.00050	0.00072	0.0760	0.1911
Optimal (μ_8) [25]	1.95	4.85	5.138	0.0166	0.0065	0.00552	0.00028	0.00027	0.0447	0.0766
Opt. (μ_8 & μ_9) [25]	1.79	4.07	3.194	0.0160	0.0078	0.00465	0.00025	0.00022	0.0363	0.0486
FPI-1	1.74	2.756	2.021	0.0090	0.0049	0.00157	$4.95e^{-05}$	$3.15e^{-05}$	0.0170	0.0400
FPI-2	**1.07**	**1.514**	**0.774**	**0.0067**	**0.0028**	**0.00091**	**$1.55e^{-05}$**	**$5.56e^{-06}$**	**0.0067**	**0.0119**

STs/PUs/PIs (given in Table 5.3) are increased in comparison with the values of non-reheat turbine given in Table 5.2 e.g., for FPI-1 controller the STs, PUs and PIs values of ΔF_1 response with non-reheat system are 1.67 s, −0.0060 Hz and ISE: $1.49e^{-05}$/ITSE: $9.07e^{-06}$/IAE: 0.0090/ITAE: 0.0134, respectively, while these values with reheat power system are 1.74 s, −0.0090 Hz and ISE: $4.95e^{-05}$/ITSE: $3.15e^{-05}$/IAE: 0.0170/ITAE: 0.0400, respectively. On the other hand, for FPI-2 controller STs, PUs and PIs values for ΔF_1 response with non-reheat system are 0.71 s, −0.0045 Hz and ISE: $4.15e^{-06}$/ITSE: $1.15e^{-06}$/IAE: 0.0030/ITAE: 0.0038, respectively and these values with reheat system are 1.07 s, −0.0067 Hz and ISE: $1.55e^{-05}$/ITSE: $5.56e^{-06}$/IAE: 0.0067/ITAE: 0.0119, respectively. It also authorizes the sluggish/degraded performance of reheat system compared to non-reheat system.

5.4.3 Multi-source hydrothermal system

To manifest the potential of FPI controllers to cope with dissimilar systems, the study is further extended to a multi-source hydrothermal system [100,103,150] as shown in Fig. 5.6. Each control area owns two generating units, one non-reheat thermal and one mechanical governor based hydro power plant. The relevant parameters are given in Appendix B.

The system results for 1.5% SLP in area-1 applied at t = 0 s using FPI controllers is shown in Figs.5.7(a-c). To make comparison, the simulation results of GA tuned PI [150] and hFA-PS tuned PI/PID controllers [150] are also shown in these figures. It is clear from Figs. 5.7(a-c) that the suggested FPI-2 controller outperforms the other considered controllers.

The numerical values of STs, PUs and PIs are given in Table 5.4. The PIs values are obtained for a simulation time of 20 s. It is observed from Table 5.4 that the performance is improving in the order: GA:PI → hFA-PS:PI → hFA-PS:PID → FPI-1 → FPI-2. It is concluded that the FPI approach demonstrate considerably better

Fig. 5.6 Transfer function model of multi-source hydrothermal power system.

Table 5.4									
Numerical values of STs, PUs and PIs with multi-source hydrothermal power system.									
Contro-ller	STs (s)			PUs (–ve) (Hz or puMW)			PIs			
	ΔF_1	ΔF_2	$\Delta Ptie_{12}$	ΔF_1	ΔF_2	$\Delta Ptie_{12}$	ISE	ITSE	IAE	ITAE
GA: PI [150]	10.48	15.45	6.292	0.0277	0.0187	0.00618	0.00090	0.00114	0.0909	0.29160
hFA-PS: PI [150]	5.35	6.18	4.480	0.0287	0.0195	0.00679	0.00090	0.00085	0.0706	0.11960
hFA-PS: PID [150]	2.95	4.53	3.309	0.0134	0.0066	0.00227	0.00011	$8.50e^{-05}$	0.0256	0.04201
FPI-1	1.84	3.09	2.112	0.0096	0.0035	0.00117	$3.73e^{-05}$	$2.08e^{-05}$	0.0140	0.03532
FPI-2	**0.90**	**1.93**	**1.038**	**0.0080**	**0.0024**	**0.00075**	**$1.65e^{-05}$**	**$5.73e^{-06}$**	**0.0070**	**0.01652**

Fig. 5.7 System response with multi-source hydrothermal for SLP of 1.5% at t = 0 s in area-1 (a) ΔF_1, (b) ΔF_2 and (c) $\Delta Ptie_{12}$.

results in terms of less STs, PUs, PIs and oscillations compared to recently published best claimed hFA-PS technique tuned PI/PID controllers [150].

5.4.4 Restructured two-area reheat thermal system

In the present study, each area of the two-area system owns two GENCOs (single reheat thermal units) and two DISCOs. The transfer function block diagram of the system is shown in Fig. 5.8. The DPM selected is given as follows:

$$
\text{DPM} = \begin{bmatrix} 0.40 & 0.25 & 0.75 & 0.30 \\ 0.30 & 0.20 & 0.00 & 0.25 \\ 0.20 & 0.20 & 0.25 & 0.25 \\ 0.10 & 0.35 & 0.00 & 0.20 \end{bmatrix}.
\tag{5.8}
$$

A hybrid transaction in scenario 3 of reference [343] is considered where all DISCOs have contracts with GENCOs. Let, the DISCO-1, DISCO-2, DISCO-3 and DISCO-4 demands $\Delta P_{L1} = 0.15$ puMW, $\Delta P_{L2} = 0.05$ puMW, $\Delta P_{L3} = 0.15$ puMW and $\Delta P_{L4} = 0.05$ puMW, respectively from GENCOs defined by Eqn. (5.8). The steady state output of GENCOs is given by Eqns. (3.29 or 5.9) as [241,343]:

$$\Delta P_{Gi} = cpf_{i1}\Delta P_{L1} + cpf_{i2}\Delta P_{L2} + cpf_{i3}\Delta P_{L3} + cpf_{i4}\Delta P_{L4}, \; i = 1, \ldots, 4. \tag{5.9}$$

Consequently, $\Delta P_{G1} = 0.2$ puMW, $\Delta P_{G2} = 0.0675$ puMW, $\Delta P_{G3} = 0.09$ puMW, $\Delta P_{G4} = 0.0425$ puMW. In addition, DISCO-1 demands 0.1 puMW of glut power. As a result, $\Delta P_{D1} = 0.3$ puMW and $\Delta P_{D2} = 0.2$ puMW. ACE participation factors (apfs) are taken as: $apf_1 = 0.75$, $apf_2 = 0.25$ and $apf_3 = apf_4 = 0.5$. Hence, $\Delta P_{G1} = 0.2 + 0.075 = 0.275$ puMW, $\Delta P_{G2} = 0.0675 + 0.025 = 0.0925$ puMW and $\Delta P_{G3}/\Delta P_{G4}$ will be unaffected. The scheduled tie-line power flow from control area-1 to control area-2 is given as the total power exported from control area-1 minus total power imported to control area-1 as stated in Eqns. (3.28 or 4.5). Hence, $\Delta Ptie_{scheduled} = 0.0675$ puMW.

The system is simulated using BFOA tuned integral (I) [343], optimal and the proposed FPI controllers. The state vector of order [17×1] chosen for optimal controller is given as:

$$[X]^T = [\Delta F_1 \Delta F_2 \Delta Ptie_{actual} \; \Delta P_{G1} \; \Delta P_{G2} \; \Delta P_{G3} \; \Delta P_{G4} \; \Delta P_{R1} \; \Delta P_{R2} \; \Delta P_{R3} \; \Delta P_{R4}$$

$$\Delta X_{E1} \Delta X_{E2} \; \Delta X_{E3} \; \Delta X_{E4} \int ACE_1 dt \int ACE_2 dt]. \tag{5.10}$$

The optimal feedback gain matrix [K^*] of order [2×17] for optimal controller is obtained via codes written in MATLAB as:

$$K^* = \begin{bmatrix} 0.3159 & -0.0597 & -0.1951 & 2.1627 & 2.1627 & -0.1941 & -0.1941 & -0.7747 & -0.7747 \\ -0.0597 & 0.3159 & 0.1951 & -0.1941 & -0.1941 & 2.1627 & 2.1627 & 0.0399 & 0.0399 \end{bmatrix}$$

$$\begin{bmatrix} 0.0399 & 0.0399 & 0.0786 & 0.0786 & -0.0141 & -0.0141 & 1.0000 & -0.0000 \\ -0.7747 & -0.7747 & -0.0141 & -0.0141 & 0.0786 & 0.0786 & 0.0000 & 1.0000 \end{bmatrix}.$$
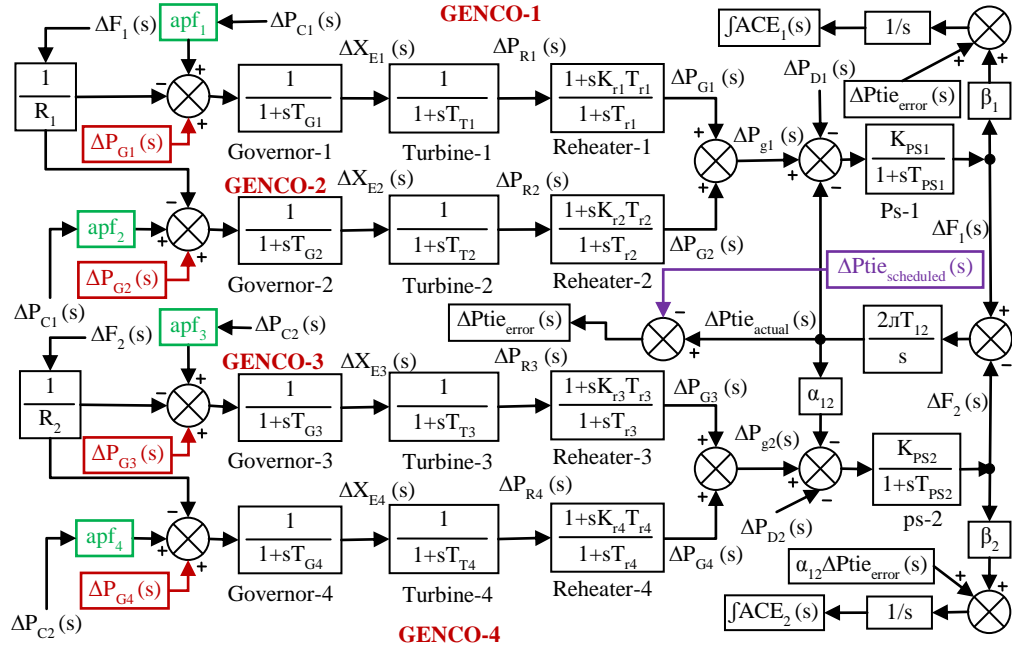
Fig. 5.8 Transfer function model of restructured reheat thermal system.

(a)

(b)

(c)

(d)
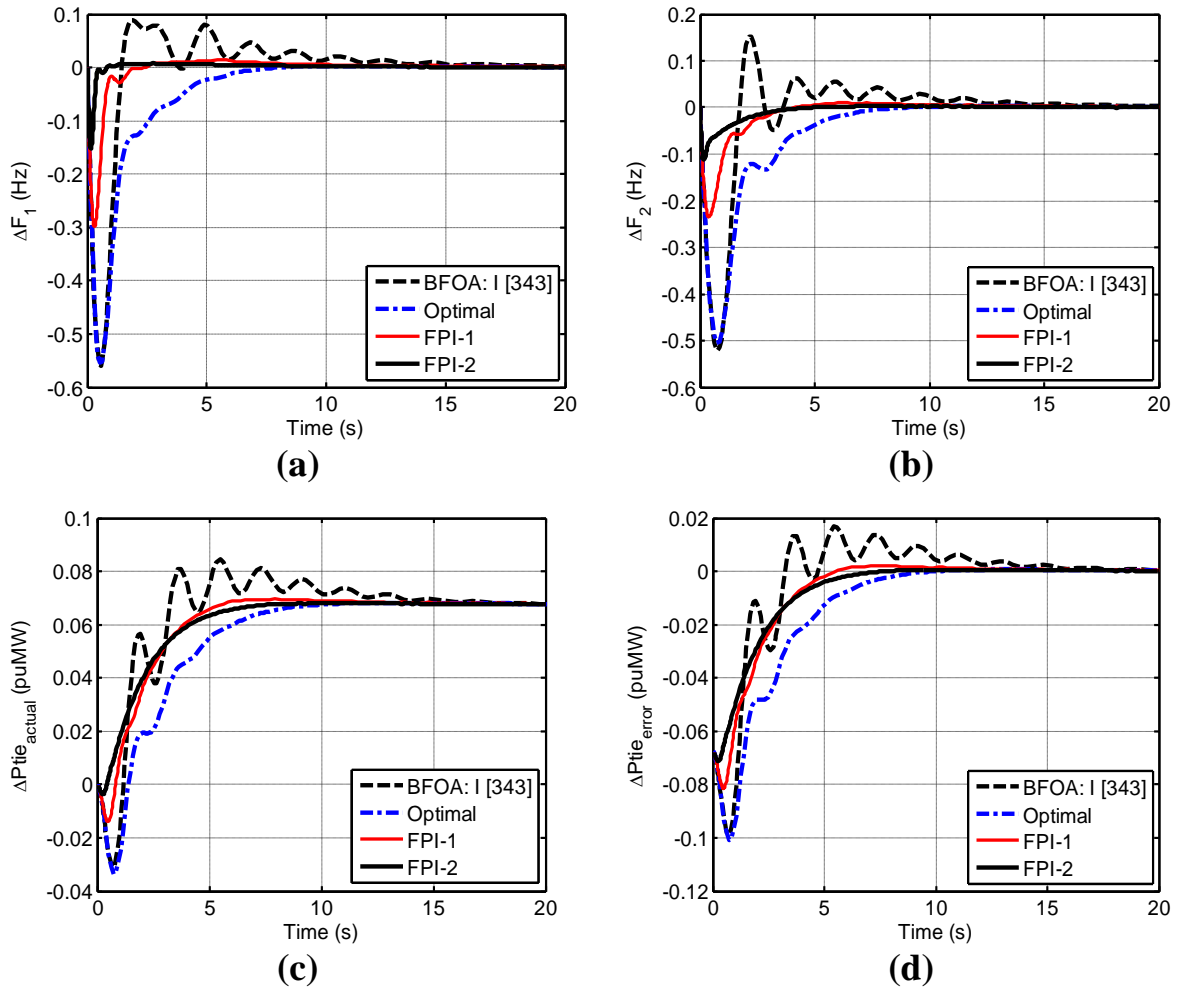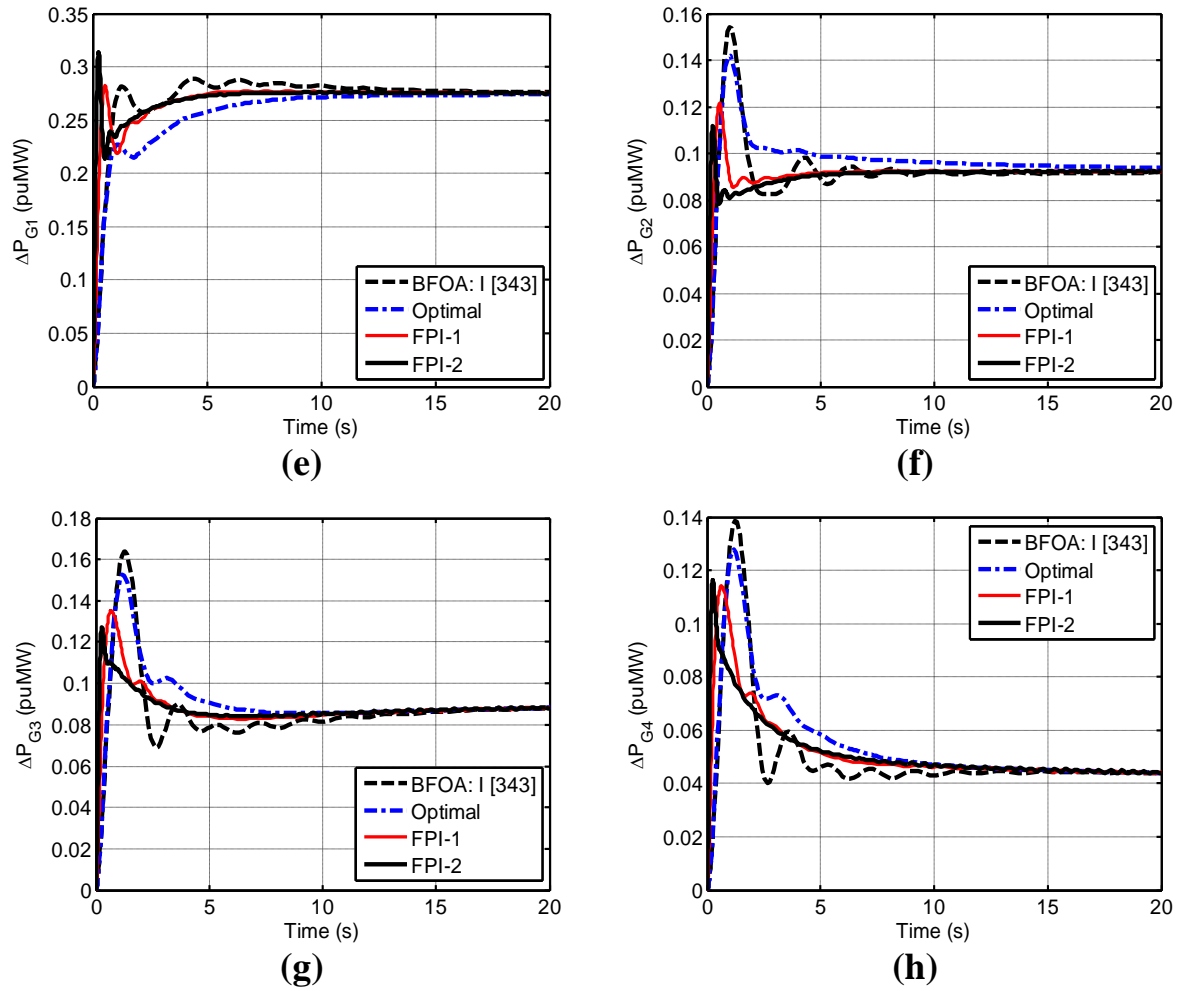
Fig. 5.9 System response with restructured reheat thermal system at SLPs in areas at t = 0 s (a) ΔF_1, (b) ΔF_2, (c) $\Delta Ptie_{actual}$,(d) $\Delta Ptie_{error}$, (e) ΔP_{G1},(f) ΔP_{G2}, (g) ΔP_{G3} and (h) ΔP_{G4}.

Table 5.5
Numerical values of STs, PUs and PIs with restructured reheat thermal power system.

Contro-ller	STs (s)			PUs (–ve) (Hz or puMW)			PIs			
	ΔF_1	ΔF_2	$\Delta Ptie_{error}$	ΔF_1	ΔF_2	$\Delta Ptie_{error}$	ISE	ITSE	IAE	ITAE
BFOA: I [343]	10.73	10.12	2.918	0.5583	0.5210	0.0988	0.48670	0.49630	2.1320	7.654
Optimal	5.38	5.93	4.235	0.5542	0.5041	0.1009	0.5547	0.5529	2.1420	4.558
FPI-1	1.55	2.82	2.712	0.2991	0.2342	0.0814	0.08141	0.05305	0.7870	2.322
FPI-2	**0.37**	**2.24**	**2.571**	**0.1513**	**0.1120**	**0.0713**	**0.01760**	**0.01292**	**0.3969**	**1.065**

The simulation results are shown in Fig. 5.9. It is palpable from Figs. 5.9(a-b) that ΔF_1

and ΔF_2 due to each controller settle to zero in steady state and therefore convince the

AGC requirements. In addition, $\Delta Ptie_{actual}$ (Fig. 5.9(c)) equates to $Ptie_{scheduled}$ in steady

state (0.0675 puMW), thus $\Delta Ptie_{error}$ settles to zero as shown in Fig. 5.9(d). The

generations are equal to the desired (calculated) values as shown in Figs. 5.9(e-g). Critical analysis of the results shown in Fig. 5.9 clearly reveals that all controllers gratify the AGC obligations and the optimal controller offers slightly improved results over BFOA optimized I controller, while significant improvement is observed with proposed FPI controllers. Additionally, the superiority of FPI-2 controller is evident from Table 5.5 with least values of STs (for a band of ±0.02), PUs and PIs (for simulation time of 20 s) for dynamic responses of ΔF_1, ΔF_2 and $\Delta Ptie_{error}$.

5.5 Conclusion

In this chapter, fuzzy PI (FPI) control strategy for AGC of interconnected traditional/restructured electrical power systems is analyzed. Two FPI i.e., FPI-1 and FPI-2 controllers are designed and applied on traditional two-area non-reheat/reheat/multi-source hydrothermal and restructured reheat thermal power systems. GA technique is used to tune output scaling factors and horizontal range of membership functions (mfs). In order to advance the dynamic performance of the system, the horizontal range of mfs of FPI-1 is optimized to get FPI-2. The proposed controllers are first implemented on a traditional two-area non-reheat thermal system. The results yielded by the FPI controllers are compared with optimal PI controllers and other conventional controllers tuned employing BFOA, GSA and hBFOA-PSO algorithms. The comparative study is performed in terms of settling times (STs), peak undershoots (PUs) and various performance indices (PIs). It is found that the suggested controllers provide better performance compared to others. Further, the study is extended to a two-area reheat thermal system and without redesigning, the FPI controllers are applied in this model and it is observed that the proposed controllers show noticeably superior concert compared to three optimal PI controllers,

103

one proportional integral (PI) and one GA based integral controllers in terms of less numerical values of STs/PUs/PIs. Furthermore, the effectiveness of the FPI controllers is tested on a multi-source hydrothermal system. It is noticed that the suggested method optimized for two-area non-reheat system ensures improved dynamic performance over conventional controllers tuned using GA and hFA-PS tuning methods. To point out the potential of the proposed approach to cope with the restructured systems, finally, the study is extended to a restructured two-area reheat thermal system and effectiveness of the method is established over optimal and BFOA tuned I controller. Consequently, the results find out from the MATLAB/SIMULINK simulations, establish that the proposed control strategy is effective, robust, simple and easy-to-implement. It attains enhanced dynamic performance and thus, improves the quality and reliability of the electric power supplied to the customers.

CHAPTER 6

BFOA BASED FUZZY PI/PID CONTROLLER FOR AGC OF TWO-AREA POWER SYSTEMS

6.1 Introduction

In industrial processes, the use of classical proportional integral derivative (PID) controller is extensive due to its simple design, effectiveness for linear systems, robustness and less cost. Though, for higher order systems with time delays, nonlinearities and uncertainties, classical PID controller might not be a capable choice. On the other hand, fuzzy logic controller (FLC) is valuable to enhance the closed-loop performance of PID controller and competent to take care of small deviations in operating point or system parameters by tuning the controller parameters. Fuzzy based PID controller is effective for all nonlinear systems, but parameters of FLC may not be most favorable as their selection is based usually on certain experiential rules. FLC tuning via rules and membership functions (mfs) is a very complicated task that enhances the complexity of the controller optimization task. Hence, FLC tuning process via rules and mfs may be avoided. Due to simplicity, the most widespread method of FLC tuning is the tuning of input and output scaling factors just like tuning of a conventional controller gains. Thus, standard rule base and mfs may be utilized for different applications and input and output scaling factors can be optimized to design an optimum fuzzy PI/PID controller [89,104,107,151,293]. A simplified fuzzy PI (FPI) configured controller is visualized for AGC of different systems [151], where tuned input scaling factors i.e., ACE and its derivative are used as the input to the FLC. The output of the FLC is connected to a conventional PI

controller with optimized gains (output scaling factors) to get the desired control signal. With standard rule base/mfs, the input/output scaling factors of FPI controller are optimized employing hybrid particle swarm optimization-pattern search (PSO-PS) [151] and hybrid differential evolution-pattern search (DE-PS) [104] tuning methods to achieve the desired performance. For higher order systems, a FPI controller during the transient phase may not display fine performance because of its internal integration operation. To arrive at an overall enhanced recitation, generally fuzzy PID (FPID) controller is suggested [89,104,107,293]. A bacterial foraging optimization algorithm (BFOA) based fuzzy integral double derivative structured controller is proposed with optimized mfs and output scaling factors for AGC of a traditional three-area hydrothermal system [99]. Though, input scaling factors are not tuned but this controller offers a good performance over its conventional counterpart. A firefly algorithm (FA) optimized FPID structured controller shows superior results in comparison to conventional I/PI/PID structured controller optimized using the same technique for AGC of a restructured four-area thermal system [293].

From the literature study, it is observed that the performance of AGC systems depends largely on the kind of optimization method used and structure of the supplementary controller utilized. In context to FLC, various intelligent techniques and structures are existing in the literature [87–111,273–296]. To the authors' best knowledge, no research is reported in the literature so far to design BFOA optimized FPI/FPID structured controller for AGC study of traditional or restructured electric power systems. Hence, additional study is required. Contrasted with the prevalent methods in the literature, the advantages of the suggested FPI/FPID controller are observed through the simulation results on different traditional and restructured system models. Moreover, the design technique is very easy to realize.

106

6.2 Bacterial foraging optimization algorithm

Recently, bacterial foraging optimization algorithm (BFOA), a powerful nature-inspired evolutionary computation technique was introduced as a new method in which the foraging (methods of locating, handling and ingesting food) behavior of Escherichia coli (E. coli) bacteria present in our intestine is mimicked. Since the maiden application of BFOA to AGC problem of a traditional three-area thermal system by Nanda et al., [142], many papers have been witnessed in the literature for different AGC systems [99,143–146,340–344]. BFOA follow the law of natural evolution, which favors species with better food searching ability and eliminates those with deprived search capability. The genes of stronger species possibly propagate in the evolution chain since they show the greater ability to reproduce better future generations. The foraging strategy of E. coli bacteria can be subdivided into four developments namely chemotaxis, swarming, reproduction, and elimination-dispersal [142]. These four operations among the bacteria are used for searching the total solution space.

6.2.1 Chemotaxis

Chemotaxis process is attained through swimming and tumbling via flagella of E. coli bacteria. In the entire lifetime, the revolution of flagella in each bacterium decides whether it should move in a pre-specified direction (swimming) or altogether in different directions (tumbling). Mathematically, tumble of any bacterium can be defined by $\phi(j)*C(i)$, where $\phi(j)$ is unit length of random direction and $C(i)$ is step length of that bacterium. Let, 'j' is the index of chemotactic step, 'k' is reproduction step and 'l' is the elimination-dispersal event, then $\theta^i(j+1,k,l)$ is the position of ith bacteria at j^{th} chemotactic step, k^{th} reproduction step and l^{th} elimination-dispersal

event. In the next chemotatic step, the position of the bacteria after a tumble is given by Eqn. (6.1).

$$\theta^i(j+1,k,l) = \theta^i(j,k,l) + C(i)\phi(j) \tag{6.1}$$

6.2.2 Swarming

During foraging the bacterium which discovered best food location provides an attraction signal till a point of time in the search period to other bacteria so that they can swarm together in a group to converge at the desired location more rapidly. In other words, the effect of swarming is to congregate the bacteria into groups and hence travel as concentric patterns of groups with high bacterial density. Mathematically swarming process is represented by

$$J_{cc}(\theta, P(j,k,l)) = \sum_{i=1}^{S} J_{cc}^i\left(\theta, \theta^i(j,k,l)\right)$$

$$= \sum_{i=1}^{S}\left[-d_{attract}\exp\left(-w_{attract}\sum_{m=1}^{p}\left(\theta_m - \theta^i_m\right)^2\right)\right] + \sum_{i=1}^{S}\left[h_{repelent}\exp\left(-w_{repelent}\sum_{m=1}^{p}\left(\theta_m - \theta^i_m\right)^2\right)\right]$$

$$\tag{6.2}$$

where $J_{cc}(\theta, P(j,k,l))$ is the relative distance of each bacterium from the optimum bacterium or the cost function value to be added to the actual cost function to be minimized to present a time varying cost function. S is the total number of bacteria and p is the total number of parameters to be optimized, θ^m is the position of the fittest bacteria and $d_{attract}$, $\omega_{attract}$, $h_{repelent}$ and $\omega_{repelent}$ are the various coefficients characterizing swarm behavior which are to be chosen accurately.

6.2.3 Reproduction

At reproduction step, the healthiest bacteria (those yielding lower value of objective function) will reproduce and the least healthy bacteria will die. The healthier bacteria

replace unhealthy one, which is eliminated owing to their poorer foraging capabilities. This makes the population of bacteria invariable in the evolution process.

6.2.4 *Elimination and dispersal*

In the evolution process, a gradual or abrupt unexpected incident in the local environment where a bacterium population lives may drastically alter the even practice of evolution. Events can occur in such a manner that all the bacteria in a region are killed due to significant increase in heat (elimination) or a group is scattered into a new location/environment due to sudden flow of water (dispersal). These events may possibly destroy the chemotactic progress, but they also have the effect to support chemotaxis, as dispersal may position a newer set of bacteria nearer
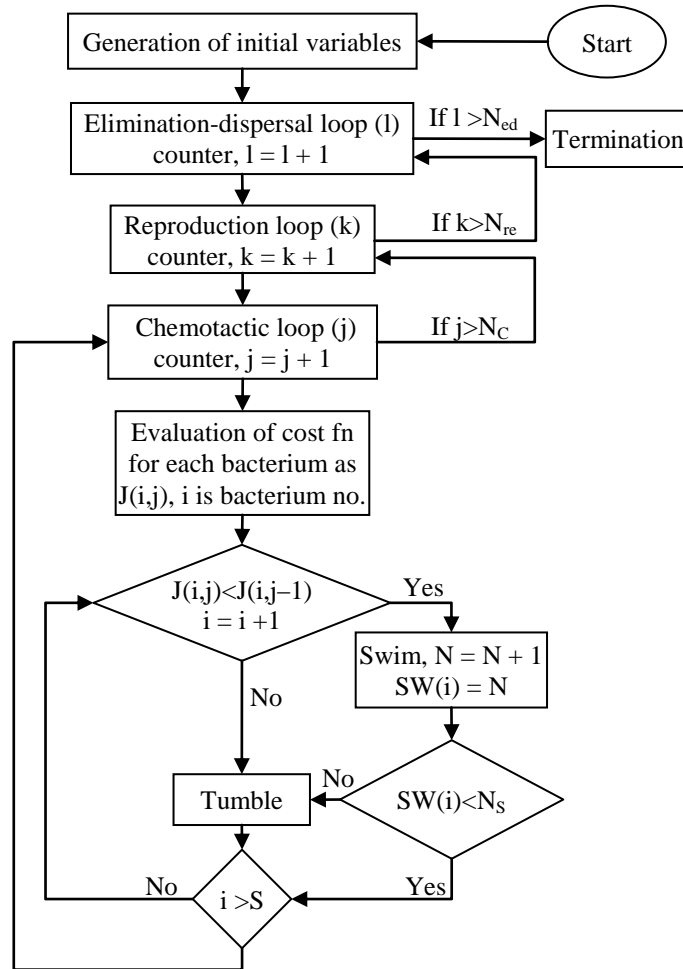
Fig. 6.1 Flow chart of BFOA for tuning FPI/FPID controller parameters.

good food locations. In a broad perspective, elimination and dispersal are elements of the population-level long-distance motile behavior. Elimination-dispersal step helps to avoid the behavior of stagnation (trapping the optimization process in a premature local optima point) often observed in such parallel search algorithms. In BFOA, to simulate this incident, some bacteria are liquidated haphazardly with a very small prospect while the new replacements are randomly loaded over the search space.

In the present simulation work, BFOA is initialized considering (a) No. of parameters to be optimized, p = 4 or 5, (b) No. of bacteria to be used for total search space, S = 6, (c) Swimming length, N_S = 3, (d) No. of iterations to be undertaken in a chemotactic loop, N_C = 5 ($N_C > N_S$), (e) Maximum no. of reproduction steps by bacteria, N_{re} = 15, (f) Maximum no. of elimination and dispersal events, N_{ed} = 2, (g) Probability with which the elimination and dispersal will prolong, P_{ed} = 0.25, (h) The location of each bacterium p specified by values attained using the trial and error method, (i) The value of step size taken in the random direction, $C(i)$, i = 1,2,…,S, is assumed to be constant for all bacteria to simplify the design approach, (j) The magnitude of secretion of attractant by a cell, $d_{attract}$ = 0.01, (k) The chemical cohesion signal diffuses (smaller makes it diffuse more), $\omega_{attract}$ = 0.04, (l) The repellant (tendency to avoid nearby cell), $h_{repelent}$ = 0.01 and (m) The width of the repellant, $\omega_{repelent}$ = 10. The value of $d_{attract}$ and $h_{repelent}$ must be equivalent so that the penalty compelled on the cost function through J_{cc} of Eqn. (6.2) will be zero when all the bacteria will have equal value i.e., they have converged. The, flow chart of BFOA is shown in Fig. 6.1.

6.3 Systems investigated

Investigations are carried out on traditional two-area non-reheat, reheat thermal, multi-source hydrothermal and restructured multi-source hydrothermal power

systems. Area capacity of each system under study is 2000 MW with nominal initial loading of 1000 MW. The model of traditional two-area reheat thermal system with FPI/FPID controller is shown in Fig. 6.2 and that of traditional/restructured multi-source hydrothermal system in Fig. 6.7. The nominal parameters of non-reheat system are taken from [145], for reheat system from [129] and for multi-source hydrothermal system from [100] and given in Appendix B. The detailed description of the models under study is provided in Chapter 3.
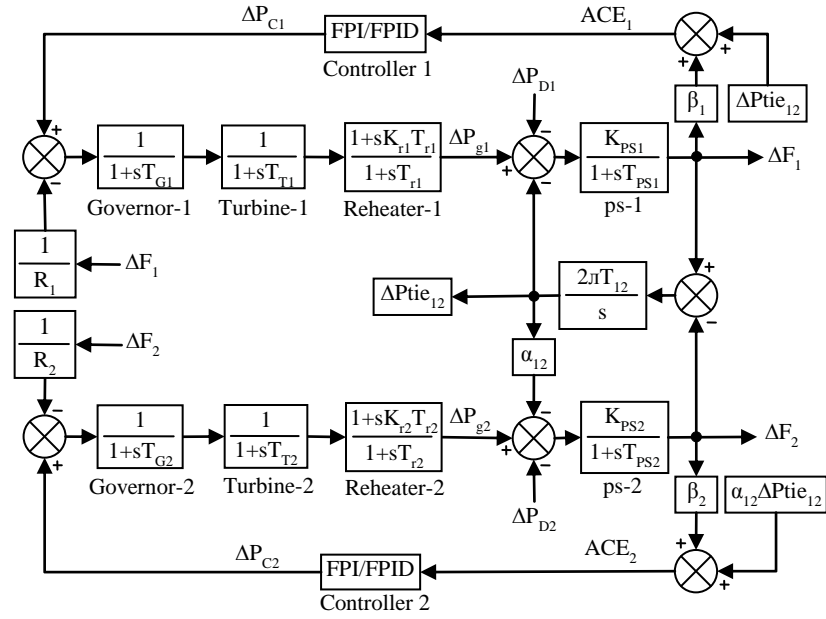

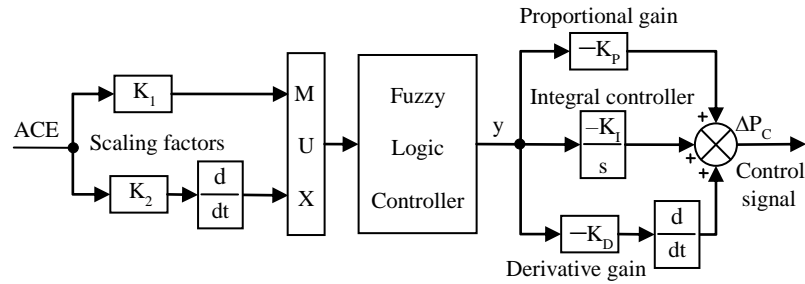**Fig. 6.2**   Model of two-area reheat thermal power system.

Fig. 6.3   Structure of FPID controller [104,107].

111

6.4   Controller structure

To solve AGC problem, FPI/FPID controller is provided in both areas of the two-area systems under study. The FPID controller structure is shown in Fig. 6.3 [104,107]. The error input is the respective area control error (ACE). ACE and derivative of ACE are the inputs to the FLC. The FLC output y is multiplied with K_P, K_I and K_D and then summed to get the output ΔP_{Ci} of FPI/FPID controller. ΔP_C is the control input of the system. The K_P, K_I and K_D represent the proportional, integral and derivative gains of the FLC, respectively. K_1/K_2 (input scaling factors) and $K_P/K_I/K_D$ (output scaling factors) are the parameters to be tuned employing BFOA via minimization of an objective function. For FPI, the derivative path will be excluded from Fig. 6.3. Usually, triangular, trapezoidal, bell and Gaussian shaped membership functions (mfs) are preferred owing to easy functional representation, less memory

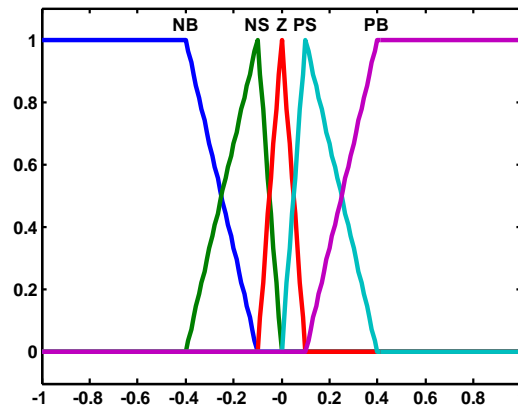**Fig. 6.4**   Membership functions of FPI/FPID controller for ACE, ACE derivative and FLC output [104,151].

Table 6.1

Rule base for ACE, ACE derivative and FLC output.

	ACE derivative				
ACE	NB	NS	Z	PS	PB
NB	NB	NB	NB	NS	Z
NS	NB	NS	NS	Z	PS
Z	NB	NS	Z	PS	PB
PS	NS	Z	PS	PS	PB
PB	Z	PS	PB	PB	PB

112

requirement for the storage and efficient in handling by the fuzzy inference system (fis). However, triangular mfs are usual in FLC designs of real time applications because of their economical and improved outcome compared to other options [104,293]. Therefore, in the present study five triangular mfs are utilized with five fuzzy linguistic variables like NB (negative big), NS (negative small), Z (zero), PS (positive small) and PB (positive big) for both inputs and output of the fuzzy controller. The mfs for ACE, ACE derivative and FLC output are shown in Fig. 6.4. Identical mfs with identical horizontal range are employed for both inputs and output of FLC [104,151,293]. Mamdani fis and centroid defuzzification method are selected for the study. The control signal of FPI/FPID controller is given by

$$\Delta P_{Ci} \text{ (FPI)} = K_P y + K_I \int y dt, \ i = 1,2, \tag{6.3}$$

$$\Delta P_{Ci} \text{ (FPID)} = K_P y + K_I \int y dt + K_D \frac{dy}{dt}, \ i = 1,2. \tag{6.4}$$

The two-dimensional rule base for ACE, ACE derivative and FLC output consisting of twenty five rules is shown in Table 6.1. Identical FPI/FPID controller is designed for the identical two-area systems.

6.5 Optimization problem

The main purpose of an optimization problem is to lessen an objective function selected for the system considering an appropriate performance index. The performance of an optimization method largely depends on the selection of a suitable performance index. In this study, integral of squared error (ISE) is used as a performance index (J) to design the BFOA-FPI/FPID controller. The mathematical expression for J, which is the amalgamation of the tie-line power flow ($\Delta Ptie_{12}$) and frequency deviations (ΔF_1 and ΔF_2) of the two-area system, is stated in Eqn. (5.4) as:

$$ISE = J = \int_0^T (\Delta F_1^2 + \Delta F_2^2 + \Delta Ptie_{12}^2) dt. \tag{6.5}$$

113

where, T is the simulation time. The optimum solution is found out at the lowest value of J. The constraints of the optimization problem are the gains/parameters of FPI/FPID controller inside some pre-specified limits. Hence, the controller design task can be developed as the following optimization problem:

Minimize J, subject to

$K_1^{min} \leq K_1 \leq K_1^{max}$, $K_2^{min} \leq K_2 \leq K_2^{max}$, $K_P^{min} \leq K_P \leq K_P^{max}$, $K_I^{min} \leq K_I \leq K_I^{max}$ (FPI controller), $\hspace{3cm}$ (6.6)

$K_1^{min} \leq K_1 \leq K_1^{max}$, $K_2^{min} \leq K_2 \leq K_2^{max}$, $K_P^{min} \leq K_P \leq K_P^{max}$, $K_I^{min} \leq K_I \leq K_I^{max}$,

$K_D^{min} \leq K_D \leq K_D^{max}$ (FPID controller). $\hspace{3cm}$ (6.7)

The superscripts min and max stand for the minimum and the maximum values of the respective parameter. The choice of the range of superscripts influences the final best solution largely. The minimum and maximum values of the parameters are selected as 0.0 and 2.0, respectively [104,151]. The motivation of minimizing J is to find out the most favorable scaling factors or gains of the controller, which may yield the desired AGC performance. Each bacterium is allowed to take all likely values within pre-specified range and J is reduced to obtain the optimal gains of the controller. The total tunable parameters for FPI (K_1, K_2, K_P and K_I) and FPID (K_1, K_2, K_P, K_I and K_D) controllers would be 4 and 5, respectively. The BFOA optimization process for each model under study is repeated 20 times and the best final solution

Table 6.2								
BFOA optimized FPI/FPID controller parameters.								
Para-meters	Non-reheat		Reheat		Multi-source		Restructured multi-source	
	BFOA: FPI	BFOA: FPID	BFOA: FPI	BFOA: FPID	BFOA: FPI	BFOA: FPID	BFOA: FPI	BFOA: FPID
K_1	1.9902	1.9999	1.1645	1.6601	1.8978	1.9904	0.8023	0.5956
K_2	0.9509	0.7990	0.6711	0.9576	1.1525	1.1099	0.4512	0.3222
K_P	0.5514	1.2914	0.5336	0.6017	0.4111	1.1532	0.9836	1.8231
K_I	0.7991	1.3991	0.7936	1.7598	0.4412	1.0502	1.2082	1.6991
K_D	−	0.0311	−	0.0121	−	0.0719	−	0.0813
An entry "−" means not applicable.								

is chosen as the gains of the controller [104,146]. The best final optimal results obtained for various power system models under study are displayed in Table 6.2. To study the comparative evaluation between the suggested approach and the other techniques published recently, the settling times (STs) and peak undershoots (PUs) of tie-line/frequency deviation results under step load perturbation (SLP) are calculated at the program written in MATLAB software. The numeric values of STs/PUs/PIs indicate the speed of a dynamic response. To set up additional comparisons, in addition to the ISE defined via Eqn. (6.5), three extra performance indices (PIs) like integral of time multiplied squared error (ITSE), integral of absolute error (IAE) and integral of time multiplied absolute error (ITAE) are also computed. These three PIs are stated by Eqns. (5.5–5.7) [100,107]. The Results in terms of STs/PUs/PIs showing best performance are **bold faced** in their respective tables.

6.6   Simulation results and discussions

6.6.1   *Two-area non-reheat thermal system*

A two-area non-reheat thermal system is simulated using data given in Appendix B and considering a big 10% SLP at t = 0 s in area-1. The system model shown in Fig. 6.2 clearly portrays the grid connections and position of SLP inputs. However, reheater blocks presented in area-1 and area-2 of Fig. 6.2 are not parts of this system. The system dynamic results for ΔF_1, ΔF_2 and $\Delta Ptie_{12}$ responses are shown in Figs. 6.5(a-c). To show the advantage of the proposed approach, the simulation results with some recently published approaches like BFOA [145], PSO [146], hybrid BFOA-PSO [146] and FA [148] tuned PI structured controller as well as PS [151] and PSO [151] tuned FPI structured controller are also displayed in Figs. 6.5(a-c). Critical examination of Figs. 6.5(a-c) clearly reveals that substantial improvements are observed with the proposed BFOA tuned FPI controller compared to PI/FPI

controller. The system dynamic performance is further enhanced by accumulating the derivative block in the FPI controller, i.e., by using FPID controller. The numerical values of the dynamic responses in terms of STs, PUs and various PIs just like ISE, ITSE, IAE and ITAE are given in Table 6.3. It is evident from Table 6.3 that with the same controller structure and with BFOA optimized FPI controller, smaller ITAE (0.0757), IAE (0.0822), ITSE (0.0009), ISE (0.0020), STs (ΔF_1 = 2.05, ΔF_2 = 4.04, $\Delta Ptie_{12}$ = 3.38) and PUs (ΔF_1 = –0.0692, ΔF_2 = –0.0264, $\Delta Ptie_{12}$ = –0.0099) values are gained compared to ITAE (0.4564), IAE (0.2374), ITSE (0.0063), ISE (0.0064), STs
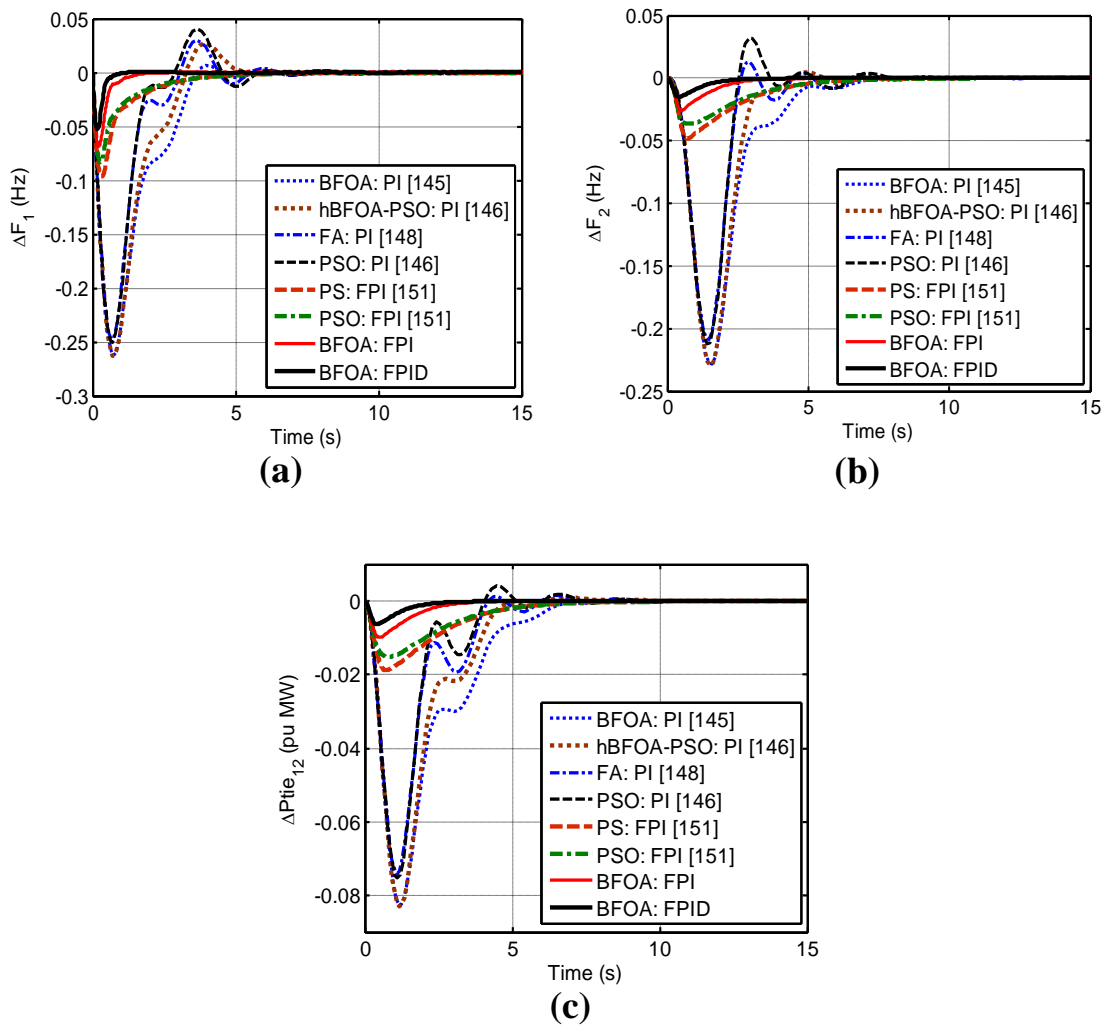

Fig. 6.5 System response with non-reheat thermal system for SLP of 10% at t = 0 s in area-1 (a) ΔF_1, (b) ΔF_2 and (c) $\Delta Ptie_{12}$.

Table 6.3

Numerical values of STs, PUs and PIs with non-reheat thermal system.

Controller	STs (s)			PUs (–ve) (Hz or puMW)			PIs			
	ΔF_1	ΔF_2	$\Delta Ptie_{12}$	ΔF_1	ΔF_2	$\Delta Ptie_{12}$	ISE	ITSE	IAE	ITAE
PSO: PI [146]	9.77	10.52	7.85	0.2500	0.2118	0.0754	0.0992	0.1119	0.7519	1.2330
FA: PI [148]	9.26	9.05	6.91	0.2473	0.2076	0.0740	0.0963	0.1068	0.7385	1.1470
BFOA: PI [145]	7.79	8.87	7.78	0.2622	0.228	0.0828	0.1409	0.1869	1.030	1.8430
hBFOA-PSO: PI [146]	7.87	7.00	7.52	0.2627	0.2293	0.0830	0.1324	0.1650	0.9255	1.4960
PS: FPI [151]	7.20	8.38	7.03	0.0966	0.0482	0.0188	0.0091	0.0087	0.2725	0.4907
PSO: FPI [151]	7.68	8.70	7.28	0.0834	0.0366	0.0151	0.0064	0.0063	0.2374	0.4564
BFOA: FPI	2.05	4.04	3.38	0.0692	0.0264	0.0099	0.0020	0.0009	0.0822	0.0757
BFOA: FPID	**1.05**	**3.16**	**2.50**	**0.0528**	**0.0154**	**0.0062**	**0.0008**	**0.0002**	**0.0428**	**0.0325**

(ΔF_1 = 7.68, ΔF_2 = 8.70, $\Delta Ptie_{12}$ = 7.28) and PUs (ΔF_1 = − 0.0834, ΔF_2 = −0.0366, $\Delta Ptie_{12}$ = −0.0151) values obtained due to PSO: FPI controller. These numerical values due to BFOA optimized FPI controller are also smaller in comparison to PS: FPI controller and PI controller tuned using PSO, FA, BFOA and hybrid BFOA-PSO approaches. It is also obvious from Table 6.3 that least ITAE (0.0325), IAE (0.0428), ITSE (0.0002), ISE (0.0008), STs (ΔF_1 = 1.05, ΔF_2 = 3.16, $\Delta Ptie_{12}$ = 2.50) and PUs (ΔF_1 = −0.0528, ΔF_2 = −0.0154, $\Delta Ptie_{12}$ = −0.0062) values are achieved with BFOA: FPID controller compared to all other controllers including BFAO: FPI. Hence, it can be concluded that the suggested BFOA: FPID approach outperforms other optimal PI/FPI structured controllers prevalent in the literature. The STs are noted in a band of 5% (±0.0005) and PIs values are taken into account for a simulation time of 15 s for the power system models under investigation.

6.6.2 Two-area reheat thermal system

The study is further extended by integrating the reheat effect in the non-reheat model. The transfer function block diagram of reheat thermal system is shown in Fig. 6.2. The simulation results of ΔF_1, ΔF_2 and $\Delta Ptie_{12}$ signals in the wake of 1% SLP in area-1 at t = 0 s are shown in Figs. 6.6(a-c). The results of BFOA tuned FPI/FPID

controller is compared with some recently published heuristic techniques such as: PSO: PI [128–129] and ABC: PI [133] controllers as shown in Figs. 6.6(a-c) and Table 6.4. Critical analysis of Figs. 6.6(a-c) and Table 6.4 clearly point out that the proposed control method exhibits good performance in comparison to other methods.
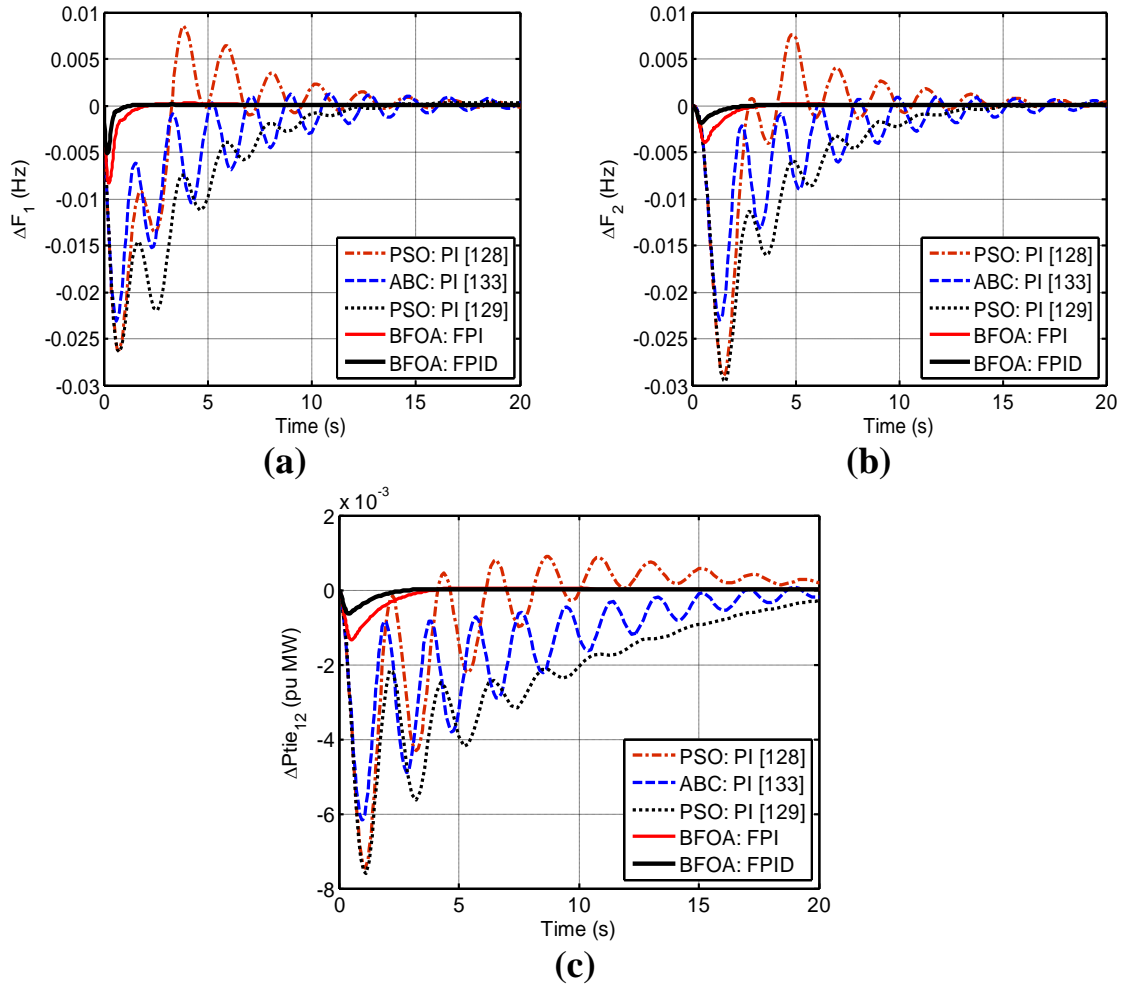

Fig. 6.6 System response with reheat thermal system for SLP of 1% at t = 0 s in area-1 (a) ΔF_1, (b) ΔF_2 and (c) $\Delta Ptie_{12}$.

Table 6.4

Numerical values of STs, PUs and PIs with reheat thermal system.

Contr-oller	STs (s)			PU (–ve) (Hz or puMW)			PIs			
	ΔF_1	ΔF_2	$\Delta Ptie_{12}$	ΔF_1	ΔF_2	$\Delta Ptie_{12}$	ISE	ITSE	IAE	ITAE
ABC: PI [133]	20.52	19.50	16.24	0.0230	0.0230	0.0061	0.00144	0.00343	0.1547	0.6377
PSO: PI [128]	17.03	18.02	15.49	0.0262	0.0289	0.0074	0.00186	0.00317	0.1444	0.4893
PSO: PI [129]	11.63	12.81	18.10	0.0265	0.0296	0.0076	0.00301	0.00745	0.2350	0.9220
BFOA: FPI	1.43	2.27	1.741	0.0083	0.0039	0.0013	$3.64e^{-05}$	$2.20e^{-05}$	0.0134	0.0269
FPID	**0.71**	**1.44**	**0.713**	**0.0051**	**0.0018**	**0.0006**	**$8.53e^{-06}$**	**$3.02e^{-06}$**	**0.0051**	**0.0084**

6.6.3 Traditional multi-source hydrothermal system

To manifest the prospective of the BFOA optimized FPI/FPID controller to cope with multi-source systems, the study is furthermore widened to a traditional multi-source hydrothermal system [100,103,150–151]. The system model is shown in Fig. 6.7 (without dotted line connections). Every control area owns two units, one non-reheat thermal and other mechanical governor equipped hydro power plant. The dynamic performance of the system for 1.5% SLP in area-1 applied at t = 0 s using proposed controller is shown in Figs. 6.8(a-c). The system performance in terms of STs, PUs and PIs of ΔF_1, ΔF_2 and $\Delta Ptie_{12}$ responses is noted in Table 6.5.
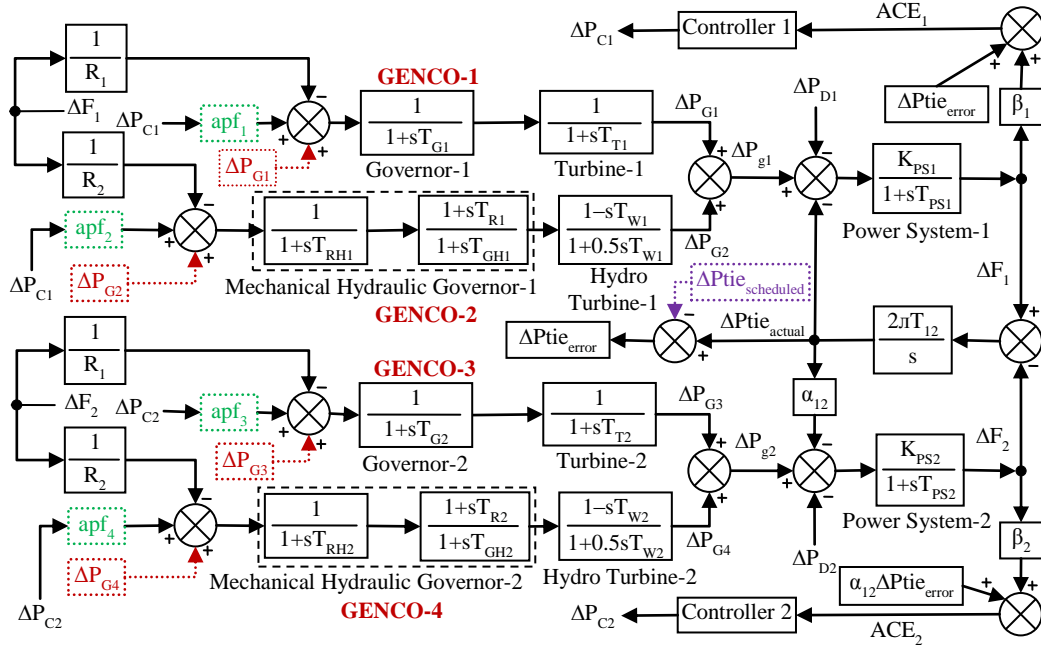

Fig. 6.7 Model of multi-source hydrothermal system (Traditional: without dotted line connections; Restructured: with dotted line connections).

Table 6.5
Numerical values of STs, PUs and PIs with traditional multi-source system.

| Controller	STs (s)			PUs (–ve) (Hz or puMW)			PIs			
	ΔF_1	ΔF_2	$\Delta Ptie_{12}$	ΔF_1	ΔF_2	$\Delta Ptie_{12}$	ISE	ITSE	IAE	ITAE
GA: PI [150]	10.48	15.45	6.292	0.0277	0.0187	0.006184	0.00098	0.00110	0.0882	0.2530
hFA-PS: PI [150]	7.38	10.26	3.054	0.0267	0.0176	0.006066	0.00076	0.00085	0.0740	0.1670
hFA-PS: PI [150]	5.35	6.18	4.480	0.0287	0.0195	0.006797	0.00093	0.00086	0.0706	0.1170
BFOA: FPI	1.41	2.86	1.923	0.0093	0.0029	0.001080	$3.42e^{-05}$	$1.74e^{-05}$	0.0123	0.0199
FPID	**0.82**	**1.79**	**1.173**	**0.0065**	**0.0019**	**0.000792**	**$1.61e^{-05}$**	**$6.06e^{-06}$**	**0.0068**	**0.0085**
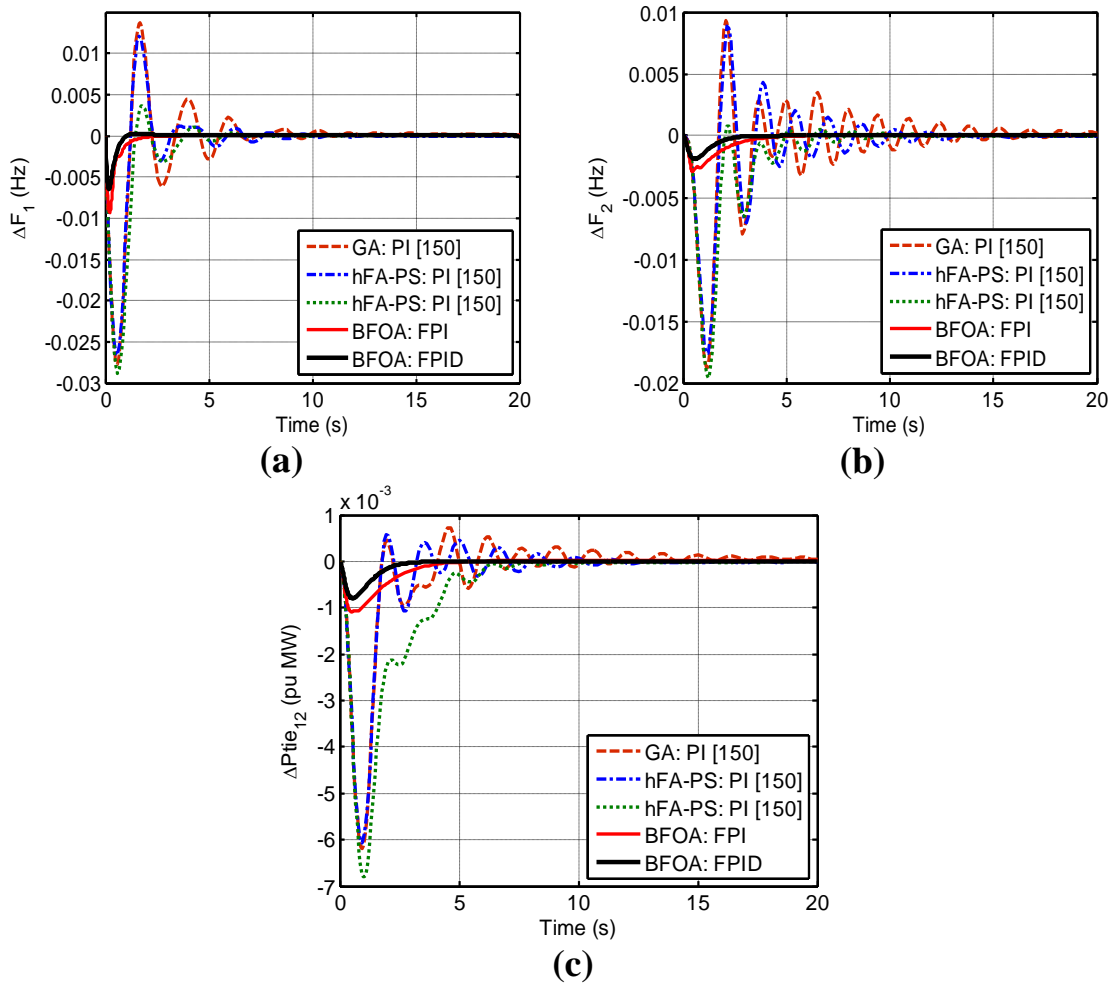
Fig. 6.8 System response with traditional multi-source hydrothermal system for SLP of 1.5% at t = 0 s in area-1 (a) ΔF_1, (b) ΔF_2 and (c) $\Delta Ptie_{12}$.

For comparison, the simulation results with GA [150] and hFA-PS [150] tuned conventional PI controllers are also given in these figures and Table 6.5. It is observed from Figs. 6.8(a-c) that BFOA based FPID controller outperforms the GA/hFA-PS based PI and BFOA based FPI controllers. Table 6.5 shows that the least numerical values of STs, PUs for ΔF_1, ΔF_2 and $\Delta Ptie_{12}$ responses and PIs are obtained with BFOA tuned FPID controller. Hence, suggested approach show better results when compared to GA [150]/hFA-PS [150] optimized PI and BFOA optimized FPI controllers.

6.6.4 Restrutured multi-source hydrothermal system

To bulge competition in modern wholesale electricity market, vast VIUs are being deregulated to amalgamate companies selling unbundled power. Due to the rising dimension and intricacy of the restructured system and introduction of considerable uncertainties and disturbances in the power system, it is preferred to exploit some novel control approaches to attain AGC objectives and secure electric power system passably. In sight of this, to express the talent of the advocated method to tackle restructured system, the study is additionally extended from traditional hydrothermal to restructured configuired hydrothermal system. The block diagram of the system is shown in Fig. 6.7 (with dotted line connections). Each area of identical two-area system owns two GENCOs and two DISCOs. GENCO-1 and GENCO-3 are non-reheat thermal while GENCO-2 and GENCO-4 are hydro units. A hybrid scenario having blend of poolco and bilateral transactions among DISCOs and GENCOs is considered for the current study. ACE participation factors (apfs) are taken as: $apf_1 = apf_2 = apf_3 = apf_4 = 0.5$ and DPM structure is given by Eqn. (6.8).

$$DPM = \begin{bmatrix} 0.10 & 0.24 & 0.33 & 0.18 \\ 0.20 & 0.16 & 0.17 & 0.22 \\ 0.27 & 0.40 & 0.50 & 0.00 \\ 0.43 & 0.20 & 0.00 & 0.60 \end{bmatrix}. \tag{6.8}$$

In these transactions, let the DISCO-1, DISCO-2, DISCO-3 and DISCO-4 demands equally 1% puMW of power from GENCOs as per Eqn. (6.8) i.e., $\Delta P_{L1} = \Delta P_{L2} = \Delta P_{L3} = \Delta P_{L4} = 0.01$ puMW. Hence, $\Delta P_{D1} = 0.02$ puMW, $\Delta P_{D2} = 0.02$ puMW and uncontracted power demand signals $\Delta P_{UC1} = \Delta P_{UC2} = 0$ puMW. The power output of GENCOs in steady state must satisfy the contracted demand of the DISCOs. Based on Eqn. (5.9), deviation in the steady state outputs of GENCOs are: $\Delta P_{G1} = 0.0085$ puMW, $\Delta P_{G2} = 0.0075$ puMW, $\Delta P_{G3} = 0.0117$ puMW, $\Delta P_{G4} = 0.0123$ puMW. The

scheduled tie-line power (ΔPtie$_{scheduled}$) flow from area-1 to 2 is the total power exported from area-1 minus total power imported to area-1 as stated by Eqns. (3.28) or (4.5) [12]. Hence, ΔPtie$_{scheduled}$= −0.004 puMW. The performance of BFOA based FPID controller is compared with BFOA based FPI controller. The simulation results of ΔF_1 and ΔF_2 are shown in Figs. 6.9(a-b) and Table 6.6. It is apparent from Figs. 6.9(a-b) and Table 6.6 that ΔF_1 and ΔF_2 responses due to FPI/FPID controller settle
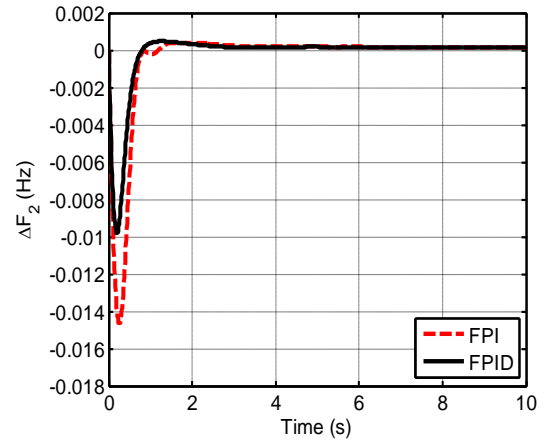
Table 6.6

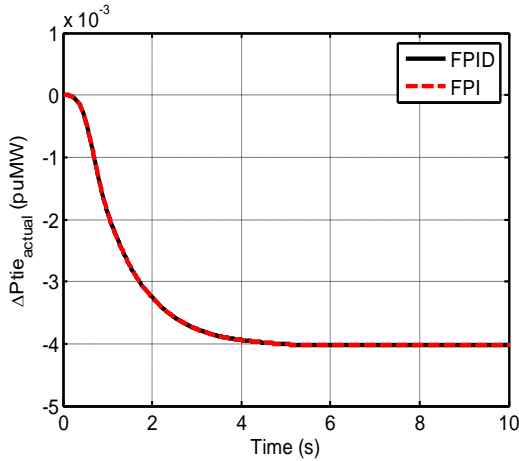Numerical values of STs, PUs and PIs with restructured multi-source power system.

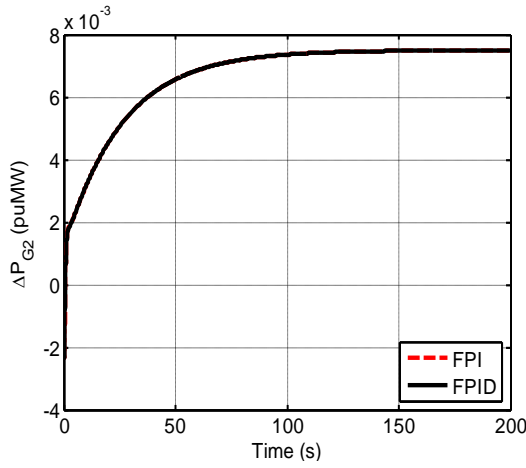| Contro-	STs (s)			PUs (–ve) (Hz or puMW)			PIs			
ller	ΔF_1	ΔF_2	ΔPtie$_{error}$	ΔF_1	ΔF_2	ΔPtie$_{error}$	ISE	ITSE	IAE	ITAE
BFOA: FPI	2.85	0.73	2.36	0.0160	0.0146	0.0000	0.00021	9.482e^{-05}	0.0297	0.0531
BFOA: FPID	**2.84**	**0.69**	**2.23**	**0.0098**	**0.0097**	0.0000	**0.00011**	**6.256e^{-05}**	**0.0245**	**0.0488**
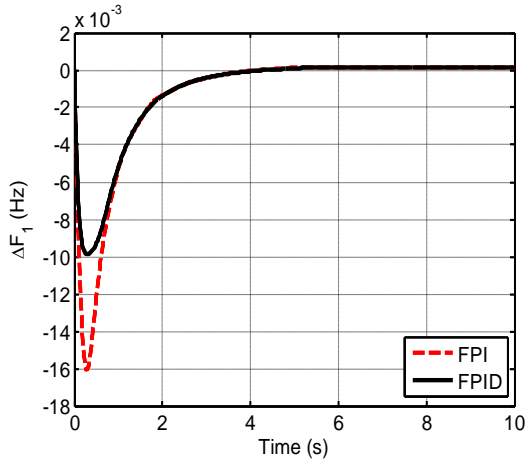
(a)

(b)

(c)
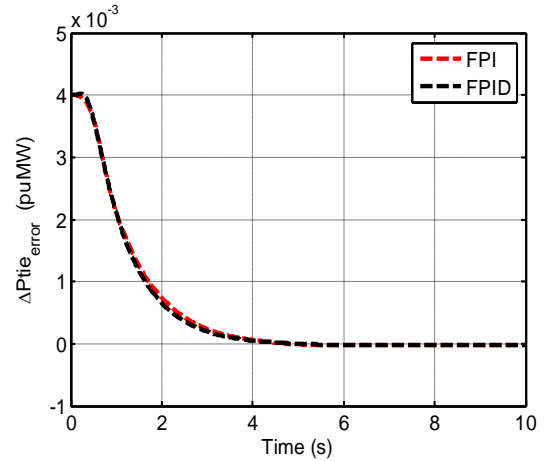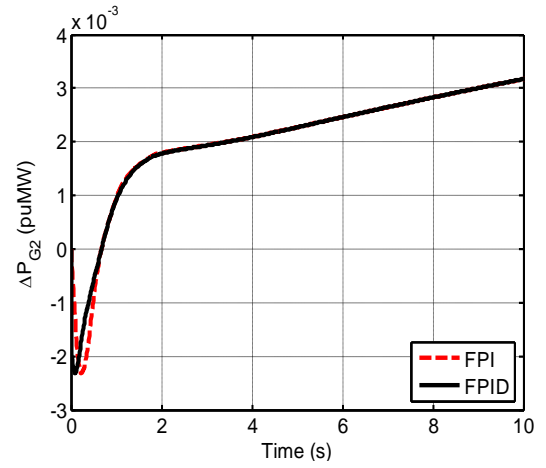

(d)
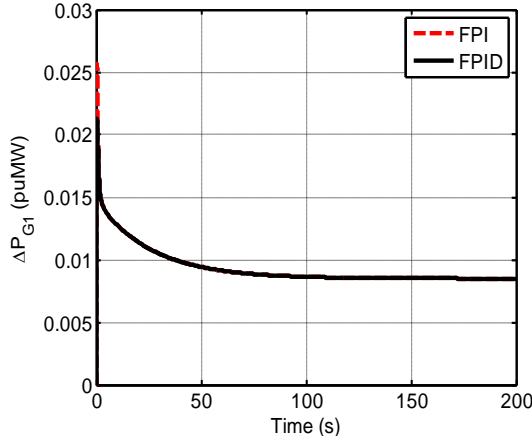
(e)
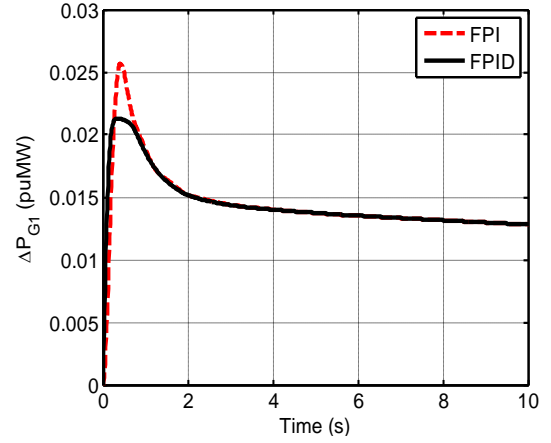
(f) Fig. 6.9(e) with Time = 0-10 s.

(g)

(h) Fig. 6.9(g) with Time = 0-10 s.
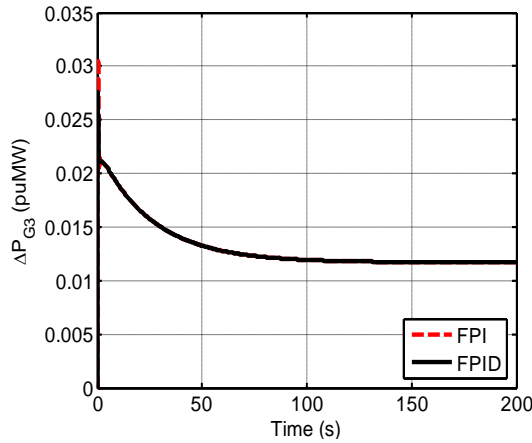
(i)
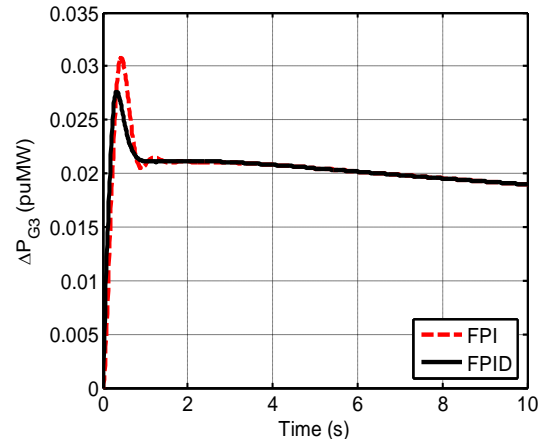
(j) Fig. 6.9(i) with Time = 0-10 s.

to zero in steady state and hence assure the AGC obligation. However, FPID shows better-quality performance compared to FPI in terms of lesser STs, PUs and PIs (Table 6.6). Fig. 6.9(c) shows that $\Delta Ptie_{actual}$ value equates to $Ptie_{scheduled}$ values of –0.004 puMW in steady state. Hence, $\Delta Ptie_{error}$ settles to zero (Fig. 6.9(d)). Addition-

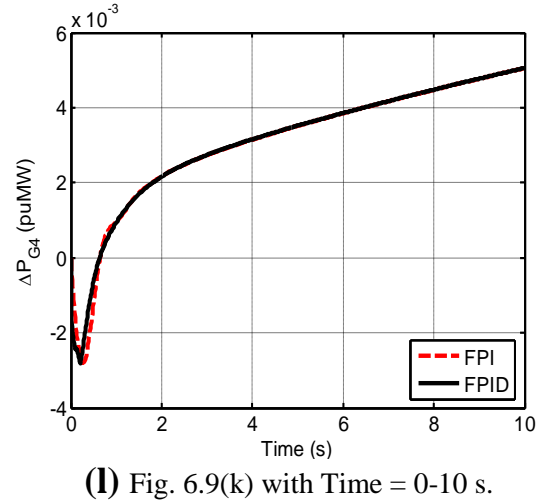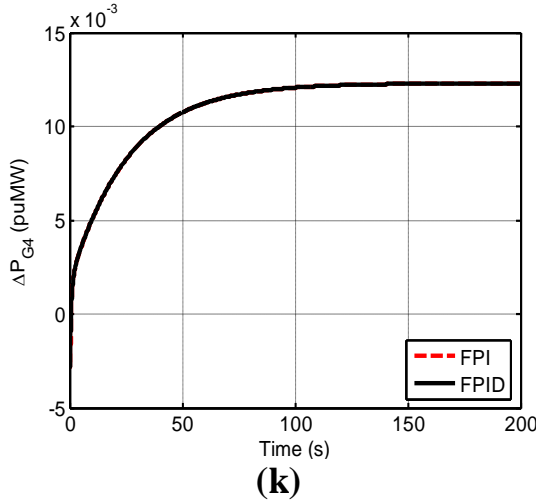**(k)**   **(l)** Fig. 6.9(k) with Time = 0-10 s.

Fig. 6.9 System response with restructured hydrothermal system for FPI/FPID at SLPs in areas at t = 0 s (a) ΔF_1, (b) ΔF_2, (c) $\Delta Ptie_{actual}$,(d) $\Delta Ptie_{error}$, (e) ΔP_{G1},(f) ΔP_{G1}, (g) ΔP_{G2}, (h) ΔP_{G2}, (i) ΔP_{G3}, (j) ΔP_{G3}, (k) ΔP_{G4} and (l) ΔP_{G4}.

ally, power generation responses of all four GENCOs attain their desired generation as showcased in Figs. 6.9(e-l). Critical analysis of Figs. 6.9(e,g,i,k) and Figs. 6.9(f,h,j,l) (reduced x-axis of Figs. 6.9(e,g,i,k)) visibly divulges that the proposed controller satisfy the AGC compulsions capably, however FPID show favorable performance in comparison to the performance offered by FPI.

6.7 Conclusion

In this chapter, BFOA optimized FPI/FPID controller is suggested for AGC of two-area interconnected traditional and restructured power systems. Firstly, a broadly accepted traditional two-area non-reheat thermal system is considered and BFOA is used to simultaneously tune the input/output scaling factors of FPI/FPID controller. To portray potential benefits yielded by the approach, results are contrasted with PI controller based on recently reported techniques like PSO/FA/BFOA/hBFOA-PSO and FPI controller based up on PS/PSO algorithms for the same system design. It is perceived that considerable progress is accomplished with the proposed method compared to recently reported PI/FPI controller. The approach is then extended to a

two-area reheat thermal system and superb dynamic system performance is observed with the suggested method over PI controller optimized via PSO/ABC technique. The approach is further implemented on a traditional two-area multi-source hydrothermal system. From the simulation results, it is observed that BFOA tuned FPID controller perform better compared to newly published GA and hFA-PS tuned PI controller as well as BFOA tuned FPI controller. The system performance indices like ISE/ITSE/IAE/ITAE, settling times and peak undershoots of frequency and tie-line power flow responses concerning systems under study disclose that the proposed approach is superior over others. To reveal the potential of BFOA optimized FPI/FPID to cope with restructured system, the approach is also extended to a restructured two-area multi-source hydrothermal system. It is observed that FPID outperforms FPI controller. It may be concluded that the proposed BFOA optimized fuzzy controller may prolifically be implemented in AGC field as well as in some other more complex power engineering problems.

CHAPTER 7

FRACTIONAL ORDER PID CONTROLLER FOR AGC OF POWER SYSTEMS

7.1 Introduction

Incessant growth in size and complexity, stochastically altering load power demands, system modeling errors and variations in electric system structures has turned AGC task an exigent one. As a result, usual control approaches may be inept to handle such erratic variations in a power system. Hence, worldwide the researchers are trying to suggest various new control strategies that blend knowledge, techniques and methodologies from diverse sources to undertake AGC problem energetically. Various optimization and control techniques such as classical continuous-discrete mode I/PI [70], BFOA based I/PI/PID [142–146], hFA-PS technique based PI/PID [150], grey wolf optimization (GWO) based PI/PID [152], differential evolution (DE) based PID [323], BFOA based fractional order PID (FOPID) [340–341] etc., structured controllers are available in the literature.

Recently, the researches employing fractional calculus (FC) based control approaches are receiving growing interest due to its additional flexibility and outstanding design performance [125,131,140,163–169,289,338,341,353]. Fractional order calculus (FOC) is a 300 years old concept in mathematics. FOC was not extensively incorporated into control engineering owing to few physical constraints and inadequate computational tools existing during last two decades. In recent years, researchers reported that FO differential equations could model various materials more adequately rather than integer order ones. The FOPID, so called $PI^\lambda D^\mu$ controller, is a generalization of integer order PID (IOPID) controller using FC. The

design of FOPID controller engrosses getting of proportional, integral, differential and integrating/differential orders, which are not essentially integer. Different evolutionary algorithms such as improved PSO [131], hybridized gravitational search algorithm (GSA) [140], ICA [163], gases Brownian motion optimization (GBMO) [164], kriging based surrogate modeling [165], robust optimization [166], chaotic multi-objective optimization [167], GA [125,289], DE [338], BFOA [340–341], flower pollination algorithm (FPA) [353] are used in tuning the FOPID controllers. The $PI^{\lambda}D^{\mu}$ controllers have been observed expedient in AGC of diverse power systems such as four-area hydrothermal gas [140], two-area multi-source [131], three-area hydro thermal [163], two-area non-reheat [164], two-area reheat thermal [167], single-area multi-source renewable power system [168], single/two-area non-reheat thermal [169], restructured two-area non-reheat thermal [289], restructured three-area thermal [341] and restructured three-area hydrothermal gas [353]. Various benefits are observed employing FOC technique for controlling the industrial process such as: no steady-state error, robustness to variations in the gain of the plant, robustness to high frequency noise, good output disturbance rejection etc.

The discussion made above unveils that over the past decade various control approaches have been proposed for AGC of traditional/restructured systems. In context to FOPID, a variety of soft computing techniques have been witnessed [125,131,140,163–168,289,338,341,353].

In light of the above, in this paper an attempt has been made to implement FOPID controller for AGC of two-area multi-source hydrothermal/thermal-gas traditional/restructured power system and BFOA is utilized to optimize controller parameters like input/output scaling factors, order of integrator (λ) and order of differentiator (μ and γ).

7.2 Systems investigated

Investigations are performed on a traditional two-area multi-source hydrothermal system, a restructured two-area multi-source hydrothermal system, a restructured two-area multi-source thermal-gas system and a restructured three-area multi-source hydrothermal system. Both areas of traditional/restructured hydrothermal system own one non-reheat thermal and one mechanical governor based hydro plant. Restructured two-area thermal-gas system is equipped with one single reheat thermal and one gas generating unit in its each area. Rated capacity of each area is 2000 MW with initial loading of 1000 MW. The block diagrams of the systems under study are shown in Figs. 7.2, 7.5 and 7.7. The nominal parameters of the systems are given in Appendix B and the list of symbols is given in Nomenclature section.

7.3 FOPID controller

In industry, recently FOPID controller has received extensive attention and investigation over broadly accepted classical PID controller. Since proposed by Alomoush [169] in AGC systems, the implementation of FOPID controller in AGC of various systems has been observed broadly in the literature [125,131,140,163–168, 289,338,341,353]. The FO controller theory deals with differential equations via FC. The FC is the generalization of the ordinary calculus. It is an expansion of $d^n y(t)/dt^n$ concept with n integer number to the concept $d^\alpha y(t)/dt^\alpha$ with α non-integer number with the view to be complex. Many definitions are accessible in the literature to portray the FO function such as the Cauchy integral formula, the Grunwald-Letnikov definition, the Riemann-Liouville definition and the Caputo definition. However, the Riemann-Liouville definition stated in Eqn. (7.1) is generally used in FO calculus.

$$aD_t^\alpha f(t) = \frac{1}{\Gamma(n-\alpha)} \frac{d^n}{dt^n} \int_a^t (t-\tau)^{n-\alpha-1} f(\tau) d\tau \tag{7.1}$$

where, $n - 1 > \alpha < n$, n is an integer and symbol $\Gamma(\cdot)$ represents Euler's gamma function and is given by Eqn. (7.2).

$$\Gamma(x) = \int_0^\infty e^{-t} t^{(x-1)} dt, \ x > 0, \tag{7.2}$$

with unique case when $x = n$,

$$\Gamma(n) = (n - 1)(n - 2) \cdots (2)(1) = (n - 1)!. \tag{7.3}$$

For convenience, the Laplace domain concept is used to illustrate the fractional differentiation-integration process. The Laplace transformation of Eqn. (7.1) under zero initial condition for the fractional derivative is given by Eqn. (7.4).

$$L\left\{aD_t^\alpha f(t)\right\} = \int_0^\infty e^{-st} aD_t^\alpha f(t) dt$$

$$= s^\alpha F(s) - \sum_{k=0}^{n-1} s^k aD_t^{\alpha-k-1} f(t)\big|_{t=0} \tag{7.4}$$

$L\{f(t)\}$ indicates the normal Laplace transformation and F(s) is the Laplace transform of f(t).

The general form of FOPID is the $PI^\lambda D^\mu$ and its transfer function is given by Eqn. (7.5).

$$G_c(s) = K_P + \frac{K_I}{s^\lambda} + K_D s^\mu \tag{7.5}$$

where, K_P, K_I, K_D are proportional, integral, derivative gains, respectively. λ and μ indicate order of integration and differentiation, respectively. Hence, in $PI^\lambda D^\mu$ controller structure, it is needed to optimize five design parameters compared to three required in PID structured controller. The FOPID requires the appropriate design of
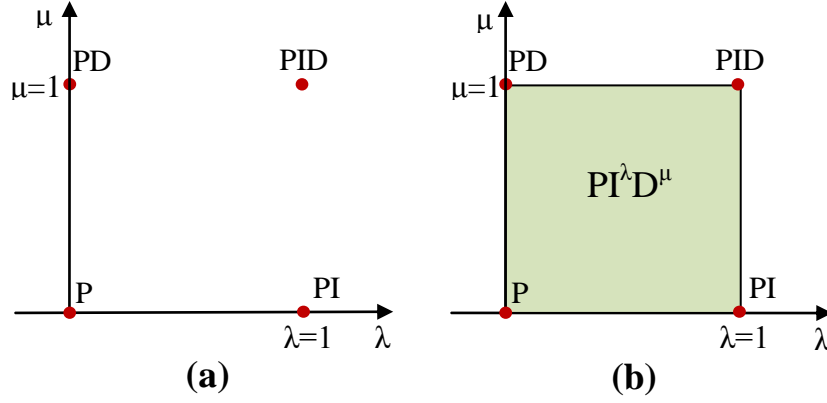
Fig. 7.1 FOPID structure based controllers.

K_P/K_I/K_D and orders λ/μ. The orders are not essentially integer, but any real numbers.

For $\lambda = 1$ and $\mu = 1$; the controller structure of Eqn. (7.5) shrinks to the conventional PID controller. Additionally, if $\lambda = 1$ and $\mu = 0$; then it turn into PI, if $\lambda = 0$ and $\mu = 1$; then it turn out to be a PD, if $\lambda = 0$ and $\mu = 0$; then it is only P, if $\lambda = 0$; then it is termed as PD$^\mu$; if $\mu = 0$; then it becomes PI$^\lambda$, if $\lambda = 1$; then it becomes PID$^\mu$ and if $\mu = 1$; then it is converted into PI$^\lambda$D controller. These integer-order controllers are represented as points in the λ-μ plane as shown in Fig. 7.1(a). The FOPID controller generalizes the PID controller and expands it from a point to the entire λ-μ plane, as shown in Fig. 7.1(b). This generalization of the PID offers a much wider selection of tuning parameters and thereby more flexibility in the controller design, which leads to more accurate control of plants or process. For simulations and industrial realization of transfer functions involving FO of s, it is necessary to approximate them with usual (integer order) transfer functions. To approximate a fractional transfer function suitably, a usual transfer function would appoint an infinite number of poles and zeroes. However, an approximation with a finite number of poles and zeroes can be obtained using the CRONE approximation proposed by Oustaloup [402]. Oustaloup's recursive distribution employs a higher order filter having an order of 2N + 1, and it provides a very good approximation or fitting to the

FO element s^α specified by Eqn. (7.6) within a specified frequency band $[\omega_L, \omega_H]$ [167–168].

$$G_f(s) = s^\alpha = K \prod_{k=-N}^{N} \frac{s + \omega_k^\iota}{s + \omega_k} \tag{7.6}$$

where α is the order of differentiation-integration and $0 < \alpha < 1$, $(2N + 1)$ is the order of the filter. K is the gain, ω_k^ι and ω_k are the zeros and poles of the analog filter respectively, and are recursively obtained as follows:

$$K = \omega_H^\alpha \tag{7.7}$$

$$\omega_k^\iota = \omega_L \left(\frac{\omega_H}{\omega_L}\right)^{\frac{k + N + \frac{1}{2}(1-\alpha)}{2N + 1}} \tag{7.8}$$

$$\omega_k = \omega_L \left(\frac{\omega_H}{\omega_L}\right)^{\frac{k + N + \frac{1}{2}(1+\alpha)}{2N + 1}}. \tag{7.9}$$

K is altered so that approximation should have unit gain at 1 rad/s frequency [289]. The choice of N is a significant deciding aspect in the feat of the approximation. Low values of N may result in simpler approximations and easiness in hardware execution but the approximation get worse due to ripple formation in magnitude and phase responses. Such ripples may be eradicated by elevating the values of N but it will turn the approximation complicated and complexity in hardware implementation. In this work, CRONE approximation is employed with N = 3, while fitting frequency range $[\omega_L, \omega_H]$ is taken as $[10^{-2}, 10^2]$ [167].

The control signal of the controller is given by Eqn. (7.10).

$$\Delta P_C = K_P(ACE) + \frac{K_I}{s^\lambda}(ACE) + K_D s^\mu(ACE), (\lambda, \mu > 0). \tag{7.10}$$

7.4 Optimization problem

For AGC problem under study, the objective function (J) employed is integral squared error (ISE) as stated in Eqns. (5.4)/(6.5) or (7.11).

$$J = \int_0^T \{\Delta F_1^2 + \Delta F_2^2 + \Delta Ptie_{12}^2\} dt. \tag{7.11}$$

where, T is the range of simulation time. $\Delta Ptie_{error}$ will replace $\Delta Ptie_{12}$ in restructured system. The problem restraints are the controller parameter limits. As a result, the FOPID controller design problem is treated as an optimization problem. The FOPID controller in each area of two-area system has five parameters to be optimized. The optimization problem can be delineated as to minimize J in view of the following constraints:

$K_{P\,min} \leq K_P \leq K_{P\,max}$, $K_{I\,min} \leq K_I \leq K_{I\,max}$, $\lambda_{min} \leq \lambda \leq \lambda_{max}$, $K_{D\,min} \leq K_D \leq K_{D\,max}$, $\mu_{min} \leq \mu \leq \mu_{max}$.

Here, λ_{min}, μ_{min}, $K_{P,I,D\,min}$ and λ_{max}, μ_{max}, $K_{P,I,D\,max}$ are the minimum and maximum values of the FOPID controller parameters, respectively. The minimum and maximum values of $K_{P,I,D}$ parameters are chosen as 0.0 and 4.0, respectively. However, λ and μ values are preferred between 0.0 and 1.0. Each bacterium is permitted to take all feasible values within this limit to minimize Eqn. (7.11) to obtain the optimal parameter values of FOPID controller.

7.5 Simulation results and discussions

7.5.1 Traditional two-area multi-source hydrothermal system

In MATLAB/SIMULINK a two-area multi-source hydrothermal power system is simulated considering 1.5% SLP at time t = 0 s in area-1. The AGC model is given in the literature [100,103,150–152] and equipped with FOPID controller in each area is

shown in Fig. 7.2 (without dotted line connections). Each area is outfitted with non-reheat thermal and mechanical governor based hydro plants. The optimized parameters of FOPID controller obtained exploiting BFOA are: $K_P = -2.9532$, $K_I = -3.9172$, $\lambda = 0.9230$, $K_D = -1.0014$ and $\mu = 0.9902$. The $\Delta Ptie_{error}$ signal shown in Fig. 7.2 will be $\Delta Ptie_{12}$ for traditional system. The system dynamic responses for ΔF_1, ΔF_2, $\Delta Ptie_{12}$, ACE_1, ACE_2, ΔP_{g1} and ΔP_{g2} are shown in Fig. 7.3. To corroborate the advantage of the FOPID controller, the simulation results with some newly published controllers like hFA-PS tuned PI/PID [150] and grey wolf optimization (GWO) tuned PID [152] controllers are also shown in Fig.7.3. Critical examination of the Figs. 7.3(a-g) clearly reveals significant improvements in the system performance due to the BFOA optimized FOPID controller compared to hFA-PS tuned PI/PID [150] and GWO tuned PID [152] structured controller in terms of STs, PUs and oscillations. The system performance in terms of numeric values of STs, PUs and various PIs such
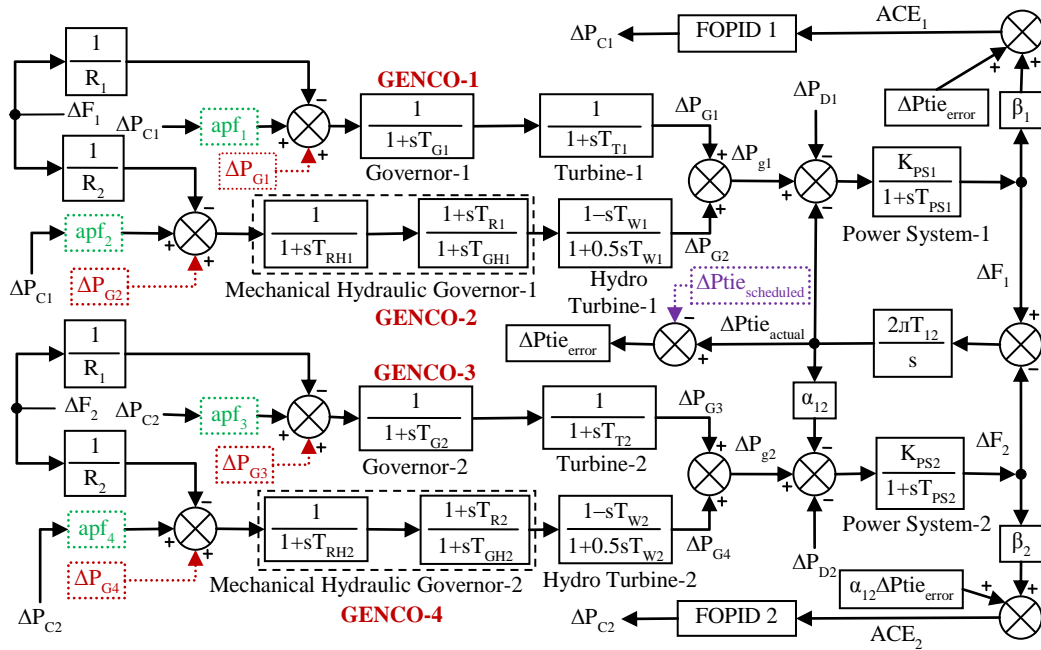

Fig. 7.2 Model of multi-area multi-source hydrothermal power system (Traditional: without dotted line connections; Restructured: with dotted line connections).

Table 7.1

Numerical values of STs, PUs and PIs with traditional multi-source hydrothermal system.

Controller	STs (s)			PUs (–ve) (Hz or puMW)			PIs			
	ΔF_1	ΔF_2	$\Delta Ptie_{12}$	ΔF_1	ΔF_2	$\Delta Ptie_{12}$	ISE	ITSE	IAE	ITAE
PI [150]	5.35	6.18	4.480	0.0287	0.0195	0.0067	$9.03e^{-04}$	$8.56e^{-04}$	0.0705	0.1177
PID [150]	2.94	4.53	3.300	0.0134	0.0066	0.0022	$1.17e^{-04}$	$8.50e^{-05}$	0.0255	0.0395
GWO[152]	1.21	3.50	2.640	0.0149	0.0069	0.0026	$1.47e^{-04}$	$9.03e^{-05}$	0.0233	0.0259
FOPID	**1.20**	**2.15**	**1.678**	**0.0115**	**0.0046**	**0.0015**	**$5.22e^{-05}$**	**$2.14e^{-05}$**	**0.0116**	**0.0121**

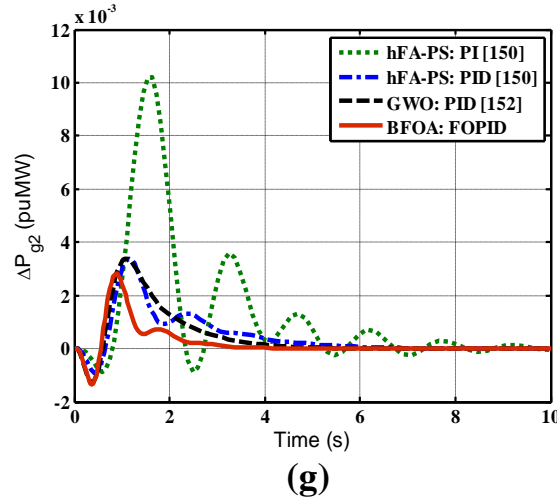(a)

(b)

(c)

(d)

(e)

(f)

(g)
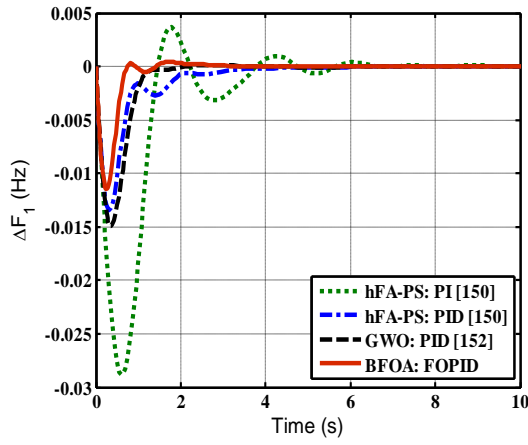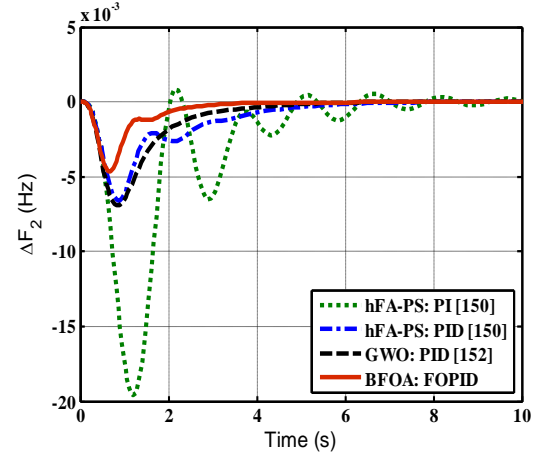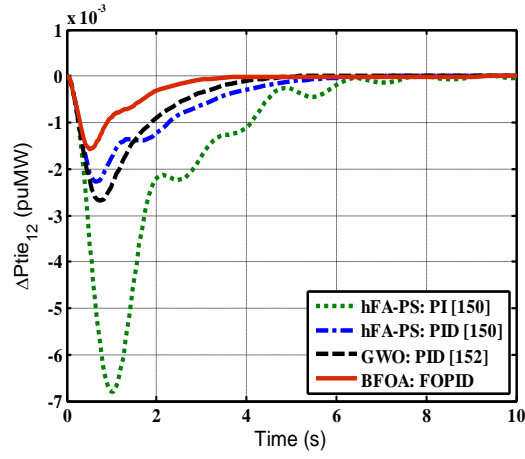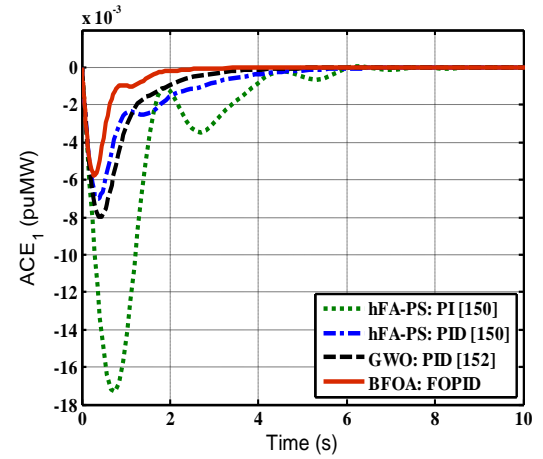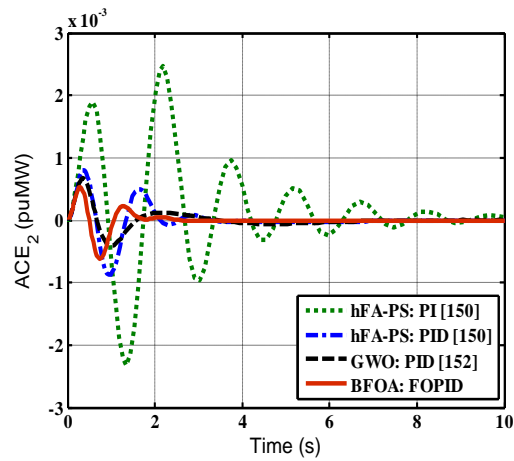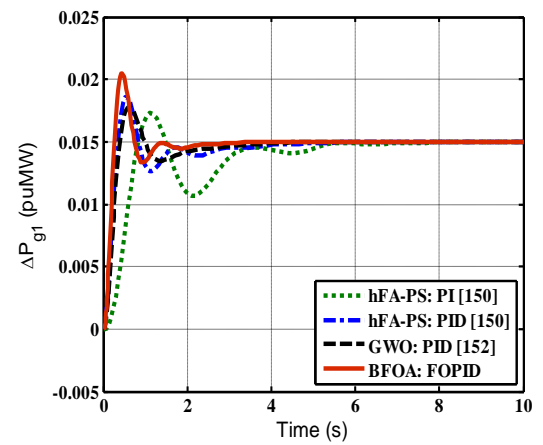
Fig. 7.3 Dynamic responses of traditional two-area two-source hydrothermal system with different types of controllers for 1.5% SLP in area-1 at time t = 0 s (a) ΔF_1 (b) ΔF_2 (c) $\Delta Ptie_{12}$, (d) ACE_1, (e) ACE_2, (f) ΔP_{g1} and (g) ΔP_{g2}.

such as ISE, ITSE, IAE and ITAE [150,169] are shown in Table 7.1. In addition to STs and PUs, the numerical values of PIs also assist to decide the best control approach among various approaches available for comparison. It is also observed from Table 7.1 and Figs 7.3(a–g) that GWO: PID [152] outperforms hFA-PS: PI/PID [150] controller. Table 7.1 also points out that BFOA: FOPID outperform GWO: PID [152] controller in terms of less STs (FOPID: ΔF_1 = 1.20, ΔF_2 = 2.15, $\Delta Ptie_{12}$ = 1.678; GWO: PID: ΔF_1 = 1.21, ΔF_2 = 3.50, $\Delta Ptie_{12}$ = 2.640), PUs (FOPID: ΔF_1 = 0.0115, ΔF_2 = 0.0046, $\Delta Ptie_{12}$ = 0.0015; GWO: PID: ΔF_1 = 0.0149, ΔF_2 = 0.0069, $\Delta Ptie_{12}$ = 0.0026) and PIs (FOPID: ISE = $5.22e^{-05}$, ITSE = $2.14e^{-05}$, IAE = 0.0116, ITAE = 0.0121; GWO: PID: ISE = $1.47e^{-04}$, ITSE = $9.03e^{-05}$, IAE = 0.0233, ITAE = 0.0259). Therefore, superior system performance in terms minimum PIs and STs/PUs in frequency and tie-line power deviations is achieved with the optimal FOPID controller compared to other controllers. Figs. 7.3(d-e) show the responses of area control errors of control areas and it is observed from Figs. 7.3(d-e) that ACE_1 and ACE_2 responses due to FOPID control approach settle faster to zero with least STs/PUs compared to PI/PID approaches. Further, Figs. 7.3(f-g) show the responses

135

of deviation in generations of control areas ($\Delta P_{g1}/\Delta P_{g2}$) under SLP in area-1. It is examined from ΔP_{g1} response (Fig. 7.3(f)) that the power generation deviation in area-1 in transient period due to FOPID control approach is more but it settle to the desired generation in less time compared to PI/PID approaches. It is observed from ΔP_{g2} response (Fig. 7.3(g)) that the power generation deviation in area-2 in transient period due to FOPID control approach is less and ST is also less compared to PI/PID controllers.

### 7.5.2 *Restructured two-area multi-source hydrothermal system* (Poolco based transactions)

To authenticate the ability of FOPID control approach in restructured system, the study is further extended from traditional multi-source hydrothermal system to restructured multi-source hydrothermal system whose model is also shown in Fig.7.2 (with dotted line connections). GENCO-1 and GENCO-3 are thermal while GENCO-2 and GENCO-4 are hydro plants. Two DISCOs in each area i.e., DISCO-1, DISCO-2 in area-1 and DISCO-3, DISCO-4 in area-2 are supposed in two-area system. The system parameters are given in Appendix B. The optimum parameter values of controller are acquired by running the BFOA codes written in .mfile and models developed in SIMULINK. The optimized values of FOPID as well as a PID controller are found out as: $K_P = -1.2965$, $K_I = -3.0843$, $\lambda = 0.7634$, $K_D = -2.9231$, $\mu = 0.8939$ for FOPID and $K_P = -1.0123$, $K_I = -1.3101$, $K_D = -0.9502$ for PID. The computer simulations are carried out using these best possible controller parameters.

In this study, only poolco based transactions are simulated where DISCOs and GENCOs of the same area negotiate power contracts. Let, $\Delta P_{L1} = \Delta P_{L2} = 0.01$ puMW and $\Delta P_{L3} = \Delta P_{L4} = 0.00$ puMW. Hence, $\Delta P_{D1} = 0.02$ puMW and $\Delta P_{D2} = 0.00$ puMW. The selected DPM structure is given by Eqn. (7.12).

$$DPM = \begin{bmatrix} 0.5 & 0.5 & 0.0 & 0.0 \\ 0.5 & 0.5 & 0.0 & 0.0 \\ 0.0 & 0.0 & 0.0 & 0.0 \\ 0.0 & 0.0 & 0.0 & 0.0 \end{bmatrix} \tag{7.12}$$

The controller output signal (ΔP_C) acts as the input to apf block of the concerned GENCO. The apf of a GENCO relates to participation in AGC, profile, bid price and capacity in the power market. It is assumed that all GENCOs participate equally in AGC task i.e., $apf_1 = apf_2 = apf_3 = apf_4 = 0.5$. In the steady state, power outputs of GENCOs essentially go with the demand of the DISCOs in contract with them. Hence, in steady state, $\Delta P_{G1} = \Delta P_{G2} = 0.01$ puMW and $\Delta P_{G3} = \Delta P_{G4} = 0.0$ puMW. The $\Delta Ptie_{scheduled} = 0$ puMW. The system simulations are carried out with the FOPID and PID controllers. STs and PUs of $\Delta F_1/\Delta F_2/\Delta Ptie_{error}$ and ISE/ITSE/IAE/ITAE for FOPID/PID controllers are given in Table 7.2. It is apparent from Table 7.2 that FOPID is superior to PID as minimum PIs value is obtained with FOPID (ISE = $9.64e^{-05}$, ITSE = $5.79e^{-05}$, IAE = 0.0223, ITAE = 0.0410) compared to PID (ISE = $2.57e^{-04}$, ITSE = $2.04e^{-04}$, IAE = 0.0426, ITAE = 0.1342). Additionally, it is clear that STs and PUs are also less with FOPID (STs: $\Delta F_1 = 1.89$, $\Delta F_2 = 3.32$, $\Delta Ptie_{error} = 2.68$;

(a)   **(b)**

(c)

(d)

(e)

(f) Fig. 7.4(e) with Time = 0-10 s.

(g)

(h)
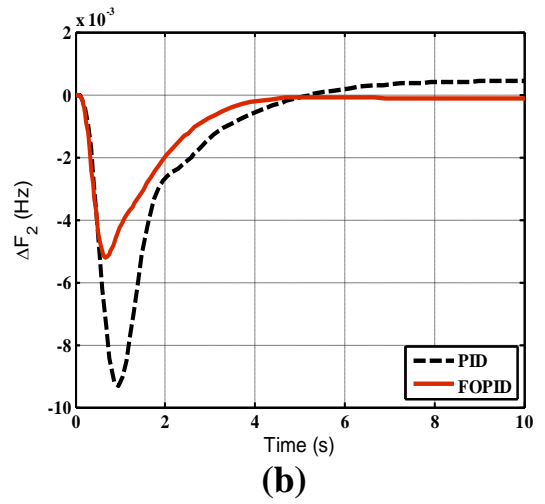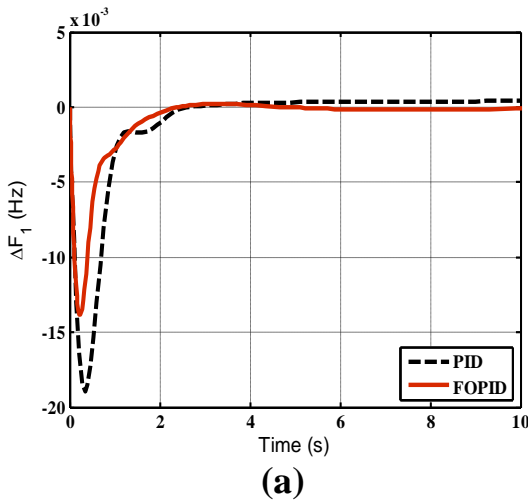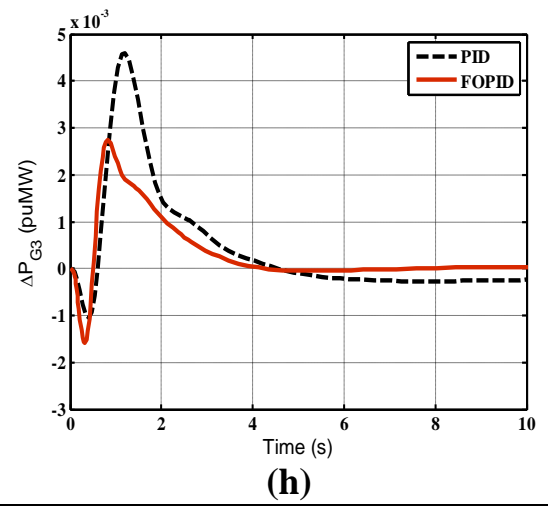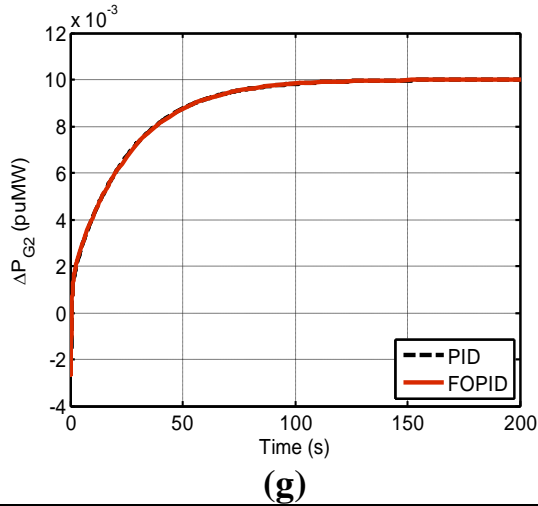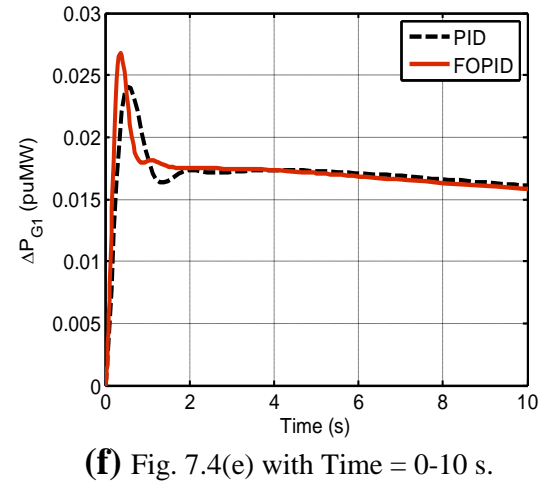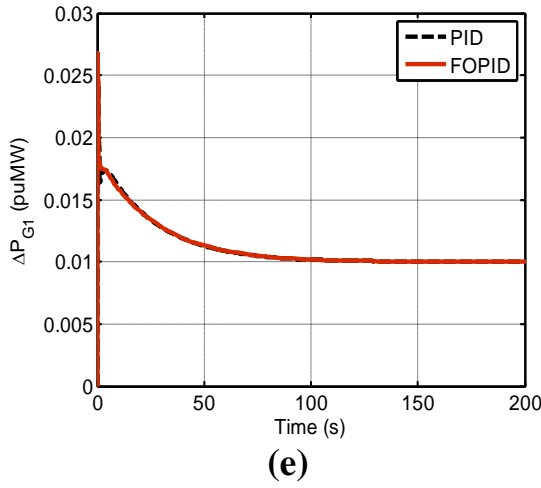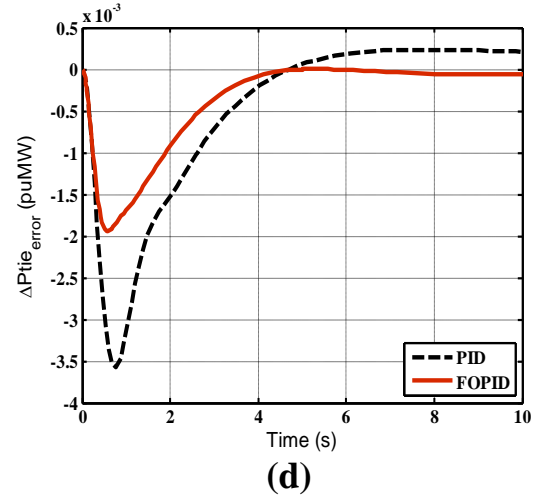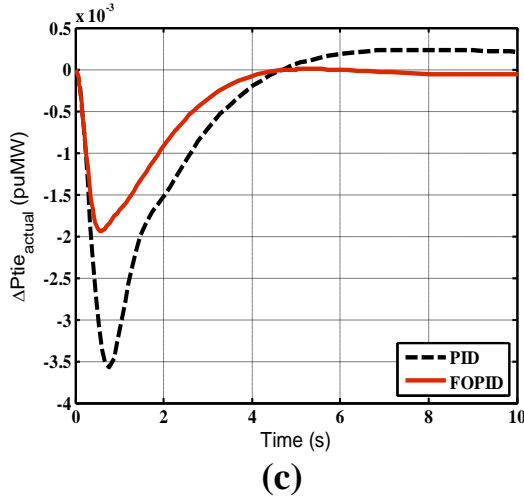
PUs: $\Delta F_1 = 0.0138$, $\Delta F_2 = 0.0052$, $\Delta Ptie_{error} = 0.0019$) compared to PID (STs: $\Delta F_1 =$ 2.23, $\Delta F_2 = 4.11$, $\Delta Ptie_{error} = 3.34$; PUs: $\Delta F_1 = 0.0190$, $\Delta F_2 = 0.0093$, $\Delta Ptie_{error} =$ 0.0035). Hence, it can be concluded that FOPID structured controller is superior to PID structured controller. The system dynamic performance is shown in Fig. 7.4. It is

(i)

(j) Fig. 7.4(i) with Time = 0-10 s.

(k)

(l)

(m)

(n)
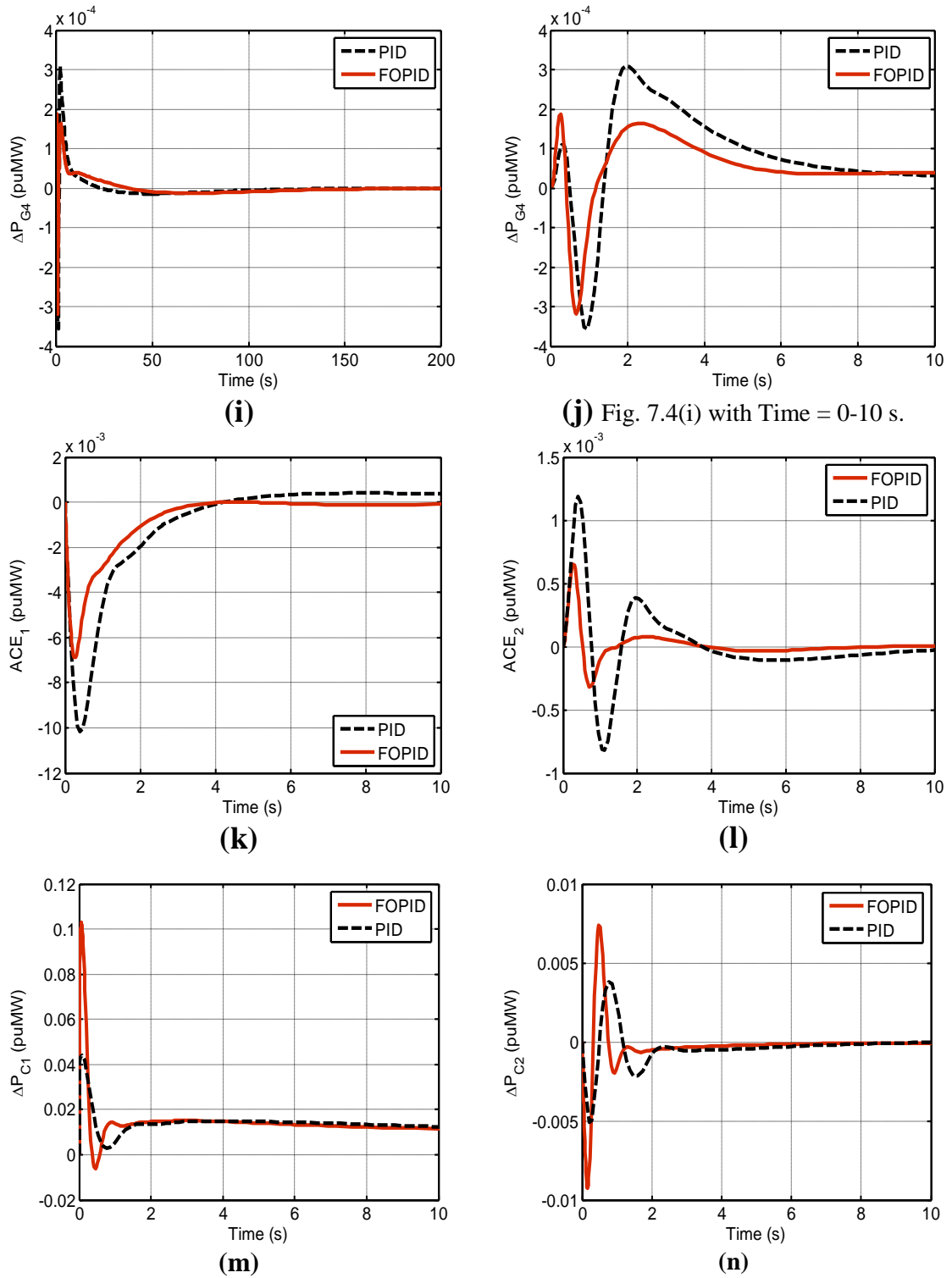
Fig. 7.4 Dynamic responses of restructured two-area two-source hydrothermal system with PID/FOPID controller for (a) ΔF_1, (b) ΔF_2, (c) $\Delta Ptie_{actual}$, (d) $\Delta Ptie_{error}$, (e) ΔP_{G1}, (f) ΔP_{G1}, (g) ΔP_{G2}, (h) ΔP_{G3}, (i) ΔP_{G4}, (j) ΔP_{G4}, (k) ACE_1, (l) ACE_2, (m) ΔP_{C1} and (n) ΔP_{C2}.

clear from Figs. 7.4(a-d) that enhanced system dynamic performance in terms minimum STs and PUs in frequency and tie-line power deviations is attained with the

Table 7.2

Numerical values of STs, PUs and PIs with restructured multi-source hydrothermal system.

Contr-oller	STs (s)			PUs (Hz) (–ve)		PUs (puMW) (–ve)	PIs			
	ΔF_1	ΔF_2	$\Delta Ptie_{error}$	ΔF_1	ΔF_2	$\Delta Ptie_{error}$	ISE	ITSE	IAE	ITAE
PID	2.23	4.11	3.34	0.0190	0.0093	0.0035	$2.57e^{-04}$	$2.04e^{-04}$	0.0426	0.1342
FOPID	**1.89**	**3.32**	**2.68**	**0.0138**	**0.0052**	**0.0019**	**$9.64e^{-05}$**	**$5.79e^{-05}$**	**0.0223**	**0.0410**
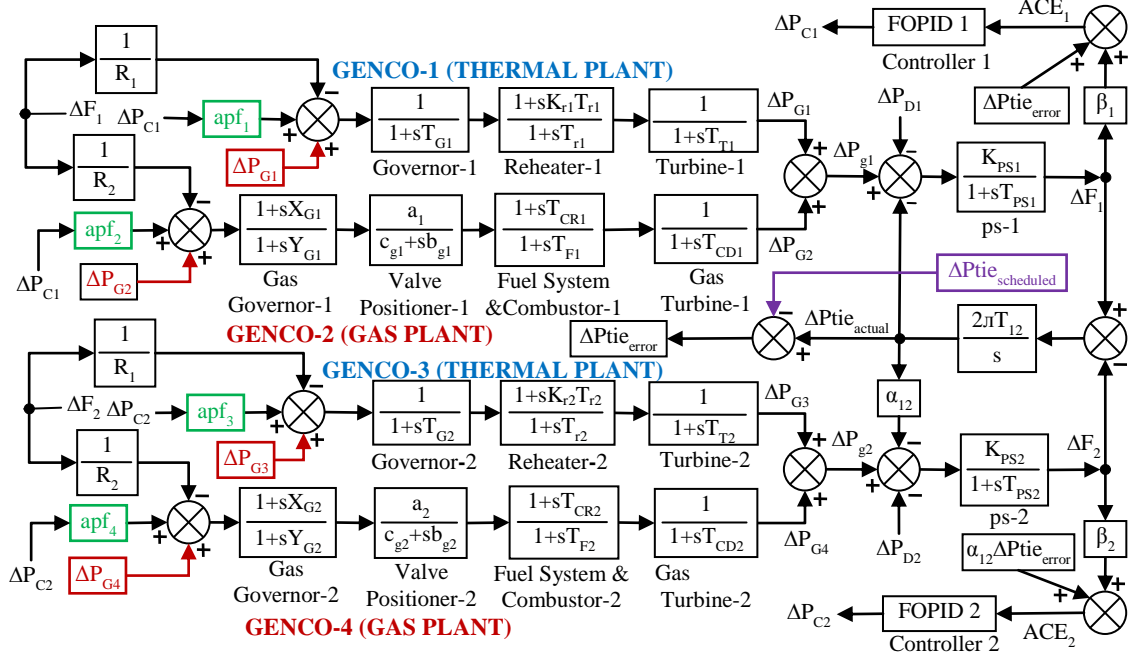
Fig. 7.5 Restructured two-area multi-source thermal gas power system model.

FOPID compared to PID controller. Further, Figs. 7.4(a-b,d) indicate that FOPID fulfill AGC condition as ΔF in each area and $\Delta Ptie_{error}$ settle to zero in the steady state. From Figs. 7.4(e-j), it is observed that steady state simulated values of GENCOs outputs match with desired value obtained using Eqn. (5.9) and Fig. 7.4(c) validates Eqn. (4.5). Figs. 7.4(k-l) display ACE results. However, FOPID show better results in Figs. 7.4(e-l). Figs. 7.4(m-n) show controller outputs ($\Delta P_{C1}/\Delta P_{C2}$) due to FOPID and PID controllers. It is observed from Figs. 7.4(m-n) that in transient state, FOPID provides more control action and acquire steady state quickly compared to PID. Hence, FOPID outperforms PID.

7.5.3 Restructured two-area multi-source thermal gas system

(poolco plus bilateral based transactions)

To demonstrate the scalability and effectiveness of the BFOA optimized FOPID controller to cope up with the dissimilar restructured systems, the study is further extended to a restructured two-area multi-source power system by believing two GENCOs i.e., thermal and gas in each control area, as shown in Fig. 7.5. The thermal plant is provided with a single reheat turbine having an appropriate generation rate constraint (GRC) of ± 0.03 pu/s. The test model is taken from [323]. In this extension study, only poolco plus bilateral case is considered. ACE participation factors used are $apf_1 = 0.75$, $apf_2 = 0.25$, $apf_3 = apf_4 = 0.5$. A big step load power of 0.1 puMW is demanded by each DISCO. Hence, $\Delta P_{D1} = \Delta P_{D2} = 0.2$ puMW. Optimized controller parameters are obtained as: $K_P = -1.3972$, $K_I = -0.9905$, $\lambda = 0.4530$, $K_D = -1.0994$, μ

Table 7.3

Numerical values of STs, PUs and PIs with restructured multi-source thermal gas system.

Control-ler	STs (s)			PUs (−ve) (Hz or puMW)			PIs			
	ΔF_1	ΔF_2	$\Delta Ptie_{error}$	ΔF_1	ΔF_2	$\Delta Ptie_{error}$	ISE	ITSE	IAE	ITAE
GA: PID [323]	14.58	14.32	6.158	0.5063	0.3718	0.0000	$5.35e^{-01}$	$9.25e^{-01}$	2.3690	7.0880
DE: PID [323]	13.85	27.16	20.38	0.4790	0.3719	0.0000	$3.93e^{-01}$	$5.03e^{-01}$	1.8500	4.6930
BFOA: FOPID	**8.95**	**5.95**	**6.450**	**0.5130**	**0.2839**	**0.0000**	**$2.69e^{-01}$**	**$2.00e^{-01}$**	**1.0780**	**1.8450**
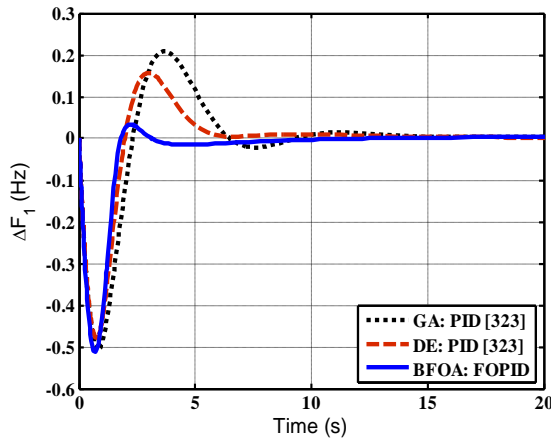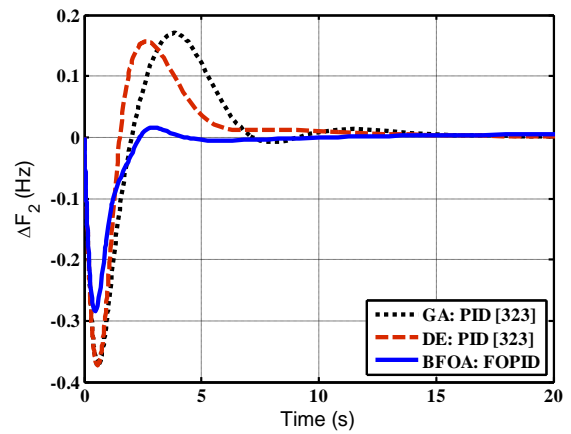
(a)   **(b)**
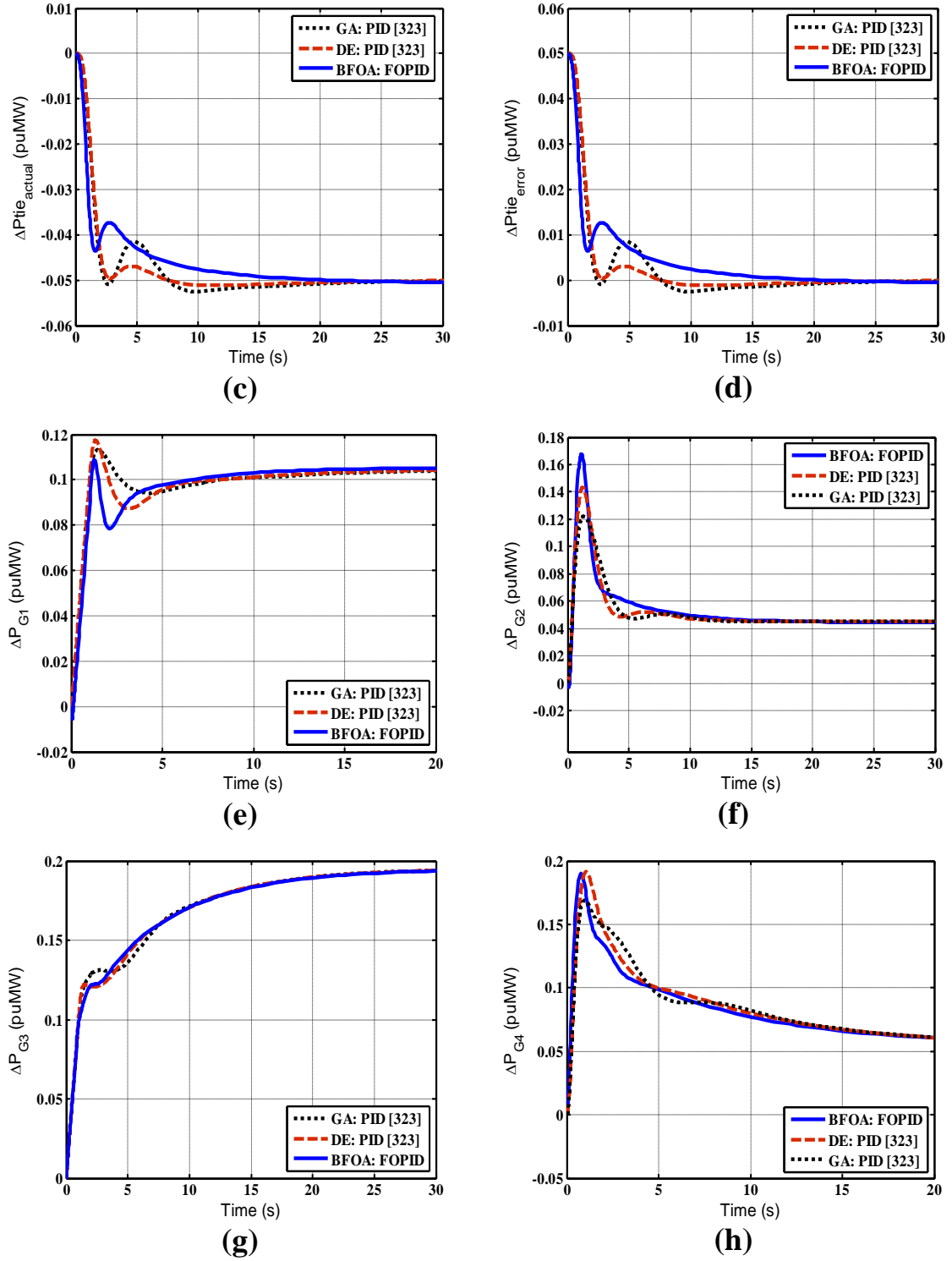
Fig. 7.6 Dynamic responses of restructured two-area multi-source thermal gas system with different controllers (a) ΔF_1 and (b) ΔF_2, (c) $\Delta Ptie_{actual}$, (d) $\Delta Ptie_{error}$, (e) ΔP_{G1} (f) ΔP_{G2}, (g) ΔP_{G3} and (h) ΔP_{G4}.

= 0.9990. The DPM is taken from [323] and is described by Eqn. (7.13).

$$
DPM = \begin{bmatrix} 0.5 & 0.25 & 0.0 & 0.3 \\ 0.2 & 0.25 & 0.0 & 0.0 \\ 0.0 & 0.25 & 1.0 & 0.7 \\ 0.3 & 0.25 & 0.0 & 0.0 \end{bmatrix} \qquad (7.13)
$$

The power system responses with BFOA tuned FOPID and DE [323]/GA [323] optimized PID controllers are displayed in Fig. 7.6. With BFOA tuned FOPID method, ΔF_1, ΔF_2 and $\Delta Ptie_{error}$ signals are rapidly driven back to zero with small values of STs/PUs/PIs as indicated in Table 7.3 and Figs. 7.6(a-b,d). However, PU for ΔF_1 response due to BFOA optimized FOPID controller is more compared to DE/GA optimized PID controller. In the steady state, deviation in tie-line power flows accurately diverge to the specified values of Eqn. (4.5) i.e., $\Delta Ptie_{scheduled} = -0.05$ puMW, as confirmed from Fig. 7.6(c). As revealed in Figs. 7.6(e-h), the actual power outputs of GENCOs, on the basis of Eqn. (5.9), suitably attain their desired values of $\Delta P_{G1} = 0.105$ puMW, $\Delta P_{G2} = 0.045$ puMW, $\Delta P_{G3} = 0.195$ puMW and $\Delta P_{G4} = 0.055$ puMW, quickly in the steady state compared to DE/GA based PID controllers.

7.5.4   *Restructured three-area multi-source hydrothermal system*

(Poolco plus bilateral with contract violation based transactions)

In order to validate the feasibility of FOPID controller, it is also implemented on a restructured three-area multi-source system. The topology of the system is shown in Fig. 7.7. The detailed configuration is shown in reference [273]. Each area of the three-area restructured system owns two DISCOs and two GENCOs (hydro and thermal). The apfs are assumed as: $apf_1 = apf_2 = apf_3 = apf_4 = 0.5$, $apf_5 = 0.6$ and $apf_6 = 0.4$. The power demands are assumed to be occurred in all three areas. In poolco plus bilateral with contract violation based transactions, it is assumed that a large step load power of 0.1 puMW is demanded by each DISCO of area-1, 2 and 3. It is

assumed that in addition to the specified contracted load demands, DISCO-1 situated in area-1, DISCO-3 situated in area-2 and DISCO-5 situated in area-3 demand 0.05 puMW, 0.04 puMW and 0.03 puMW of surplus power, respectively. Hence, $\Delta P_{UC1} = 0.05$ puMW, $\Delta P_{UC2} = 0.04$ puMW and $\Delta P_{UC3} = 0.03$ puMW. Therefore, area load demands will be as: $\Delta P_{D1} = 0.25$ puMW, $\Delta P_{D2} = 0.24$ puMW and $\Delta P_{D3} = 0.23$ puMW. Eqn. (5.9) is modified in three-area system to find out the actual generated powers of the GENCOs to Eqn. (7.14).

$$\Delta P_{Gi} = cpf_{i1}\Delta P_{L1} + cpf_{i2}\Delta P_{L2} + cpf_{i3}\Delta P_{L3} +$$

$$cpf_{i4}\Delta P_{L4} + cpf_{i5}\Delta P_{L5} + cpf_{i6}\Delta P_{L6}, \; i = 1,\ldots,6. \tag{7.14}$$

Eqn. (7.15) portrays the DPM for this scenario [273].

$$DPM = \begin{bmatrix} 0.25 & 0 & 0.25 & 0 & 0.5 & 0 \\ 0.5 & 0.25 & 0 & 0.25 & 0 & 0 \\ 0 & 0.5 & 0.25 & 0 & 0 & 0 \\ 0.25 & 0 & 0.5 & 0.75 & 0 & 0 \\ 0 & 0.25 & 0 & 0 & 0.5 & 0 \\ 0 & 0 & 0 & 0 & 0 & 1 \end{bmatrix} \tag{7.15}$$

The optimum parameters of the controllers are obtained using BFOA. The tuned parameters of FOPID as well as a PID controller are optimized such as: $K_P = -2.9243$, $K_I = -2.6879$, $\lambda = 0.9491$, $K_D = -1.7991$, $\mu = 0.9997$ (for FOPID) and $K_P = -1.3655$, $K_I = -1.3792$, $K_D = -0.6852$ (for PID). The computer simulation results in terms of numerical values of STs/PUs/PIs are depicted in Table 7.4. The results of frequency deviation of all three areas, power deviations of GENCOs and deviations in the tie-line power flows are shown in Figs. 7.8(a-r). Using, Eqns. (7.14-7.15) and apfs, the steady state power outputs of various GENCOs are obtained as: $\Delta P_{G1} = 0.125$ puMW (Figs. 7.8(h-i)), $\Delta P_{G2} = 0.125$ puMW (Figs. 7.8(j-k)), $\Delta P_{G3} = 0.095$ puMW (Figs. 7.8(l-m)), $\Delta P_{G4} = 0.17$ puMW (Figs. 7.8(n-o)), $\Delta P_{G5} = 0.093$ puMW (Fig. 7.8(p)) and

$\Delta P_{G6} = 0.112$ puMW (Figs. 7.8(q-r)). It is observed from Figs. 7.8(h-r) that these power signals converge properly to the desired values in the steady state. Further, Eqn.(3.5) for tie-line scheduled power will be modified in three-area system as indicated in Eqns. (7.16-7.17).

$$\Delta Ptie_{21,scheduled} = \sum_{i=3}^{4} \sum_{j=1}^{2} cpf_{ij} \Delta P_{Lj} - \sum_{i=1}^{2} \sum_{j=3}^{4} cpf_{ij} \Delta P_{Lj}, \tag{7.16}$$

$$\Delta Ptie_{31,scheduled} = \sum_{i=5}^{6} \sum_{j=1}^{2} cpf_{ij} \Delta P_{Lj} - \sum_{i=1}^{2} \sum_{j=5}^{6} cpf_{ij} \Delta P_{Lj}. \tag{7.17}$$

Hence, from Eqns. (7.16) and (7.17), $\Delta Ptie_{21,scheduled} = 0.025$ puMW and $\Delta Ptie_{31,scheduled} = -0.025$ puMW as revealed in Figs. 7.8(d) and (f), respectively. Signals ΔF_1 (Fig. 7.8(a)), ΔF_2 (Fig. 7.8(b)), ΔF_3 (Fig. 7.8(c)), $\Delta Ptie_{21,error}$ (Fig. 7.8(e))
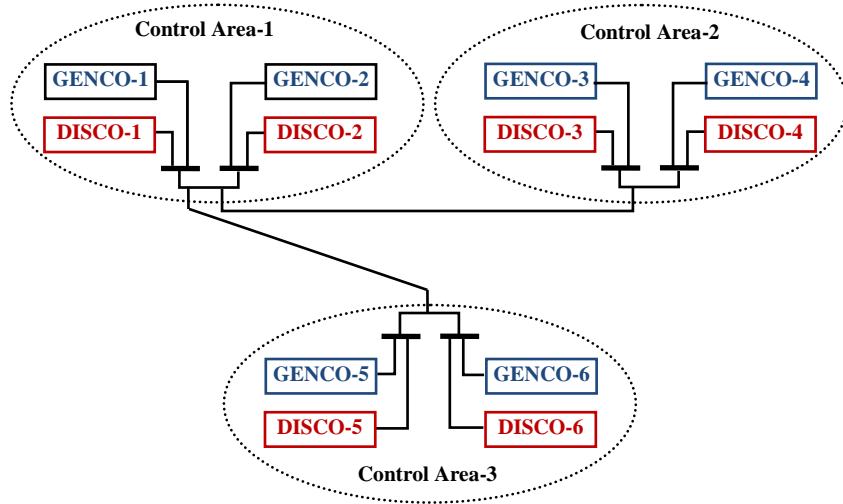
Fig. 7.7 Configuration diagram of a restructured three-area power system [273].

(c)

(d)

(e)

(f)

(g)

(h)
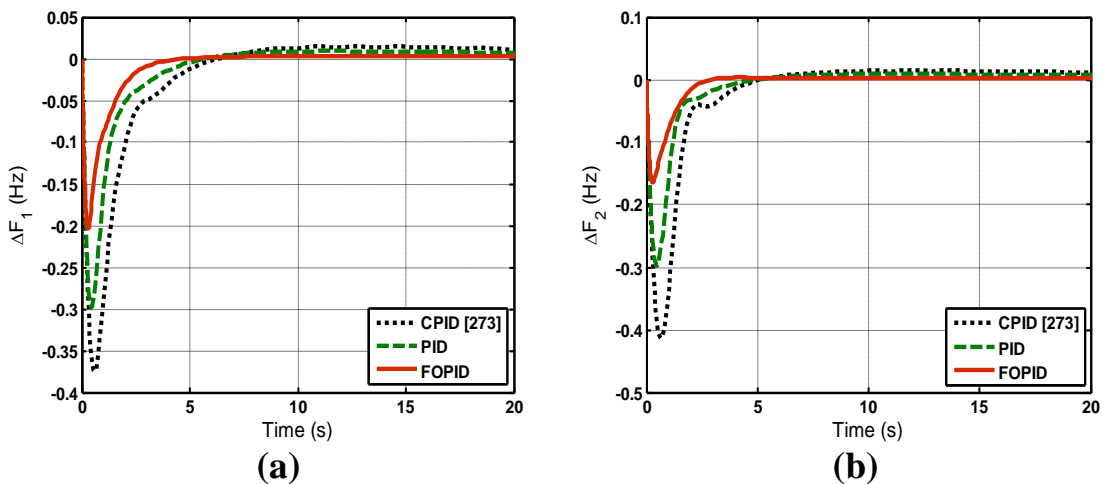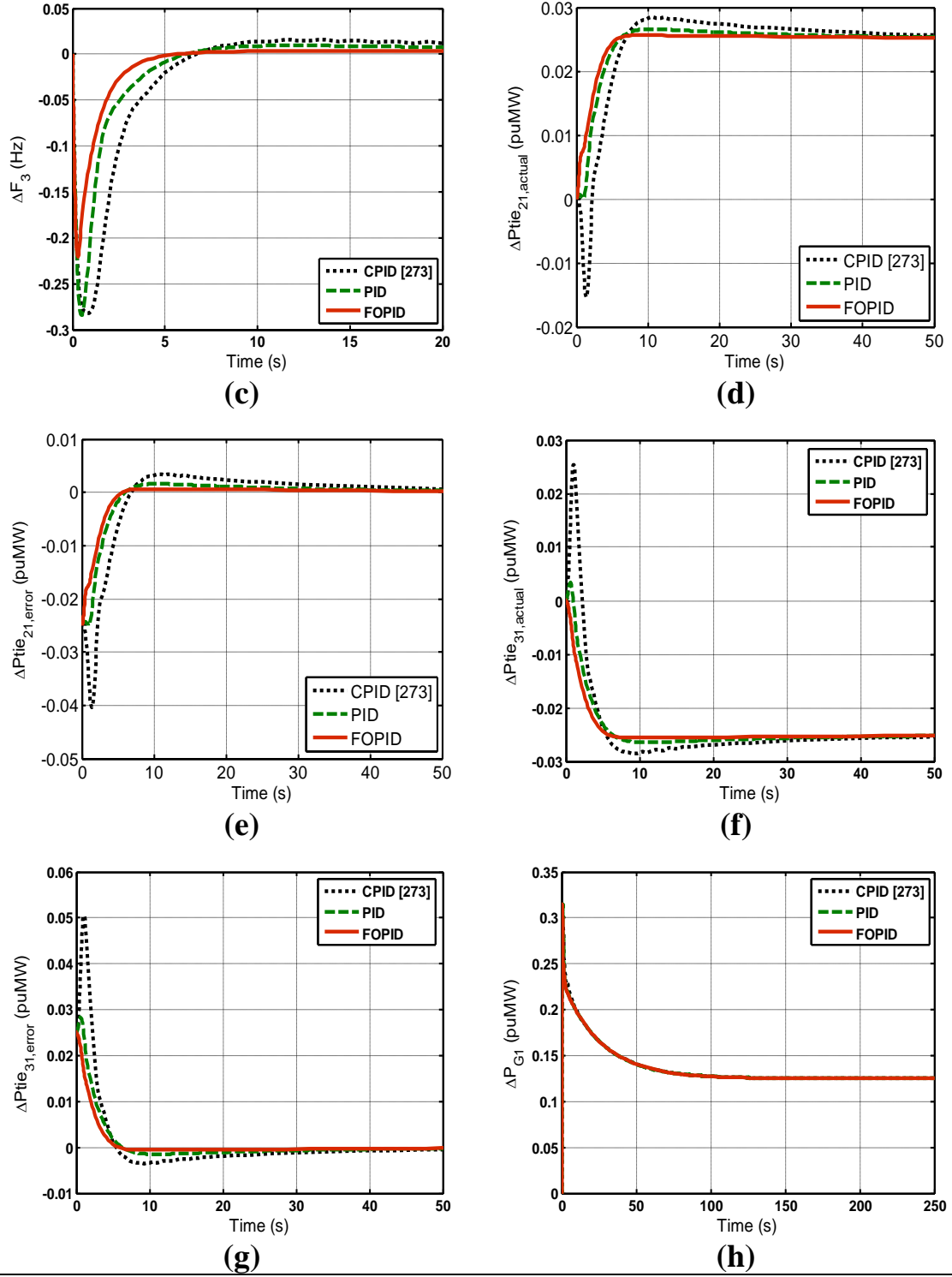
and $\Delta Ptie_{31,error}$ (Fig. 7.8(g)) are driven back quickly to zero in steady state. This is a required condition for an effective AGC control scheme. To demonstrate the advantage of BFOA tuned PID controller over a conventional PID (CPID) controller, the simulation results of CPID are also shown in Figs. 7.8(a-r). The optimized param-
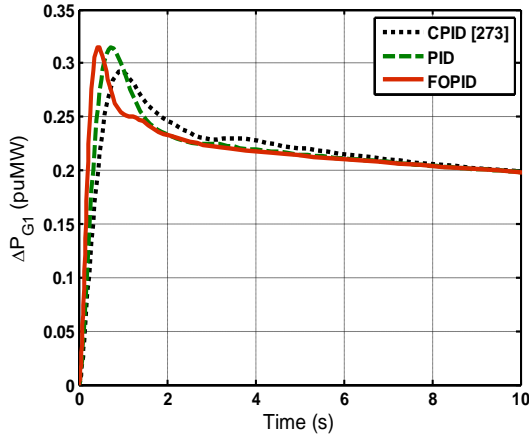
(i) Fig. 7.8(h) with Time = 0-10 s.
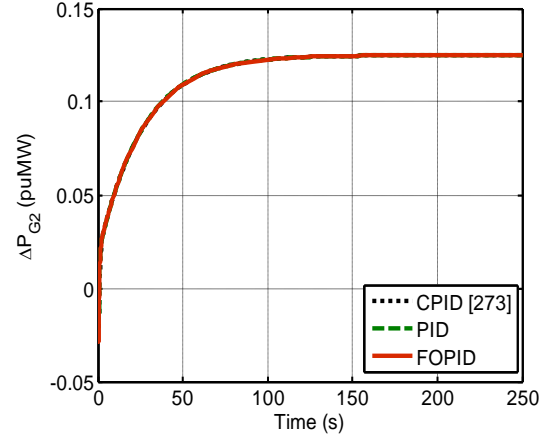
(j)
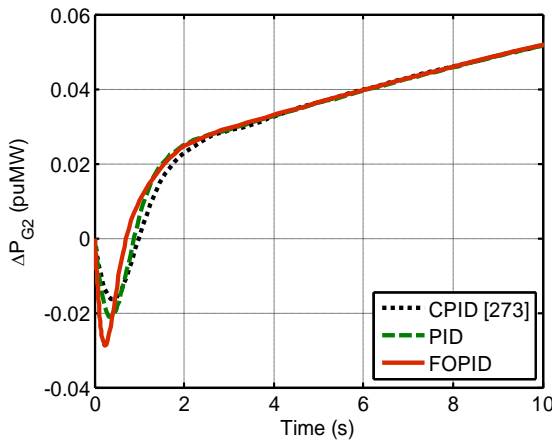
(k) Fig. 7.8(j) with Time = 0-10 s.
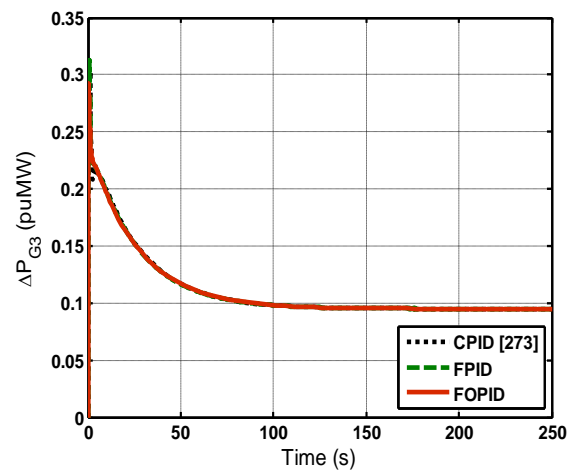
(l)
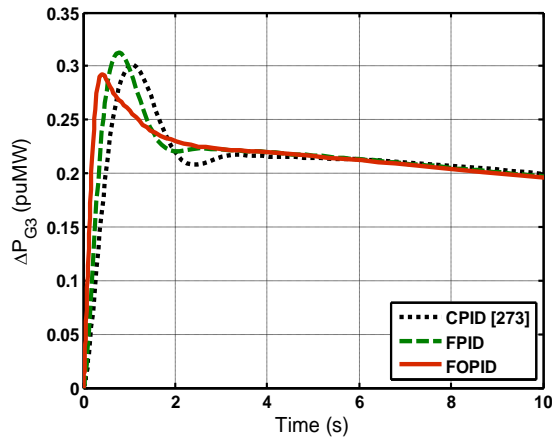
(m) Fig. 7.8(l) with Time = 0-10 s.
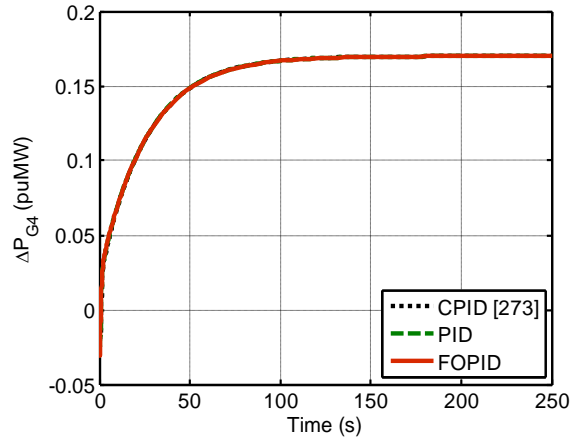
(n)

eters of CPID are employed from [273]. It is conferred from Figs. 7.8(a-d) and STs/PUs/PIs given in Table 7.4 that BFOA tuned PID exhibit superior performance compared to CPID and BFOA FOPID compared to BFOA tuned PID. However, peak undershoot due to CPID for ΔF_3 response is superior compared to BFOA tuned PID
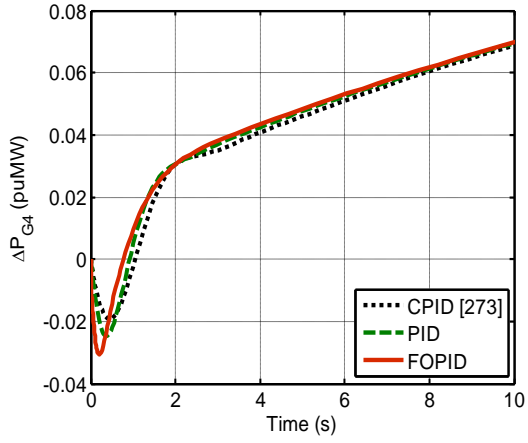
(o) Fig. 7.8(n) with Time = 0-10 s.
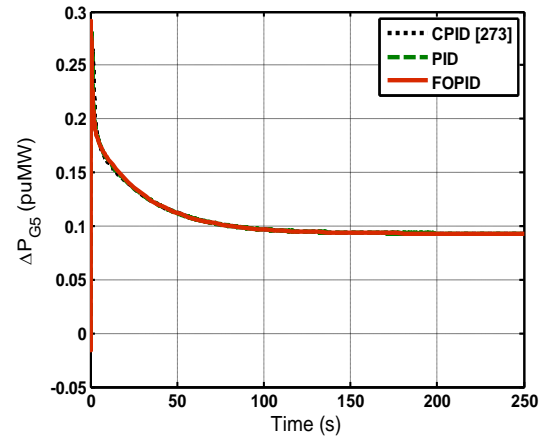
(p)
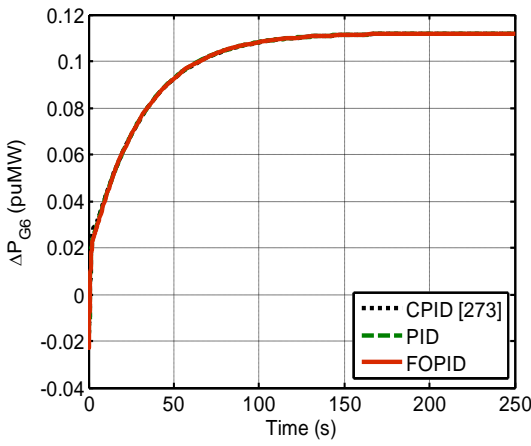
(q)
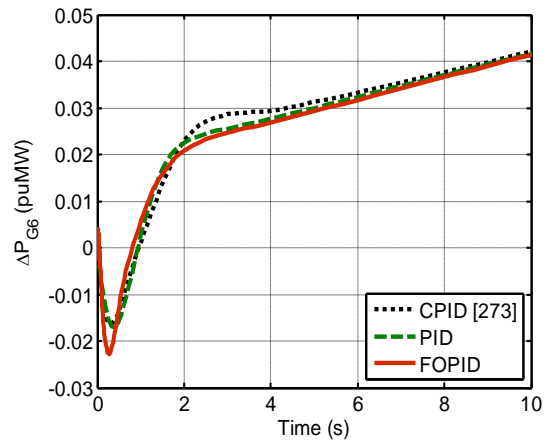
(r) Fig. 7.8(q) with Time = 0-10 s.

Fig. 7.8 Dynamic responses of three-area restructured multi-source hydrothermal power system with different controllers (a) ΔF_1 and (b) ΔF_2, (c) ΔF_3, (d) $\Delta Ptie_{21,actual}$, (e) $\Delta Ptie_{21,error}$, (f) $\Delta Ptie_{31,actual}$, (g) $\Delta Ptie_{31,error}$, (h) ΔP_{G1}, (i) ΔP_{G1}, (j) ΔP_{G2}, (k) ΔP_{G2}, (l) ΔP_{G3}, (m) ΔP_{G3}, (n) ΔP_{G4}, (o) ΔP_{G4}, (p) ΔP_{G5}, (q) ΔP_{G6} and (r) ΔP_{G6}.

Table 7.4

Numerical values of STs, PUs and PIs with restructured three-area multi-source system.

Controller type	STs (s)				PUs (Hz) (–ve)		
	ΔF_1	ΔF_2	ΔF_3	$\Delta Ptie_{21,error}$	ΔF_1	ΔF_2	ΔF_3
CPID [273]	106.46	106.15	106.58	55.69	0.3749	0.4139	0.2825
PID	93.45	92.87	95.37	38.17	0.2976	0.2975	0.2844
FOPID	**84.75**	**84.49**	**84.96**	**23.40**	**0.2038**	**0.1640**	**0.2205**

Controller type	PUs (puMW) (–ve)	PIs			
	$\Delta Ptie_{21,error}$	ISE	ITSE	IAE	ITAE
CPID [273]	0.0404	$4.25e^{-01}$	$4.53e^{-01}$	2.4240	7.1610
PID	0.0251	$2.02e^{-01}$	$1.66e^{-01}$	1.5190	4.2220
FOPID	**0.0250**	**$7.69e^{-02}$**	**$5.06e^{-02}$**	**0.8502**	**1.8110**

controller (CPID = −0.2825 and BFOA based PID = −0.2844). It is noticed that in restructured system, the proposed approach works well and the type of contract not only affects the area power demand, the scheduled tie-line power flow is also altered.

7.6   Conclusion

Fractional order PID (FOPID) controller is suggested for AGC problem solution in two-area traditional as well as restructured multi-source power systems. The parameters of FOPID controller are optimized exploiting BFOA. At first, a traditional two-area multi-source hydrothermal system is considered and the advantage of FOPID is established over PI/PID controller optimized using hFA-PS and PID controller optimized using GWO techniques. To show the effectiveness of the method, the approach is also extended to restructured two-area multi-source hydrothermal and thermal gas systems. The analysis of the simulation results discloses the efficacy of FOPID controller over BFOA optimized PID and DE/GA optimized PID controllers. Finally, the study is extended to a restructured three-area multi-source hydrothermal power system. It is revealed that the suggested controller work satisfactorily on various types of restructured power system models and satisfies the AGC obligation efficiently under various transactions taking place in deregulated environment. Hence, FOPID controller may be a suitable choice to solve AGC problem in traditional as well as restructured power systems.

CHAPTER 8

FRACTIONAL ORDER FUZZY PID CONTROLLER FOR AGC OF POWER SYSTEMS

8.1 Introduction

Although usual integer order (IO) controllers are widely recognized for their simplicity but there is no guarantee that they would provide the best results under practically constrained environments. It is also observed that the IO based classical controllers are not efficient in attaining excellent dynamic performances when subjected to ample change in size of SLP. To conquer these troubles, authors in Refs. [125,131,140,149,158,163–169,289,338,340–341,353] have introduced fractional order (FO) based classical controller to solve multi/single-area AGC problem. The chief benefits linked with FOPID controller is its two extra tuning knobs (parameters) known as λ (non-integer order of integrator) and μ (non-integer order of differentiator) that offers additional flexibility for amendment of system dynamics. However, owing to this benefit of FOPID, the majority of the history researches were centered only on employing classical IO controller in conjunction with an appropriate optimization techniques and very less attempt has been made to design and implement FOPID AGC controller. But recently, the concept of FO systems has been drawing more attentions because the improvements in computation power permit simulation and implementation of such systems with sufficient exactness. The major unease of FOPID controllers is the fine tuning of their parameters. The literature survey illustrates that recently various optimization techniques have been utilized to enhance the performance of FOPID controller via tuning its parameters for AGC systems for instance improved PSO in two-area hydrothermal gas multi-source system [131],

different variants of gravitational search algorithm (GSA) in four-area hydro-thermal gas system [140], firefly algorithm (FA) in three-area reheat thermal system [149], cat swarm optimization (CSO) for three-area non-reheat thermal system [158], imperialist competitive algorithm (ICA) in three-area hydrothermal system [163], gases Brownian motion optimization (GBMO) in two-area non-reheat thermal system [164], kriging based surrogate modeling in a single-area hybrid-source system [165], GA in two-area traditional/deregulated non-reheat thermal system [125,289], BFOA in two-area deregulated non-reheat thermal system [340]/three-area deregulated reheat thermal system [341] etc. Performance of FOPID is tried to improve employing a new classical controller termed as two-degree-of-freedom-FOPID (2-DOF-FOPID) optimized using a FA in a three-area reheat thermal system where it shows enhanced results compared to classical I/PI/PID/FOI/FOPI/FOPID/2-DOF-FOPID controller [149]. Additionally, FOPID is integrated with fuzzy logic termed as fractional order fuzzy PID (FOFPID) and chaotic PSO to enhance the performance of FOFPID in a single-area hybrid-source power system [168]. It is observed that the FOFPID controller outperforms PID and fuzzy PID controller structures.

The literature survey reveals that in the past decade various methods have been proposed by the researchers to improve the performance of FOPID controller in AGC of various types of traditional and restructured power systems. It is also observed that no work is available in the literature about the implementation of FOFPID structured controller in AGC of multi-area single/multi-source power system. However, a FOFPID controller is proposed for a single-area multi-source system [168]. Hence, extra study of FOFPID controller for AGC of multi-area multi-source traditional/restructured power system is requisite.

In the light of above discussions, in this chapter, a maiden attempt is made to implement a FOFPID controller for AGC of two-area multi-source traditional/restructured power system and BFOA is used to optimize the controller parameters. In this study, a comparison is tried to report between standard PID, FOPID and designed FOFPID controllers to show the advantage of the FOFPID control scheme.

8.2   Systems investigated

The systems investigated in this chapter are same as described in Chapter 6. Hence, study has been conducted on traditional/restructured two-area multi-source hydrothermal system, restructured two-area multi-source thermal gas system and restructured three-area multi-source hydrothermal system.

8.3   FOFPID controller

FOFPID controller is shown in Fig. 8.1. FLC uses ACE and ACE derivative with fractional order as input signals. The FLC output (i.e., y) is multiplied with FOPID to get output ΔP_C of the controller. ΔP_C described by Eqn. (8.1) is the control input to the system.

$$\Delta P_C = K_P y + \frac{K_I}{s^\lambda} y + K_D s^\mu y, \ (\lambda, \mu > 0). \tag{8.1}$$

K_1, K_2 (input scaling factors), γ (order of input differentiator), $K_P/K_I/K_D$ (output scaling factors), λ (order of output integrator) and μ (order of output differentiator) are the parameters to be optimized employing BFOA via minimizing an appropriate objective function i.e., Eqn. (7.11). In the current study, five triangular mfs are selected for inputs (ACE, fractional rate of ACE derivative) and output of FLC as shown in Fig. 6.4 [104,151]. Identical mfs with equal horizontal range are engaged for inputs and output of the FLC. The two-dimensional rule base for ACE, fractional rate
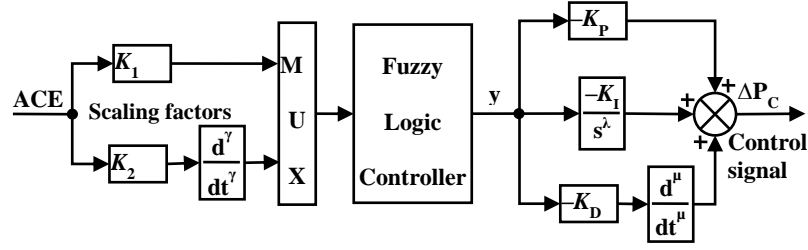
Fig. 8.1 Structure of FOFPID controller [104,107].

of ACE derivative and FLC output consisting of twenty five rules is revealed in Table 6.1. Mamdani fis and centroid defuzzification method are used in this study. Identical controllers are designed for the identical two/three-area systems.

8.4 Optimization problem

The FOFPID controller design problem can be treated as an optimization problem. Each out of two FOFPID controllers used in two-area system has eight parameters to be optimized. The optimization problem can be described as to minimize J (7.11) in sight of the following constraints:

$K_{1\ min} \leq K_1 \leq K_{1\ max}$, $K_{2\ min} \leq K_2 \leq K_{2\ max}$, $\gamma_{min} \leq \gamma \leq \gamma_{max}$, $K_{P\ min} \leq K_P \leq K_{P\ max}$, $K_{I\ min} \leq K_I \leq K_{I\ max}$, $\lambda_{min} \leq \lambda \leq \lambda_{max}$, $K_{D\ min} \leq K_D \leq K_{D\ max}$, $\mu_{min} \leq \mu \leq \mu_{max}$.

where, γ_{min}, λ_{min}, μ_{min}, $K_{1,2,P,I,D\ min}$ and γ_{max}, λ_{max}, μ_{max}, $K_{1,2,P,I,D\ max}$ are the minimum and maximum values of FOFPID structured controller parameters, respectively. The minimum and maximum values of $K_{1,2,P,I,D}$ parameters are selected as 0.0 and 4.0, respectively. Though, γ, λ and μ values are selected between 0.0 and 1.0. The tunable parameters for FOPID (K_P, K_I, K_D, λ and μ) controller would be five; though, their numbers will be three in case of conventional PID (K_P, K_I and K_D) controller.

153

8.5 Simulation results and discussions

To study the dynamic performance of the systems under concern against SLP in any control area, the models and programs of the systems are developed on an Intel Core2 Duo processor of 1.66 GHz and 2 GB of RAM computer in the MATLAB /SIMULINK version 7.5.0 (R2007b) using the data shown in Appendix B. The BFOA tuning procedure for every model under study is repeated 50 times and the best final solution among 50 runs are chosen as the controller parameters to be used in computer simulations [150,323]. The results indicating advantage are **bold faced** in the relevant tables.

8.5.1 Traditional two-area multi-source hydrothermal system

A traditional two-area multi-source hydrothermal power system is simulated considering 1.5% SLP at time t = 0 s in area-1. The AGC system model is shown in Fig.7.2 (without dotted line connections). However, FOPID controller stickered in Fig. 7.2 will be replaced with FOFPID controller in the current study. The FOFPID controller parameters are optimized employing BFOA as: K_1 = 1.9996, K_2 = 0.9043, γ = 0.9359, K_P = 1.2192, K_I = 1.9390, λ = 0.9953, K_D = 0.0791 and μ = 0.9999. The system dynamic responses for ΔF_1, ΔF_2, $\Delta Ptie_{12}$, ACE_1, ΔP_{g1} and ΔP_{g2} responses are shown in Fig. 8.2. To confirm the superiority of the proposed FOFPID controller, the dynamic responses due to BFOA tuned FOPID for the same system are also given in Fig. 8.2 and Table 8.1. Critical analysis of Fig. 8.2 and Table 8.1 clearly reveals that the performance of FOFPID controller show advantage over FOPID controller in terms of lesser STs (FOFPID: ΔF_1 = 0.55 s, ΔF_2 = 0.98 s, $\Delta Ptie_{12}$ = 0.45 s, ACE_1 = 0.0567 s; FOPID: ΔF_1 = 1.20 s, ΔF_2 = 2.15 s, $\Delta Ptie_{12}$ = 1.678 s, ACE_1 = 1.5190 s), PUs (FOFPID: ΔF_1 = –0.0038 Hz, ΔF_2 = –0.0007 Hz, $\Delta Ptie_{12}$ = –0.0003 puMW, ACE_1 =

–0.00171 puMW; FOPID: $\Delta F_1 = -0.0115$ Hz, $\Delta F_2 = -0.0046$ Hz, $\Delta Ptie_{12} = -0.0015$ puMW, $ACE_1 = -0.00575$ puMW) and PIs (FOFPID: ISE = $2.81e^{-06}$, ITSE = $7.73e^{-07}$, IAE = 0.0026, ITAE = 0.0035; FOPID: ISE = $5.22e^{-05}$, ITSE = $2.14e^{-05}$, IAE = 0.0116, ITAE = 0.0121). Consequently, better system dynamic performance in terms minimum PIs and STs/PUs in frequency, tie-line power and area control error deviations is achieved employing FOFPID controller compared to FOPID. It is also

Table 8.1
Numerical values of STs, PUs and PIs with traditional two-area multi-source hydrothermal system.

Controller type	STs (s)				PUs (Hz)		PUs (puMW)	
	ΔF_1	ΔF_2	$\Delta Ptie_{12}$	ACE_1	ΔF_1	ΔF_2	$\Delta Ptie_{12}$	ACE_1
FOPID	1.20	2.15	1.678	1.5190	−0.0115	−0.0046	−0.0015	−0.00575
FOFPID	**0.55**	**0.98**	**0.450**	**0.0567**	**−0.0038**	**−0.0007**	**−0.0003**	**−0.00171**
-	PIs							
-	ISE		ITSE		IAE		ITAE	
FOPID	$5.22e^{-05}$		$2.14e^{-05}$		0.0116		0.0121	
FOFPID	**$2.81e^{-06}$**		**$7.73e^{-07}$**		**0.0026**		**0.0035**	
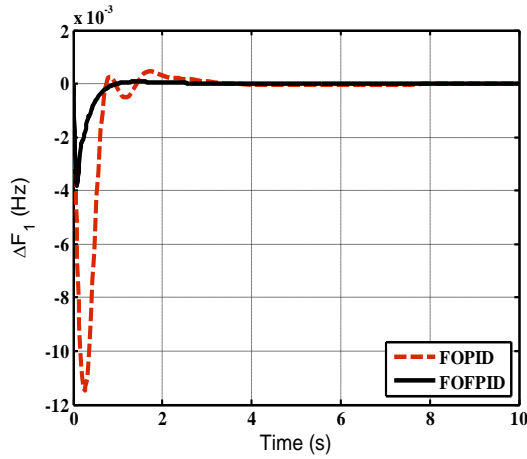
(a)
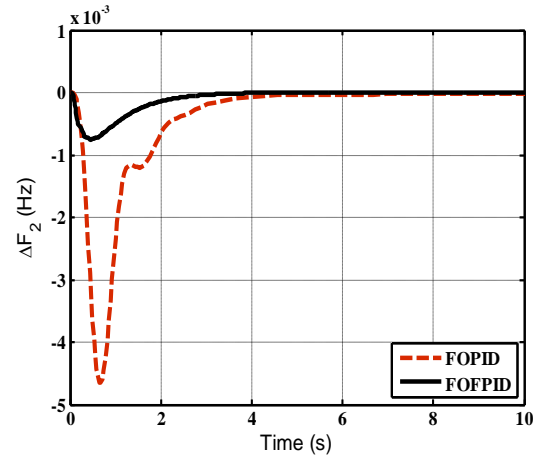
(b)
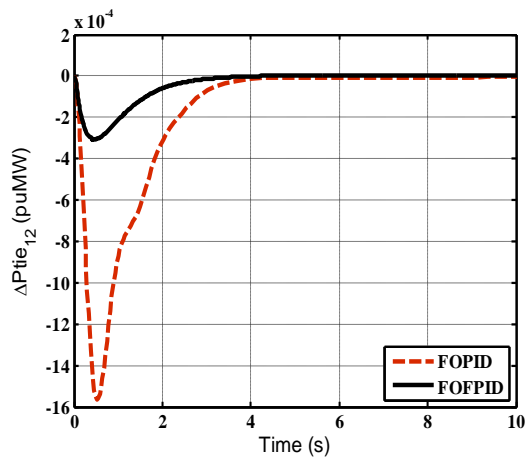
(c)
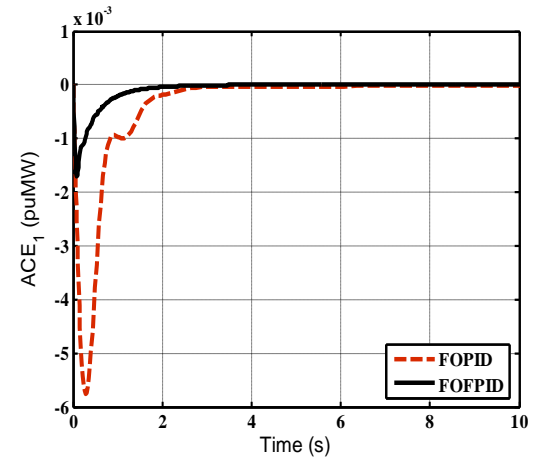
(d)

Fig. 8.2 Dynamic responses of traditional two-area multi-source hydrothermal system with different types of controllers for 1.5% SLP in area-1 at time t = 0 s (a) ΔF_1 (b) ΔF_2 (c) $\Delta Ptie_{12}$, (d) ACE_1, (e) ΔP_{g1} and (f) ΔP_{g2}.

Table 8.2

Numerical values of STs, PUs and PIs with restructured multi-source hydrothermal system.

Contr-oller	STs (s)			PUs (–ve) (Hz or puMW)			PIs			
	ΔF_1	ΔF_2	$\Delta Ptie_{error}$	ΔF_1	ΔF_2	$\Delta Ptie_{error}$	ISE	ITSE	IAE	ITAE
FOPID	1.89	3.32	2.68	0.0138	0.0052	0.0019	$9.64e^{-05}$	$5.79e^{-05}$	0.0223	0.0410
FOFPID	**0.79**	**1.97**	**1.19**	**0.0085**	**0.0022**	**0.0008**	**$2.04e^{-05}$**	**$7.12e^{-06}$**	**0.0079**	**0.0147**

observed from Figs. 8.2(a-b) that the frequency deviation belonging to area where SLP is applied shows more PU compared to area without SLP. It is observed from Figs. 8.2(e-f) that the generaions in area-1 and 2 settle to the desired values of 0.015 puMW and 0 puMW, respectively due to both FOFPID and FOPID controllers but the responses due to FOFPID controller observed more healthier compared to FOPID responses.

8.5.2   Restructured two-area multi-source hydrothermal system

   (poolco based transactions)

The block diagram of restructured multi-source hydrothermal power system is shown in Fig. 7.2 (with dotted line connections). In model two GENCO and two DISCOs are
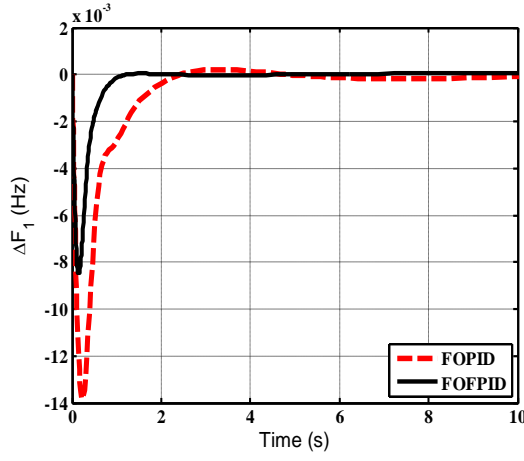
(a)
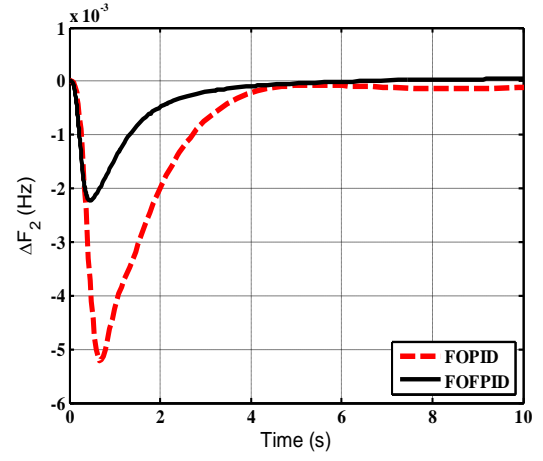
(b)
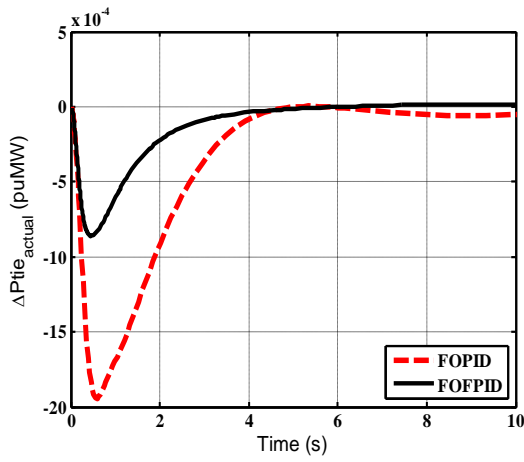
(c)
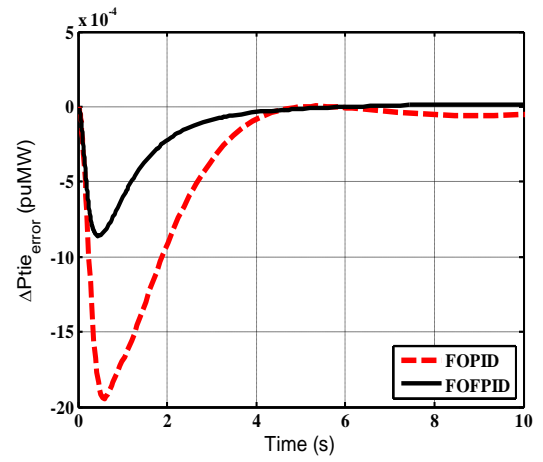
(d)
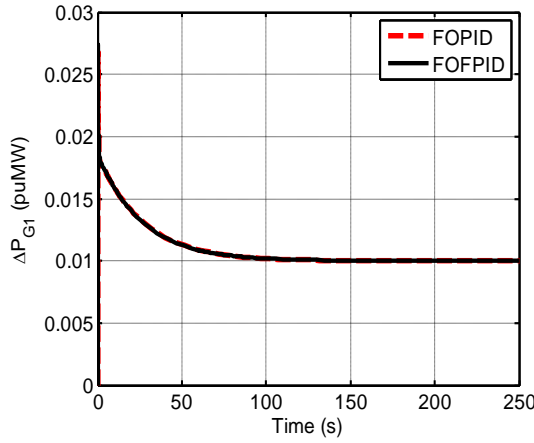
(e)
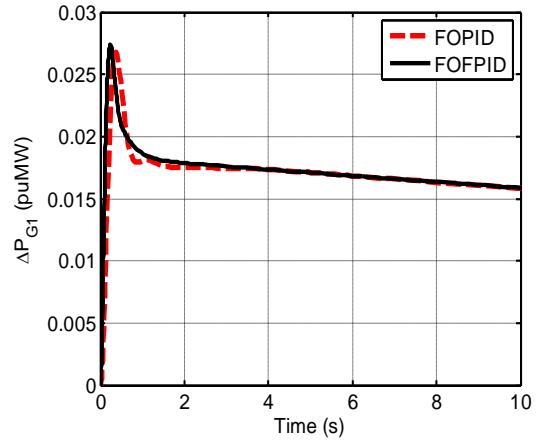
(f) Fig. 8.3(e) with Time t = 0-10 s.

assumed in each area. The optimum parameter values of BFOA optimized FOFPID controller is as: $K_1 = 0.5031$, $K_2 = 0.4630$, $\gamma = 0.9075$, $K_P = 1.9986$, $K_I = 3.0992$, $\lambda = 0.9563$, $K_D = 0.1584$ and $\mu = 0.7984$. Let, $\Delta P_{L1} = \Delta P_{L2} = 0.01$ puMW and $\Delta P_{L3} = \Delta P_{L4}$
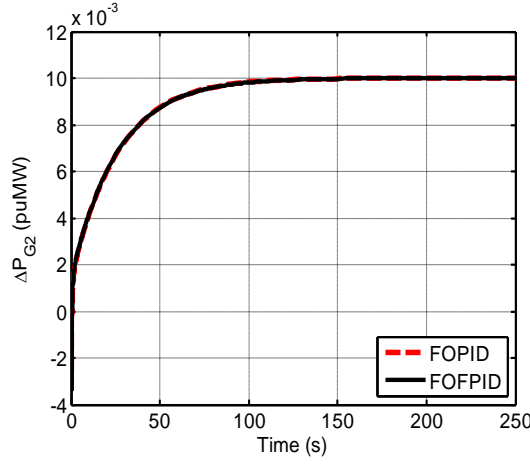
(g)
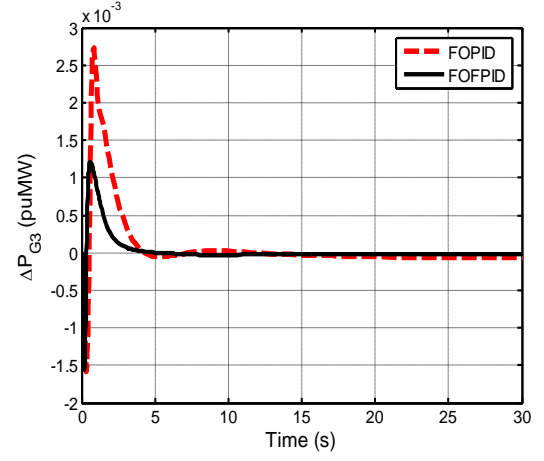
(h)
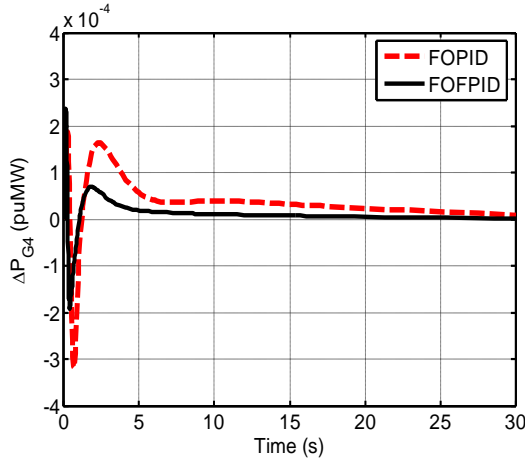
(i)
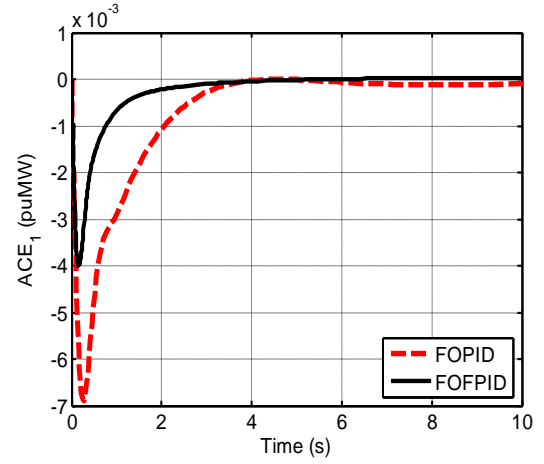
(j)
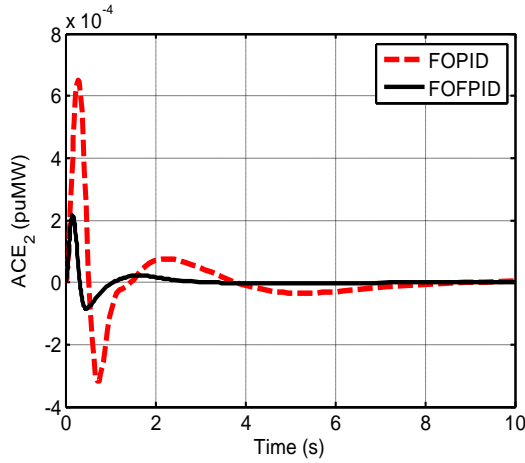
(k)
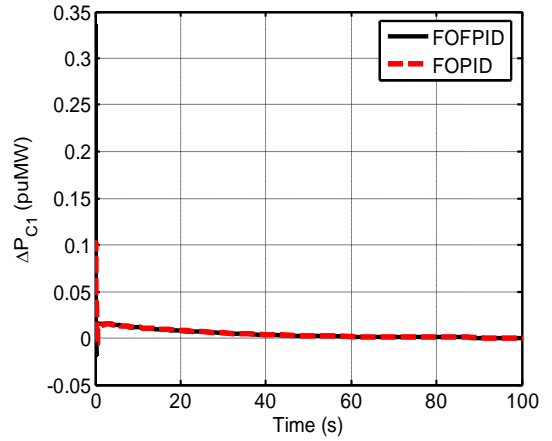
(l)

= 0.00 puMW. The selected DPM structure is given by Eqn. (7.12). Simulations of the system are carried out with the suggested FOFPID controller and compared with FOPID controller designed in Chapter 6. STs/PUs of $\Delta F_1/\Delta F_2/\Delta Ptie_{error}$ and PIs for FOFPID and FOPID controllers are given in Table 8.2. It is clear from Table 8.2 that

(m) Fig. 8.3(l) with Time t = 0–10 s. **(n)**
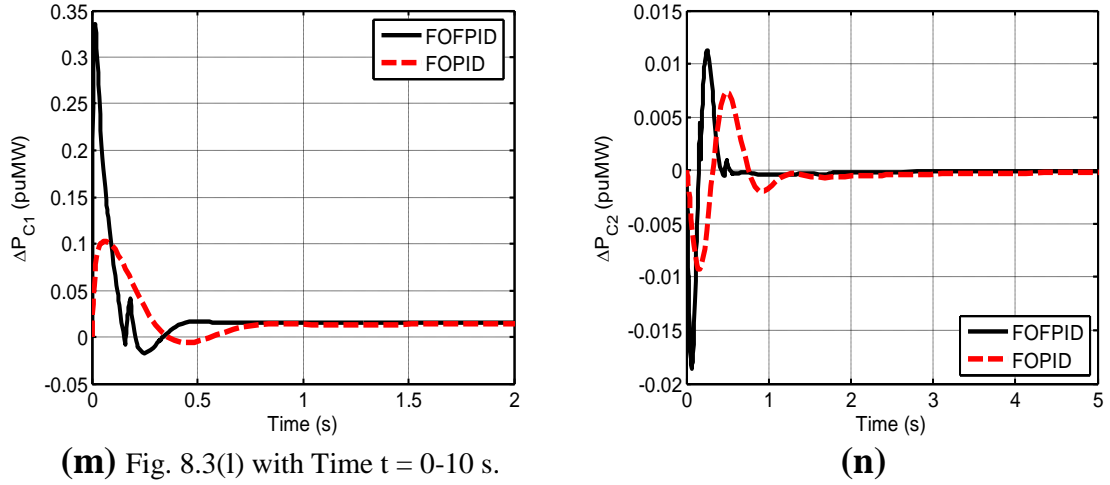
Fig. 8.3 Dynamic responses of restructured two-area two-source hydrothermal system with FOPID/FOFPID controller for (a) ΔF_1, (b) ΔF_2, (c) $\Delta Ptie_{actual}$, (d) $\Delta Ptie_{error}$, (e) ΔP_{G1}, (f) ΔP_{G1}, (g) ΔP_{G2}, (h) ΔP_{G3}, (i) ΔP_{G4}, (j) ACE_1, (k) ACE_2, (l) ΔP_{C1}, (m) ΔP_{C1} and (n) ΔP_{C2}.

FOFPID perform superiorly as minimum PIs values are acquired with FOFPID (ISE = $2.04e^{-05}$, ITSE = $7.12e^{-06}$, IAE = 0.0079, ITAE = 0.0147) compared to FOPID (ISE = $9.64e^{-05}$, ITSE = $5.79e^{-05}$, IAE = 0.0223, ITAE = 0.0410). Furthermore, it is apparent that STs and PUs values are also less with FOFPID (STs: ΔF_1 = 0.79 s, ΔF_2 = 1.97 s, $\Delta Ptie_{error}$ = 1.19 s; PUs: ΔF_1 = 0.0085 Hz, ΔF_2 = 0.0022 Hz, $\Delta Ptie_{error}$= 0.0008 puMW) compared to FOPID (STs: ΔF_1 = 1.89 s, ΔF_2 = 3.32 s, $\Delta Ptie_{error}$ = 2.68 s; PUs: ΔF_1 = 0.0138 Hz, ΔF_2 = 0.0052 Hz, $\Delta Ptie_{error}$ = 0.0019 puMW). The dynamic performance of the system is shown in Figs. 8.3(a-n). It is apparent from Figs. 8.3(a-d) that improved system dynamic responses in terms minimum STs and PUs in frequency and tie-line power error variations is attained via FOFPID controller in comparison to FOPID controller. Further, From Figs. 8.3(e-i), it is noted that steady state simulated values of GENCOs outputs match with the desired values. In these figures FOFPID controller work superbly. Figs. 8.3(j-k) show the responses of ACEs where FOFPID controller show lesser PUs and STs. Figs. 8.3(l-n) show the responses of controller outputs i.e., ΔP_{C1} and ΔP_{C2}. Figs. 8.3(l-n) indicate that FOFPID controller show greater control

action in the dynamic periods in both areas and settle to the desired value quickly compared to FOPID controller. Hence, a favored performance is exerted by the suggested FOFPID controller.

8.5.3 Restructured two-area multi-source thermal gas system
(poolco plus bilateral based transactions)

The study is further extended to a restructured two-area multi-source thermal gas power system by considering two GENCOs (thermal and gas) plus two DISCOs in each control area as stated in section 7.5.3. The block diagram of the system is shown in Fig. 7.5. Poolco plus bilateral transactions case is considered in which all four GENCOs contribute in the AGC task. The DISCOs have contracts with the GENCOs as per apfs as: $apf_1 = 0.75$, $apf_2 = 0.25$, $apf_3 = apf_4 = 0.5$ and DPM stated in Eqns. (7.13) and (8.2).

Table 8.3

Numerical values of STs, PUs and PIs with restructured multi-source thermal gas system.

Cont-roller	STs (s)			PUs (–ve) (Hz or puMW)			PIs			
	ΔF_1	ΔF_2	$\Delta Ptie_{error}$	ΔF_1	ΔF_2	$\Delta Ptie_{error}$	ISE	ITSE	IAE	ITAE
FO PID	8.95	5.95	6.450	0.5130	0.2839	0.0000	$2.69e^{-01}$	$2.00e^{-01}$	1.0780	1.8450
FO FPID	**5.86**	**1.55**	**3.998**	**0.2374**	**0.1128**	0.0000	**$4.67e^{-02}$**	**$3.43e^{-02}$**	**0.4901**	**0.7724**
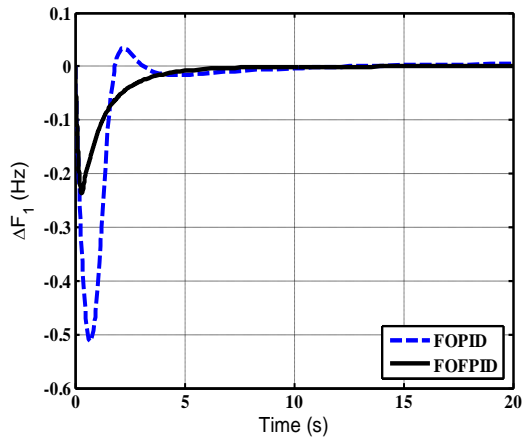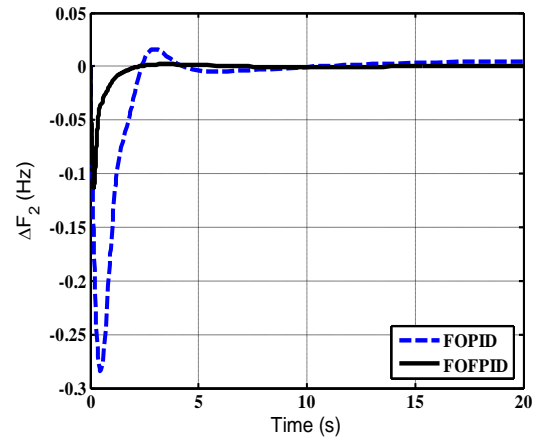
(a)   (b)
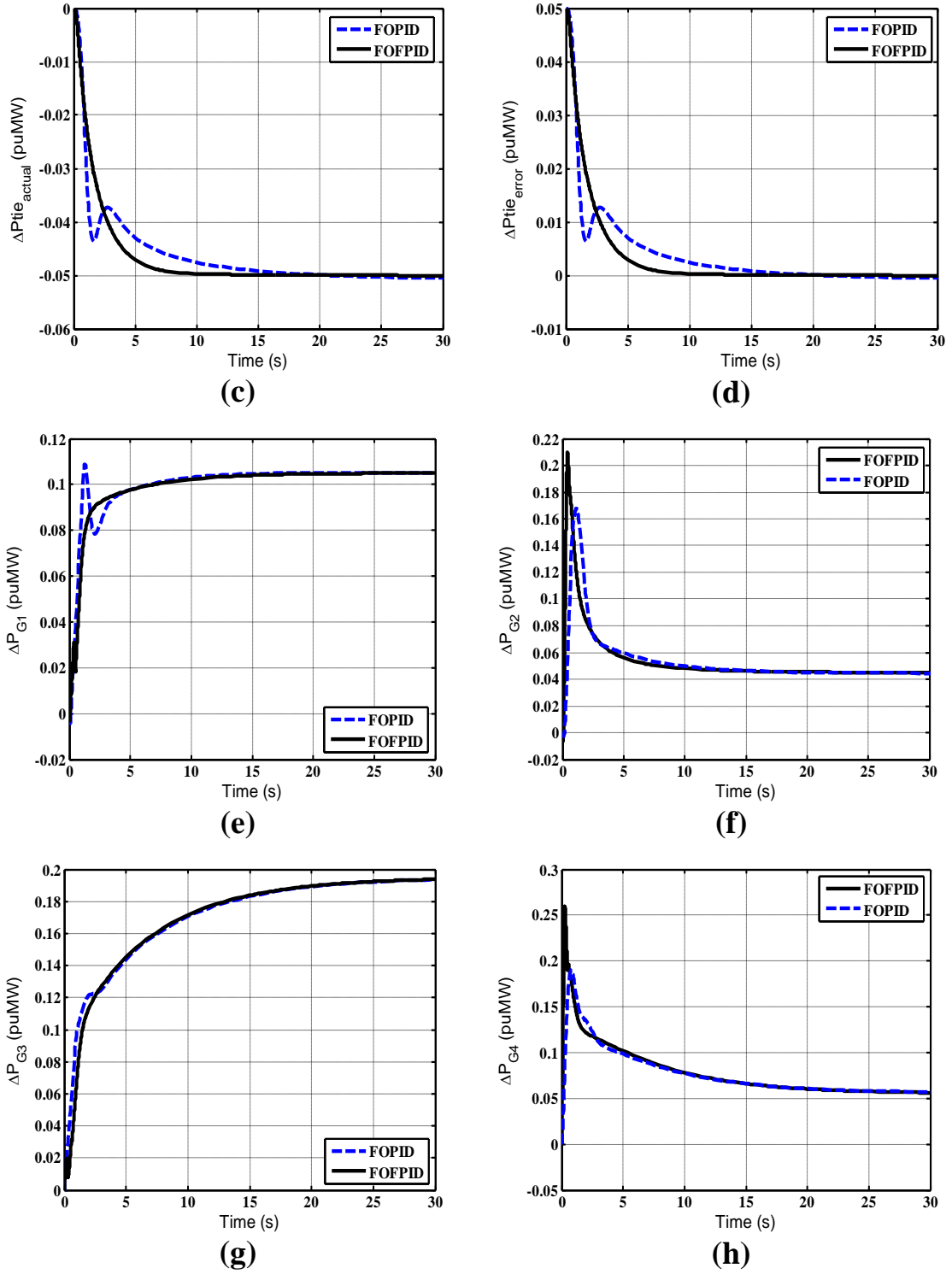
Fig. 8.4 Dynamic responses of two-area restructured multi-source thermal gas system with different controllers for poolco plus bilateral based transactions (a) ΔF_1, (b) ΔF_2, (c) $\Delta Ptie_{actual}$, (d) $\Delta Ptie_{error}$, (e) ΔP_{G1}, (f) ΔP_{G2}, (g) ΔP_{G3} and (f) ΔP_{G4}.

$$DPM = \begin{bmatrix} 0.5 & 0.25 & 0.0 & 0.3 \\ 0.2 & 0.25 & 0.0 & 0.0 \\ 0.0 & 0.25 & 1.0 & 0.7 \\ 0.3 & 0.25 & 0.0 & 0.0 \end{bmatrix} \qquad (8.2)$$

Let, $\Delta P_{L1} = \Delta P_{L2} = \Delta P_{L3} = \Delta P_{L4} = 0.1$ puMW. Optimized controller parameters are obtained using BFOA as: $K_1 = 1.9971$, $K_2 = 1.9990$, $\gamma = 0.9973$, $K_P = 2.2361$, $K_I = 2.7321$, $\lambda = 0.0993$, $K_D = 0.4179$ and $\mu = 0.9992$. System responses with BFOA tuned FOFPID and FOPID (simulated in Chapter 7) controllers are shown in Fig. 8.4. With FOFPID controller, ΔF_1, ΔF_2 and $\Delta Ptie_{error}$ responses driven back to zero quickly with slight values of STs, PUs and PIs as designated in Table 8.3 and Figs. 8.4(a-b,d). Additionally, in the steady state, $\Delta Ptie_{actual}$ response properly touched the specified value of Eqn. (4.5) i.e., $\Delta Ptie_{scheduled/actual} = -0.05$ puMW as verified from Fig. 8.4(c). As shown in Figs. 8.4(e-h), the actual power generations of GENCOs, according to Eqn. (5.9), correctly reach their preferred values comparably quickly in the steady state i.e., $\Delta P_{G1} = 0.105$ puMW, $\Delta P_{G2} = 0.045$ puMW, $\Delta P_{G3} = 0.195$ puMW and $\Delta P_{G4} = 0.055$ puMW. However, in all these responses, in comparison to FOPID controller, FOFPID controller shows smooth, fast and hence better dynamic responses.

8.5.4 *Restructured three-area multi-source hydrothermal system*
(poolco plus bilateral with contract violation based transactions)

To validate the capability of the FOFPID controller in multiple multi-area restructured power systems, the study is also expanded to a restructured three-area system. The topology of the system is shown in Fig. 7.7. The detailed interconnections of the three-area system are shown in [273]. Each area of the system consists of two DISCOs and two GENCOs. Two GENCOs in an area have a single reheat thermal plant and a hydro plant with mechanical governor. The apfs are assumed to be $apf_1 =$

apf$_2$ = apf$_3$ = apf$_4$ = 0.5, apf$_5$ = 0.6 and apf$_6$ = 0.4. Let, Let, $\Delta P_{L1} = \Delta P_{L2} = \Delta P_{L3} = \Delta P_{L4}$ = $\Delta P_{L5} = \Delta P_{L6}$ = 0.1 puMW, ΔP_{UC1} = 0.05 puMW, ΔP_{UC2} = 0.04 puMW and ΔP_{UC3} = 0.03 puMW. Therefore, ΔP_{D1} = 0.25 puMW, ΔP_{D2} = 0.24 puMW and ΔP_{D3} = 0.23 puMW. Eqn. (7.15) portrays the DPM for this scenario [273]. The optimum parameters of the controller are obtained using BFOA. The optimized parameters of FOFPID are acquired as: K_1 = 1.9961, K_2 = 0.5861, γ = 0.9999, K_P = 1.5402, K_I = 1.9912, λ = 0.9743, K_D = 1.0941 and μ = 0.3241. The computer simulation results of the system in terms of numerical values of STs/PUs/PIs for ΔF_1, ΔF_2, ΔF_3 and $\Delta Ptie_{21,error}$ are depicted in Table 8.4. It is revealed from Table 8.4 that FOFPID controller show very less values of STs/PUs/PIs for $\Delta F_1/\Delta F_2/\Delta F_3/\Delta Ptie_{21,error}$ responses compared to FOPID controller e.g., STs of ΔF_1, ΔF_2, ΔF_3 and $\Delta Ptie_{21,error}$ responses with FOFPID are 9.63 s, 9.72 s, 5.02 s and 4.56 s, respectively while these values with FOPID controller are 84.75 s, 84.49 s, 84.96 s and 23.40 s, respectively. However, PU for $\Delta Ptie_{21,error}$ signal is same (i.e., –0.0250 puMW) with both FOFPID and FOPID controllers. The superiority of FOFPID controller is also visible in Figs. 8.5(a), 8.5(b), 8.5(c), 8.5(e) and 8.5(g) concerned with ΔF_1, ΔF_2, ΔF_3, $\Delta Ptie_{21,error}$ and $\Delta Ptie_{31,error}$ responses, respectively. In these figures, deviated responses, due to SLPs

Table 8.4

Numerical values of STs, PUs and PIs with restructured three-area multi-source system.

Controller type	STs (s)				PUs (–ve) (Hz)		
	ΔF_1	ΔF_2	ΔF_3	$\Delta Ptie_{21,error}$	ΔF_1	ΔF_2	ΔF_3
FOPID	84.75	84.49	84.96	23.40	0.2038	0.1640	0.2205
FOFPID	**9.63**	**9.72**	**5.02**	**4.56**	**0.1275**	**0.1125**	**0.1371**

Controller type	PUs (–ve) (puMW)	PIs			
	$\Delta Ptie_{21,error}$	ISE	ITSE	IAE	ITAE
FOPID	0.0250	$7.69e^{-02}$	$5.06e^{-02}$	0.8502	1.8110
FOFPID	**0.0250**	**$1.96e^{-02}$**	**$8.55e^{-03}$**	**0.3632**	**0.4733**

(a)

(b)

(c)

(d)

(e)

(f)
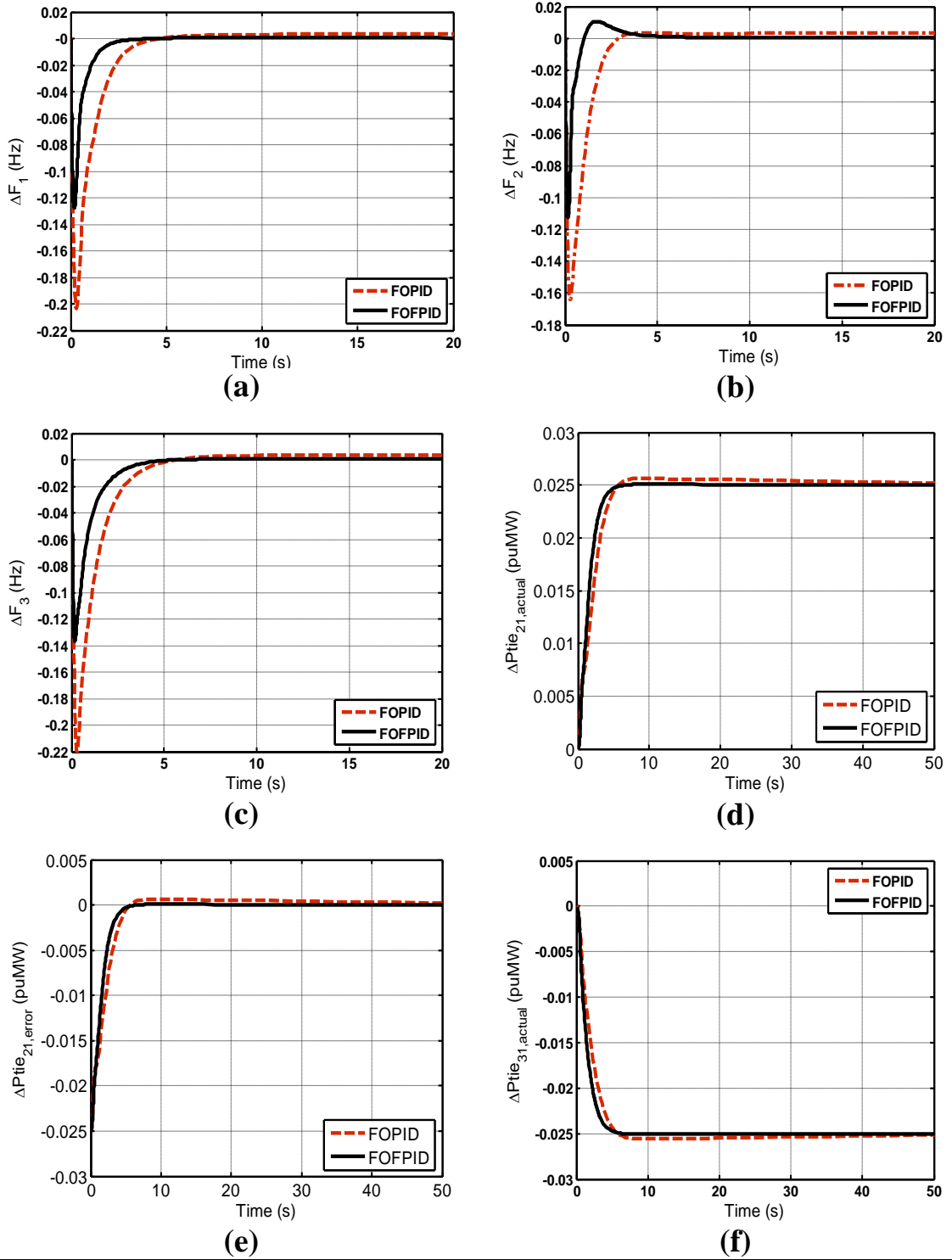
in control areas, go back to their desired zero positions in steady state swiftly with FOFPID compared to FOPID controller. The dynamic responses of actual tie-line power flows and power deviations of GENCOs are shown in Figs. 8.5(d,f,h-r). Using, Eqns. (7.14-7.15), the steady state power outputs of various GENCOs are obtained as:

164
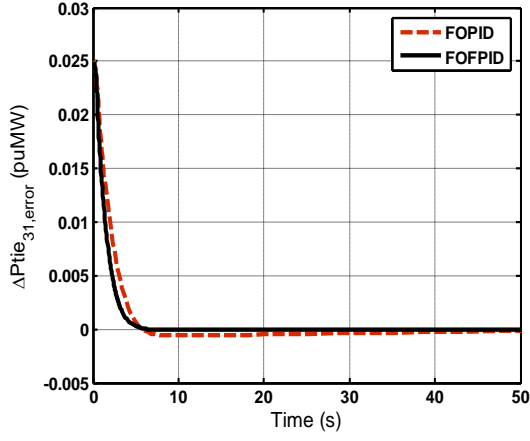
(g)
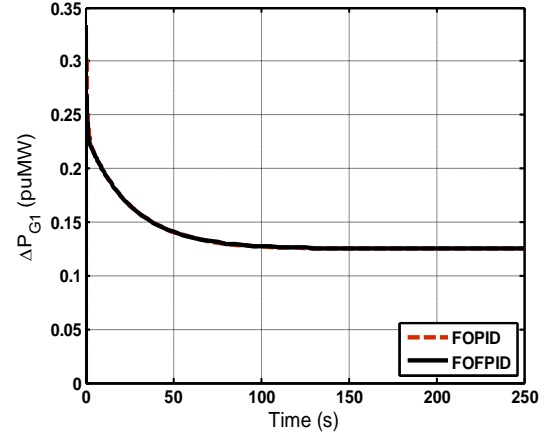
(h)
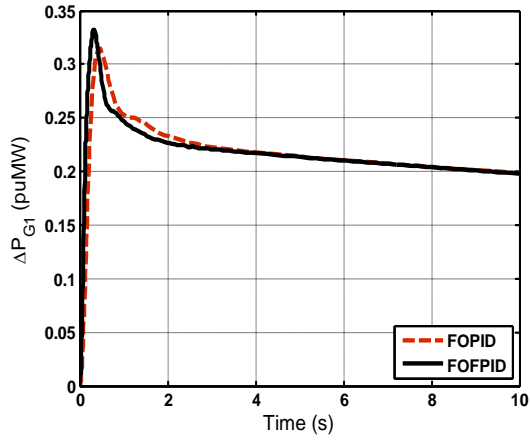
(i) Fig. 8.5(h) with Time = 0-10 s.
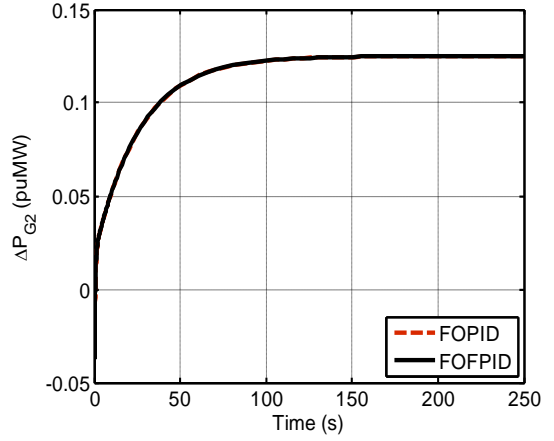
(j)
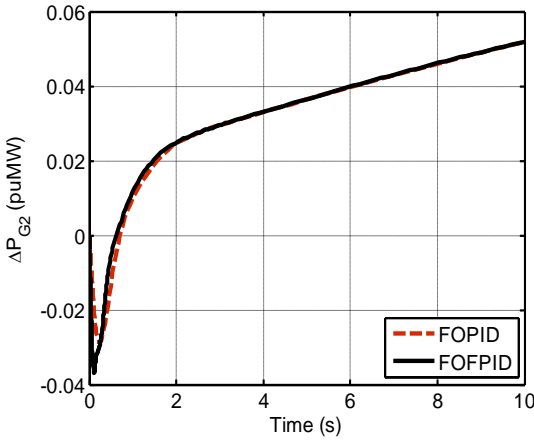
(k) Fig. 8.5(j) with Time = 0-10 s.

(l)
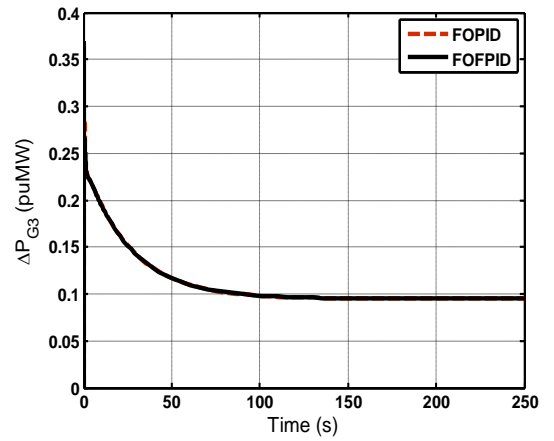
ΔP_{G1} = 0.125 puMW (Figs. 8.5(h-i)), ΔP_{G2} = 0.125 puMW (Figs. 8.5(j-k)), ΔP_{G3} = 0.095 puMW (Figs. 8.5(l-m)), ΔP_{G4} = 0.17 puMW (Figs. 8.5(n-o)), ΔP_{G5} = 0.093 puMW (Fig. 8.5(p)) and ΔP_{G6} = 0.112 puMW (Figs. 8.5(q-r)). It is observed from Figs. 8.5(h-r) that these power signals converge properly to the desired values in the

165
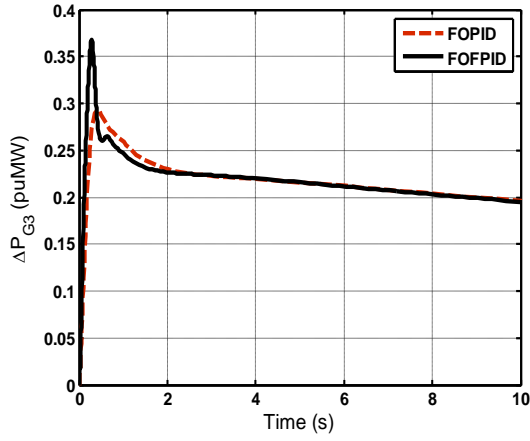
(m) Fig. 8.5(l) with Time = 0-10 s.
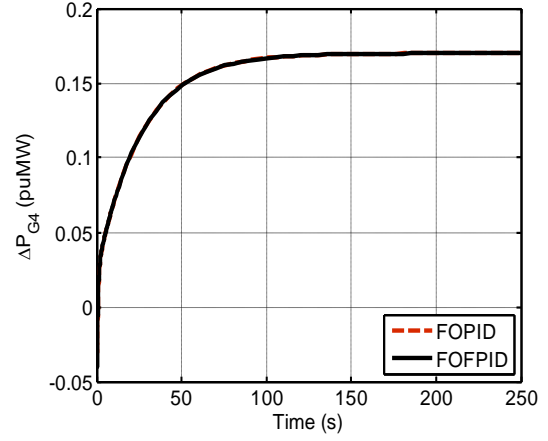
(n)
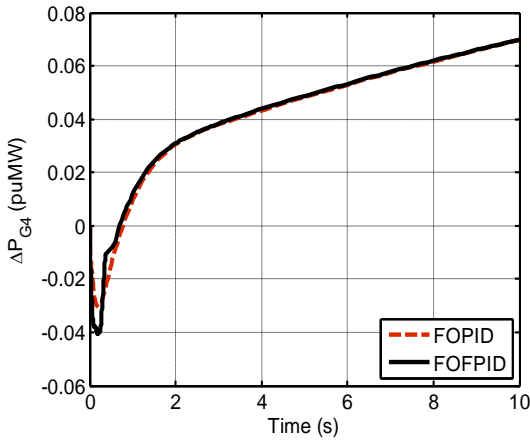
(o) Fig. 8.5(n) with Time = 0-10 s.
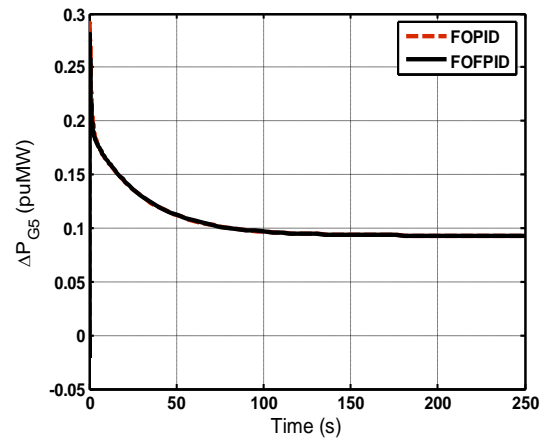
(p)
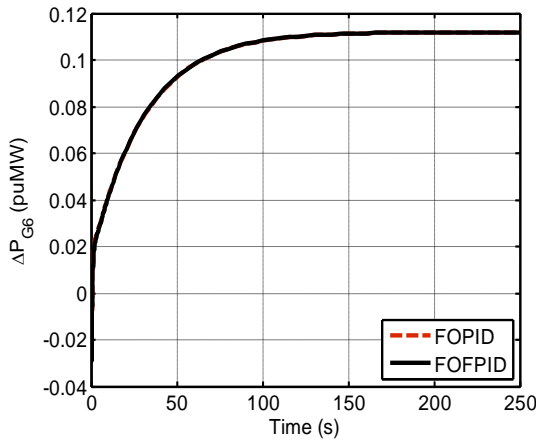
(q)
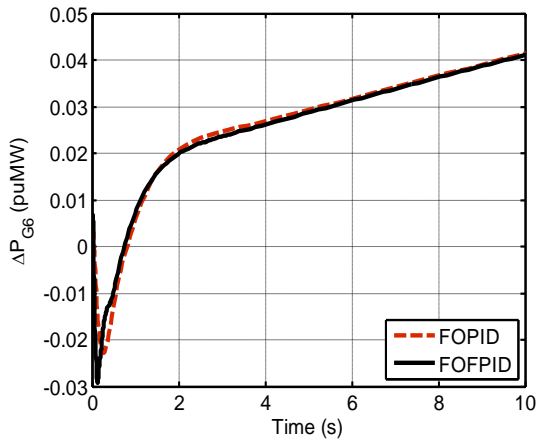
(r) Fig. 8.5(q) with Time = 0-10 s.

Fig. 8.5 Dynamic responses of three-area restructured multi-source hydrothermal power system with different types of controllers for poolco plus bilateral with contract violation based transactions (a) ΔF_1 and (b) ΔF_2, (c) ΔF_3, (d) $\Delta Ptie_{21,actual}$, (e) $\Delta Ptie_{21,error}$, (f) $\Delta Ptie_{31,actual}$, (g) $\Delta Ptie_{31,error}$, (h) ΔP_{G1}, (i) ΔP_{G1}, (j) ΔP_{G2}, (k) ΔP_{G2}, (l) ΔP_{G3}, (m) ΔP_{G3}, (n) ΔP_{G4}, (o) ΔP_{G4}, (p) ΔP_{G5}, (q) ΔP_{G6} and (r) ΔP_{G6}.

steady state with both FOFPID and FOPID controllers. However, FOFPID controller displays better results. Further, from Eqns. (7.16) and (7.17) $\Delta Ptie_{21,scheduled} = 0.025$ puMW and $\Delta Ptie_{31,scheduled} = -0.025$ puMW as revealed by $\Delta Ptie_{21,actual}$ and $\Delta Ptie_{31,actual}$ responses in Figs. 8.5(d) and 8.5(f), respectively. It is observed that FOFPID controller show superior performance over the performance offered by FOPID controller.

8.6   Conclusion

A maiden attempt is made to propose a FOFPID controller for multi-area multi-source traditional and restructured AGC systems. The parameters of FOFPID controller are tuned utilizing BFOA. Firstly, a traditional two-area multi-source hydrothermal system is considered and advantage of FOFPID controller is confirmed over BFOA tuned FOPID. To validate the effectiveness of proposed approach, the approach is also extended to restructured two-area multi-source hydrothermal, restructured two-area multi-source thermal gas and restructured three-area multi-source hydrothermal systems. Critical analysis of the obtained results divulges the efficacy of FOFPID controller over FOPID controller in terms of less numerical value of STs, PUs and PIs. It is also experienced that FOFPID controller satisfies the AGC requirement in different power transactions taking place under deregulated environment more effectively than FOPID controller does. Hence, FOFPID controller can be favored as a supplementary controller in multiple multi-area traditional and restructured power systems.

CHAPTER 9

AGC OF RESTRUCTURED POWER SYSTEM INCORPORATING SYSTEM NONLINEARITIES

9.1 Introduction

Practical power system is nonlinear in nature having a variety of physical constraints and nonlinearities. These constraints are imposed by communication channels, filters, governor-turbine, crossover elements in thermal and the penstock behavior in hydro plants. The physical constraints affect overall dynamics of power system including AGC responses by rising overshoot, undershoot, number of oscillations and settling time and therefore corrupt the performance of the designed controller [122]. Consequently, to study the insight of an AGC problem, it is necessary to comprise the main inherent constraints and nonlinearities in the system model under study. The chief constraints that influence the system performance significantly are time delay (TD) [107,122,150,157,353,359,399] generation rate constraint (GRC) [38,46,58,68, 97–98,107,262,381,387,399], boiler dynamics (BD) [82,97–98,288,368,400] and governor deadband or deadzone (DZ) nonlinearity [57,68,97,98,288,293,399–400] as described below:

Time delay

The time delay (TD) in an electric power system is owing to the delays in the communication channels (CCs), filters and signal processing units. The TD in an AGC system mostly subsist on the CCs between the control center and operating stations; particularly on the measured frequency and tie-line power flow from remote terminal units (RTUs) to the control center and the delay up/down signal from control

center to individual generation units. The TD creates noteworthy challenge in the AGC analysis due to the restructuring, growth in physical setups, complexity and functionality of interconnected system. The existence of the TD degrades the performance of an AGC system appreciably and may turn the system unstable [122,150]. It is observed that the generation/frequency control recital declines when the TD increases [122,353]. In order to please the desired performance for a complex multi-area AGC system, the controller adopted should be capable to work efficiently in the presence of the TD otherwise system may become unstable.

Generation rate constraint

In the real world, electric power plants cannot change their power outputs too hastily owing to the limitations of thermal and mechanical movements termed as generation rate constraint (GRC). GRC is given in a percentage of the rated output of the generator per unit of time. It offers big challenge to the control approaches employed because they radically persuade the system dynamic performance. In a pragmatic AGC study, GRC impacts must be integrated. Under the non appearance of GRC, undesirably, generators are anticipated to chase large temporary disturbances that may turn power generation network to unstable [122]. The time results of the system in the presence of GRC show larger overshoots and longer settling times in comparison to the system having no GRC. Further, if the parameters of the controller are not optimized properly, the power system may turn unstable in the presence of GRC [122]. Most of the larger reheat thermal generating units have fairly low GRC around ±3%/min [142,359,360]. For gas units ±20%/min GRC is used usually [353], while for hydro units, larger values of GRC of +270% per minute i.e., 4.5%/s for raising generation and −360% per minute i.e., 6%/s for lowering generation are considered [353,360].

Boiler dynamics

Boiler is used to produce steam under pressure. It receives feed water preheated in the economizer and outputs saturated steam. Recirculation boiler uses a drum to separate steam from the recirculation water aiming to proceed it to the superheater as a heatable vapor. Thus, the recirculation boilers are referred to as drum type boiler. The change in generation is started by turbine control valves and the boiler controls respond with essential control action, changes in steam flow and changes in throttle pressure, the combustion rate and hence output of the boiler. To launch long-term dynamics of fuel and steam flow on the boiler drum pressure, boiler dynamics (BD) are incorporated in thermal units. Fig. 9.1 shows the boiler dynamics model of a coal fired well-tuned drum type boiler [82,97–98,368,400]. The transfer function models of pressure control unit and fuel system are given in Eqns. (9.1-9.2).

$$G_{PC} = \frac{K_{IB}(1+sT_{IB})(1+sT_{RB})}{s(1+0.1sT_{RB})} \tag{9.1}$$

$$G_{FS} = \frac{e^{-sT_D}}{1+sT_f} \tag{9.2}$$
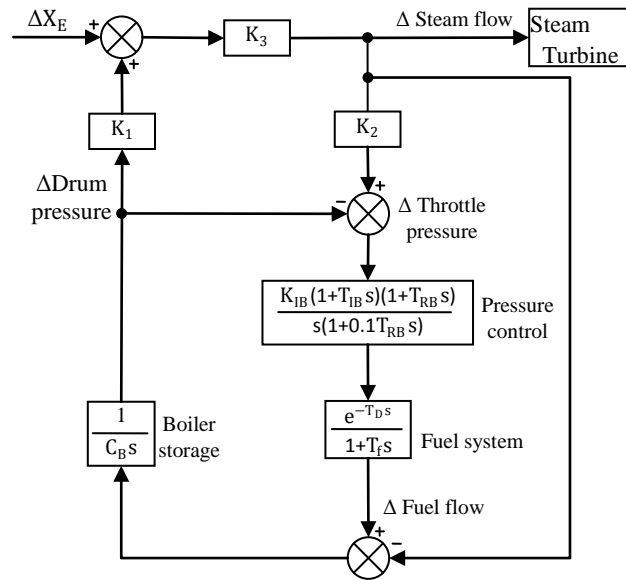
Fig. 9.1   Block diagram representing boiler dynamics in thermal turbine.

Employing 2nd order Pade approximation method, e^{-sT_D} can be approximated as specified in Eqn. (9.3):

$$e^{-sT_D} = \frac{1 - \frac{sT}{2} + \frac{s^2 T^2}{2}}{1 + \frac{sT}{2} + \frac{s^2 T^2}{2}} \tag{9.3}$$

The linear transfer function model of BD is derived using signal flow graph technique as:

$$G_{BD} = \frac{K_3(1 + G_1 G_2)}{1 - K_1 K_2 K_3 G_1 G_2 + G_1 G_2 + K_1 K_3 G_2} \tag{9.4}$$

where, $G_1 = G_{PC} \times G_{FS}$ and $G_2 = 1/sC_B$. The BD parameters and nomenclatures are stated in Appendix B and Nomenclature section, respectively. This contains the long-term dynamics of fuel and steam flow on boiler drum pressure. Demonstrations for combustion controls are also included. Although, the model is principally a drum type boiler, similar responses are observed for once through boilers and pressurized water reactors. The model is effective to study the coal-fired units with weakly tuned (oscillatory) combustion controls, coal fired units with fine-tuned controls and well-tuned oil or gas fired units. In traditional steam units, variation in generation is started by turbine control valves and the boiler controls respond with essentially immediate control action upon sensing changes in the steam flow and deviations in pressure.

Governor deadband/zone

The speed governor deadband (GDB) or deadzone (DZ) is another significant concern in power system performance. By altering the input signal, the speed governor does not reacts instantly until the input attains a specific value. The GDB is the total magnitude of a sustained speed change where there is no resulting change in valve position. Because of the GDB, an up/down in speed takes place before the position of the valve adjusts. Consequently, GDB significantly affects the dynamic

Fig. 9.2 SIMULINK model of restructured three-area multi-source hydrothermal system.
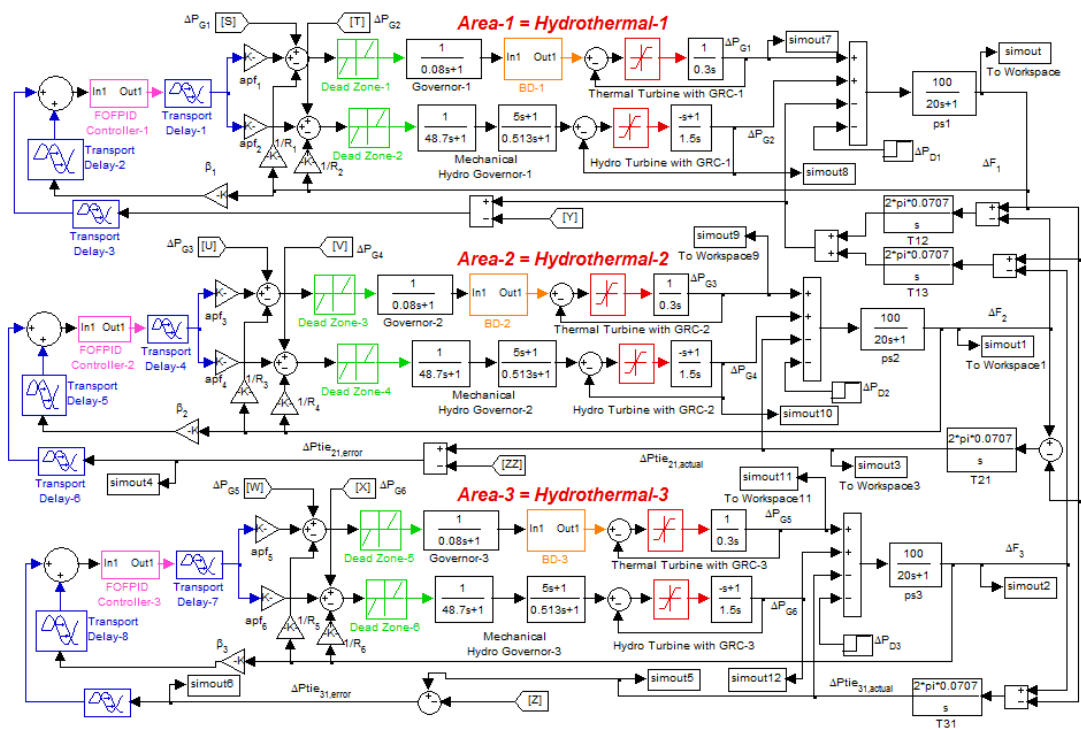
performance of AGC system as it turns the system oscillatory. GDB is stated in per cent of rated speed. In traditional power system operating environment, the effect of GDB on performance of AGC regulator has been investigated in [68,97–98,107,122, 131–132,138,150,164,167,400–401] and various AGC strategies in restructured power systems are conducted in [288,293,351,353,359,368,371].

9.2   System studied

The system considered is a restructured three-area multi-source hydrothermal with area capacities of 2000 MW. The areas are equipped with non-reheat turbine and mechanical governor based hydro turbine plants. Hence, each area owns two GENCOs and let two DISCOs as stated in Chapters 7 or 8. The time delays (TD) are considered in area frequencies, tie-line power flows and the controller output signals. The TD of 5ms is considered in these specified signals. The GRC for hydro plant is

considered 270%/min for raising generation (+0.045 pu/s) and 360%/min for lowering generation (−0.06 pu/s) [131–132,150,353,368–369,371]. However, GRC of ±0.1 pu/s for non-reheat type thermal units is taken from [273,399]. The boiler dynamics (BD) are considered in between governor and turbines of each thermal GENCO. The standard magnitude or maximum limit value of deadzone (DZ) for governors of steam turbines is taken as ±0.0006 pu or ±0.06% (±0.036 Hz) [150,399–400] and for hydro governors, a DZ of ±0.0002 or ±0.02% (±0.012Hz) is considered [401]. The SIMULINK model of system is shown in Fig. 9.2.

9.3 Results and analysis

9.3.1 Restructured three-area multi-source hydrothermal system

Only FOFPID controller with optimum parameter values obtain in Chapter 8 via BFOA is employed for simulations in a restructured three-area multi-source hydrothermal system incorporating TD, GRC, BD and DZ physical constraints. To demonstrate the efficacy of FOFPID controller, poolco plus bilateral with contract violation based transactions are considered to perform the simulations as prospects of the system to turn unstable are high in this worst case. The DPM used in the simulations is given in Eqn. (7.15). As stated in previous chapters, the apfs used are: $apf_1 = apf_2 = apf_3 = apf_4 = 0.5$, $apf_5 = 0.6$ and $apf_6 = 0.4$, demands of DISCOs are: $\Delta P_{L1} = \Delta P_{L2} = \Delta P_{L3} = \Delta P_{L4} = \Delta P_{L5} = \Delta P_{L6} = 0.1$ puMW and uncontracted power demands of DISCOs are: $\Delta P_{UC1} = 0.05$ puMW, $\Delta P_{UC2} = 0.04$ puMW and $\Delta P_{UC3} = 0.03$ puMW. Therefore, $\Delta P_{G1} = 0.125$ puMW, $\Delta P_{G2} = 0.125$ puMW, $\Delta P_{G3} = 0.095$ puMW, $\Delta P_{G4} = 0.17$, $\Delta P_{G5} = 0.093$ puMW, $\Delta P_{G6} = 0.112$ puMW, $\Delta Ptie_{21,scheduled} = 0.025$ puMW and $\Delta Ptie_{31,scheduled} = -0.025$ puMW.

The simulation results of the system for frequencies of all three areas, actual/error tie-line power flows and power outputs of all six GENCOs of the system without GRC, with GRC and with GRC/DZ/BD/TD are shown in Figs. 9.3(a-r). It is observed from Figs. 9.3(a-r) that in the presence of GRC in thermal and hydro turbines, the sys-

(a)

(b)

(c)

(d)

(e)

(f)
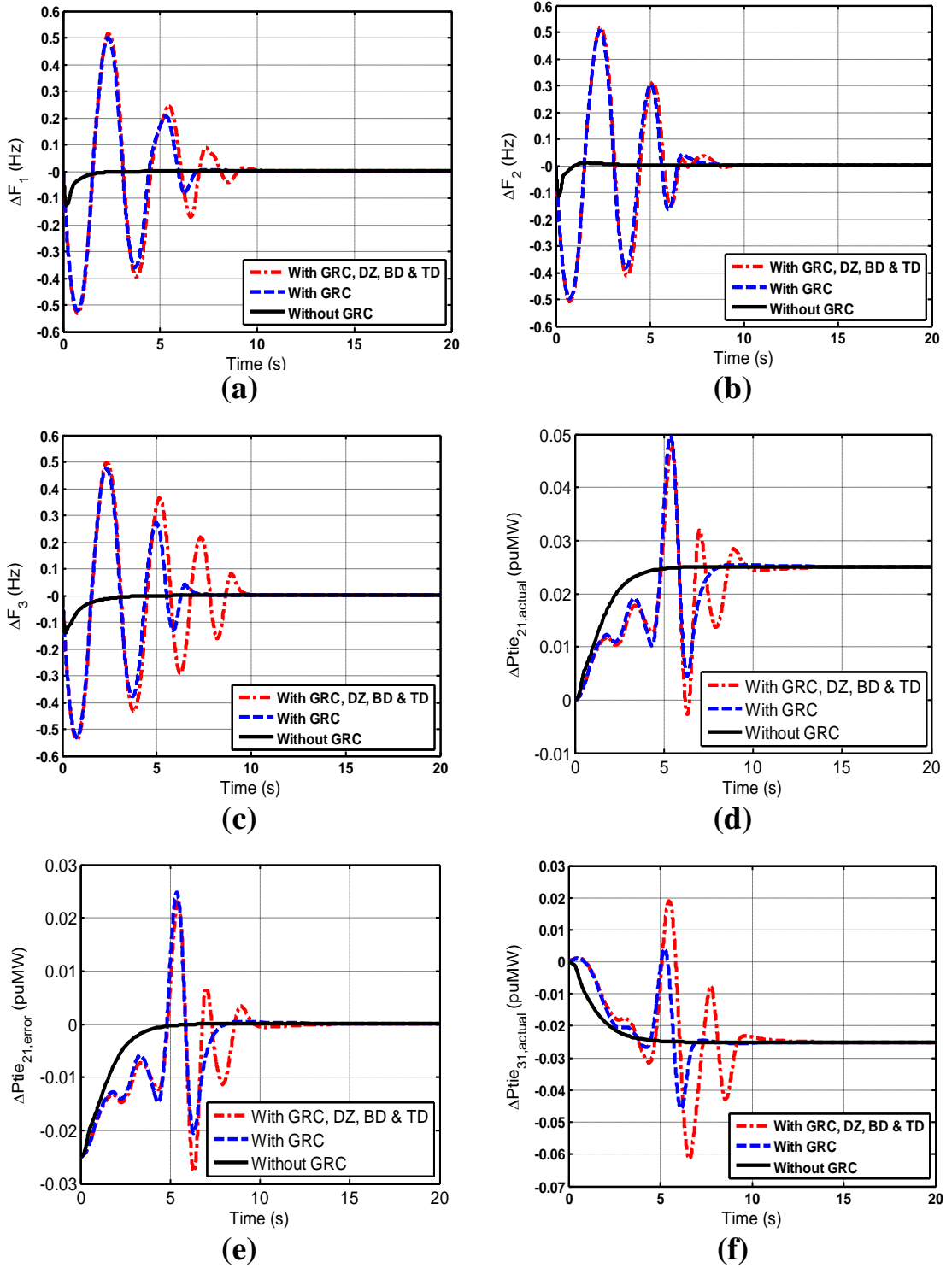
tem results get deteriorated. The results of the system with GRC show larger PUs, longer STs, high numeric values of PIs, more peak overshoots and larger oscillations in comparison to the system without GRC. Similar simulation results are observed for the system having GRC/DZ/BD/TD in compared to the system having only GRC.
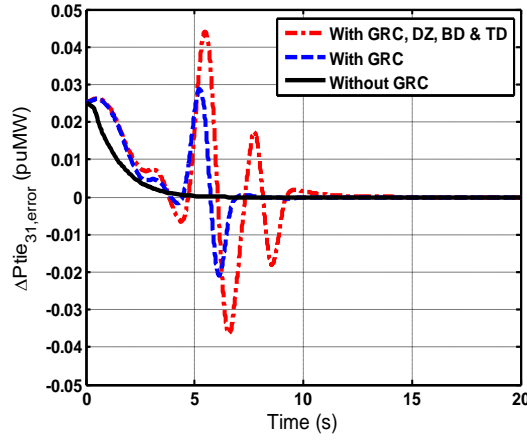
(g)
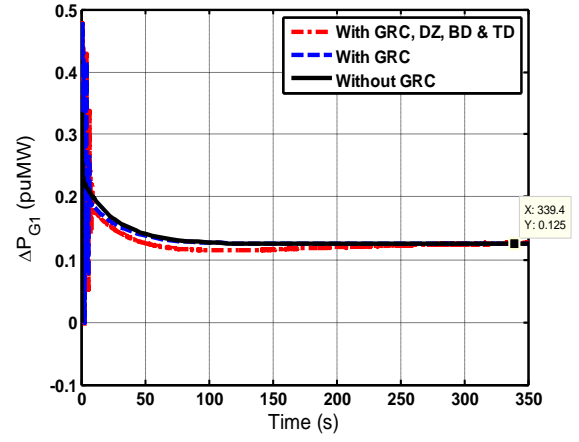
(h)
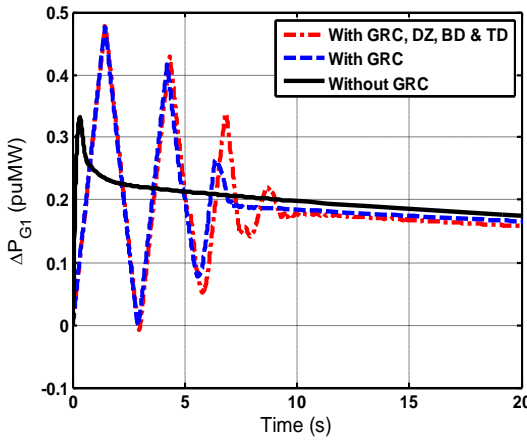
(i) Fig. 9.3(h) with Time = 0-20 s.

(j)
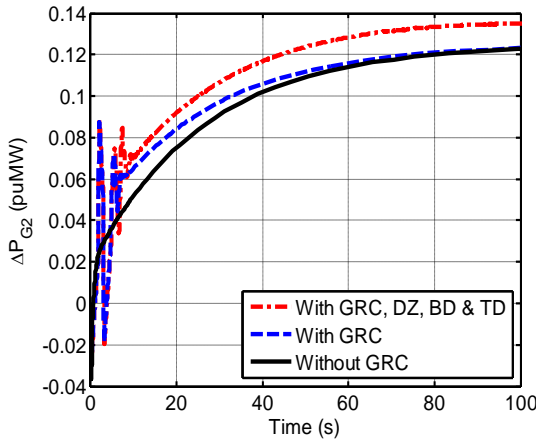
(k) Fig. 9.3(j) with Time = 0-100 s.

(l)

175
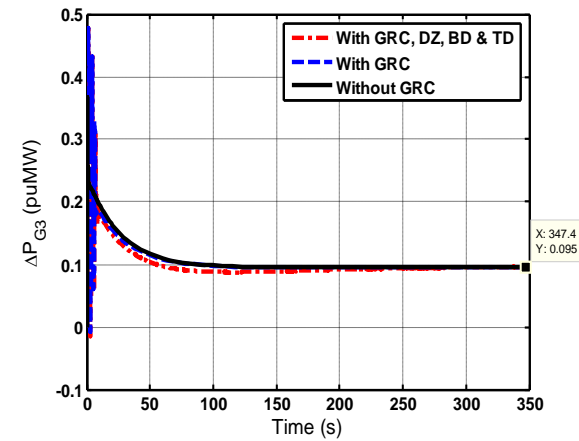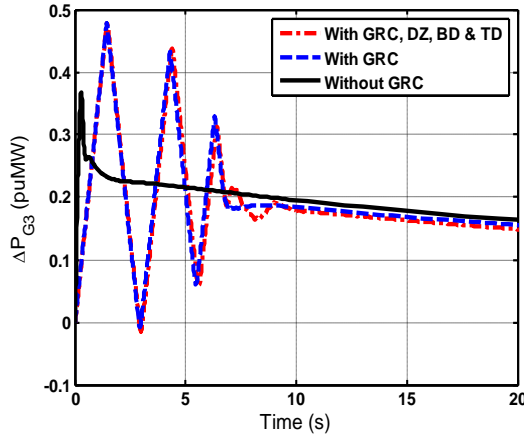
(m) Fig. 9.3(l) with Time = 0–20 s.
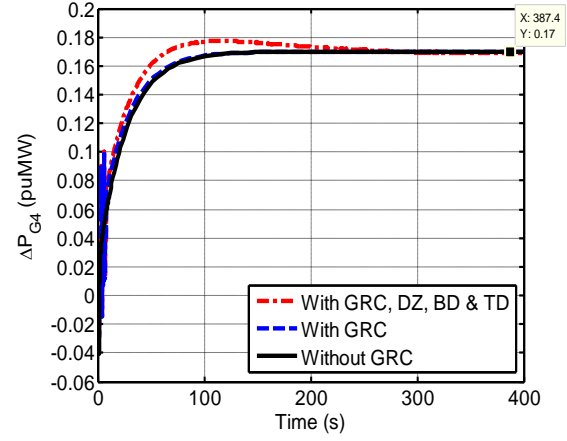
(n)
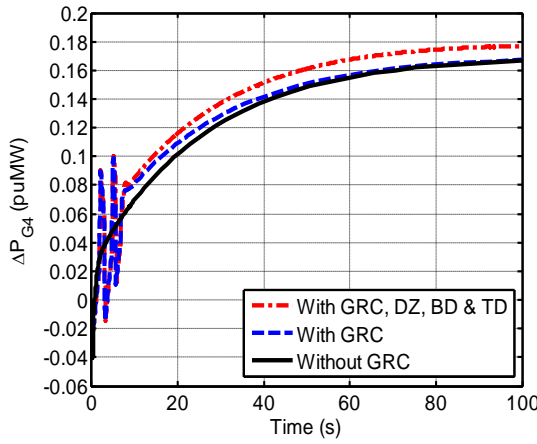
(o) Fig. 9.3(n) with Time = 0–100 s.
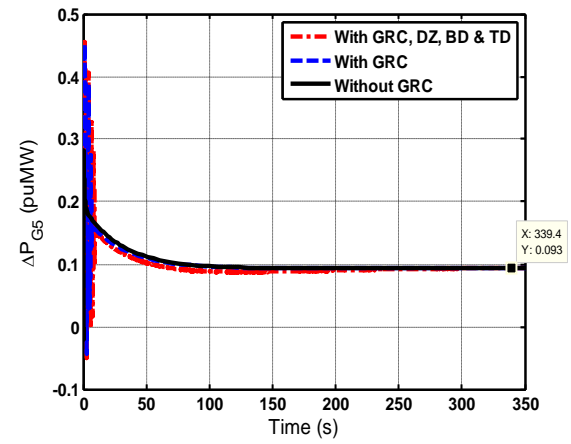
(p)
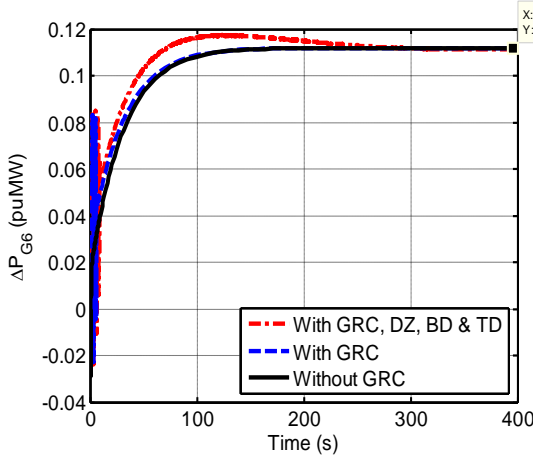
(q)
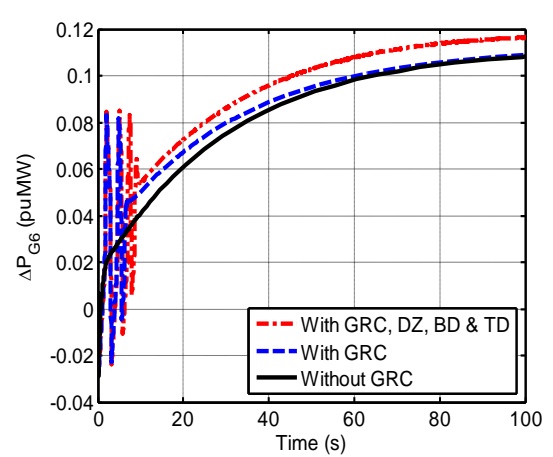
(r) Fig. 9.3(q) with Time = 0–100 s.

Fig. 9.3 Dynamic responses of three-area restructured multi-source hydrothermal power system in the presence/absence of nonlinearities (a) ΔF_1, (b) ΔF_2, (c) ΔF_3, (d) $\Delta Ptie_{21,actual}$, (e) $\Delta Ptie_{21,error}$, (f) $\Delta Ptie_{31,actual}$, (g) $\Delta Ptie_{31,error}$, (h) ΔP_{G1}, (i) ΔP_{G1}, (j) ΔP_{G2}, (k) ΔP_{G2}, (l) ΔP_{G3}, (m) ΔP_{G3}, (n) ΔP_{G4}, (o) ΔP_{G4}, (p) ΔP_{G5}, (q) ΔP_{G6} and (r) ΔP_{G6}.

Table 9.1

Numerical values of STs, PUs and PIs with restructured three-area multi-source system.

Controller type	STs (s)					PUs (−ve) (Hz)		
	ΔF_1	ΔF_2	ΔF_3	$\Delta Ptie_{21,error}$	$\Delta Ptie_{31,error}$	ΔF_1	ΔF_2	ΔF_3
Without GRC	**9.63**	**9.72**	**5.02**	**4.56**	**4.55**	**0.1275**	**0.1125**	**0.1371**
With GRC	12.67	11.58	13.34	7.81	6.85	0.5218	0.4971	0.5305
With GRC, TD, BD & DZ	25.48	29.08	22.50	10.76	11.27	0.5355	0.5080	0.5395

-	PUs (−ve) (puMW)		PIs				
	$\Delta Ptie_{21,error}$	$\Delta Ptie_{31,error}$	ISE	ITSE	IAE	ITAE	
Without GRC	**0.0250**	**0.000**	**0.1963**	**0.00855**	**0.3632**	**0.4733**	
With GRC	0.0205	0.0208	1.6730	3.73100	5.1280	13.9500	
With GRC, TD, BD & DZ	0.0277	0.0365	1.9920	5.21900	6.1530	20.2000	

Table 9.1 presents a comparative data analysis for some of the important states of the system without GRC, with GRC and with GRC/DZ/BD/TD. It is revealed from Table 9.1 that STs/PUs/PIs of the system without GRC are: $\Delta F_1 = 9.63$ s, $\Delta F_2 = 9.72$ s, $\Delta F_3 = 5.02$ s, $\Delta Ptie_{21,error} = 4.56$ s, $\Delta Ptie_{31,error} = 4.55$ s/$\Delta F_1 = 0.1275$ Hz, $\Delta F_2 = 0.1125$ Hz, $\Delta F_3 = 0.1371$ Hz, $\Delta Ptie_{21,error} = 0.0250$ puMW, $\Delta Ptie_{31,error} = 0$ puMW/ISE: 0.1963, ITSE: 0.00855, IAE: 0.3632, ITAE: 0.4733 and these values respectively for the system with GRC are $\Delta F_1 = 12.67$ s, $\Delta F_2 = 11.58$ s, $\Delta F_3 = 13.34$ s, $\Delta Ptie_{21,error} = 7.81$ s, $\Delta Ptie_{31,error} = 6.85$ s/$\Delta F_1 = 0.5218$ puMW, $\Delta F_2 = 0.4971$ puMW, $\Delta F_3 = 0.5305$ puMW, $\Delta Ptie_{21,error} = 0.0205$ puMW, $\Delta Ptie_{31,error} = 0.0208$ puMW/ISE: 1.6730, ITSE: 3.73100, IAE: 5.1280, ITAE: 13.9500. Hence, the system results get degraded as all values, except PU of $\Delta Ptie_{21,error}$, increase in the presence of GRC compared to the system without GRC. The performance of the system is further corrupted when the effects of DZ, BD and TD are also incorporated in addition to the effect of GRC as clearly indicated in Table 9.1 and Figs. 9.3(a-r).

9.3.2   Simulations with variable contract violation

In realistic power system, uncontracted power demands (ΔP_{UC}) of DISCOs may exist in any one or in all the areas concurrently [341]. If controller is not robust enough to
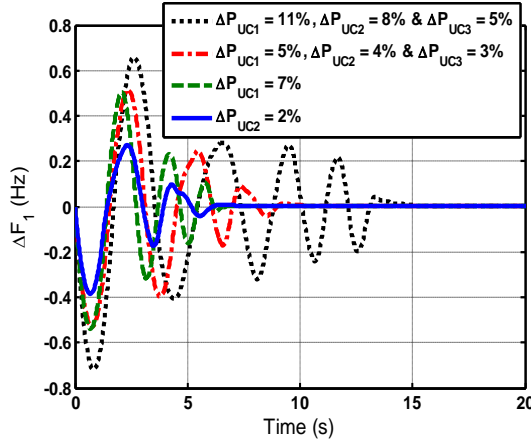
(a)
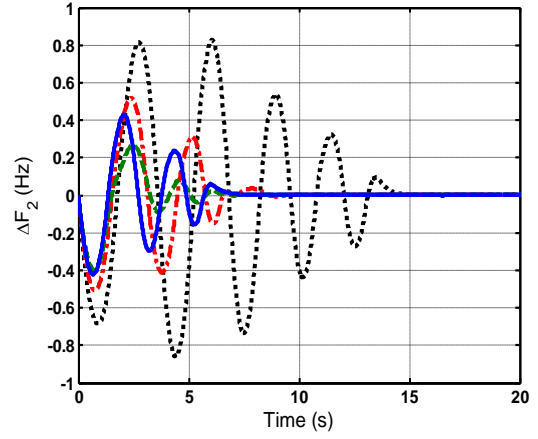
(b)
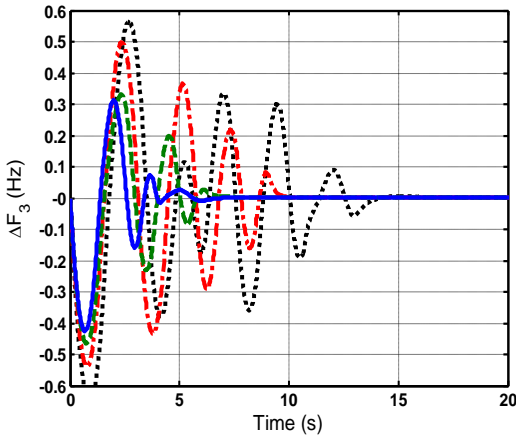
(c)
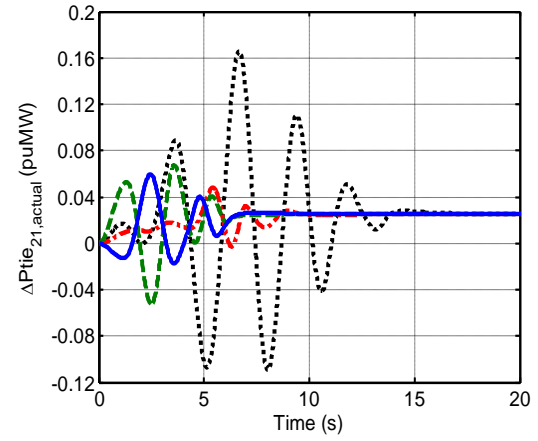
(d)
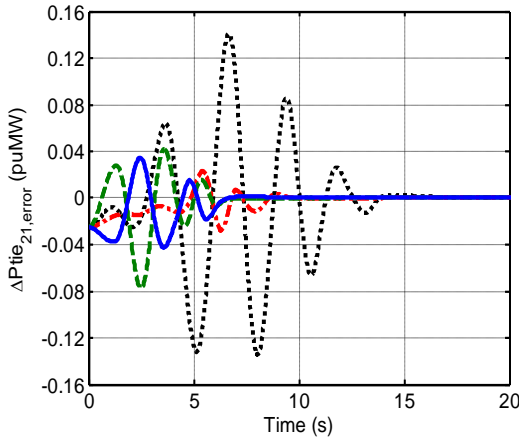
(e)
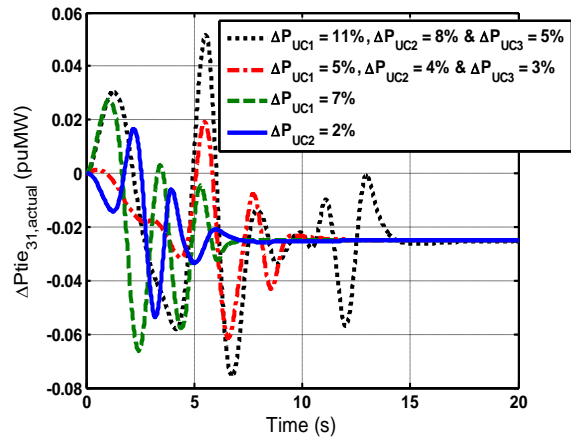
(f)

deal with such circumstances, system will certainly turn unstable. In this section, the simulations of restructured three-area multi-source hydrothermal power system under poolco plus bilateral transactions are realized for various combination of sizes and locations of ΔP_{UC} of the DISCOs in contract with the GENCOs. Three more ΔP_{UC}

patterns are included in the existing ΔP_{UC} pattern i.e., ΔP_{UC1} = 5% puMW, ΔP_{UC2} = 4% puMW and ΔP_{UC3} = 3% puMW. Randomly, in first case ΔP_{UC} is selected as: ΔP_{UC1} = 7% puMW, ΔP_{UC2} = 0% puMW, ΔP_{UC3} = 0% puMW, in second case ΔP_{UC} is selected as: ΔP_{UC1} = 0% puMW, ΔP_{UC2} = 2% puMW, ΔP_{UC3} = 0% puMW and in third
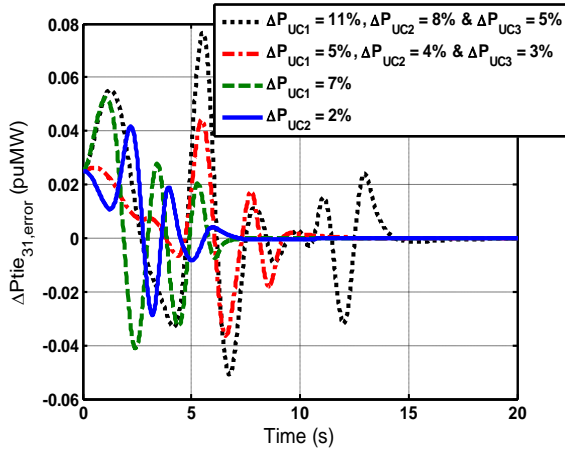
(g)
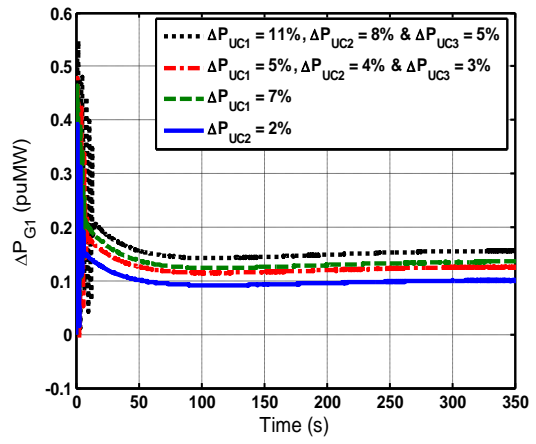
(h)
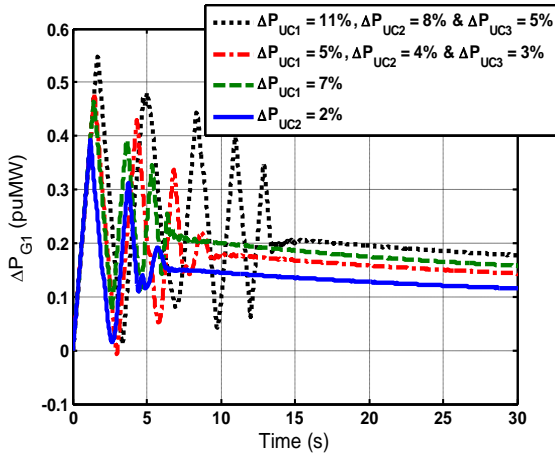
(i) Fig. 9.4(h) with Time = 0-30 s.
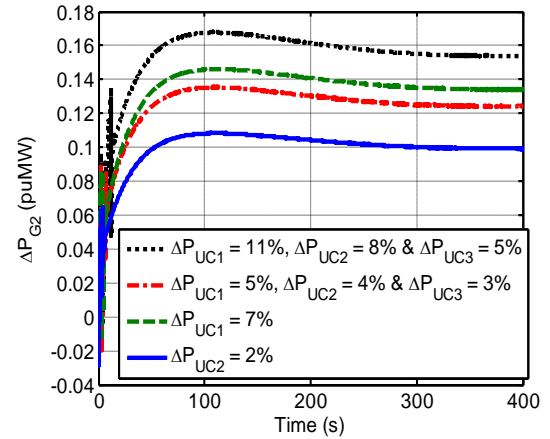
(j)
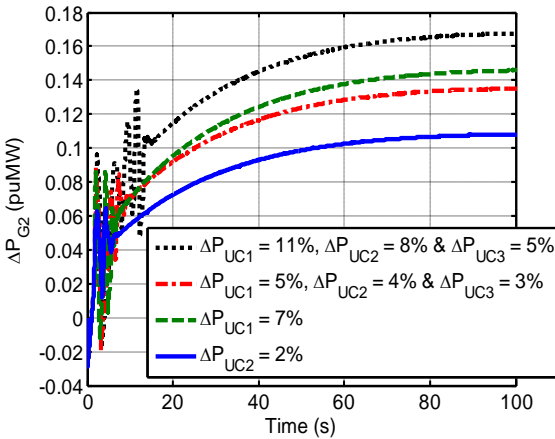
(k) Fig. 9.4(j) with Time = 0-100 s.

(l)

179
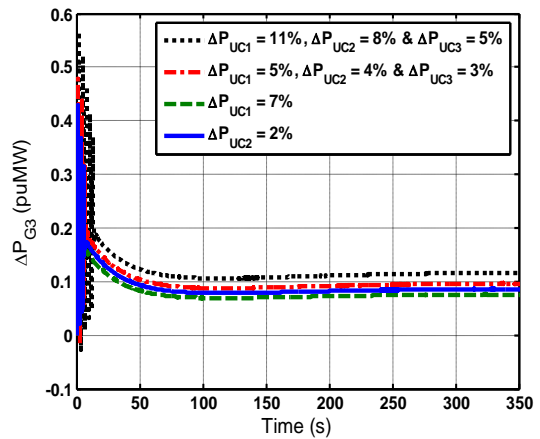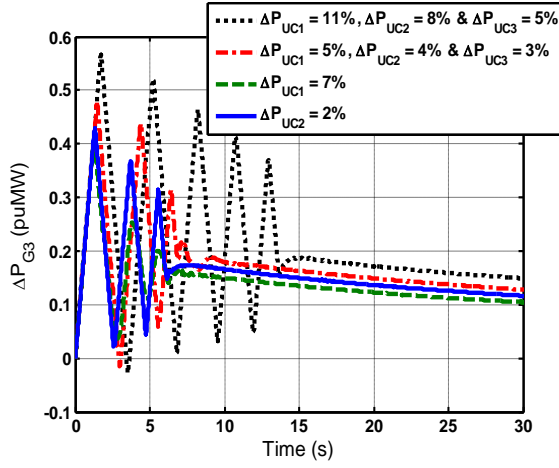
(m) Fig. 9.4(l) with Time = 0-30 s.
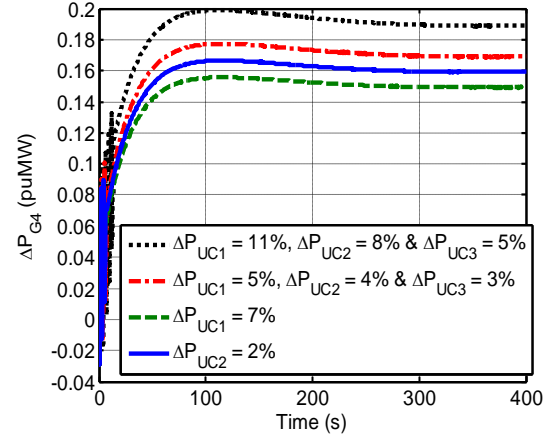
(n)
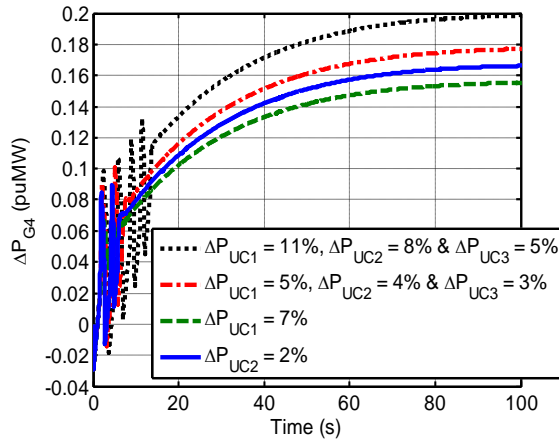
(o) Fig. 9.4(n) with Time = 0-100 s.
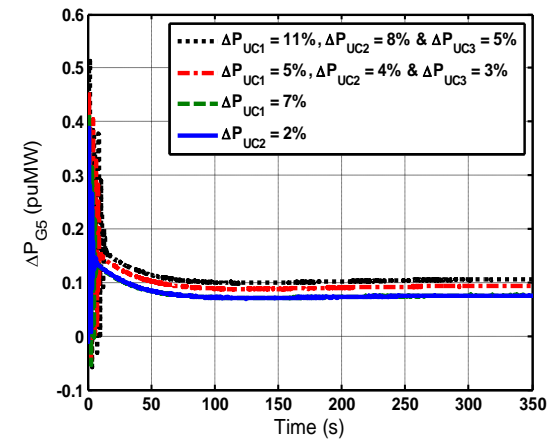
(p)
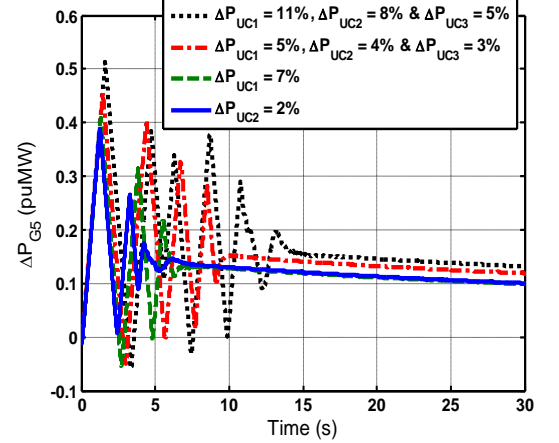
(q) Fig. 9.4(p) with Time = 0-30 s.
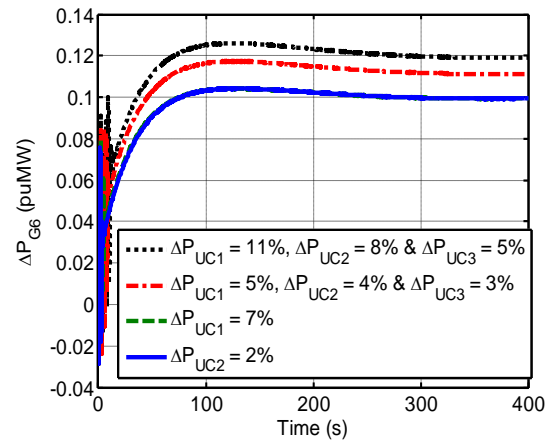
(r)

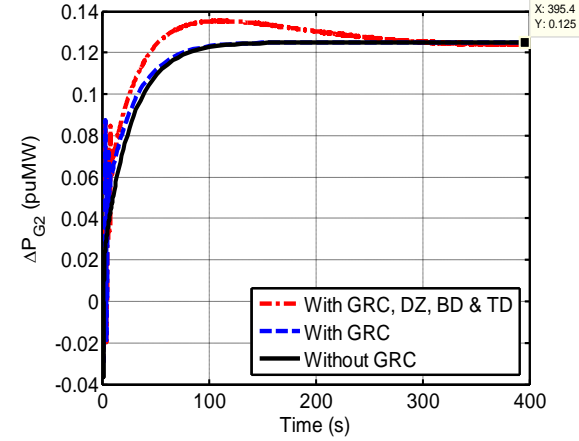**Fig. 9.4** Dynamic responses of three-area restructured multi-source hydrothermal power system under varied uncontracted power demands (a) ΔF_1, (b) ΔF_2, (c) ΔF_3, (d) $\Delta Ptie_{21,actual}$, (e) $\Delta Ptie_{21,error}$, (f) $\Delta Ptie_{31,actual}$, (g) $\Delta Ptie_{31,error}$, (h) ΔP_{G1}, (i) ΔP_{G1}, (j) ΔP_{G2}, (k) ΔP_{G2}, (l) ΔP_{G3}, (m) ΔP_{G3}, (n) ΔP_{G4}, (o) ΔP_{G4}, (p) ΔP_{G5}, (q) ΔP_{G5} and (r) ΔP_{G6}.

case ΔP_{UC} is selected as: $\Delta P_{UC1} = 11\%$ puMW, $\Delta P_{UC2} = 8\%$ puMW, $\Delta P_{UC3} = 5\%$ puMW. In first case, considering employed DPM, apfs and Eqn. (7.14), the steady state power outputs of GENCOs are calculated as: $\Delta P_{G1} = 0.135$ puMW, $\Delta P_{G2} = 0.135$ puMW, $\Delta P_{G3} = 0.075$ puMW, $\Delta P_{G4} = 0.15$, $\Delta P_{G5} = 0.075$ puMW and $\Delta P_{G6} = 0.1$ puMW. In second case, ΔP_G will be as: $\Delta P_{G1} = 0.1$ puMW, $\Delta P_{G2} = 0.1$ puMW, $\Delta P_{G3} = 0.085$ puMW, $\Delta P_{G4} = 0.16$, $\Delta P_{G5} = 0.075$ puMW and $\Delta P_{G6} = 0.1$ puMW. In third case, ΔP_G will be as: $\Delta P_{G1} = 0.155$ puMW, $\Delta P_{G2} = 0.155$ puMW, $\Delta P_{G3} = 0.115$ puMW, $\Delta P_{G4} = 0.19$, $\Delta P_{G5} = 0.105$ puMW and $\Delta P_{G6} = 0.12$ puMW. The simulation results of the system are shown in Figs. 9.4(a-r). From Figs. 9.4(a-c,e,g), it is observed that deviation in frequency of areas and tie-line error power flows settle to zero in steady state. However, maximum oscillations in the responses are observed in third case where values of ΔP_{UC} are biggest. It is experienced from Figs. 9.4(a-g) that variation in the values of ΔP_{UC} do not affect the steady state responses but only transient responses of ΔF_1, ΔF_2, ΔF_3, $\Delta Ptie_{21,scheduled}$, $\Delta Ptie_{31,scheduled}$, $\Delta Ptie_{21,error}$ and $\Delta Ptie_{31,error}$ will be affected. However, STs, PUs and numbers of oscillation in the responses have increased with the increase in ΔP_{UC} in the control areas as demonstrated in case third i.e., $\Delta P_{UC1} = 11\%$, $\Delta P_{UC2} = 8\%$ & $\Delta P_{UC3} = 5\%$. It should be noted that both steady state and transient responses of GENCOs power outputs will be affeted under variation in ΔP_{UC} in control areas. From Figs. 9.4(h-r), it is observed that under variable values of uncontracted power demands, suggested FOFPID controller works well and deviation in power outputs of GENCOs matches with the desired values in the steady state, however, the quality of the responses degrades at bigger uncontracted power demands.

Though, the controller is optimized for the system having no GRC, the beauty of FOFPID controller is that it works excellently in the presence of GRC, GRC/DZ/BD/TD and at variable/bigger values of ΔP_{UC} without showing any requirement of redesigning it and without showing any sign of instability in the system. Hence, robustness of the controller is confirmed.

9.4 Conclusion

Fractional order fuzzy PID (FOFPID) controller is implemented for the first time in AGC of restructured multi-area multi-source hydrothermal system considering appropriate GRC/DZ/BD/TD and poolco plus bilateral plus contract violation based transactions. Controller designed and optimized employing BFOA technique for linear system is implemented on the same system with GRC/DZ/BD/TD physical constraints. Performance of the controller with the system without GRC is compared with the system with GRC and with GRC/DZ/BD/TD. It is seen that a desirable performance is achieved using FOFPID controller, however, in the presence of GRC and GRC/DZ/BD/TD, the system performance degrades drastically. The controller is also tested against different amounts and positions of uncontracted power demands to check the robustness. Investigations clearly reveal that the controller is found to perform well when the system is subjected to higher degree of uncontracted demands and simultaneous occurrence of uncontracted demands. Thus, controller parameters like K_1, K_2, K_P, K_I, K_D, γ, λ and μ obtained for the system without GRC are robust enough and need not be retuned for the system having appropriate GRC or GRC/DZ/BD/TD or wide changes in the size and location of contract violations. Thus, the main objective of designing a suitable controller to perform satisfactorily

under uncertain environments has been fruitfully attained to supply reliable power
with quality to the end users.

CHAPTER 10

CONCLUSIONS

10.1 Overview of the work

This chapter presents an overview of the contributions made in the present thesis. In this thesis, an attempt is made to present various strategies on AGC of multi-area-multi-source restructured as well as traditional interconnected power systems. To solve AGC problem in restructured and traditional power systems, some new control strategies have been proposed in this thesis. To compare and thus validate the results of the proposed controllers, the study is conducted on various traditional and restructured multi-area power systems available in the literature. Along with the proposed control strategies, some restructured two-area multi-source power systems are also proposed in the existing thesis. The main findings of the works done in this thesis are stated as follows:

A. Optimal AGC of two-area restructured multi-source systems

The optimal PI structured controllers are designed to solve AGC problem of restructured two-area multi-source hydrothermal and hydrothermal/gas power systems interconnected via AC and AC/DC parallel tie-lines. It is observed that optimal PI controllers work satisfactorily and meet AGC requirements under various types of possible power market transactions. AC/DC parallel tie-lines show stabilizing effect on power system performance in comparison to AC tie-line. The patterns of open/closed loop eigenvalues confirm the enhanced stability of the system with AC/DC parallel tie-lines. The frequency deviation is found more in the area in which DISCOs violate the contract agreement. After comparison of dynamic responses of

multi-source hydrothermal system with single-source thermal system, it is observed that the performance of hydrothermal system is sluggish/poor compared to thermal system.

B. *AGC of power systems using GA based fuzzy logic controller*

GA is employed to optimize FPI controllers for AGC of two-area traditional non-reheat thermal, reheat thermal, multi-source hydrothermal and restructured reheat thermal power system models. The output scaling factors of FPI are optimized using GA to get FPI-1 and horizontal range of membership functions (mfs) of FPI-1 is then optimized via GA to get FPI-2 controller. The FPI-1 and 2 optimized only for non-reheat model work superbly on other systems without retuning. From the system results, it is concluded FPI-2 outperforms FPI-1 in terms of better responses having less numerical values of settling time, peak undershoot and various performance indices. FPI-2 outsmarts even the conventional and intelligent control approaches prevalent in the literature.

C. *BFOA tuned fuzzy PI/PID controller for AGC of two-area power systems*

BFOA optimized FPI/FPID controller is proposed to solve AGC problem of two-area traditional non-reheat thermal, reheat thermal, multi-source hydrothermal and restructured multi-source hydrothermal power systems. It is observed from the system outcomes on MATLAB platform that BFOA tuned FPID outperforms BFOA tuned FPI and various other intelligent algorithms tuned PI/FPI controller available in the recent literature.

185

D. Fractional order PID controller for AGC of power systems

BFOA tuned FOPID controller is proposed for AGC of traditional two-area multi-source hydrothermal, restructured two-area multi-source hydrothermal, restructured two-area multi-source thermal gas and restructured three-area multi-source hydrothermal power system models. From the simulation results, it observed that BFOA tuned FOPID controller outperforms hFA-PS tuned PI and conventional/BFOA/GA/DE/hFA-PS/GWO tuned PID controllers.

E. Fractional order fuzzy PID controller for AGC of power systems

The fuzzy and fractional order concepts are mingled to evolve a new controller termed as FOFPID controller tuned via BFOA. The efficacy of the proposed controller is tested on traditional two-area multi-source hydrothermal, restructured two-area multi-source hydrothermal, restructured two-area multi-source thermal gas and restructured three-area multi-source hydrothermal power system models. From the simulation results, it is observed that proposed BFOA tuned FOFPID controller show superior performance in comparison to BFOA tuned FOPID controller in terms of least values of settling time, peak undershoot and various performance indices.

F. AGC of restructured power system incorporating system nonlinearities

BFOA tuned FOFPID controller is tested on restructured three-area multi-source hydrothermal system with nonlinearities such as GRC, DZ, BD and TD. A desired performance is obtained in the presence of GRC/DZ/BD/TD with FOFPID controller optimized for linear system. However, in the presence of GRC or GRC/DZ/BD/TD the system performance degrades drastically without system instability under worst poolco plus bilateral with contract violation case. Further, system dynamic responses

186

clearly reveal that the controller is found to perform well when the three-area system is subjected to higher degree of uncontracted demands and simultaneous occurrence of uncontracted demands. Hence, proposed controller is a robust controller and may be a suitable choice to solve AGC problem in various traditional and restructured power systems.

10.2 Scope for the future research

In the present study it has been tried to propose some good designs of AGC controllers for AGC of power systems interconnected in traditional and restructured modes in presence or absence of AC/DC parallel transmission links. The proposed controllers have demonstrated very promising results. However, there are various areas, which need further research to provide better AGC controller designs for various types of power system structures. These areas are stated as follows:

1. The current study is limited only to two/three-area traditional/restructured interconnected power system but this work can further be extended to four/five-area power systems.

2. Since all the system states may not be accessible for measurement. Consequently, the studies may be performed in future by considering sub-optimal control strategies.

3. In this study, the design of FPI controller is carried out employing GA and the design of PID, FPI/FPID, FOPID and FOFPID controllers is carried out using BFOA but more fruitful results may be obtained by using some other new intelligent optimization techniques.

4. Some other forms of supplementary controllers such as neural, neural-fuzzy, two degree of freedom PID (2-DOF-PID), 2-DOF-FOPID, 2-DOF-FPID, 2-DOF-

FOFPID (2-DOF-FOFPID), fuzzy tilt integral derivative (FTID) etc., in conjunction with some new tuning techniques may be implemented in future studies on restructured as well as traditional power systems.

5. The design of AGC controllers is carried out in continuous mode but further studies may be carried out to design AGC controllers in discrete mode.

6. In the present study, it is assumed that control areas of power system have multi-sources of power generations like thermal and hydro or thermal or gas in each area. However, further studies may be done by considering diverse sources like hydro, thermal, gas, wind, diesel, nuclear etc. in each control area of multi-area traditional/restructured power system.

7. The current study is performed on assuming that AGC loop does not interact with the automatic voltage regulator (AVR) loop due to inertial differences between them. In future, AGC studies in restructured power systems can be realized in the presence of AVR loop in each area.

8. The impact of various FACTS and energy storing devices can be studied for solving AGC problem of multi-area multi-source multi-unit restructured power systems.

REFERENCES

[1]   O. I. Elgerd, *Electric Energy Systems Theory: An introduction*. 2nd ed. 42nd reprint. New Delhi: McGraw Hill Education, 2014, pp. 299–362.

[2]   P. Kundur, *Power System Stability and Control*. 5th reprint. New Delhi: Tata McGraw Hill, 2008, pp. 377–448.

[3]   H. Saadat, *Power System Analysis*. 1st ed. 15th reprint. New Delhi: Tata McGraw-Hill, 2002, pp. 527–585.

[4]   H. Bevrani, *Robust Power System Frequency Control*. 1st ed. New York: Springer-Verlag, 2009.

[5]   D. Das, *Electrical Power Systems*. 1st ed. reprint. Delhi: New Age International Pub., 2010, pp. 307–355.

[6]   H. Bevrani and T. Hiyama, *Intelligent Automatic Generation Control*. 1st ed. Boca Raton, FL: CRC Press, Apr. 2011.

[7]   F. C. Schweppe and S. K. Mitter, "Hierarchical system theory and electric power systems," In *Proc. of the Symposium on Real-Time Control of Electric Power Systems*, Baden, Switzerland, p. 259–277, 1971.

[8]   F. C. Schweppe, M. C. Caramanis, R. D. Taboors, and R. E. Bohn, *Spot Pricing of Electricity*, Kluwer Academic Publishers: Boston, USA, 1988.

[9]   M. Ilic, F. Galiana and L. Fink, *Power System Restructuring: Engineering and Economics*, Kluwer Academic Publishers: Boston, USA, 1998.

[10]   M. A. Einhorn and R. Siddiqi, *Electricity Transmission Pricing and Technology*, Kluwer Academic Publishers: Boston, USA, 1996.

[11]   S. Stoft, *Power Systems Economics*: *Designing Markets for Electricity*, Wiley-IEEE Press: New York, 2002.

[12]   V. Donde, M. A. Pai, and I. A. Hiskens, "Simulation and optimization in an AGC system after deregulation," *IEEE Trans. Power Syst.*, vol. 16, no. 3, pp. 481–489, Aug. 2001.

[13]   J. Kumar, K.-H. Ng, and G. Sheble, "AGC simulator for price-based operation Part I: A model," *IEEE Trans. Power Syst.*, vol. 12, no. 2, pp. 527–532, May 1997.

[14]   J. Kumar, K.-H. Ng, and G. Sheble, "AGC simulator for price-based operation-part II: Case study results," *IEEE Trans. Power Syst.*, vol. 12, no. 2, pp. 533–538, May 1997.

[15]   N. Cohn, "Some aspects of tie-line bias control on interconnected power systems," *AIEE Trans. Power App. Syst.*, vol. 75, no. 3, pt. III, pp. 1415–1436, Feb. 1957.

[16]   C. Concordia and L. K. Kirchmayer, "Tie-line power and frequency control of electric power systems," *AIEE Trans. Power App. Syst.*, vol. 72, no. 2, pt. 3, pp. 562–572, Jun. 1953.

[17]   C. Concordia and L. K. Kirchmayer, "Tie-line power and frequency control of electric power systems-Part II," *AIEE Trans. Power App. Syst.*, vol. 73, no. 1, pt. III, pp. 133–146, Apr. 1954.

[18]   C. Concordia, H. S. Shott, and C. N. Weygandt, "Control of tie-line power swings," *AIEE Trans. Elect. Eng.*, vol. 61, no. 6, pp. 306–314, Jun. 1942.

[19]   R. P. Aggarwal and F. R. Bergseth, "Large signal dynamics of load-frequency control systems and their optimization using nonlinear programming: I & II," *IEEE Trans. Power App. Syst.*, vol. PAS-87, no. 2, pp. 527–538, Feb. 1968.

[20]   C. E. Fosha and O. I. Elgerd, "The megawatt-frequency control problem: a new approach via optimal control theory," *IEEE Trans. Power App. Syst.*, vol. PAS-89, no. 4, pp. 563–577, Apr. 1970.

[21]   M. Calovic, "Linear regulator design for a load frequency control," *IEEE Trans. Power App. Syst.*, vol. PAS-91, no. 6, pp. 2271–2285, Nov. 1972.

[22]   M. S. Calovic, "Automatic generation control: decentralized area-wise optimal solution," *Elect. Power Syst. Res.*, vol. 7, no. 2, 115–139, Apr. 1984.

[23]   M. L. Kothari and J. Nanda, "Application of optimal control strategy to automatic generation control of a hydrothermal system," *IEE Proc. Control Theory Appl.*, vol. 135no.4, , pt. D, pp. 268–274, Jul. 1988.

[24]   Ibraheem and P. Kumar, "A novel approach to the matrix Riccati equation solution: an application to optimal control of interconnected power systems," *Elect. Power Compon. Syst.*, vol. 32, no. 1, pp. 33–52, Jan. 2004.

[25]   C. M. Liaw and K. H. Chao, "On the design of an optimal automatic generation controller for interconnected power systems," *Int. J. Contr.*, vol. 58, no. 1, pp. 113–127, Jul. 1993.

[26]   C. M. Liaw, "A modified optimal load-frequency controller for interconnected power systems," *Optim. Contr. Appl. Meth.*, vol. 12, no. 3, pp. 197–204, Jul./Sep. 1991.

[27]   Ibraheem, P. Kumar, and S. Khatoon, "Effect of parameter uncertainties on dynamic performance of an interconnected power system with AC/DC links," *Int. J. Power Energy Syst.*, vol. 25, no. 3, pp. 196–210, 2005.

[28] N. Hasan, Ibraheem, and P. Kumar, "Optimal AGC of interconnected power system with modified area control error," *Int. J. Power Energy Syst.*, vol. 32, no. 4, 160–166, 2012.

[29] N. Hasan, Ibraheem, and P. Kumar, "Optimal automatic generation control of interconnected power system considering new structures of matrix Q," *Elect. Power Compon. Syst.*, vol. 41, no. 2, pp. 136–156, Jan. 2013.

[30] Ibraheem, Nizamuddin, and T. S. Bhatti, "AGC of two area power system interconnected by AC/DC links with diverse sources in each area," *Int. J. Elect. Power Energy Syst.*, vol. 55, pp. 297–304, Feb. 2014.

[31] Ibraheem, Nizamuddin, and T. S. Bhatti, "AGC of two area interconnected power system with diverse sources in each area," *J. Elect. Eng.*, vol. 13, no. 4, pp. 202–209, 2013.

[32] Ibraheem, K. R. Niazi, and G. Sharma, "Study on dynamic participation of wind turbines in automatic generation control of power systems," *Elect. Power Compon. Syst.*, vol. 43, no. 1, pp. 44–55, 2015.

[33] S. C. Tripathy, N. Mital, and T. S. Bhatti, "Decentralized sub-optimal automatic generation control of hydro thermal power system using state variable model," *J. Inst. Eng. India*, vol. 64, pt. EL, pp. 69–74, Aug. 1983.

[34] O. P. Malik, G. S. Hope, S. C. Tripathy, and N. Mital, "Decentralized suboptimal load-frequency Control of a hydro-thermal power system using the state variable model," *Elect. Power Syst. Res.*, vol. 8, no. 3, pp. 237–247, May 1985.

[35] M. Aldeen and H. Trinh, "Load-frequency control of interconnected power systems via constrained feedback control schemes," *Comput. Elect. Eng.*, vol. 20, no. 1, pp. 71–88, Jan. 1994.

[36] Ibraheem, P. Kumar, N. Hasan, and Nizamuddin, "Sub-optimal automatic generation control of interconnected power system using output vector feedback control strategy," *Elect. Power Compon. Syst.*, vol. 40, no. 9, pp. 977–994, Jun. 2012.

[37] N. Hasan, Ibraheem, P. Kumar, and Nizamuddin, "Sub-optimal automatic generation control of interconnected power system using constrained feedback control strategy," *Int. J. Elect. Power Energy Syst.*, vol. 43, no. 1, pp. 295–303, Dec. 2012.

[38] K. P. S. Parmar, S. Majhi, and D. P. Kothari, "Load frequency control of a realistic power system with multi-source power generation," *Int. J. Elect. Power Energy Syst.*, vol. 42, no. 1, pp. 426–433, Nov. 2012.

[39] G. Sharma, I. Nasiruddin, and K. R. Niazi, "Optimal automatic generation control of asynchronous power systems using output feedback control strategy with dynamic participation of wind turbines," *Elect. Power Compon. Syst.*, vol. 43, no. 4, pp. 384–398, 2015.

[40] G. Sharma, I. Nasiruddin, K. R. Niazi, and R. C. Bansal, "Optimal AGC of a multi-area power system with parallel AC/DC tie lines using output vector feedback control strategy," *Int. J. Elect. Power Energy Syst.*, vol. 81, pp. 22–31, Oct. 2016.

[41] W.-C. Chan and Y.-Y. Hsu, "Automatic generation control of interconnected power systems using variable-structure controllers," *IEE Proc. Gener. Transm. Distrib.*, vol. 128, no. 5, pt. C, pp. 269–279, Sep. 1981.

[42] N. N. Bengiamin and W. C. Chan, "Variable structure control of electric power generation," *IEEE Trans. Power App. Syst.*, vol. PAS-101, no. 2, pp. 376–380, Feb. 1982.

[43] W.-C. Chan and Y.-Y. Hsu, "Optimal control of electric power generation using variable structure controllers," *Elect. Power Syst. Res.*, vol. 6, no. 4, pp. 269–278, Dec. 1983.

[44] Y. Y. Hsu and W. C. Chan, "Optimal variable structure controller for the load-frequency control of interconnected hydrothermal power systems," *Int. J. Elect. Power Energy Syst.*, vol. 6, no. 4, pp. 221–229, Oct. 1984.

[45] A. Kumar, O. P. Malik, and G. S. Hope, "Power generation control using dual-mode control," *Elect. Mach. Power Syst.*, vol. 9, nos. 4-5, pp. 335–345, Jan. 1984.

[46] A. Kumar, O. P. Malik, and G. S. Hope, "Variable-structure-system control applied to AGC of an interconnected power system," *IEE Proc. Gener. Transm. Distrib.*, vol. 132, pt. C, no. 1, pp. 23–29, Jan. 1985.

[47] A. Y. Sivaramakrishnan, M. V. Hariharan, and M. C. Srisaiam, "Switched control of frequency of interconnected power systems using variable structure," *Int. J. Syst. Sc.*, vol. 16, no. 11, pp. 1409–1424, Nov. 1985.

[48] M. L. Kothari, D. Das, S. V. Singh, D. P. Kothari, and J. Nanda, "Variable structure controllers for AGC of interconnected power system," *J. Inst. Eng. India*, vol. 72, pt. El, pp. 79–82, Aug. 1991.

[49] D. Das, M. L. Kothari, D. P. Kothari, and J. Nanda, "Variable structure control strategy to automatic generation control of interconnected reheat thermal system," *IEE Proc. Contr. Theory Appl.*, vol. 138, no. 6, pt. D, pp. 579–585, Nov. 1991.

[50] T. S. Bhatti and D. P. Kothari, "Variable structure load-frequency control of isolated wind-diesel-micro hydro hybrid power systems," *J. Inst. Eng. India*, vol. 83, pt. EL, pp. 52–56, 2002.

[51] G. Ray, S. Dey, and T. K. Bhattacharyya, "Multi-area load frequency control of power systems: a decentralized variable structure approach," *Elect. Power Compon. Syst.*, vol. 33, no. 3, pp. 315–331, Dec. 2004.

[52] E. V. Bohn and S. M. Miniesy, "Optimum load-frequency sampled-data control with randomly varying system disturbances," *IEEE Trans. Power App. Syst.*, vol. PAS-91, no. 5, pp. 1916–1923, Sep. 1972.

[53] F. P. deMello, R. J. Mills, and W. F. B'Rells, "Automatic generation control, Part II-Digital control techniques," *IEEE Trans. Power App. Syst.*, vol. PAS-92 , no. 2, pp. 716–724, Mar. 1973.

[54] M. L. Kothari, J. Nanda, and L. Hari, "Selection of sampling period for automatic generation control," *Elect. Mach. Power Syst.*, vol. 25, no. 10, pp. 1063–1077, Dec. 1997.

[55] M. L. Kothari, P. S. Satsangi, and J. Nanda, "Sampled-data automatic generation control of interconnected reheat thermal systems considering generation rate constraints," *IEEE Trans. Power App. Syst.*, vol. PAS-100, no. 5, pp. 2334–2342, May 1981.

[56] J. Nanda, M. L. Kothari, and P. S. Satsangi, "Automatic generation control of an interconnected hydrothermal system in continuous and discrete modes considering generation rate constraints," *IEE Proc. Control Theory Appl.*, vol. 130, no. 1, pt. D, pp. 17–27, Jan. 1983.

[57] A. Kumar and O. P. Malik, "Discrete analysis of load frequency control problem," *IEE Proc. Gener. Transm. Distrib.*, vol. 131, no. 4, pp. 144–145, Jul. 1984.

[58] S. C. Tripathy, T. S. Bhatti, C. S. Jha, O. P. Malik, and G. S. Hope, "Sampled data automatic generation control analysis with reheat steam turbines and governor dead-band effects," *IEEE Trans. Power App. Syst.*, vol. PAS-103, no. 5, pp. 1045–1051, May 1984.

[59] T. Hiyama, "Optimisation of discrete-type load-frequency regulators considering generation-rate constraints," *IEE Proc. Gener. Transm. Distrib.*, vol. 129, pt. C, no. 6, pp. 285–289, Nov. 1985.

[60] Y.-Y. Hsu and C.-J. Wu, "The design of sampled- data load frequency controllers using parameter plane methods," *J. Chinese Inst. Eng.*, vol. 9, no. 1, pp. 89–96, Jan. 1986.

[61] T. S. Bhatti, "Sampled data interactive excitation and AGC of power systems," In *Proc. on Recent Trends in Electrical Energy Systems,* New Delhi, India, 1986, p. 144–154.

[62] A. Kumar, O. P. Malik, and G. S. Hope, "Discrete variable structure controller for load frequency control of multiarea interconnected power systems," *IEE Proc. Gener. Transm. Distrib.*, vol. 134, no. 2, pt. C, pp. 116–122, Mar. 1987.

[63] A. Kumar, "Discrete load frequency control of interconnected power system," *Int. J. Energy Syst.*, vol. 9, no. 2, pp. 73–77, 1989.

[64] M. L. Kothari, J. Nanda, D. P. Kothari, and D. Das, "Discrete-mode automatic generation control of a two-area reheat thermal system with new area control error," *IEEE Trans. Power Syst.*, vol. 4, no. 2, pp. 730–738, May 1989.

[65] L. Hari, M. L. Kothari, and J. Nanda, "Optimum selection of speed regulation parameters for automatic generation control in discrete mode considering

generation rate constraints," *IEE Proc. Gener. Transm. Distrib.*, vol. 138, no. 5, pt. C, pp. 401–406, Sep. 1991.

[66] M. L. Kothari, J. Nanda, D. P. Kothari, and D. Das, "Discrete mode automatic generation control of a two-area reheat thermal system with a new area control error considering generation rate constraint," *J. Inst. Eng. India*, vol. 72, pt. EL, pp. 297–303, Feb. 1992.

[67] C. S. Indulkar, "Analysis of megawatt-frequency control problem using sampled-data theory," *J. Inst. Eng. India*, vol. 73, pt. EL, pp. 129–133, 1992.

[68] S. C. Tripathy and K.-P. Juengst, "Sampled data automatic generation control with superconducting magnetic energy storage in power systems," *IEEE Trans. Energy Convers.*, vol. 12, no. 2, pp. 187–192, Jun. 1997.

[69] S. Chowdhury, S. P. Chaudhury, and S. Choudhuri, "Advanced digital load frequency control with unknown deterministic power demand for interconnected power systems," *J. Inst. Eng. India*, vol. 80, pt. EL, pp. 87–95, Nov. 1999.

[70] J. Nanda, A. Mangla, and S. Suri, "Some new findings on automatic generation control of an interconnected hydrothermal system with conventional controllers," *IEEE Trans. Energy Convers.*, vol. 21, no. 1, pp. 187–194, Mar. 2006.

[71] Ibraheem, P. Kumar, and D. P. Kothari, "Recent philosophies of automatic generation control strategies in power systems," *IEEE Trans. Power Syst.*, vol. 20, no. 1, pp. 346–357, Feb. 2005.

[72] H. Shayeghi, H. A. Shayanfar, and A. Jalili, "Load frequency control strategies: a state-of-the-art survey for the researcher," *Energy Convers. Manage.*, vol. 50, no. 2, pp. 344–353, Feb. 2009.

[73] S. K. Pandey, S. R. Mohanty, and N. Kishor, "A literature survey on load-frequency control for conventional and distribution generation power systems," *Renewab. Sustain. Energy Rev.*, vol. 25, pp. 318–334, Sep. 2013.

[74] A. Pappachen and A. P. Fathima, "Critical research areas on load frequency control issues in a deregulated power system: A state-of-the-art-of-review," *Renewab. Sustain. Energy Reviews*, vol. 72, pp. 163–177, May 2017.

[75] R. Shankar, S. R. Pradhan, K. Chatterjee, and R. Mandal, "A comprehensive state of the art literature survey on LFC mechanism for power system," *Renewab. Sustainab. Energy Reviews*, vol. 76, no. 6, pp. 1185–1207, Sep. 2017.

[76] A. Demiroren, N. S. Sengor, and H. L. Zeynelgil, "Automatic generation control by using ANN technique," *Elect. Power Compon. Syst.*, vol. 29, no. 10, pp. 883–896, Oct. 2001.

[77] H. L. Zeynelgil, A. Demiroren, and N. S. Sengor, "Load frequency control for power system with reheat steam turbine and governor deadband non-linearity by using neural network controller," *Eur. Trans. Elect. Power*, vol. 12, no. 3, pp.

179–184, May/Jun. 2002.

[78] H. L. Zeynelgil, A. Demiroren, and N. S. Sengor, "The Application of ANN technique to automatic generation control of multi-area power system," *Int. J. Elect. Power Energy Syst.*, vol. 24, no. 5, pp. 345–354, Jun. 2002.

[79] A. Demiroren, H. L. Zeynelgil, and N. S. Sengor, "Automatic generation control for power system with SMES by using neural network controller," *Elect. Power Compon. Syst.*, vol. 31, no. 1, pp. 1–25, Jan. 2003.

[80] A. Demiroren, H. L. Zeynelgil, and N. S. Sengor, "The application of NN technique to automatic generation control for the power system with three areas including SMES units," *Eur. Trans. Elect. Power*, vol. 13, no. 4, pp. 227–238, Jul./Aug. 2003.

[81] A. Demiroren, H. L. Zeynelgil, and N. S. Sengor, "Automatic generation control using ANN technique for multi-area power system with SMES units," *Elect. Power Compon. Syst.*, vol. 32, no. 2, pp. 193–213, Feb. 2004.

[82] A. Demiroren and E. Yesil, "Automatic generation control with fuzzy logic controllers in the power system including SMES units," *Int. J. Elect. Power Energy Syst.*, vol. 26, no. 4, pp. 291–305, May 2004.

[83] Y. Oysal, "A comparative study of adaptive load frequency controller designs in a power system with dynamic neural network models," *Energy Convers. Manage.*, vol. 46, nos. 15–16, pp. 2656–2668, Sep. 2005.

[84] M. Luy, I. Kocaarslan, E. Cam, and M. C. Taplamacioglu, "Load frequency control in a single area power system by artificial neural network (ANN)," *University Pitesti-Electron. Comput. Sc., Sc. Bulletin*, vol. 2, no. 8, pp. 26–29, 2008.

[85] R. Francis and I. A. Chidambaram, "Application of modified dynamic neural network for the load frequency control of a two area thermal reheat power system," *Int. Review Automat. Contr.*, vol. 6, no. 1, pp. 47–53,Jan. 2013.

[86] D. Qian, S. Tong, H. Liu, and X. Liu, "Load frequency control by neural-network-based integral sliding mode for nonlinear power systems with wind turbines," *Neurocomput.*, vol. 173, pt. 3, pp. 875–885, Jan. 2016.

[87] C. S. Indulkar and B. Raj, "Application of fuzzy controller to automatic generation control," *Elect. Mach. Power Syst.*, vol. 23, no. 2, pp. 209–220, Mar. 1995.

[88] S. P. Ghoshal, "Multi-area frequency and tie-line power flow control with fuzzy logic based integral gain scheduling," *J. Inst. Eng. India*, vol. 84, pt. EL, pp. 135–141, Dec. 2003.

[89] E. Yesil, M. Guzelkaya, and I. Eksin, "Self tuning fuzzy PID type load and frequency controller," *Energy Convers. Manage.*, vol. 45, no. 3, pp. 377–390, Feb. 2004.

[90] E. Cam and I. Kocaarslan, "Load-frequency control in two area power system," *Karabuk University's J. Tek.*, vol. 7, no. 2, pp. 197–203, Apr.-Jun. 2004.

[91] E. Cam and I. Kocaarslan, "Load frequency control in two area power systems using fuzzy logic controller," *Energy Convers. Manage.*, vol. 46, no. 2, pp. 233–243, Jan. 2005.

[92] E. Cam and I. Kocaarslan, "A fuzzy gain scheduling PI controller application for an interconnected electrical power system," *Elect. Power Syst. Res.*, vol. 73, no. 3, pp. 267–274, Mar. 2005.

[93] I. Kocaarslan and E. Cam, "Fuzzy logic controller in interconnected electrical power systems for load-frequency control," *Int. J. Elect. Power Energy Syst.*, vol. 27, no. 8, pp. 542–549, Oct. 2005.

[94] S. Pothiya, I. Ngamroo, S. Runggeratigul, and P. Tantaswadi, "Design of optimal fuzzy logic based PI controller using multiple tabu search algorithm for load frequency control," *Int. J. Contr.*, *Automat. Syst.*, vol. 4, no. 2, pp. 155–164, Apr. 2006.

[95] E. Cam, "Application of fuzzy logic for load frequency control of hydroelectrical power plants," *Energy Convers. Manage.*, vol. 48, no. 4, pp. 1281–1288, Apr. 2007.

[96] L. H. Hassan, H. A. F. Mohamed, M. Moghavvemi, and S. S. Yang, "Automatic generation control of power system with fuzzy gain scheduling integral and derivative controller," *Int. J. Power, Energy, Artificial Intell.*, vol. 1, no. 1, pp. 29–33, Aug. 2008.

[97] S. Pothiya and I. Ngamroo, "Optimal fuzzy logic-based PID controller for load-frequency control including superconducting magnetic energy storage units," *Energy Convers. Manage.*, vol. 49, no. 10, pp. 2833–2838, Oct. 2008.

[98] B. Anand and A. E. Jeyakumar, "Load frequency control with fuzzy logic controller considering non-linearities and boiler dynamics," *ICGST-ACSE J.*, vol. 8, no. 3, pp. 15–20, Jan. 2009.

[99] L. C. Saikia, N. Sinha, and J. Nanda, "Maiden application of bacterial foraging based fuzzy IDD controller in AGC of a multi-area hydrothermal system," *Int. J. Elect. Power Energy Syst.*, vol. 45, no. 1, pp. 98–106, Feb. 2013.

[100] K. R. M. V. Chandrakala, S. Balamurugan, and K. Sankaranarayanan, "Variable structure fuzzy gain scheduling based load frequency controller for multi source multi area hydro thermal system," *Int. J. Elect. Power Energy Syst.*, vol. 53, pp. 375–381, Dec. 2013.

[101] E. Yesil, "Interval type-2 fuzzy PID load frequency controller using big bang-big crunch optimization," *Applied. Soft Comput.*, vol. 15, pp. 100–112, Feb. 2014.

[102]   H. A. Yousef, K. AL-Kharusi, M. H. Albadi, N. Hosseinzadeh, "Load frequency control of a multi-area power system: an adaptive fuzzy logic approach," *IEEE Trans. Power Syst.*, vol. 29, no. 4, pp. 1822–1930, Jul. 2014.

[103]   V. Chandrakala, B. Sukumar, and K. Sankaranarayanan, "Load frequency control of multi-source multi-area hydro thermal system using flexible alternating current transmission system devices," *Elect. Power Compon. Syst.*, vol. 42, no. 9, pp. 927−934, Jul. 2014.

[104]   R. K. Sahu, S. Panda, and N. K. Yegireddy, "A novel hybrid DEPS optimized fuzzy PI/PID controller for load frequency control of multi-area interconnected power systems," *J. Process Contr.*, vol. 24, no. 10, pp. 1596–1608, Oct. 2014.

[105]   B. K. Sahu, S. Pati, S. Panda, "Teaching-learning based optimization algorithm based fuzzy-PID controller for automatic generation control of multi-area power system," *Applied Soft Comput.*, vol. 27, pp. 240–249, Feb. 2015.

[106]   D. K. Chaturvedi, R. Umrao, O. P. Malik, "Adaptive polar fuzzy logic based load frequency controller," *Int. J. Elect. Power Energy Syst.*, vol. 66, pp. 154–159, Mar. 2015.

[107]   R. K. Sahu, S. Panda, and P. C. Pradhan, "Design and analysis of hybrid firefly algorithm-pattern search based fuzzy PID controller for LFC of multi area power systems," *Int. J. Elect., Power Energy Syst.*, vol. 69, pp. 200–212, Jul. 2015.

[108]   H. Yousef, "Adaptive fuzzy logic load frequency control of multi-area power system," *Int. J. Elect. Power Energy Syst.*, vol. 68, pp. 384–395, Jun. 2015.

[109]   M. H. Khooban and T. Niknam, "A new intelligent online fuzzy tuning approach for multi-area load frequency control: self adaptive modified bat algorithm," *Int. J. Elect. Power Energy Syst.*, vol. 71, pp. 254–261, Oct. 2015.

[110]   V. Jeyalakshmi and P. Subburaj, "PSO-scaled fuzzy logic to load frequency control in hydrothermal power system," *Soft Comput.*, vol. 20, no. 7, pp. 2577–2594, Jul. 2016.

[111]   R. Khezri, S. Golshannavaz, S. Shokoohi, and H. Bevrani, "Fuzzy logic based fine-tuning approach for robust load frequency control in a multi-area power system," *Elect. Power Compon. Syst.*, vol. 44, no. 18, pp. 2073–2083, Oct. 2016.

[112]   H. H. Chung, M. K. Chung, and G. H. Han, "Design of an adaptive neuro-fuzzy inference precompensator for load frequency control of two-area power systems," *J. Korean Society Marine Eng.*, vol. 24, no. 2, pp. 72–81, 2000.

[113]   S. H. Hosseini and A. H. Etemadi, "Adaptive neuro-fuzzy inference system based automatic generation control," *Elect. Power Syst. Res.*, vol. 78, no. 7, pp. 1230–1239, Jul. 2008.

[114]   G. Panda, S. Panda, and C. Ardil, "Hybrid neuro fuzzy approach for automatic generation control of two–area interconnected power system," *Int. J. Comput. Intell.*, vol. 5, no. 1, pp. 80–84, 2009.

[115] G. Panda, S. Panda, and C. Ardil, "Automatic generation control of interconnected power system with generation rate constraints by hybrid neuro fuzzy approach," *Int. J. Elect. Power Energy Syst. Eng.*, vol. 2, no. 1, pp. 13–18, 2009.

[116] Y. Oguz, I. Guney, and H. Erdal, "Modeling of hybrid wind-gas power generation system and adaptive neuro-fuzzy controller to improve the system performance," *Comput. Appl. Eng. Educat.*, vol. 18, no. 4, pp. 669–683, Dec. 2010.

[117] C. S. Rao, S. S. Nagaraju, and P. S. Raju, "Adaptive neuro-fuzzy inference system for automatic generation control of interconnected hydrothermal plant," *Int. J. Knowledge-Based Intell. Eng. Syst.,* vol. 15, no. 2, pp. 71–78, Apr. 2011.

[118] S. R. Khuntia and S. Panda, "Simulation study for automatic generation control of a multi-area power system by ANFIS approach," *Applied Soft Comput.*, vol. 12, no. 1, pp. 333–341, Jan. 2012.

[119] M. S. Kahkeshi and F. Sheikholeslam, "A fuzzy wavelet neural network load frequency controller based on genetic algorithm," *Int. J. Tech. Physical Prob. Eng.*, vol. 4, no. 2, issue 11, pp. 81–89, Jun. 2012.

[120] M. I. Mosaad and F. Salem, "LFC based adaptive PID controller using ANN and ANFIS techniques," *J. Elect. Syst. Informat. Tech.*, vol. 1, no. 3, pp. 212–222, Dec. 2014

[121] A. D. Falehi and A. Mosallanejad, "Neoteric HANFISC–SSSC based on MOPSO technique aimed at oscillation suppression of interconnected multi-source power systems," *IET Gener. Transm. Distrib.*, vol. 10, no. 7, pp. 1728–1740, May 2016.

[122] H. Golpira, H. Bevrani, and H. Golpira, "Application of GA optimization for automatic generation control design in an interconnected power system," *Energy Convers. Manage.*, vol. 52, no. 5, pp. 2247–2255, May 2011.

[123] Y. L. Abdel-Magid and M. M. Dawoud, "Optimal AGC tuning with genetic algorithms," *Elect. Power Syst. Res.*, vol. 38, no. 3, pp. 231–238, Sep. 1996.

[124] I. A. Chidambaram and B. Paramasivam, "Genetic algorithm based decentralized controller for load-frequency control of interconnected power systems with RFB considering TCPS in the tie-line," *Int. J. Electron. Eng. Res.*, vol. 1, no. 4, pp. 299–312, 2009.

[125] C. Ismayil, R. S. Kumar, and T. K. Sindhu, "Optimal fractional order PID controller for automatic generation control of two-area power systems," *Int. Trans. Elect. Energy Syst.,* vol. 25, no. 12, pp. 3329–3348, Dec. 2015.

[126] K. R. M. V. Chandrakala and S. Balamurugan, "Simulated annealing based optimal frequency and terminal voltage control of multi source multi area system," *Int. J. Elect. Power Energy Syst.*, vol. 78, pp. 823–829, Jun. 2016.

[127] R. N. Rao and P. R. K. Reddy, "PSO based tuning of PID controller for a load frequency control in two area power system," *Int. J. Eng. Res. Applicat.*, vol. 1, no. 4, pp. 1499–1505, Nov.-Dec. 2011.

[128] Y. L. Abdel-Magid and M. A. Abido, "AGC tuning of interconnected reheat thermal systems with particle swarm optimization," In *Proc. of 10th IEEE Int. Conf. on Electronics, Circuits and Systems*, 14-17 December, 2003, vol. 1, p. 376–379.

[129] H. Gozde, M. C. Taplamacioglu, I. Kocaarslan, and M. A. Senol, "Particle swarm optimization based PI-controller design to load-frequency control of a two area reheat thermal power system," *J. Therm. Sc. Tech.*, vol. 30, no. 1, pp. 13–21, 2010.

[130] H. Gozde and M. C. Taplamacioglu, "Automatic generation control application with craziness based particle swarm optimization in a thermal power system," *Int. J. Elect. Power Energy Syst.*, vol. 33, no. 1, pp. 8–16, Jan. 2011.

[131] J. Morsali, K. Zare, and M. T. Hagh, "Applying fractional order PID to design TCSC-based damping controller in coordination with automatic generation control of interconnected multi-source power system," *Eng. Sc. Tech., an Int. J.*, vol. 20, no. 1, pp. 1–17, Feb. 2017.

[132] K. Zare, M. T. Hagh and J. Morsali, "Effective oscillation damping of an interconnected multi-source power system with automatic generation control and TCSC," *Int. J. Elect. Power Energy Syst.*, vol. 65, pp. 220–230, Feb. 2015.

[133] H. Gozde, M. C. Taplamacioglu, and I. Kocaarslan, "Comparative performance analysis of artificial bee colony algorithm in automatic generation control for interconnected reheat thermal power system," *Int. J. Elect. Power Energy Syst.,* vol. 42, no. 1, pp. 167–178, Nov. 2012.

[134] K. Naidu, H. Mokhlis, and A. H. A. Bakar, "Multiobjective optimization using weighted sum artificial bee colony algorithm for load frequency control," *Int. J. Elect. Power Energy Syst.*, vol. 55, pp. 657–667, Feb. 2014.

[135] M. Elsisi, M. Soliman, M. A. S. Aboelela, and W. Mansour, "ABC based design of PID controllers for two area load frequency control with nonlinearities. *Telkomnika Indonesian J. Elect. Eng.*, vol. 16, no. 1, pp. 58–64, Oct. 2015.

[136] S. Duman and N. Yorukeren, "Automatic generation control of the two area non-reheat thermal power system using gravitational search algorithm," *Przeglad Elektrotechniczny (Elect. Review)*, vol. 88, no. 10a, pp. 254–259, 2012.

[137] R. K. Sahu, S. Panda, U. K. Rout, "Application of gravitational search algorithm for load frequency control of multi area power system," *J. Bioinformatics Intell. Contr.*, vol. 2, no. 3, pp. 200–211, Sep. 2013.

[138] R. K. Sahu, S. Panda, and S. Padhan, "Optimal gravitational search algorithm for automatic generation control of interconnected power systems," *Ain Shams Eng. J.*, vol. 5, no. 3, pp. 721–733, Sep. 2014.

[139] M. Elsisi, M. Soliman, M. A. S. Aboelela, and W. Mansour, "GSA-based design of dual proportional integral load frequency controllers for nonlinear hydrothermal power system," *Int. J. Elect., Comput., Energetic, Electron. Communicat. Eng.*, vol. 9, no. 8, pp. 893–899, 2015.

[140] P. Dahiya, V. Sharma, and R. Naresh, "Solution approach to automatic generation control problem using hybridized gravitational search algorithm optimized PID and FOPID controllers," *Advances Elect. Comput. Eng.,* vol. 15, no. 2, pp. 23–34, May 2015.

[141] M. Elsisi, M. Soliman, M. A. S. Aboelela, and W. Mansour, "Dual proportional integral controller of two-area load frequency control based gravitational search algorithm," *Telkomnika Indonesian J. Elect. Eng.*, vol. 15, no. 1, pp. 26–35, Jul. 2015.

[142] J. Nanda, S. Mishra, and L. C. Saikia, "Maiden application of bacterial foraging-based optimization technique in multiarea automatic generation control," *IEEE Trans. Power Syst.*, vol. 24, no. 2, pp. 602–609, May 2009.

[143] I. Nasiruddin, T. S. Bhatti, and N. Hakimuddin, "Automatic generation control in an interconnected power system incorporating diverse source power plants using bacteria foraging optimization technique," *Elect. Power Compon. Syst.*, vol. 43, no. 2, pp. 189–199, 2015.

[144] E. S. Ali and S. M. Abd-Elazim, "Optimal PID tuning for load frequency control using bacteria foraging optimization algorithm," In *Proc. of the 14th International Middle East Power Systems Conference (MEPCON'10)*, Cairo, Egypt, 19-21 December 2010, paper id 191, p. 410–415.

[145] E. S. Ali and S. M. Abd-Elazim, "Bacteria foraging optimization algorithm based load frequency controller for interconnected power system," *Int. J. Elect. Power Energy Syst.*, vol. 33, no. 3, pp. 633–638, Mar. 2011.

[146] S. Panda, B. Mohanty, and P. K. Hota, "Hybrid BFOA-PSO algorithm for automatic generation control of linear and nonlinear interconnected power systems," *Applied Soft Comput.*, vol. 13, no. 12, pp. 4718–4730, Dec. 2013.

[147] L. V. S. Kumar, G. V. N. Kumar, and S. Madichetty, "Pattern search algorithm based automatic online parameter estimation for AGC with effects of wind power," *Int. J. Elect. Power Energy Syst.*, vol. 84, pp. 135–142, Jan. 2017.

[148] S. Padhan, R. K. Sahu, and S. Panda, "Application of firefly algorithm for load frequency control of multi-area interconnected power system," *Elect. Power Compon. Syst.*, vol. 42, no. 13, pp. 1419–1430, Oct. 2014.

[149] S. Debbarma, L. C. Saikia, and N. Sinha, "Automatic generation control using two degree of freedom fractional order PID controller," *Int. J. Elect. Power Energy Syst.*, vol. 58, pp. 120–129, Jun. 2014.

[150] R. K. Sahu, S. Panda, and S. Padhan, "A hybrid firefly algorithm and pattern search technique for automatic generation control of multi area power systems," *Int. J. Elect. Power Energy Syst.*, vol. 64, pp. 9–23, Jan. 2015.

[151] R. K. Sahu, S. Panda, and G. T. C. Sekhar, "A novel hybrid PSO-PS optimized fuzzy PI controller for AGC in multi area interconnected power systems," *Int. J. Elect. Power Energy Syst.*, vol. 64, pp. 880–893, Jan. 2015.

[152] D. Guha, P. K. Roy, and S. Banerjee, "Load frequency control of interconnected power system using grey wolf optimization," *Swarm Evolution. Comput.*, vol. 27, pp. 97–115, Apr. 2016.

[153] M. Elsisi, M. Soliman, M. A. S. Aboelela, and W. Mansour, "Bat inspired algorithm based optimal design of model predictive load frequency control," *Int. J. Elect. Power Energy Syst.*, vol. 83, pp. 426–433, Dec. 2016.

[154] U. Salma, "Design of load frequency controller using multi objective bat algorithm," *J. Elect. Eng.*, vol. 15, no. 3, pp. 106–112, 2015.

[155] A. K. Barisal, "Comparative performance analysis of teaching learning based optimization for automatic load frequency control of multi-source power systems," *Int. J. Elect. Power Energy Syst.*, vol. 66, pp. 67–77, Mar. 2015.

[156] B. Mohanty, "TLBO optimized sliding mode controller for multi-area multi-source nonlinear interconnected AGC system," *Int. J. Elect. Power Energy Syst.*, vol. 73, pp. 872–881, Dec. 2015.

[157] B. Mohanty, S. Panda, and P. K. Hota, "Controller parameters tuning of differential evolution algorithm and its application to load frequency control of multi-source power system," *Int. J. Elect. Power Energy Syst.*, vol. 54, pp. 77–85, Jan. 2014.

[158] R. K. Chekka and P. V. R. Rao, "Fractional order automatic generation controller for a multi area interconnected system using evolutionary algorithms," *Int. J. Applied Eng. Res.*, vol. 11, no. 4, pp. 2999–2205, 2016.

[159] A. Y. Abdelaziz and E. S. Ali, "Cuckoo Search algorithm based load frequency controller design for nonlinear interconnected power system," *Int. J. Elect. Power Energy Syst.*, vol. 73, pp. 632–643, Dec. 2015.

[160] A. Y. Abdelaziz and E. S. Ali, "Load frequency controller design via artificial cuckoo search algorithm," *Elect. Power Compon. Syst.*, vol. 44, no. 1, pp. 90–98, Jan. 2016.

[161] P. Dash, L. C. Saikia, and N. Sinha, "Flower pollination algorithm optimized PI-PD cascade controller in automatic generation control of a multi-area power system," *Int. J. Elect. Power Energy Syst.*, vol. 82, pp. 19–28, Nov. 2016.

[162] K. Jagatheesan, B. Anand, S. Samanta, N. Dey, V. Santhi, A. S. Ashour, and V. E. Balas, "Application of flower pollination algorithm in load frequency control of

multi-area interconnected power system with nonlinearity," *Neural Comput. Appl.*, vol. 28, no. 1, pp. 475–488, Dec. 2017.

[163]   S. A. Taher, M. H. Fini, and S. F. Aliabadi, "Fractional order PID controller design for LFC in electric power systems using imperialist competitive algorithm," *Ain Shams Eng. J.*, vol. 5, no. 1, pp. 121–135, Mar. 2014.

[164]   A. Zamani, S. M. Barakati, S. Yousofi-Darmian, "Design of a fractional order PID controller using GBMO algorithm for load-frequency control with governor saturation consideration," *ISA Trans.*, vol. 64, pp. 56–66, Sep. 2016.

[165]   I. Pan and S. Das, "Kriging based surrogate modeling for fractional order control of microgrids," *IEEE Trans. Smart Grid*, vol. 6, no. 1, pp. 36–44, Jan. 2015.

[166]   I. Pan and S. Das, "Fractional order AGC for distributed energy resources using robust optimization," *IEEE Trans. Smart Grid*, vol. 7, no. 5, pp. 2175–2186, Sep. 2016.

[167]   I. Pan, S. Das, "Fractional order load-frequency control of interconnected power systems using chaotic multi-objective optimization," *Applied Soft Comput.*, vol. 29, pp. 328–344, Apr. 2015.

[168]   I. Pan, S. Das, "Fractional order fuzzy control of hybrid power system with renewable generation using chaotic PSO," *ISA Trans.*, vol. 62, pp. 19–29, May 2016.

[169]   M. I. Alomoush, "Load frequency control and automatic generation control using fractional-order controllers," *Elect. Eng.*, vol. 91, no. 7, pp. 357–368, Mar. 2010.

[170]   Y. R. Sood, N. P. Padhy and H. O. Gupta, "Restructuring power industry-A bibliographical survey," In *Proc. of IEEE Power Engineering Society Winter Meeting*, 27-31 Jan. 2002, New York, USA, vol. 1, p. 163–167.

[171]   Y. R. Sood, N. P. Padhy, and H. O. Gupta, "Wheeling of power under deregulated environment of power system: A bibliographical survey," *IEEE Trans. Power Syst.*, vol. 17, no. 3, pp. 870–878, Aug. 2002.

[172]   S. Dhanalakshmi, S. Kannan, and K. Mahadevan, "Market modes for deregulated environment-A review," In *Proc. IEEE Int. Conf. on Emerging Trends in Electrical and Computer Technology*, 23-24 March 2011, Tamil Nadu, India, p. 82–87.

[173]   V. Nanduri and T. K. Das, "A survey of critical research areas in the energy segment of restructured electric power markets," *Int. J. Elect. Power Energy Syst.*, vol. 31, no. 5, pp. 181–191, Jun. 2009.

[174]   S. K. Aggarwal, L. M. Saini, and A. Kumar, "Electricity price forecasting in deregulated markets: A review and evaluation," *Int. J. Elect. Power Energy Syst.*, vol. 31, no. 1, pp. 13–22, Jan. 2009.

[175]   A. G. Kagiannas, D. T. Askounis, and J. Psarras, "Power generation planning: A survey from monopoly to competition," *Int. J. Elect. Power Energy Syst.*, vol. 26, no. 6, pp. 413–421, Jul. 2004.

[176]   R. J. Thomas, "Introduction to the minitrack on restructuring the electric power industry: emerging issues, methods and tools," In *Proc. of the 32nd Annual Hawaii Int. Conf. on Systems Sciences*, 5-8 January 1999, Maui, Hawaii, p. 82–87.

[177]   R. W. Ferrero and S. M. Shahidehpour, "Energy interchange in deregulated power systems," *Int. J. Elect. Power Energy Syst.*, vol. 18, no.4, pp. 251–258, May 1996.

[178]   N. G. Hingorani, "Role of FACTS in a deregulated market," In *Proc. IEEE Power Engineering Society Summer Meeting*, Seattle, Washington USA, 16-20 July 2000, vol. 3, p. 1463–1467.

[179]   A. Kazemi and H. Andami, "FACTS devices in deregulated electric power systems: a review," In *Proc. IEEE Int. Conf. on Electric Utility Deregulation, Restructuring and Power Technologies*, 5-8 April 2004, vol. 1, p. 337–342.

[180]   T. Amakasu, "Power technology development schemes for the deregulated electrical power industry," In *Proc. IEEE Int. Conf. on Electric Utility Deregulation and Restructuring and Power Technologies*, London, UK, 4-7 April 2000, p. XVIII–XXXII.

[181]   S. I. Alamarchuk and N. I. Varopai, "Power industry in Russia: Current state and restructuring," In *Proc. IEEE/PES Transmission & Distribution Conf. & Exposition: Asia and Pacific*, 18-18 August 2005, p. 1–6.

[182]   I. Kurihari, "Restructuring of the electric power industry and the current state of the power market in Japan," In *Proc. IEEE Power Engineering Society General Meeting*, 18-22 June 2006, p. 1–6.

[183]   J. Jhong and Y. Ni, "Power industry restructuring in China," In *Proc. IEEE Power Engineering Society General Meeting*, 18-22 June 2006, p. 1–5.

[184]   F. F. Wu, W. Fushuan, and G. Duan, "Generation planning and investment under deregulated environment: Comparison of USA and China," In *Proc. IEEE Power Engineering Society General Meeting*, 6-10 June 2004, vol. 2, p. 1324–1328.

[185]   M. H. Asgari, M. J. Tabatabaei, R. Riahi, A. Mazhabjafari, M. Mirzaee, and H. R. Bagheri, "Establishment of regulation service market in Iran restructured power system," In *Proc. IEEE Canadian Conf. on Electrical and Computer Engineering*, Canada, 4-7 May 2008, p. 713–718.

[186]   A. Berizzi, C. Bovo, M. Delfanti, A. Silvestri, and P. Marannino, "Cost analysis of the frequency regulation service for the Italian system," In *IEEE Porto Power Tech. Proc.*, 10-13 September 2001, vol. 1, p. 1–6.

[187]   L. Grilli, "Deregulated electricity market and auctions: The Italian case," *iBusiness*, vol. 2, no. 3, pp. 238–242, Sep. 2010.

[188] T. MacGregor, "Electricity restructuring in Britain: not a model to follow," *IEEE Spectrum*, vol. 38, no. 6, pp. 15–19, Jun. 2001.

[189] Y. Ni, J. Zhong, and H. Liu, "Deregulation of power systems in Asia: Special consideration in developing countries," In *Proc. IEEE Power Engineering Society General Meeting*, 16-16 June 2005, vol. 3, p. 2876–2881.

[190] S. A. Khaparde, "Power sector reform and restructuring in India," In *Proc. IEEE Power Engineering Society General Meeting*, Khaparde, South Africa, 6-10 June 2004, vol. 2, p. 2328–2335.

[191] S. N. Singhand S. C. Srivastava, "Electric power industry restructuring in India: present scenario and future prospect," In *Proc. IEEE Int. Conf. on Electric Utility Deregulation, Restructuring and Power Tech.*, 5-8 April 2004, p. 20–23.

[192] K. T. Madrewar, W. A. Gavhane, A. H. Kardile, and U. D. Shiurkar, "Adaptive approach in deregulation of Indian power system," In *Proc. IEEE Int. Conf. on Energy Syst. and Appl.*, Pune, India, 30 October-1 November 2015, p. 167–172.

[193] R. N. Nayak, Y. K. Sehgal and M. Gupta, "Change in approach to planning and operation of power systems under open access regime-Indian experience," In *Proc. IEEE Power Tech. Russia*, St. Petersburg , Russia, 27-30 June 2005, p. 1–6.

[194] H. L. Bajaj and D. Sharma, "Power sector reforms in India," In *Proc. Int. Conf. on Power Electronics, Drives and Energy Systems*, 12-15 December 2006, p. 1–5.

[195] H. Rudnick, "Planning in a deregulated environment in developing countries: Bolivia, Chile, and Peru," *IEEE Power Eng. Review*, vol. 16, no.7, pp. 18–19, Jul. 1996.

[196] A. M. Pirbazari, "Ancillary services definitions, markets and practices in the world," In *Proc. IEEE/PES on Transm. Distrib. Conf. Exposition*, Latin America, 8-10 November 2010, p. 32–36.

[197] A. Motamedi and M. Fotuhi-Firuzabad, "Ancillary service markets," In *Proc. IEEE Large Eng. Syst. Conf. Power Eng.*, 10-12 October 2007, p. 316–320.

[198] S. S. Oren, "Design of ancillary service markets," In *Proc. IEEE 34th Annual Hawaii Int. Conf. on Syst. Sc.*, Maui, Hawaii, 6-6 January 2001, p. 1–9.

[199] K. W. Cheung, "Ancillary service market design and implementation in North America: From theory to practice," In *Proc. IEEE 3rd Int. Conf. on Elect. Utility Deregulation, Restructuring and Power Tech.*, NanJing China, 6-9 April 2008, p. 66–73.

[200] K. W. Cheung, M. Xingwang, and D. Sun, "Functional design of ancillary service markets under the framework of standard market design for ISO New England", In *Proc. Int. Conf. Power Syst. Tech.*, 22-26 October 2006, p. 1–7.

[201] D. Zheng and W. Zhou, "A design for regional ancillary services auction markets in China," In *Proc. IEEE Bologna Power Tech. Conf.*, Bologna, 23-26 June 2003, vol. 4, p. 1–4.

[202]   O. Gjerde, "Ancillary services-state of the art in the Nordic market," In *Proc. IEEE Power Engineering Society General Meeting*, 24-28 June 2007, p. 1–2.

[203]   2007 IEEE Summer Power Meeting "Panel session on "Experience with bidding ancillary services in RTO markets" operating ancillary service markets in California," In *Proc. IEEE Power Engineering Society General Meeting*, 24-28 June 2007, p. 1–1.

[204]   B. Keshavamurthy, "Panel session on "Experience with operating GENCO assets in RTO markets": PJM's experience with operating energy and ancillary-service markets," In *Proc. IEEE Power Energy Society General Meeting*, 26-30 July 2009, p. 1–1.

[205]   Y. Li and J. N. Jiang, "Experience with operating the ancillary-service markets in ERCOT," In *Proc. IEEE Power Engineering Society General Meeting*, 24-28 June 2007, p. 1–6.

[206]   J. H. T. Hernandez, M. Jimenez-Guzman, and G. Gutierrez-Alcaraz, "Ancillary reactive power service allocation cost in deregulated markets: a methodology," *Int. J. Elect. Power Energy Syst.*, vol. 27, nos. 5-6, pp. 371–378, Jun.-Jul. 2005.

[207]   Y. G. Rebours, D. S. Kirschen, M. Trotignon, and S. Rossignol, "A survey of frequency and voltage control ancillary services-Part I: Technical features," *IEEE Trans. Power Syst.*, vol. 22, no. 1, pp. 350–357, Feb. 2007.

[208]   Y. G. Rebours, "Some salient features of the management of frequency and voltage control ancillary services," In *Proc. IEEE Power Engineering Society General Meeting*, 24-28 June 2007, p. 1–6.

[209]   E. E. El-Araby and N. Yorino, "A hybrid PSO technique for procuring VAR ancillary service in the deregulated electricity markets," *Int. J. Elect. Power Energy Syst.*, vol. 32, no. 6, pp. 664–670, Jul. 2010.

[210]   R. D. Christie and A. Bose, ''Load frequency control issues in power system operations after deregulation," *IEEE Trans. Power Syst.*, vol. 11, no. 3, pp. 1191–1200, Aug. 1996.

[211]   H. Bevrani, A. Rezazadeh, and M. Teshnehlab "Comparison of existing LFC approaches in deregulated environment," In Proc. *IEE 5th Int. Conf. on Power Syst. Manage. Contr.*, London, U.K, 17-19 April 2002, p. 238–243.

[212]   N. Bekhouche, "Automatic generation control before and after deregulation," In *Proc. of the Thirty-Fourth Southeastern Symposium Syst. Theory*, Huntsville, Alabama, 18-19 March 2002, p. 321–323.

[213]   V. Donde, M. A. Pai and I. A. Hiskens, "Automatic generation control: traditional versus restructured scenario," In *Proc. 11th National Conf. on Power Systems*, Bangalore, India, 2000.

[214] N. Bengiamin and L. Wang, "Assessment of automatic generation control (AGC) in a deregulated environment," In *Proc. IEEE Power Engineering Society Winter Meeting*, Califorrnia, USA, 2000, vol. 2, p. 1331–1336.

[215] K. Genki and K. Masakazu, "Study on social welfare evaluation by LFC methods under deregulation," In *Proc. Int. Conf. on Elect. Eng.*, Okinawa, Japan, 2000, p. 1–6.

[216] O. P. Malik, "Control considerations in a deregulated electric utility environment," *IEEE Canadian Review-Fall/Automne,* Magazine, Canada, 2000, p. 9–11.

[217] J. Zhong and K. Bhattacharya, "Frequency linked pricing as an instrument for frequency regulation in deregulated electricity markets," In *Proc. IEEE Power Engineering Society Annual General Meeting*, Toronto, 13-17 July 2003, vol. 2, p. 566–571.

[218] K. V. V. Reddy, A. Kumar, and S. Chanana, "Frequency linked pricing as an instrument for frequency regulation market and ABT mechanism," In *Proc. IEEE Int. Conf. on Power Electronics, Drives Energy Syst.*, New Delhi, India, 12-15 December 2006, p. 1–7.

[219] J.-J. Wang, W.-D. Li, W.-L. Zhao, and Y.-L. Zhao, "A novel strategy for allocation cost of automatic generation control in electricity market environment," In *Proc. IEEE 2nd Int. Conf. Signal Processing Syst.*, Dalian, China, 5-7 July 2010, vol. 3, p. V3-237–V3-240.

[220] S. Chanana and A. Kumar, "A price based automatic generation control using unscheduled interchange price signals in Indian electricity systems," *Int. J. Eng. Sc. Tech.*, vol. 2, no. 2, pp. 23–30, Feb. 2010.

[221] S. K. Parida, S. N. Singh, and S. C. Srivastava, "An integrated approach for optimal frequency regulation service procurement in India," *Energy Policy*, vol. 37, no. 8, pp. 3020–3034, Aug. 2009.

[222] J. Katende and F. N. Okafor, "Automatic generation control performance of the Nigerian power system after deregulation," In *Proc. IEEE 2nd Africon Conf.*, Africa, 15-17 September 2004, vol. 2, p. 717–722.

[223] B. H. Baken and K. Uhlen, "Market based AGC with online bidding of regulating reserves," In *Proc. IEEE Power Engineering Society Summer Meeting*, Vancouver, Canada, 15-19 July 2001, vol. 2, p. 848–853.

[224] I. Egido, F. Fernandez-Bernal, L. Rouco, E. Porras, J. L. Ruiz-Mendoza, and A. Saiz-Chicharro, "An overview of an AGC for a de-regulated power system," In *Proc. IEEE 5th Int. Conf. on Power Syst. Manage. Contr.*, London, England, 17-19 April 2002, p. 250–255.

[225] B. H. Bakken and O. S. Grande, "Automatic generation control in a deregulated power system," *IEEE Trans. Power Syst.*, vol. 13, no. 4, pp. 1401–1406, Nov. 1998.

[226]   E. D. Tuglie and F. Torelli, "Load following control schemes for deregulated energy markets," *IEEE Trans. Power Systems*, vol. 21, no. 4, pp. 1691–1698, Nov. 2006.

[227]   E. Nobile, A. Bose, and K. Tomsovic, "Feasibility of a bilateral market for load following," *IEEE Trans. Power Syst.*, vol. 16, no. 4, pp. 782–787, Nov. 2001.

[228]   R. J. Abraham, D. Das, and A. Patra, "Load following in a bilateral market with local controllers," *Int. J. Elect. Power Energy Syst.*, vol. 33, no. 10, pp. 1648–1657, Dec. 2011.

[229]   D. Rerkpreedapong and A. Feliachi, "Decentralized load frequency control for load following services," In *IEEE Power Eng. Society Winter Meeting.*, New York, USA, January 27-31, 2002, vol. 2, no. 1, p. 1252–1257.

[230]   S. Balamurugan and R. R. Lekshmi, "Control strategy development for multi source multi area restructured system based on GENCO and TRANSCO reserve," *Int. J. Elect. Power Energy Syst.*, vol. 75, pp. 320–327, Feb. 2016.

[231]   A. P. S. Meliopoulos, G. J. Cokkinides, and A. G. Bakirtzis, "Load-frequency control service in a deregulated environment," *Decision Support Syst.*, vol. 24, nos. 3-4, pp. 243–250, Jan. 1999.

[232]   Z. Wang, X. Zhao, F. Wen, D. Gan, M. Huang, and W. Sun, "Forecasting and procurement of AGC capacity requirement in electricity market environment," In *Proc. IEEE Int. Conf. on Electric Utility Deregulation, Restructuring Power Tech.*, 5-8 April 2004, p. 723–728.

[233]   B. Delfino, F. Fornari, and S. Massucco, "Load-frequency control and inadvertent interchange evaluation in restructured power systems," *IEE Proc. Gener. Transm. Distrib.*, vol. 149, no. 5, pp. 607–614, Sep. 2002.

[234]   A. P. Fathima and M. A. Khan, "Performance analysis of the frequency related market structure in the deregulated power system," *Int. J. Power Syst. Power Electron.*, vol. 1, no. 1, pp. 53–61, Jul. 2008.

[235]   Y.-H. Moon, H.-S. Ryu, and J.-K. Park, "A new paradigm of automatic generation control under the deregulated environments," In *Proc. IEEE Power Engineering Society Winter Meeting*, Singapore, 23-27 January 2000, vol. 1, p. 21–25.

[236]   S. M. Pujara and C. D. Kotwal, "An inclusive review on load frequency control in deregulated market," *Int. J. Elect. Eng. Informat.*, vol. 8, no. 3, pp. 594–610, Sep. 2016.

[237]   S. Sinha, R. Patel, and R. Prasad, "Application of AI supported optimal controller for automatic generation control of a restructured power system with parallel AC-DC tie lines," *Eur. Trans. Elect. Power*, vol. 22, no. 5, pp. 645–661, Jul. 2012.

[238]   N. Hasan, "Optimal AGC regulator design for deregulated power system using pole-placement technique," *Int. J. Eng. Manage. Res.*, vol. 2, no. 4, pp. 19–25, Aug. 2012.

[239] N. Hasan, "Optimal AGC of deregulated interconnected power system with parallel AC/DC link," *Int. J. Mod. Eng. Res.*, vol. 2, no. 4, pp. 2789–2794, July–Aug 2012.

[240] U. Gupta and S. N. Chaphekar, "Design of full order optimal controller for interconnected deregulated power system for AGC," *Int. J. Comput. Eng. Res.*, vol. 8, no. 3, pp. 594–610, Sep. 2016.

[241] Ibraheem, P. Kumar, N. Hasan, and Y. Singh, "Optimal automatic generation control of interconnected power system with asynchronous tie-lines under deregulated environment," *Elect. Power Compon. Syst.*, vol. 40, no. 10, pp. 1208–1228, Jul. 2012.

[242] P. Kumar, S. A. Kazmi, and N. Yasmeen, "Comparative study of automatic generation control in traditional and deregulated power environment," *World J. Model. Simulat.*, vol. 6, no. 3, pp. 189–197, Aug. 2010.

[243] B. Tyagi and S. C. Srivastava, "A LQG based load frequency controller in a competitive electricity environment," *Int. J. Emerging Elect. Power Syst.*, vol. 2, no. 2, art. 4, Mar. 2005.

[244] B. Tyagi and S. C. Srivastava, "A decentralized automatic generation control scheme for competitive electricity markets," *IEEE Trans. Power Syst.*, vol. 21, no. 1, pp. 312–320, Feb. 2006.

[245] K. P. S. Parmar, S. Majhi, and D. P. Kothari, "LFC of an interconnected power system with multi-source power generation in deregulated power environment," *Int. J. Elect. Power Energy Syst.*, vol. 57, pp. 277–286, May 2014.

[246] E. Rakhshani and J. Sadeh, "Practical viewpoints on load frequency control problem in a deregulated power system, " *Energy Convers. Manage.*, vol. 51, no. 6, pp. 1148–1156, Jun. 2010.

[247] E. Rakhshani and J. Sadeh, "Reduced-order observer control for two-area LFC system after deregulation," *Contr. Intell. Syst.*, vol. 38, no. 4, pp. 185–193, 2010.

[248] E. Rakhshani and J. Sadeh, "Reduced-order observer control for two-area LFC system after deregulation," *Contr. Intell. Syst.*, vol. 38, no. 4, pp. 185–193, 2010.

[249] E. Rakhshani, "Intelligent linear-quadratic optimal output feedback regulator for a deregulated automatic generation control system," *Elect. Power Compon. Syst.*, vol. 40, no. 5, pp. 513–533, Mar. 2012.

[250] E. Rakhshani, A. Luna, J. Sadeh, and P. Rodriguez, "PSO based optimal output feedback controller for two-area LFC system," In *Proc. of IEEE 20th Mediterranean Conf. Contr. Automat.*, 3-6 July 2012, p. 1284–1289.

[251] E. Rakhshani and J. Sadeh, "Multi-area load frequency control in a deregulated power system using optimal output feedback method," In *Proc. of 5th Int. Conf. Eur. Electricity Market*, Lisboa, 28-30 May 2008, p. 1–6.

[252]   F. Liu, S. Mei, Y. Song, and Q. Lu, "Optimal load frequency control in deregulated power systems," In *Proc. IEEE Int. Conf. Power Systems Tech.*, Kunming, China, 13-17 October 2002, vol. 2, p. 944–948.

[253]   H. Bevrani, Y. Mitani, and K. Tsuji, "Robust LFC in a deregulated environment: multi-objective control approach," *IEEJ Trans. Power Energy*, vol. 124, no. 12, pp. 1409–1416, 2004.

[254]   A. Feliachi, "On load-frequency control in a deregulated environment," In *Proc. of IEEE Int. Conf. on Cont. Appl.*, Michigan, USA, 15-18 September 1996, p. 437–441.

[255]   H. Bevrani, Y. Mitani, and K. Tsuji, "Robust AGC: traditional structure versus restructured scheme," *IEEJ Trans. Power Energy*, vol. 124, no. 5, pp. 751–761, Aug. 2004.

[256]   H. Bevrani, Y. Mitani, and K. Tsuji, "PI-based multi-objective load-frequency control in a restructured power system," In *Proc. Int. Conf. SICE 2004*, 4-6 August 2004, vol. 2, p. 1745–1750.

[257]   T. A. Kumar, G. Venu, and N. V. Ramana, "Load frequency control of multi area power system in deregulated environment with robust controllers in coordination with frequency controllable HVDC link," In *Proc. IEEE Int. Conf. Energy Efficient Technol. Sustainab.*, 7-8 April 2016, p. 473–478.

[258]   H. Bevrani, Y. Mitani, and K. Tsuji, "Robust AGC in a competitive environment," In *Proc. IEEE 39th Int. Universities Power Eng. Conf.*, Bristol, UK, 6-8 September 2004, vol. 1, p. 722–726.

[259]   H. Bevrani, Y. Mitani, and K. Tsuji, "Robust decentralized AGC in a restructured power system," *Energy Convers. Manage.*, vol. 45, nos. 15–16, pp. 2297–2312, Sep. 2004.

[260]   H. Shayeghi and H. A. Shayanfar, "Design of decentralized robust LFC in a competitive electricity environment," *J. Elect. Eng.*, vol. 56, nos. 9–10, pp. 225–236, 2005.

[261]   H. Bevrani, Y. Mitani, K. Tsuji, and H. Bevrani, "Bilateral based robust load frequency control," *Energy Convers. Manage.*, vol. 46, nos. 7–8, pp. 1129–1146, May 2005.

[262]   H. S. Moghanlou and H. A. Shayanfar, "Robust decentralized LFC design in restructured power system," *Int. J. Emerging Elect. Power Syst.*, vol. 6, no. 2, art. 4, Aug. 2006.

[263]   H. Bevrani and T. Hiyama, "Robust decentralised PI based LFC design for time delay power systems," *Energy Convers. Manage.*, vol. 49, no. 2, pp. 193–204, Feb. 2008.

[264]   S. A. Taher and R. Hematti, "Robust decentralized load frequency control using multi variable QFT method in deregulated power systems," *American J. Applied Sc.*, vol. 5, no. 7, pp. 818–828, Jul. 2008.

[265] H. Shayeghi, A. Jalili, H. A. Shayanfar, "A robust mixed H_2/H_∞ based LFC of a deregulated power system including SMES," *Energy Convers. Manage.*, vol. 49, no. 10, pp. 2656–2668, Oct. 2008.

[266] A. Huddar and P. S. Kulkarni, "A robust method of tuning a decentralized proportional-integral load frequency controller in a deregulated environment using genetic algorithms," *Elect. Power Compon. Syst.*, vol. 37, no. 3, pp. 265–286, Feb. 2009.

[267] J. Rezvantalab, M. H. Kazemi, and A. K. Seddigh, "Multi-area robust decentralized load frequency controller design in a restructured power system using quantitative feedback theory," In *Proc. IEEE Int. Conf. Elect. Power Energy Convers. Syst.*, Tehran, Iran, 10-12 November 2009, p. 1–6.

[268] S. K. Pandey, N. Kishor, and S. R. Mohanty, "A novel decentralized robust MIMO-PID load frequency controller via iterative LMI approach in deregulated environment," In *Proc. IEEE Students Conf. Eng. Syst.*, Allahabad, India,12-14 April 2013, p. 1–6.

[269] C. S. Rao, S. S. Nagaraju, and P. S. Raju, "Improvement of dynamic performance of AGC under open market scenario employing TCPS and AC-DC parallel tie line," *Int. J. Recent Trends Eng.*, vol. 1, no. 3, pp. 1–6, May 2009.

[270] C. S. Rao, Z. Naghizadeh, and S. Mahdavi, "Improvement of dynamic performance of hydrothermal system under open market scenario using asynchronous tie-lines," *World J. Model. Simulat.*, vol. 4, no. 2, pp. 153–160, 2008.

[271] R. K. Selvaraju and G. Somaskandan, "Design of artificial cooperative search algorithm based load frequency controller for interconnected deregulated power systems with AC-DC parallel tie-lines," *Australian J. Basic Applied Sc.*, vol. 8, no. 13, pp. 326–338, Aug. 2014.

[272] R. K. Selvaraju and G. Somaskandan, "Artificial cooperative search algorithm based load frequency controller for multi-area deregulated power system with coordinated control of TCPS, RFB and AC-DC parallel tie-lines," *ARPN J. Eng. Applied Sc.*, vol. 10, no. 14, pp. 6080–6091, Aug. 2015.

[273] H. Shayeghi, H. A. Shayanfar, and A. Jalili, "Multi-stage fuzzy PID power system automatic generation controller in deregulated environments," *Energy Convers. Manage.*, vol. 47, nos. 18–19, pp. 2829–2845, Nov. 2006.

[274] H. Shayeghi, A. Jalili, and H. A. Shayanfar, "Robust modified GA based multi-stage fuzzy LFC," *Energy Convers. Manage.*, vol. 48, no. 5, pp. 1656–1670, May 2007.

[275] A. P. Fathima and M. A. Khan, "Design of a new market structure and robust controller for the frequency regulation service in the deregulated power system," *Elect. Power Compon. Syst.*, vol. 36, no. 8, pp. 864–883, Jun. 2008.

[276] H. Shayeghi, A. Jalili, and H. A. Shayanfar, "Multi-stage fuzzy load frequency control using PSO," *Energy Convers. Manage.,* vol. 49, no. 10, pp. 2570–2580, Oct. 2008.

[277] H. Guo-Lian, L. Rui, Z. Jianhua, Z. Qiaoqia, and F. Chanming, "T-S model based fuzzy logic controller for AGC system after deregulation considering DPM," In *Proc. IEEE Chinese Contr. Decision Conf.*, 17-19 June 2009, p. 2231–2236.

[278] C. S. Rao, S. S. Nagaraju, and P. S. Raju, "Automatic generation control of TCPS based hydrothermal system under open market scenario: a fuzzy logic approach," *Int. J. Elect. Power Energy Syst.*, vol. 31, nos. 7–8, pp. 315–322, Sep. 2009.

[279] N. Taghizadegan, N. M. Tabatabaei, A. Demiroren, and N. S. Boushehri, "LFC dynamic response improvement using fuzzy logic based control of TCPS in deregulated power system," *Int. J. Tech. Physical Problems Eng.*, vol. 3, no. 4, issue 9, pp. 86–90, Dec. 2011.

[280] G. R. Pratap, R. Umrao, and D. K. Chaturvedi, "Automatic generation control with polar fuzzy controller considering generation rate constraint in deregulated power system," in *Proc. of Int. Conf. Comput., Commun., Appll.*, Nagapattinam, Tamil Nadu, 30–31 February 2012, p. 610–615.

[281] J. Javidan and A. Ghasemi, "A novel fuzzy RPID controller for multiarea AGC with IABC optimization," *J. Eng.*, vol. 2013, art. id 510572, pp. 13, 2013.

[282] Y. P. Verma and A. Kumar, "Load frequency control in deregulated power system with wind integrated system using fuzzy controller," *Frontiers in Energy*, vol. 7, no. 2, pp. 245–254, Jun. 2013.

[283] H. Hosseini, B. Tousi, N. Razmjooy, and M. Khalilpour, "Design robust controller for automatic generation control in restructured power system by imperialist competitive algorithm," *IETE J. Res.*, vol. 59, no. 6, pp 745–752, Nov.-Dec. 2013.

[284] C. Ismayil, K. R. Sreerama, and T. K. Sindhu, "Fuzzy logic and genetic algorithm based automatic generation control of two-area deregulated power systems," *Int. Review Elect. Eng.*, vol. 9, no. 1, pp. 186–199, 2014.

[285] S. H. Rouhani, A. Sheikholeslami, R. Ahmadi, and H. Hosseini, "Using optimal fuzzy logic controller to improve transient fluctuations in deregulated power system with random variable load," *J. Intell. Fuzzy Syst.: Appl. Eng. Tech.*, vol. 27, no. 6, pp 3145–3157, Jun. 2014.

[286] Y. K. Bhateshvar, H. D. Mathur, and H. Siguerdidjane, "Impact of wind power generating system integration on frequency stabilization in multi-area power system with fuzzy logic controller in deregulated environment," *Frontiers Energy*, vol. 9, no. 1, pp. 7–21, Mar. 2015.

[287] Y. K. Bhateshvar, H. D. Mathur, H. Siguerdidjane, and S. Bhanot, "Frequency stabilization for multi-area thermal-hydro power system using genetic algorithm-optimized fuzzy logic controller in deregulated environment," *Elect. Power Compon. Syst.*, vol. 43, no. 2, pp. 146–156, 2015.

[288] V. S. Vakula and K. R. Sudha, "Differential evolutionary algorithm based structure preserving controller in three area deregulated environment," *J. Intell. Fuzzy Syst.: Appl. Eng. Tech.*, vol. 28, no. 1, pp. 85–105, 2015.

[289] I. Chathoth, S. K. Ramdas, and S. T. Krishnan, "Fractional-order proportional-integral-derivative-based automatic generation control in deregulated power systems," *Elect. Power Compon. Syst.*, vol. 43, no. 17, pp. 1931–1945, 2015.

[290] R. K. Sahu, G. T. C. Sekhar and S. Panda, "DE optimized fuzzy PID controller with derivative filter for LFC of multi source power system in deregulated environment," *Ain Shams Eng. J.*, vol. 6, no. 2, pp. 511–530, Jun. 2015.

[291] T. S. Gorripotu, R. K. Sahu, and S. Panda, "AGC of a multi-area power system under deregulated environment using redox flow batteries and interline power flow controller," *Eng. Sc. Tech., an Int. J.*, vol. 18, no. 4, pp. 555–578, Dec. 2015.

[292] S. Srikanth, K. R. Sudha, and Y. B. Raju, "Fuzzy C-means load frequency controller in deregulated power environment," *Int. J. Fuzzy Computat. Modelling*, vol. 2, no.1, pp. 27–49, Jan. 2016.

[293] G. T. C. Sekhar, R. K. Sahu, A. K. Baliarsingh, and S. Panda, "Load frequency control of power system under deregulated environment using optimal firefly algorithm," *Int. J. Elect. Power Energy Syst.*, vol. 74, pp. 195–211, Jan. 2016.

[294] Y. K. Bhateshvar and H. D. Mathur, "Power frequency oscillation suppression using two-stage optimized fuzzy logic controller for multigeneration system," *Advances Fuzzy Syst.*, vol. 2016, art. id 8308109, pp. 13, 2016.

[295] P. Anitha and P. Subburaj, "Hybrid fuzzy controller based frequency regulation in restructured power system," *Circuits Syst.*, vol. 7, no. 6, pp. 759–770, May 2016.

[296] K. Sabahi, S. Ghaemi, and S. Pezeshki, "Gain scheduling technique using MIMO type-2 fuzzy logic system for LFC in restructure power system," *Int. J. Fuzzy Syst.*, vol. 28, no. 1, pp. 475–488, Dec. 2017.

[297] H. Bevrani, T. Hiyama, Y. Mitani, K. Tsuji, and M. Teshnehlab, "Load-frequency regulation under a bilateral LFC scheme using flexible neural networks," *Int. J. Eng. Intell. Syst. Elect. Eng. Communicat.*, vol. 14, no. 2, pp. 109–117, Jun. 2006.

[298] H. Shayeghi, H. A. Shayanfar, and O. P. Malik, "Robust decentralized neural networks based LFC in a deregulated power system," *Elect. Power Syst. Res.*, vol. 77, nos. 3–4, pp. 241–251, Mar. 2007.

[299] B. P. Padhy and B. Tyagi, "Artificial neural network based multi area automatic generation control scheme for a competitive electricity market environment," In *Proc. IEEE Int. Conf. Power Systems*, Kharagpur, India, 27-27 December 2009, p. 1–6.

[300] K. Sabahi, E. Narimani, and A. Faramarzi, "Dynamic neural network for AGC in restructure power system," In *Proc. IEEE Int. Conf. Power Energy*, Kuala Lumpur, Malaysia, 29 Novovember-1 December 2010, p. 594–599.

[301] S. Bhangade, H. O. Gupta and B. Tyagi, "Artificial neural network based automatic generation control scheme for deregulated electricity market," In *Conf. Proc. IPEC*, 27-29 October 2010, p. 1158–1163.

[302] C. S. Rao, "Load frequency control of hydrothermal system under restructured environment: a hybrid genetic-neural network approach," *Int. J. Distribut. Energy Resources*, vol. 8, no. 1, pp. 47–59, Jan.–Mar. 2012.

[303] B. Ogbonna and S. N. Ndubisi, "Neural network based load frequency control for restructuring power industry," *Nigerian J. Tech.*, vol. 31, no. 1, pp. 40–47, Mar. 2012.

[304] H. A. Shyanfar and H. Shayeghi, "Design of decentralized neuron based LFC in a deregulated power system," In *Proc. 6th WSEAS Int. Conf. Automat. Informat.*, Buenos Aires, Argentina, 1-3 March 2005, p. 127–132.

[305] C. S. Rao, "Adaptive neuro-fuzzy based inference system for load frequency control of hydrothermal system under deregulated environment," *Int. J. Eng. Sc. Tech.*, vol. 2, no. 12, pp. 6954–6962, Dec. 2010.

[306] C. S. Rao, "Adaptive neuro fuzzy based load frequency control of multi area system under open market scenario," In *Proc. of IEEE Int. Conf. Advances Eng., Sc. Manage.*, Nagapattinam, India, 30-31 March 2012, p. 5–10.

[307] S. B. Shree and N. Kamaraj, "Hybrid neuro fuzzy approach for automatic generation control in restructured power system," *Int. J. Elect. Power Energy Syst.*, vol. 74, pp. 274–285, Jan. 2016.

[308] S. B. Shree and N. Kamaraj, "Hybrid neuro fuzzy controller for automatic generation control of multi area deregulated power system," *Circuits Syst.*, vol. 7, no. 4, pp. 292–306, Apr. 2016.

[309] B. S. Solaiappan and K. Nagappan, "AGC for multisource deregulated power system using ANFIS controller," *Int. Trans. Elect. Energy Syst.*, vol. 27, no. 3, e2270, Mar. 2017.

[310] A. Pappachen and A. P. Fathima, "Load frequency control in deregulated power system integrated with SMES–TCPS combination using ANFIS controller," *Int. J. Elect. Power Energy Syst.*, vol. 82, pp. 519–534, Nov. 2016.

[311] Y. L. Karnavas, "AGC tuning of an interconnected system after deregulation using genetic algorithms," In *Proc. 5th WSEAS Int. Conf. on Power Systems and Electromagnetic Compatibility*, Corfu, Greece, 23-25 August 2005, p. 218–223.

[312] Y. L. Karnavas, "On the optimal control of interconnected power systems in a re-structured environment using genetic algorithms," *WSEAS Trans. Syst.*, vol. 4, no. 8, pp. 1248–1258, Aug. 2005.

[313] A. Demiroren and H. L. Zeynelgil, "GA application to optimization of AGC in three-area power system after deregulation," *Int. J. Elect. Power Energy Syst.*, vol. 29, no. 3, pp. 230–240, Mar. 2007.

[314] C. S. Rao, S. S. Nagaraju, and P. S. Raju, "A modified genetic approach to hydrothermal system with thyristor controlled phase shifter under open market system," *Int. Review Elect. Eng.*, vol. 2, no. 4, pp. 507–514, Aug. 2007.

[315] N. Sinha, L. L. Lai, and V. G. Rao, "GA optimized PID controllers for automatic generation control of two area reheat thermal systems under deregulated environment," In *Proc. IEEE 3rd Int. Conf. Elect. Utility Deregulation, Restructuring Power Tech.*, Nanjing, China, 6-9 April 2008, p. 1186–1191.

[316] R. Pradhan and S. Panda, "Application of genetic algorithm based PSS for two-area AGC system in deregulated scenario," In *Proc. IEEE World Cong. Nature, Biologically Inspired Comput.*, Coimbatore, India, 9–11 December 2009, p. 1207–1212.

[317] Y. L. Karnavas and K. S. Dedousis, "Overall performance evaluation of evolutionary designed conventional AGC controllers for interconnected electric power system studies in a deregulated market environment," *Int. J. Eng. Sc. Tech.*, vol. 2, no. 3, pp. 150–166, 2010.

[318] S. Farook and P. S. Raju, "Optimization of feedback controller in restructured power system using evolutionary genetic algorithms," *Int. J. Eng. Sc. Tech.*, vol. 3, no. 5, pp. 4074–4083, May 2011.

[319] S. Farook and P. S. Raju, "Robust tuning of PID controller to optimize bilateral contracts in deregulated power system using evolutionary algorithms," *Int. J. Eng. Res. App.*, vol. 1, no. 2, pp. 165–172, Jul.–Aug. 2011.

[320] S. Farook and P. S. Raju, "AGC controllers to optimize LFC regulation in deregulated power system," *Int. J. Advances Eng. Tech.*, vol. 1, no. 5, pp. 278–289, Nov. 2011.

[321] S. B. Shree and S. Somaselvakumar, "Genetic algorithm based decentralized load frequency control in deregulated environment," *Int. J. Advanced Trends Comput. Sc. Eng.*, vol. 2, no. 2, pp. 128–133, 2013.

[322] M. Deepak and R. J. Abraham, "Load following in a deregulated power system with thyristor controlled series compensator," *Int. J. Elect. Power Energy Syst.*, vol. 65, pp. 136–145, Feb. 2015.

[323] P. K. Hota and B. Mohanty, "Automatic generation control of multi source power generation under deregulated environment," *Int. J. Elect. Power Energy Syst.*, vol. 75, pp. 205–214, Feb. 2016.

[324] N. Kumar, V. Kumar, and B. Tyagi, "Multi area AGC scheme using imperialist competition algorithm in restructured power system," *Applied Soft Comput.*, vol. 48, pp. 160–168, Nov. 2016.

[325] S. A. Taher, R. Hematti, A. Abdolalipour, and S. H. Tabei, "Optimal decentralized load frequency control using HPSO algorithms in deregulated power systems," *American J. Applied Sc.*, vol. 5, no. 9, pp. 1167–1174, 2008.

[326] C. S. Rao, S. S. Nagaraju, and P. S. Raju, "AGC tuning of TCPS based hydrothermal system under open market scenario with particle swarm optimization," *J. Elect. Syst.*, vol. 4, no. 2, pp. 1–13, 2008.

[327] P. Bhatt, R. Roy, and S. P. Ghoshal, "Optimized multi area AGC simulation in restructured power systems," *Int. J. Elect. Power Energy Syst.*, vol. 32, no. 4, pp. 311–322, May 2010.

[328] P. Bhatt, R. Roy, and S. P. Ghoshal, "Coordinated control of SSSC and SMES in competitive electricity market for load frequency control," In *Proc. 11th IEEE Int. Conf. Probabilistic Methods Applied Power Syst.*, Singapore, 14–17 June 2010, p. 42–47.

[329] P. Bhatt, S. P. Ghoshal, and R. Roy, "Automatic generation control of two-area interconnected hydro-hydro restructured power system with TCPS and SMES," *ACEEE Int. J. Elect. Power Eng.*, vol. 1, no. 2, pp. 1–5, Jul. 2010.

[330] K. Subbaramaiah, V. C. J. Mohan, and V. C. V. Reddy, "Improvement of dynamic performance of SSSC and TCPS based hydrothermal system under deregulated scenario employing PSO based dual mode controller," *Eur. J. Scientific Res.*, vol. 57, no.2, pp. 230–243, Aug. 2011.

[331] C. Jain and H. K. Verma, "Hybrid chaotic particle swarm optimization based gains for deregulated automatic generation control," *Int. J. Electron. Communicat. Comput. Eng.*," vol. 2, no. 2, pp. 1–9, 2011.

[332] C. Jain, H. K. Verma, and L. D. Arya, "A novel statistically tracked particle swarm optimization method for automatic generation control," *J. Mod. Power Syst. Clean Energy*, vol. 2, no. 4, pp. 396–410, Dec. 2014.

[333] D. Lakshmi, A. P. Fathima, and R. Muthu, "Simulation of the two-area deregulated power system using particle swarm optimization," *Int. J. Elect. Eng. Informat.*, vol. 8, no. 1, pp. 93–107, Mar. 2016.

[334] C. S. Rao, S. S. Nagaraju, and P. S. Raju, "Ant colony system algorithm for automatic generation control of hydrothermal system under open market scenario," In *Proc. IET-UK Int. Conf. Information Communication Techn. Elect. Sc.*, Dr. M.G.R. University, Chennai, Tamil Nadu, 20-22 December 2007, p. 112–119.

[335] H. Shayeghi and A. Ghasemi "Market based LFC design using artificial bee colony," *Int. J. Tech. Physical Prob. Eng.*, vol. 3, no. 1, issue 6, pp. 1–10, Mar. 2011.

[336] S. A. Taher, S. M. Nosratabadi, and M. R. Sheibani, "Optimal load frequency control method using artificial bee colony algorithm in deregulated power systems including SMES," *Intell. Syst. Elect. Eng.*, vol. 1, no. 1, pp. 23–42, Winter 2011.

[337] O. Abedinia, H. A. Shayanfar, B. Wyns, and A. Ghasemi, "Design of robust PSS to improve stability of composed LFC and AVR using ABC in deregulated

environment," In *World Congress in Comput. Sc., Comput. Eng., and Applied Comput.*, Las Vegas, Nevada, USA, 18-21 July 2011.

[338]   S. Farook, "Coordinated tuning of fractional order PID and TCPAR in a composite deregulated power system using evolutionary differential algorithm," *J. Elect. Eng.*, vol. 15, no. 3, pp. 98–105, 2015.

[339]   K. S. Shaik, Y. M. shuaib, and J. beevi, "Automatic generation control integrated with renewable energy using particle swarm optimization and differential evolutionary algorithm," *Int. Res. J. Eng. Tech.*, vol. 3, no. 5, pp. 1677–1684, May 2016.

[340]   L. C. Saikia and S. Debbarma, "Application of a non-integer order controller in AGC of a two area thermal system under deregulated environment: A preliminary study," In *IET Int. Conf. Sustainable Energy Intel. Syst.*, Chennai, India, 20-22 July 2011, p. 390–395.

[341]   S. Debbarma, L. C. Saikia, N. Sinha, "AGC of a multi-area thermal system under deregulated environment using a non-integer controller," *Elect. Power Syst. Res.*, vol. 95, pp. 175–183, Feb. 2013.

[342]   R. Thirunavukarasu, B. Paramasivam, and I. A. Chidambaram, "Power system restoration assessment indices computation for a restructured power system with bacterial foraging optimized load-frequency controller," *Int. J. Comput. Appl.*, vol. 78, no. 16, pp. 41–54, Sep. 2013.

[343]   I. A. Chidambaram and B. Paramasivam, "Optimized load-frequency simulation in restructured power system with redox flow batteries and interline power flow controller," *Int. J. Elect. Power Energy Syst.*, vol. 50, pp. 9–24, Sep. 2013.

[344]   R. Thirunavukarasu and I. A. Chidambaram, "PI^2 controller based coordinated control with redox flow battery and unified power flow controller for improved restoration indices in a deregulated power system," *Ain Shams Eng. J.*, vol. 7, no. 4. pp. 1011–1027, Dec. 2016.

[345]   M. Ponnusamy, B. Banakara, S. S. Dash, and M. Veerasamy, "Design of integral controller for load frequency control of static synchronous series compensator and capacitive energy source based multi area system consisting of diverse sources of generation employing imperialistic competition algorithm," *Int. J. Elect. Power Energy Syst.,* vol. 73, pp. 863–871, Dec. 2015.

[346]   O. Abedinia, M. S. Naderi, and A. Ghasemi, "Robust LFC in deregulated environment: fuzzy PID using HBMO," In *Proc. IEEE 10th Int. Conf. Environment, Elect. Eng.*, Rome, 8-11 May 2011, p. 1–4.

[347]   H. Shayeghi, H. A. Shayanfar, and A. Ghasemi, "Honey bee mating optimization based LFC design in a deregulated power system," In *Proc. World Congress in Comp. Sc., Comp. Eng. Applied Computing*, Las Vegas, Nevada, USA, 18-21 July 2011.

[348] O. Abedinia, N. Amjady, and M. S. Naderi, "Multi-stage fuzzy PID load frequency control via SPHBMO in deregulated environment," In *Proc. of IEEE 11th Int. Conf. Environment Elect. Eng.*, Venice, 18-25 May 2012, p. 473–478.

[349] H. Ebrahimian, V. Babazadeh, and S. Javanshir, "Combination of PSS and LFC for improving the power system stability in deregulated environment using HBMO," *J. Current Res. Sc.*, vol. 3, no. 5, pp. 128–1333, 2015.

[350] O. Abedinia, N. Amjady, K. Kiani, and H. A. Shayanfar, "Fuzzy PID based on firefly algorithm: load frequency control in deregulated environment," In *Proc. Int. Conf. Artificial Intelligence*: *The World Congress in Computer Sc., Computer Eng. Applied Computing*, Nevada, USA,16-19 July 2012.

[351] T. S. Gorripotu, R. K. Sahuu, and S. Panda, "Application of firefly algorithm for AGC under deregulated power system," *Chapter in Computational Intelligence in Data Mining, vol. 1, vol. 31 of the series Smart Innovation Syst. Tech.*, pp. 677–687, Dec. 2014.

[352] D. Lakshmi, A. P. Fathima, and R. Muthu, "A novel flower pollination algorithm to solve load frequency control for a hydro-thermal deregulated power system," *Circuits Syst.*, vol. 7, no. 4, pp. 166–178, Apr. 2016.

[353] S. Debbarma and A. Dutta, "Utilizing electric vehicles for LFC in restructured power systems using fractional order controller," *IEEE Trans. Smart Grid*, vol. 8, no. 6, pp. 2554–2564, Nov. 2017.

[354] P. K. Sanapala and V. S.Vakula, "Harmony search algorithm in optimal design of load frequency controller in deregulated environment," *Int. J. Emerging Tech. Comput. Applied Sc.*, vol.4, no. 5, pp. 476–486, Mar.-May 2013.

[355] O. Abedinia, N. Amjady, A. Ghasemi, and H. Shayeghi, "Multi-stage fuzzy load frequency control based on multi-objective harmony search algorithm in deregulated environment," *J. Operat. Automat. Power Eng.*, vol. 1, no. 1, pp. 63–73, Mar. 2013.

[356] R. Shankar, K. Chatterjee, and R. Bhushan, "Impact of energy storage system on load frequency control for diverse sources of interconnected power system in deregulated power environment," *Int. J. Elect. Power Energy Syst.*, vol. 79, pp. 11–26, Jul. 2016.

[357] C. K. Shiva and V. Mukherjee, "Automatic generation control of multi-unit multi-area deregulated power system using a novel quasi-oppositional harmony search algorithm," *IET Gener. Transm. Distrib.*, vol. 9, no. 15, pp. 2398–2408, Nov. 2015.

[358] C. K. Shiva and V. Mukherjee, "A novel quasi-oppositional harmony search algorithm for AGC optimization of three-area multi-unit power system after deregulation," *Eng. Sc. Tech., an Int. J.*, vol. 19, no. 1, pp. 395–420, Mar. 2016.

[359] C. K. Shiva and V. Mukherjee, "Design and analysis of multi-source multi-area deregulated power system for automatic generation control using quasi-

oppositional harmony search algorithm," *Int. J. Elect. Power Energy Syst.*, vol. 80, pp. 382–395, Sep. 2016.

[360]   B. Mohanty and P. K. Hota, "Comparative performance analysis of fruit fly optimisation algorithm for multi-area multi-source automatic generation control under deregulated environment," *IET Gener. Transm. Distrib.*, vol. 9, no. 14, pp. 1845–1855, Oct. 2015.

[361]   A. Rahman, L. C. Saikia, and N. Sinha, "Load frequency control of a hydro-thermal system under deregulated environment using biogeography-based optimised three-degree-of-freedom integral-derivative controller," *IET Gener. Transm. Distrib.*, vol. 9, no. 15, pp. 2284–2293, Nov. 2015.

[362]   R. K. Selvaraju and G. Somaskandan, "Impact of energy storage units on load frequency control of deregulated power systems," *Energy*, vol. 97, pp. 214–228, Feb. 2016.

[363]   N. Kumar, V. Kumar, and B. Tyagi, "Optimization of PID parameters using BBBC for multiarea AGC scheme in deregulated power system," *Turkish J. Elect. Eng. Comp. Sc.*, vol. 24, no. 5, pp. 4105–4116, 2016.

[364]   N. Yousefi and K. Yavariyan, "Load frequency control in deregulated environment based on fuzzy PID and SPGSA," *GMP Review*, vol. V16, pp. 295–303, 2015.

[365]   P. Dahiya, V. Sharma, and R. Naresh, "Automatic generation control using disrupted oppositional based gravitational search algorithm optimized sliding mode controller under deregulated environment," *IET Gener. Transm. Distrib.*, vol. 10, no. 16, pp. 3995–4005, Dec. 2016.

[366]   S. Farook and P. S. Raju, "Evolutionary hybrid genetic-firefly algorithm for optimizing LFC regulation in a deregulated power system," *J. Elect. Eng.*, vol. 13, no. 1, pp. 132–139, 2013.

[367]   J. Morsali, K. Zare, and M. T. Hagh, "MGSO optimised TID-based GCSC damping controller in coordination with AGC for diverse-GENCOs multi-DISCOs power system with considering GDB and GRC non-linearity effects," *IET Gener. Transm. Distrub.*, vol. 11, no. 1, pp. 193–208, Jan. 2017.

[368]   R. K. Sahu, T. S. Gorripotu, and S. Panda, "A hybrid DE–PS algorithm for load frequency control under deregulated power system with UPFC and RFB," *Ain Shams Eng. J.*, vol. 6, no. 3, pp. 893–911, Sep. 2015.

[369]   J. Nanda, M. Sreedhar, and A. Dasgupta, "A new technique in hydro thermal interconnected automatic generation control system by using minority charge carrier inspired algorithm," *Int. J. Elect. Power Energy Syst.*, vol. 68, pp. 259–268, Jun. 2015.

[370]   R. Roy and S. P. Ghoshal, "Optimized AGC simulation for restructured multi-area power systems," *J. Inst. Eng. India*, vol. 89, pt. EL, pp. 29–35, Mar. 2009.

[371] S. Dhundhara and Y. P. Verma, "Evaluation of CES and DFIG unit in AGC of realistic multisource deregulated power system," *Int. Trans. Elect. Energy Syst.*, vol. 27, no. 5, e2304, May 2017.

[372] K. Chatterjee, "Effect of battery energy storage system on load frequency control under deregulation," *Int. J. Emerging Elect. Power Syst.,* vol. 12, no. 3, art. 2, pp. 1–25, Jun. 2011.

[373] D. Menniti, A. Pinnarelli, N. Scordino, and N. Sorrentino, "Using a FACTS device controlled by a decentralised control law to damp the transient frequency deviation in a deregulated electric power system," *Elect. Power Syst. Res.*, vol. 72, no. 3, pp. 289–298, Dec. 2004.

[374] J. Raja and C. C. A. Rajan, "New robust energy storage devices for deregulated AGC problems," *Global J. Res. Eng., Elect. Electron. Eng.*, vol. 13, no. 12, ver. 1, pp. 37–54, 2013.

[375] M. Ma, C. Zhang, X. Liu, and H. Chen, "Distributed model predictive load frequency control of multi-area power system after deregulation," *IEEE Trans. Ind. Electron.*, vol. 64, no. 6, pp. 5129–5139, Jun. 2017.

[376] L. H. Fink and P. J. M. van Son, "On system control within a restructured industry," *IEEE Trans. Power Syst.*, vol. 13, no. 2, pp.611–616, May 1998.

[377] M. L. Kothari, N. Sinha, and M. Rafi, "Automatic generation control of an interconnected power system under deregulated environment," In *Proc. of IEEE Power Quality*, Hyderabad, India, 18 June 1998, p. 95–102.

[378] F. Liu, Y. H. Song, J. Ma, S. Mei, and Q. Lu, "Optimal load-frequency control in restructured power systems," *IEE Proc. Gener. Transm. Distrib.*, vol. 150, no. 1, pp. 87–95, Jan. 2003.

[379] M. Parida and J. Nanda, "Automatic generation control of a hydro-thermal system in deregulated environment," In *Proc. of 8th IEEE Int. Conf. Elect. Machines Syst.*, Nanjing, China, 27-29 September 2005, vol. 2, p. 942–947.

[380] Y. Liu, F. F. Wu, and K. L. Teo, "Optimal control of nonlinear system for generator bidding in deregulated power markets," In *Proc. IEEE Power Engineering Society, General Meeting*, 12-16 June2005, vol. 1, p. 395–399.

[381] N. Taghizadegan and M. R. Feyzi, "A novel and flexible method for modeling, trading and simulation of an AGC system in a restructured environment," *WSEAS Trans. Power Syst.*, vol. 1, no. 6, pp. 1095–1100, Jun. 2006.

[382] B. Stojkovic, "An efficient approach for the load-frequency control and its role under the conditions of deregulated environment," *Eur. Trans. Elect. Power,* vol. 16, no. 4, pp. 423–435, Jul./Aug. 2006.

[383] H. S. Moghanlou and H. A. Shayanfar, "Robust decentralized LFC design in a restructured power system," *Int. J. Emerging Elect. Power Syst.*, vol. 6, no. 2, art. 4, Aug. 2006.

[384]   J. H. Zhang, J. H. Hao, and G. L. Hou, "Automatic generation controller design in deregulated and networked environment using predictive control strategy," *IFAC Proc. Vol.*, vol. 41, no. 2, pp. 9410–9414, 2008.

[385]   S. K. Sinha, R. Prasad, and R. N. Patel, "Automatic generation control of restructured power systems with combined intelligent techniques," *Int. J. Bio-Inspired Comput,*, vol. 2, no.2, pp. 124–131, 2010.

[386]   A. K. Chakraborty and T. Bhattacharjee, "Fuzzy system approach to power purchases in a power pool of a deregulated power system," *Int. J. Artificial Intel. Soft Comput.*, vol. 3, no. 1, pp. 39–49, 2012.

[387]   W. Tan, H. Zhang, and M. Yu, "Decentralized load frequency control in deregulated environments," *Int. J. Elect. Power Energy Syst.*, vol. 41, no. 1, pp. 16–26, Oct. 2012.

[388]   F. Daneshfar and E. Hosseini, "Load-frequency control in a deregulated environment based on bisection search," *Iranian J. Elect. Electronic Eng.*, vol. 8, no. 4, pp. 303–310, Dec. 2012.

[389]   F. Daneshfar, "Intelligent load-frequency control in a deregulated environment: continuous-valued input, extended classifier system approach," *IET Gener. Transm. Distrib.*, vol. 7, no. 6, pp. 551–559, Jun. 2013.

[390]   L. S. Rao and N. V. Ramana, "Design of robust controller for load frequency control in deregulated hydro-thermal system using sliding mode controlled strategies," *J. Int. Review Modelling Simulat.*, vol. 6, no. 3, pp. 893−902, Jun. 2013.

[391]   F. Daneshfar, "Load-frequency control in a deregulated environment based on reinforcement learning," *J. Contr. Syst. Eng.*, vol. 1, no. 1, pp. 9–16, Jun. 2013.

[392]   S. Srikanth, K. R. Sudha, and Y. B. Raju, "Load frequency control in deregulated power system using fuzzy c-means," *Int. J. Comput. Appl.*, vol. 74, no. 11, pp. 34–41, Jul. 2013.

[393]   A. G. D. Kumar and N. V. Ramana, "Design of a new discrete sliding mode optimal controller for load frequency control in multi area deregulated power system," *Int. Review Modelling Simulat.*, vol. 6, no. 4, pp. 1183–1189, Aug. 2013.

[394]   M. Eidiani and H. Zeynal, "New approach using structure-based modeling for simulation of real power/frequency dynamics in deregulated power systems," *Turkish J. Elect. Eng. Comp. Sc.*, vol. 22, no. 5, pp. 1130–1146, 2014.

[395]   M. Prathibha and M. Bhavani, "Automatic generation control in restructured power system with wind integrated system," *Int. J. Innovat. Res. Sc. Eng. Tech.*, vol. 3, no. 3, pp. 461–466, Mar. 2014.

[396]   W. Tan, Y. Hao, and D. Li, "Load frequency control in deregulated environments via active disturbance rejection," *Int. J. Elect. Power Energy Syst.*, vol. 66, pp. 166–177, Mar. 2015.

[397] S. Srikanth, K. R. Sudha, and Y. B. Raju, "Fuzzy load frequency controller in deregulated power environment by principal component analysis," *Int. J. Fuzzy Logic Syst.*, vol. 6, no.1, pp. 13–30, Jan. 2016.

[398] S. Srikanth, K. R. Sudha, and Y. B. Raju, "Fuzzy C-means load frequency controller in deregulated power environment," *Int. J. Fuzzy Computat. Modelling*, vol. 2, no.1, pp. 27–49, Jan. 2016.

[399] Q. Zhu, L. Jiang, W. Yao, C.-K. Zhang, and C. Luo, "Robust load frequency control with dynamic demand response for deregulated power systems considering communication delays," *Elect. Power Compon. Syst.*, vol. 45, no. 1, pp. 75–87, Jan. 2017.

[400] S. C. Tripathy, R. Balasubramanian, and P. S. C. Nair, "Effect of superconducting magnetic energy storage on automatic generation control consideration governor deadband and boiler dynamics," *IEEE Trans. Power Syst.*, vol. 7, no. 3, pp. 1266–1273, Aug. 1992.

[401] C. W. Taylor, K. Y. Lee, and D. P. Dave, "Automatic generation control analysis with governor deadband effects," *IEEE Trans. Power App. Syst.*, vol. PAS-98, no. 6, pp. 2030–2036, Nov./Dec. 1979.

[402] A. Oustaloup, X. Moreau, and M. Nouillant, "The CRONE suspension," *Contr. Eng. Practice*, vol. 4, no. 8, pp. 1101–1108, Aug. 1996.

Appendix A. State Space Model Matrices:

Restructured two-area multi-source hydrothermal system:

For the two-area multi-source hydrothermal restructured power system model interconnected via AC/DC links, the system matrix A is of the order of 18×18 and its non-zero ($a_{i,j}$) elements are given as:

$$a_{1,1} = -\frac{1}{T_{P1}} \qquad a_{1,2} = -\frac{K_{P1}}{T_{P1}} \qquad a_{1,4} = \frac{K_{P1}}{T_{P1}} \qquad a_{1,5} = \frac{K_{P1}}{T_{P1}} \qquad a_{1,8} = \frac{K_{r1}K_{P1}}{T_{P1}}$$

$$a_{1,9} = -\frac{2K_{P1}}{T_{P1}} \qquad a_{1,13} = -\frac{2T_{R1}K_{P1}}{T_{GH1}T_{P1}} \qquad a_{1,18} = -\frac{K_{P1}}{T_{P1}} \qquad a_{2,1} = 2\pi T_{12} \qquad a_{2,3} = -2\pi T_{12}$$

$$a_{3,2} = -\frac{\alpha_{12}K_{P2}}{T_{P2}} \qquad a_{3,3} = -\frac{1}{T_{P2}} \qquad a_{3,6} = \frac{K_{P2}}{T_{P2}} \qquad a_{3,7} = \frac{K_{P2}}{T_{P2}} \qquad a_{3,10} = \frac{K_{r2}K_{P2}}{T_{P2}}$$

$$a_{3,11} = -\frac{2K_{P2}}{T_{P2}} \qquad a_{3,15} = -\frac{2T_{R2}K_{P2}}{T_{GH2}T_{P2}} \qquad a_{3,18} = -\frac{\alpha_{12}K_{P2}}{T_{P2}} \qquad a_{4,4} = -\frac{1}{T_{r1}} \qquad a_{4,8} = \frac{1-K_{r1}}{T_{r1}}$$

$$a_{5,5} = -\frac{2}{T_{W1}} \qquad a_{5,9} = \frac{6}{T_{W1}} \qquad a_{5,13} = \frac{6T_{R1}}{T_{GH1}T_{W1}} \qquad a_{6,6} = -\frac{1}{T_{r2}} \qquad a_{6,10} = \frac{1-K_{r2}}{T_{r2}}$$

$$a_{7,7} = -\frac{2}{T_{W2}} \qquad a_{7,11} = \frac{6}{T_{W2}} \qquad a_{7,15} = \frac{6T_{R2}}{T_{GH2}T_{W2}} \qquad a_{8,8} = -\frac{1}{T_{t1}} \qquad a_{8,12} = \frac{1}{T_{t1}}$$

$$a_{9,9} = -\frac{1}{T_{GH1}} \qquad a_{9,13} = \frac{T_{GH1}-T_{R1}}{T_{GH1}^2} \qquad a_{10,10} = -\frac{1}{T_{t2}} \qquad a_{10,14} = \frac{1}{T_{t2}} \qquad a_{11,11} = -\frac{1}{T_{GH2}}$$

$$a_{11,15} = \frac{T_{GH2}-T_{R2}}{T_{GH2}^2} \qquad a_{12,1} = -\frac{1}{R_{t1}T_{g1}} \qquad a_{12,12} = -\frac{1}{T_{g1}} \qquad a_{13,1} = -\frac{1}{R_{h1}T_{RH1}} \qquad a_{13,13} = -\frac{1}{T_{RH1}}$$

$$a_{14,3} = -\frac{1}{R_{t2}T_{g2}} \qquad a_{14,14} = -\frac{1}{T_{g2}} \qquad a_{15,3} = -\frac{1}{R_{h2}T_{RH2}} \qquad a_{15,15} = -\frac{1}{T_{RH2}} \qquad a_{16,1} = \beta_1$$

$$a_{16,2} = 1 \qquad a_{16,18} = 1 \qquad a_{17,2} = \alpha_{12} \qquad a_{17,3} = \beta_2 \qquad a_{17,18} = \alpha_{12}$$

$$a_{18,1} = \frac{K_{dc}}{T_{dc}} \qquad a_{18,3} = -\frac{K_{dc}}{T_{dc}} \qquad a_{18,18} = -\frac{1}{T_{dc}}$$

The control matrix B is of the order of 18×2 and its non-zero elements $(b_{i,j})$ are given as:

$$b_{12,1} = \frac{apf}{T_g} \quad b_{13,1} = \frac{apf_{h1}}{T_{RH1}} \qquad b_{14,2} = \frac{apf_{t2}}{T_{g2}} \quad b_{15,2} = \frac{apf_{h2}}{T_{TRH2}}$$

The disturbance matrix Γ is of the order of 18×6 and its non-zero elements $(d_{i,j})$ are given as:

$$d_{1,1} = -\frac{K_{P1}}{T_{P1}} \quad d_{1,2} = -\frac{K_{P1}}{T_{P1}} \quad d_{1,5} = -\frac{K_{P1}}{T_{P1}} \quad d_{3,3} = -\frac{K_{P2}}{T_{P2}} \quad d_{3,4} = -\frac{K_{P2}}{T_{P2}} \quad d_{3,6} = -\frac{K_{P2}}{T_{P2}}$$

$$d_{12,1} = \frac{cpf_{11}}{T_{g1}} \quad d_{12,2} = \frac{cpf_{12}}{T_{g1}} \quad d_{12,3} = \frac{cpf_{13}}{T_{g1}} \quad d_{12,4} = \frac{cpf_{14}}{T_{g1}} \quad d_{13,1} = \frac{cpf_{21}}{T_{RH1}} \quad d_{13,2} = \frac{cpf_{22}}{T_{RH1}}$$

$$d_{13,3} = \frac{cpf_{23}}{T_{RH1}} \quad d_{13,4} = \frac{cpf_{24}}{T_{RH1}} \quad d_{14,1} = \frac{cpf_{31}}{T_{g2}} \quad d_{14,2} = \frac{cpf_{32}}{T_{g2}} \quad d_{14,3} = \frac{cpf_{33}}{T_{g2}} \quad d_{14,4} = \frac{cpf_{34}}{T_{g2}}$$

$$d_{15,1} = \frac{cpf_{41}}{T_{RH2}} \quad d_{15,2} = \frac{cpf_{42}}{T_{RH2}} \quad d_{15,3} = \frac{cpf_{43}}{T_{RH2}} \quad d_{15,4} = \frac{cpf_{44}}{T_{RH2}} \quad d_{16,1} = cpf_{31} + cpf_{41}$$

$$d_{16,2} = cpf_{32} + cpf_{42} \qquad d_{16,3} = -(cpf_{13} + cpf_{23}) \qquad d_{16,4} = -(cpf_{14} + cpf_{24})$$

$$d_{17,1} = \alpha_{12}(cpf_{31} + cpf_{41}) \qquad d_{17,2} = \alpha_{12}(cpf_{32} + cpf_{42}) \qquad d_{17,3} = -\alpha_{12}(cpf_{13} + cpf_{23})$$

$$d_{17,4} = -\alpha_{12}(cpf_{14} + cpf_{24})$$

The output matrix C, the state cost weighting matrix Q and the control cost weighting matrix R are taken identity matrices of 18×18, 18×18, and 2×2 dimensions respectively.

Restructured two-area multi-source hydrothermal/gas system:

For the restructured two-area multi-source hydrothermal/gas power system model interconnected via AC/DC links, the system matrix A is of the order of 19×19 and its nonzero $(a_{i,j})$ elements are stated as:

$$a_{1,1} = -\frac{1}{T_{P1}} \qquad a_{1,3} = -\frac{K_{P1}}{T_{P1}} \qquad a_{1,4} = \frac{K_{P1}}{T_{P1}} \qquad a_{1,5} = \frac{K_{P1}}{T_{P1}} \qquad a_{1,8} = \frac{K_{r1}K_{P1}}{T_{P1}}$$

$$a_{1,9} = -\frac{2K_{P1}}{T_{P1}} \qquad a_{1,14} = -\frac{2T_{R1}K_{P1}}{T_{GH1}T_{P1}} \qquad a_{1,19} = -\frac{K_{P1}}{T_{P1}} \qquad a_{2,2} = -\frac{1}{T_{P2}} \qquad a_{2,3} = -\frac{\alpha_{12}K_{P2}}{T_{P2}}$$

$$a_{2,6} = \frac{K_{P2}}{T_{P2}} \qquad a_{2,7} = \frac{K_{P2}}{T_{P2}} \qquad a_{2,10} = \frac{K_{r2}K_{P2}}{T_{P2}} \qquad a_{2,19} = -\frac{\alpha_{12}K_{P2}}{T_{P2}} \qquad a_{3,1} = 2\pi T_{12}$$

$$a_{3,2} = -2\pi T_{12} \qquad a_{4,4} = -\frac{1}{T_{r1}} \qquad a_{4,8} = \frac{1-K_{r1}}{T_{r1}} \qquad a_{5,5} = -\frac{2}{T_W} \qquad a_{5,9} = \frac{6}{T_W}$$

$$a_{5,14} = \frac{6T_R}{T_{GH}T_W} \qquad a_{6,6} = -\frac{1}{T_{r2}} \qquad a_{6,10} = \frac{1-K_{r2}}{T_{r2}} \qquad a_{7,7} = -\frac{1}{T_{CD}} \qquad a_{7,11} = \frac{1}{T_{CD}}$$

$$a_{7,12} = -\frac{T_{CR}}{T_F T_{CD}} \qquad a_{8,8} = -\frac{1}{T_{t1}} \qquad a_{8,13} = \frac{1}{T_{t1}} \qquad a_{9,9} = -\frac{1}{T_{GH}} \qquad a_{9,14} = \frac{T_{GH}-T_R}{T_{GH}^2}$$

$$a_{10,10} = -\frac{1}{T_{t2}} \qquad a_{10,15} = \frac{1}{T_{t2}} \qquad a_{11,11} = -\frac{1}{T_F} \qquad a_{11,12} = \frac{T_F+T_{CR}}{T_F^2} \qquad a_{12,2} = -\frac{aX}{R_g bY}$$

$$a_{12,12} = -\frac{c}{b} \qquad a_{12,16} = \frac{a}{b} \qquad a_{13,1} = -\frac{1}{R_{t1}T_{g1}} \qquad a_{13,13} = -\frac{1}{T_{g1}} \qquad a_{14,1} = -\frac{1}{R_h T_{RH}}$$

$$a_{14,14} = -\frac{1}{T_{RH}} \qquad a_{15,1} = -\frac{1}{R_{t2}T_{g2}} \qquad a_{15,15} = -\frac{1}{T_{g2}} \qquad a_{16,2} = \frac{X-Y}{R_g Y^2} \qquad a_{16,16} = -\frac{1}{Y}$$

$$a_{17,1} = \beta_1 \qquad a_{17,3} = 1 \qquad a_{17,19} = 1 \qquad a_{18,2} = \beta_2 \qquad a_{18,3} = \alpha_{12}$$

$$a_{18,19} = \alpha_{12} \qquad a_{19,1} = \frac{K_{dc}}{T_{dc}} \qquad a_{19,2} = -\frac{K_{dc}}{T_{dc}} \qquad a_{19,19} = -\frac{1}{T_{dc}}$$

The control matrix B is of the order of 19×2 and its nonzero elements ($b_{i,j}$) are given

by:

$$b_{12,2} = \frac{aapf_g X}{bY} \qquad b_{13,1} = \frac{apf_{t1}}{T_{g1}} \qquad b_{14,1} = \frac{apf_h}{T_{RH}} \qquad b_{15,2} = \frac{apf_{t2}}{T_{g2}} \qquad b_{16,2} = \frac{apf_g(Y-X)}{Y^2}$$

The disturbance matrix Γ is of the order of 19×6 and its nonzero elements ($d_{i,j}$) are

given as:

$$d_{1,1} = -\frac{K_{P1}}{T_{P1}} \qquad d_{1,2} = -\frac{K_{P1}}{T_{P1}} \qquad d_{1,5} = -\frac{K_{P1}}{T_{P1}} \qquad d_{2,3} = -\frac{K_{P2}}{T_{P2}} \qquad d_{2,4} = -\frac{K_{P2}}{T_{P2}} \quad d_{2,6} = -\frac{K_{P2}}{T_{P2}}$$

$$d_{12,1} = \frac{acpf_{41}X}{bY} \quad d_{12,2} = \frac{acpf_{42}X}{bY} \quad d_{12,3} = \frac{acpf_{43}X}{bY} \quad d_{12,4} = \frac{acpf_{44}X}{bY} \quad d_{13,1} = \frac{cpf_{11}}{T_{g1}} \qquad d_{13,2} = \frac{cpf_{12}}{T_{g1}}$$

$$d_{13,3} = \frac{cpf_{13}}{T_{g1}} \qquad d_{13,4} = \frac{cpf_{24}}{T_{g1}} \qquad d_{14,1} = \frac{cpf_{21}}{T_{RH}} \qquad d_{14,2} = \frac{cpf_{22}}{T_{RH}} \qquad d_{14,3} = \frac{cpf_{23}}{T_{RH}} \quad d_{14,4} = \frac{cpf_{24}}{T_{RH}}$$

$$d_{15,1} = \frac{cpf_{31}}{T_{g2}} \qquad d_{15,2} = \frac{cpf_{32}}{T_{g2}} \qquad d_{15,3} = \frac{cpf_{33}}{T_{g2}} \qquad d_{15,4} = \frac{cpf_{34}}{T_{g2}} \qquad d_{16,1} = \frac{cpf_{41}(Y-X)}{Y^2}$$

$$d_{16,2} = \frac{cpf_{42}(Y-X)}{Y^2}$$ 　　　　 $$d_{16,3} = \frac{cpf_{43}(Y-X)}{Y^2}$$ 　　　　 $$d_{16,4} = \frac{cpf_{44}(Y-X)}{Y^2}$$

$d_{17,1} = cpf_{31} + cpf_{41}$ 　　　　 $d_{17,2} = cpf_{32} + cpf_{42}$ 　　　　 $d_{17,3} = -(cpf_{13} + cpf_{23})$

$d_{17,4} = -(cpf_{14} + cpf_{24})$ 　　　　 $d_{18,1} = \alpha_{12}(cpf_{31} + cpf_{41})$ 　　　　 $d_{18,2} = \alpha_{12}(cpf_{32} + cpf_{42})$

$d_{18,3} = -\alpha_{12}(cpf_{13} + cpf_{23})$ 　　　　 $d_{18,4} = -\alpha_{12}(cpf_{14} + cpf_{24})$

The output matrix C, the state cost weighting matrix Q and the control cost weighting matrix R for the proposed restructured multi-source power system model are taken identity matrices of 19×19, 19×19 and 2×2 dimensions respectively.

Appendix B. System Data:

Chapter4.

Multi-area multi-source hydrothermal system [1,23,56]:

$P_{r1} = P_{r2} = 2000$ MW, $Ptie_{max} = 200$ MW, Base power $= 2000$ MVA, $\Delta P_{Di}^0 = 1000$ MW, $F^0 = 60$ Hz, $\alpha_{12} = (-P_{r1}/P_{r2}) = -1$, $D_i = (\partial \Delta P_{Di}^0/\partial fP_{ri}) = 8.33 \times 10^{-3}$ puMW/Hz, $H_i = 5$ MWs/MVA, $T_{Gi} = 0.08$ s, $T_{Ti} = 0.3$ s, $K_{ri} = 0.5$, $T_{ri} = 10$ s, $R_{ti} = R_{hi} = 2.4$ Hz/puMW, $K_{PSi} = (1/D_i) = 120$ Hz/puMW, $T_{PSi} = (2H_i/F^0 D_i) = 20$ s, $B_i = (\beta_i = D_i + 1/R_{ti}) = 0.425$ puMW/Hz, $\delta = 0.31$ pu, $\sigma = (R_{hi} = F^0 \sigma) = 0.04$ pu, $T_{Ri} = 5$ s, $T_{RHi} = 48.7$ s, $T_{GHi} = 0.513$ s, $T_{Wi} = 1$ s, $\delta_{12} = (\delta_1 - \delta_2) = 30^0$, $T_{12} = 0.1\cos\delta_{12}$ puMW/rad, $2\pi T_{12} = 0.545$ puMW/Hz, $K_{dc} = 1$, $T_{dc} = (L_{dc}/R_{dc}) = 0.2$ s.

Multi-area multi/single-source power systems[1,23,56,241]:

$P_{r1} = P_{r2} = 2000$ MW, $Ptie_{max} = 200$ MW, Base power $= 2000$ MVA, $\Delta P_{Di}^0 = 1000$ MW, $F^0 = 60$ Hz, $\alpha_{12} = -1$, $D_i = 8.33 \times 10^{-3}$ puMW/Hz, $H_i = 5$ MWs/MVA, $T_{Gi} = 0.08$ s, $T_{Ti} = 0.3$ s, $K_{ri} = 0.3$, $T_{ri} = 5$ s, $R_i = R_{ti} = R_{hi} = 2.4$ Hz/puMW, $K_{PSi} = 120$

Hz/puMW, T_{PSi} = 20 s, β_i = 0.4249 puMW/Hz, T_{12} = 0.0867 puMW/rad, T_{RHi} = 48.7 s, T_{GHi} = 0.513s, T_{Ri} = 5 s, T_{Wi} = 1 s, σ = 0.04, δ = 0.31, δ_{12} = 30^0, K_{dc} = 1, T_{dc} = 0.2 s.

Multi-area multi-source hydrothermal/gas system [1,38]:

P_{r1} = P_{r2} = 2000 MW, $Ptie_{max}$ = 200 MW, Base power = 2000 MVA, ΔP_{Di}^0 = 1000 MW, F^0 = 60 Hz, α_{12}= –1, D_i = 8.33 $\times$ 10^{-3} puMW/Hz, H_i = 5 MW s/MVA, T_{gi} = 0.08 s, T_{ti} = 0.3 s, K_{ri} = 0.3, T_{ri} = 10 s, R_{ti} = R_h = R_g = 2.4 Hz/puMW, K_{Pi} = 120 Hz/puMW, T_{Pi} = 20 s, B_i = β_i = 0.425 puMW/Hz, T_{12} = 0.086 puMW/rad, σ = 0.04 pu, δ_{12} = 30^0, T_{RH} = 28.75 s, T_{GH} =0.2 s, T_R = 5 s, T_W = 1 s, a = 1, b = 0.05 s, c = 1, X = 0.6 s, Y = 1 s, T_{CR} = 0.01 s, T_F = 0.23 s, T_{CD} = 0.2 s, K_{dc} = 1, T_{dc} = 0.2 s.

Chapter 5.

Traditional non-reheat/reheat and restructured reheat thermal system [25,124, 136,144,146,150,343]:

P_{ri} = 2000 MW, ΔP_{Di}^0 = 1000 MW, α_{12} = –1, F^0 = 60 Hz, D_i = 0.00833 puMW/Hz, H_i = 5 s, R_i = 2.4 Hz/puMW, β_i = 0.425 puMW/Hz), K_{PSi} = 120, T_{PSi} = 20 s, δ_i = 30^0, $Ptie_{max}$ = 0.1P_{ri} MW, $2\pi T_{12}$ = 0.545 pu MW/Hz, T_{Gi} = 0.08 s, T_{Ti} = 0.3 s, K_{ri} = 0.5, T_{ri} = 10 s.

Multi-source hydrothermal power system [100,150,152]:

P_{ri} = 2000 MW, ΔP_{Di}^0 = 1000 MW, α_{12} = –1, F^0 = 60 Hz, D_i = 0.00833 puMW/Hz, R_1 =2 Hz/puMW , R_2 = 2.4 Hz/puMW, β_i = 0.425 puMW/Hz, K_{PSi} = 100, T_{PSi} = 20 s δ_i = 45^0, $Ptie_{max}$ = 0.1P_{ri} MW, T_{12} = 0.0707puMW/rad, T_{Gi} = 0.08 s, T_{Ti} = 0.3 s, T_{RHi} = 48.7 s, T_{Ri} = 5 s, T_{GHi} = 0.513 s, T_{Wi} = 1 s.

Chapter 6.

Non-reheat thermal system [145–146,148,151]:

P_{ri} = 2000 MW, ΔP_{Di}^0 = 1000 MW, α_{12} = −1, F^0 = 60 Hz, D_i = 0.00833 puMW/Hz, H_i = 5 s, R_i = 2.4 Hz/puMW, β_i = 0.425 puMW/Hz, K_{PSi} = 120, T_{PSi} = 20 s, δ_i = 30^0, $Ptie_{max}$ = 0.1P_{ri} MW, $2\pi T_{12}$ = 0.545 pu MW/Hz, T_{Gi} = 0.08 s, T_{Ti} = 0.3 s.

Reheat thermal system [128–129,133]:

P_{ri} = 2000 MW, ΔP_{Di}^0 = 1000 MW, α_{12} = −1, F^0 = 60 Hz, D_i = 0.00833 puMW/Hz, H_i = 5 s, R_i = 2.4 Hz/puMW, β_i = 0.425 puMW/Hz, K_{PSi} = 120, T_{PSi} = 20 s, δ_i = 30^0, $Ptie_{max}$ = 0.1P_{ri} MW, T_{12} = 0.086puMW/rad, T_{Gi} = 0.08 s, T_{Ti} = 0.3 s, K_{ri} = 0.5, T_{ri} = 10 s.

Traditional/restructured multi-source hydrothermal power system [100,150,152]:

P_{ri} = 2000 MW, ΔP_{Di}^0 = 1000 MW, α_{12} = −1, F^0 = 60 Hz, D_i = 0.00833 puMW/Hz, R_1 =2 Hz/puMW, R_2 = 2.4 Hz/puMW, β_i = 0.425 puMW/Hz, K_{PSi} = 100, T_{PSi} = 20 s, δ_i = 45^0, $Ptie_{max}$ = 0.1P_{ri} MW, T_{12} = 0.0707puMW/rad, T_{Gi} = 0.08 s, T_{Ti} = 0.3 s, T_{RHi} = 48.7 s, T_{Ri} = 5 s, T_{GHi} = 0.513 s, T_{Wi} = 1 s.

Chapters 7-9.

Traditional/restructured two/three-area multi-source hydrothermal system [100,150,152]:

P_{r1} = P_{r2} = 2000 MW, $Ptie_{max}$ = 200 MW, Base power = 2000 MVA, ΔP_{Di}^0 = 1000 MW, F^0 = 60 Hz, α_{12}= −1, β_1 = 0.425, R_1 = 2 Hz/puMW, R_2 = 2.4 Hz/puMW, K_{PSi} =

100, T_{PSi} = 20, T_{Gi} = 0.08 s, T_{Ti} = 0.3 s, T_{RHi} = 48.7 s, T_{Ri} = 5 s, T_{GHi} = 0.513 s, T_{Wi} = 1 s, T_{12} = 0.0707 puMW/rad.

Restructured two-area multi-source thermal gas system [323]:

P_{r1} = P_{r2} = 2000 MW, $Ptie_{max}$ = 200 MW, Base power = 2000 MVA, ΔP_{Di}^0 = 1000 MW, F^0 = 60 Hz, α_{12} = −1, D_i = 8.33 × 10^{-3} puMW/Hz, H_i = 5 MW s/MVA, T_{Gi} = 0.06 s, T_{Ti} = 0.3 s, K_{ri} = 0.3, T_{ri} = 10 s, R_1 = 3.0784 Hz/puMW, R_2 = 4.9809 Hz/puMW, K_{PSi} = 120 Hz/puMW, T_{PSi} = 20 s, β_i = 0.4312 puMW/Hz, T_{12} = 0.02712 puMW/rad, a_i = 1, c_{gi} = 1, b_{gi} = 0.049 s, X_i = 0.6 s, Y_i = 1.1 s, T_{CRi} = 0.01 s, T_{Fi} = 0.239 s, T_{CDi} = 0.2 s.

BIODATA

Name   :   Yogendra Arya

Fathers Name   :   Mr. Mange Ram Arya

Mothers Name   :   Late Mrs. Jaswanti Devi

Date of Birth   :   03.03.1976

Email IDs   :   mr.y.arya@gmail.com, yarya@msit.in

Academics Qualifications

Qualification	Passing Year	Board/University	Subjects	% of marks
10th	1992	CBSE	Hindi, English, Maths, Science, Social Science	75.40
12th	1994	CBSE	Physics, Chemistry, Biology, Hindi, English	62.40
Diploma	1997	BTE, Delhi	Electrical Engineering	76.70
A.M.I.E.	2008	IE(I) Kolkata	Electrical Engineering	58.33
M.Tech.	2010	DCRUST, Murthal, Haryana	Electrical Engineering (I&C)	78.47
Total teaching experience = 7 Years.				
Currently working as an Assistant Professor with Maharaja Surajmal Institute of Technology, C4, Janakpuri, New Delhi-110058, India.				

LIST OF PUBLICATIONS

[1] Yogendra Arya and Narendra Kumar, "AGC of a multi-area multi-source hydrothermal power system interconnected via AC/DC parallel links under deregulated environment," *International Journal of Electrical Power and Energy Systems*, vol. 75, pp. 127–138, Feb. 2016, (Elsevier), **Indexing: SCI**, **Impact Factor** = 3.289.

DOI: https://doi.org/10.1016/j.ijepes.2015.08.015.

[2] Yogendra Arya and Narendra Kumar, "Fuzzy gain scheduling controllers for AGC of two-area interconnected electrical power systems," *Electric Power Components and Systems*," vol. 44, no. 7, pp. 737–751, Apr. 2016, (Taylor & Francis), **Indexing: SCI**, **Impact Factor** = 1.220.

DOI: https://doi.org/10.1080/15325008.2015.1131765.

[3] Yogendra Arya, Narendra Kumar, and Ibraheem, "AGC of a two-area multi-source power system interconnected via AC/DC parallel links under restructured power environment," *Optimal Control Applications and Methods*, vol. 37, no. 4, pp. 590–607, Jul.-Aug. 2016, (Wiley), **Indexing: SCI**, **Impact Factor** = 1.558.
DOI: 10.1002/oca.2181.

[4] Yogendra Arya and Narendra Kumar, "BFOA-scaled fractional order fuzzy PID controller applied to AGC of multi-area multi-source electric power generating systems," *Swarm and Evolutionary Computation*, vol. 32, pp. 202–218, Feb. 2017, (Elsevier), **Indexing: SCI**, **Impact Factor** = 3.893.

DOI: https://doi.org/10.1016/j.swevo.2016.08.002.

[5] Yogendra Arya and Narendra Kumar, "Design and analysis of BFOA-optimized fuzzy PI/PID controller for AGC of multi-area traditional/restructured electrical power systems," *Soft Computing*, vol. 21, no. 21, pp. 6435–6452, Nov. 2017, (Springer), **Indexing: SCI**, **Impact Factor = 2.472**.

DOI: https://doi.org/10.1007/s00500-016-2202-2.

ADDITIONAL PAPERS:

[6] Yogendra Arya and Narendra Kumar, "Optimal AGC with redox flow batteries in multi-area restructured power systems," *Engineering Science and Technology, an International Journal*, vol. 19, no. 3, pp. 1145–1159, Sep. 2016, (Elsevier), **Indexing: Scopus, ESCI (Emerging Sources Citation Index)**.
DOI: https://doi.org/10.1016/j.jestch.2015.12.014.

[7] Yogendra Arya, Narendra Kumar, and S.K. Gupta, "Optimal automatic generation control of two-area power systems with energy storage units under deregulated environment," *Journal of Renewable and Sustainable Energy*, vol. 9, no. 6, pp. 064105–20, Nov. 2017, (American Institute of Physics), **Indexing: SCI**, **Impact Factor = 1.135**.

DOI: https://doi.org/10.1063/1.5018338.

[8] Yogendra Arya and Narendra Kumar, "Optimal control strategy-based AGC of electrical power systems: A comparative performance analysis," *Optimal Control Applications and Methods*, vol. 38, no. 6, pp. 982–992, Nov.-Dec. 2017, (Wiley), **Indexing: SCI**, **Impact Factor = 1.558**.

DOI: 10.1002/oca.2304.